
Electronic Thesis and Dissertation Repository

6-26-2020 10:00 AM

Determining geological controls on nutrient availability at different depths in the soils of the Pelee Island Winery

Lindsay M. Blythe, *The University of Western Ontario*

Supervisor: Webb, Elizabeth, *The University of Western Ontario*

Joint Supervisor: Corcoran, Patricia, *The University of Western Ontario*

A thesis submitted in partial fulfillment of the requirements for the Master of Science degree in Geology

© Lindsay M. Blythe 2020

Follow this and additional works at: <https://ir.lib.uwo.ca/etd>



Part of the [Geochemistry Commons](#), [Geology Commons](#), and the [Soil Science Commons](#)

Recommended Citation

Blythe, Lindsay M., "Determining geological controls on nutrient availability at different depths in the soils of the Pelee Island Winery" (2020). *Electronic Thesis and Dissertation Repository*. 7105.
<https://ir.lib.uwo.ca/etd/7105>

This Dissertation/Thesis is brought to you for free and open access by Scholarship@Western. It has been accepted for inclusion in Electronic Thesis and Dissertation Repository by an authorized administrator of Scholarship@Western. For more information, please contact wlsadmin@uwo.ca.

Abstract

Terroir describes a sense of place that can give a unique flavour to wines grown in different environments. We explored the role of soil in the terroir at Canada's most southern vineyard, Pelee Island Winery. This study examined the abundance of major nutrients, trace and rare earth elements of minerals and plant extractable nutrients from 19 soils across the vineyard to a depth of 2 m. We found that bedrock does not influence the element content of Pelee Island soils, the parent materials of the soils are tills and there are geochemical, mineralogical and grain size differences between the two soil types on the island. Nutrient distribution throughout the soil profile was controlled by soil weathering with organic matter concentrating most nutrients in surface soils. Agricultural and anthropogenic influences had minimal effects on soil nutrient concentrations.

Keywords

Pelee Island, winery, vineyard, terroir, Brookston, Toledo, soil geochemistry, bioavailability, pedogenesis, plant extractable nutrients

Summary for Lay Audience

Pelee Island is the southernmost point and has the longest growing season in Canada making it an ideal place to grow grapes to produce quality wines. We examined the elemental concentrations of the soil minerals and nutrients in the soils easily mobilized by plants (plant extractable nutrients) in order to understand variations in grape productivity across the island. This work will lead to a better understanding of how the soil contributes to the terroir, or sense of place that contributes to the flavours of Pelee Island wines. The aims of this study were to determine if bedrock has any influence on soil composition, to distinguish geochemical differences between the two main soil types on the island – Brookston and Toledo, and to understand how soils processes and agricultural and anthropogenic influences affect nutrient distribution within the soil profiles across Pelee Island. Results from the geochemical analysis conclude a few important findings. First, bedrock does not influence the composition of Pelee Island soils. Second, weathering intensities between Brookston and Toledo soils differ causing differences in elemental distributions throughout their soil profiles. Brookston soils are shallower and less leached resulting in higher abundance of Ca in surface soils and lower abundances of Fe and Mn in deep soils compared to Toledo soils. Third, nutrients used by plants are generally highest in surface soils where they are held by organic matter. Lastly, anthropogenic (i.e. airborne pollutants) and agricultural (i.e. fertilizers) influences had minimal effects on soil nutrient concentrations. These results will enable Pelee Island Winery to enhance their soil management practices and improve grape quality to produce quality wines.

List of Abbreviations

CEC	Cation exchange capacity
DTPA	Diethylene triamine penta-acetic acid
EDTA	Ethylene diamine tetra-acid
LOI	Loss on ignition
MMI	Mobile metal ion
NASC	North American shale composite
PEN	Plant extractable nutrients
PCA	Principle component analysis
REE	Rare earth element
UAN	Urea ammonium nitrate
XRD	X-ray diffraction
XRF	X-ray fluorescence

Co-Authorship Statement

I declare that I am the sole author of this thesis and all work included is original. Dr. Elizabeth Webb and Dr. Patricia Corcoran devised and directed the project and acted as editors of all written work and advisors on data presentation and interpretation. Dr. Gerhard Pratt and Jacob Kukovica performed the Pelee Island seismic survey and compiled the data into a report that is included in an appendix at the end of the thesis. Dr. Mark Biesinger set up and performed the principal component analysis used to make graphs and interpretations in the discussion chapter.

Acknowledgments

I am very thankful to everyone who has helped in the completion of this project over the past two years. I would first like to thank my supervisors Dr. Elizabeth Webb and Dr. Patricia Corcoran for their tremendous support, guidance, and words of encouragement throughout this process. Their investment in me as a developing earth scientist is much appreciated and has allowed me to work towards both my professional and personal goals. Thank you to Patricia for not letting me forget the value of a list, of taking things one step at a time, and for her thorough editing of the final product. Thank you to Liz for the countless hours she has dedicated towards mentorship and editing. Her unwavering support throughout this experience has given me the confidence to see this process through to the end, and she has taught me that the hardest part is just getting started.

This project would also not have been possible without the support of our industry and university collaborators. This project was funded by the Pelee Island Winery, NSERC CRD grant and the J. Malcom Slack Earth Sciences Award. Thanks to Jon Jacobs and Kimberly Law for their lab assistance, and to Bruno Friesen for his help in the field and for graciously providing lunches and fine wines. Thanks also to the staff at Pelee Island Winery for their help in soil collection and for coordinating field transportation, and my lab mates Zhaoming Jang and Ramen Tolo for their help in the field. Your positive attitudes and willingness to help made field work an enjoyable experience! Thanks also to those people who offered their time to aid in the data analysis for this project. Thanks to Dr. Gerhard Pratt and Jacob Kukovika for setting up the seismic survey and compiling data into a geophysical report. I am also grateful to Mark Biesinger for his help processing and interpreting PCA data. His help with the visualization and interpretation of my data was a major break-through for this project and I greatly appreciated his input. Thanks to my friends and colleagues in the Earth Science department for helping me navigate grad school and for reminding me to enjoy my time as a grad student. Lastly to my parents Joe and Audrey and my sisters Jennifer and Meghan Blythe for their love and encouragement over the past two years. Their endless support will never go unnoticed or unappreciated, and I am very grateful for everything they do and continue to do to support me.

Table of Contents

Abstract.....	ii
Summary for Lay Audience.....	iii
List of Abbreviations	ivi
Co-Authroship Statement.....	v
Acknowledgements.....	vi
Table of Contents.....	vii
List of Tables	xi
List of Figures.....	xiii
List of Appendices	xvii
Chapter 1.....	1
1 Introduction.....	1
1.1 Literature Review.....	1
1.2 Background.....	5
1.2.1 Geological History of Pelee Island	5
1.2.2 Glacial History of Pelee Island	8
1.3 Soil Formation Processes.....	11
1.3.1 Weathering.....	11
1.3.2 Parent Material – Effect on Soil Formation.....	13
1.3.3 Using REE to Trace Parent Materials in Soils.....	13
1.3.4 Soil Drainage on Pelee Island and Implications for Pedogenetic Processes.....	13
1.3.5 Pelee Island Soils	14
1.3.6 Plant Nutrition – Macro and Micronutrients and Trace Elements	17

1.3.7	Reactions in Soil Horizons and soil pH, HCO ₃ ⁻ Content, and Organic Matter	18
1.3.8	Distribution of Elements in the Soil Profile.....	20
1.4	Puropose and Objectives.....	22
Chapter 2	24
2	Methodology	24
2.1	Location and Climate of Pelee Island.....	24
2.2	Sample Collection.....	24
2.3	Sample Description and Preparation.....	29
2.4	Sample Analysis.....	31
2.4.1	Soil Minerology, Geochemistry, and Plant Extractable Nutrients.....	31
2.4.2	Bedrock Geochemistry.....	33
2.4.3	Glacial Till Geochemistry.....	33
2.4.4	Grapes and Fertilizer Geochemistry	34
2.5	Soil Depth Seismic Survey	34
Chapter 3	36
3	Results	36
3.1	Depth to Bedrock	36
3.2	Soil Properties.....	37
3.2.1	Profile Description, Organic Matter and CO ₃ ⁻ Content	37
3.2.2	Soil pH	39
3.2.3	Grain Size.....	42
3.3	Soil and Bedrock Minerology.....	44
3.4	Geochemistry of Pelee Island Soils, Till, and Bedrock	45
3.4.1	Major Element Soil Composition	45
3.4.2	Soil, Bedrock, and Till Trace Elements	52

3.4.3	Soil and Bedrock REE Patterns	58
3.4.4	Pelee Island Fertilizers	62
3.4.5	Plant Extractable Nutrients	65
3.4.6	Grape Elemental Contents	69
Chapter 4	70
4	Discussion	70
4.1	Soil Weathering Profile.....	70
4.2	Relationship Between Soil and Bedrock.....	72
4.2.1	Rare Earth Elements	72
4.3	Using PCA to Identify Controls on Pelee Island Soil Geochemistry	76
4.4	Mineral Principal Components	79
4.4.1	Mineral PC1	79
4.4.2	Mineral PC2	91
4.4.3	Mineral PC3	99
4.4.4	Mineral PC4	103
4.4.5	Mineral PC5	108
4.5	Plant Extractable Nutrient Principal Components	113
4.5.1	Measuring Bioavailability in Soil	113
4.5.2	Plant Extractable Nutrients PC1	117
4.5.3	Plant Extractable Nutrients PC2	123
4.5.4	Plant Extractable Nutrients PC3, PC4, PC5.....	128
4.6	Relationship of PEN to Soil Minerology	129
Chapter 5	132
5	Conclusions	132
5.1	Depth to Bedrock	132

5.2 Effect of Bedrock on Soil Composition of Pelee Island.....	132
5.3 Using PCA to Identify Geochemical Differences Among Soil Samples.....	133
5.3.1 Minerological Variability.....	133
5.3.2 PEN Variability.....	134
5.3.3 Soil Horizon and Weathering Profiles in Brookston and Toledo Soils ..	135
5.3.4 Soil Elemental Difference Among Vineyard Fields on Pelee Island.....	136
5.3.5 Agricultural and Anthropogenic Inputs and Effect on Soil Composition	137
5.4 Future Work	137
References	139
Appendices.....	152
Curriculum Vitae	177

List of Tables

Table 2.1. Reported average monthly temperatures and precipitation on Pelee Island from 2002-2019 (Weather Atlas 2020).....	24
Table 2.2. Summary table of sampling information for Pelee Island	26
Table 2.3. Weather on Pelee Island on sampling days.....	27
Table 2.4. Sample identification and GPS locations of bedrock and till samples. Note that glacial tills were sampled from one location and on Figure 2.1 are labeled as GT	29
Table 2.5. Types of fertilizers used on Pelee Island and their sample identification.....	29
Table 3.1. Average thicknesses of soil, till, and depth to bedrock on Pelee Island determined by the seismic survey.	36
Table 3.2. Organic matter content, measured in weight percent (dry), of each soil sample arranged by field and sampling depth on Pelee Island as determined by LOI.	38
Table 3.3. Carbonate content, measured in weight percent, of each soil sample arranged by field and sampling depth on Pelee Island as determined by LOI.	39
Table 3.4. pH values of each soil sample arranged by field and sampling depth on Pelee Island.	40
Table 3.5. Relative mineralogical abundance results from XRD of select fields at each of the soil sampling depths on Pelee Island	44
Table 3.6. Relative mineralogical abundances in bedrock samples from Pelee Island.....	45
Table 3.7. Calculated average major oxide concentrations (%) at each soil sampling depth on Pelee Island as determined by XRF.	51
Table 3.8. Average, maximum, and minimum trace and REE values of soils, tills, and bedrock on Pelee Island as determined by ICP-MS.....	54
Table 3.9. Comparison of average trace element concentrations for sections 1 and 2 of Pelee Island soils and in Ontario soils analyzed by Sheppard et al. (2009).....	56
Table 3.10. Major element concentration values (weight %) of fertilizers used on Pelee Island as determined by ICP-MS.	63
Table 3.11. Trace element concentration values (ppm) of fertilizers used on Pelee Island as determined by ICP-MS.	63

Table 3.12. Pelee Island fertilizer sample IDs and descriptions	63
Table 3.13. Calculated average plant extractable nutrient concentrations at each soil sampling depth on Pelee Island as determined by ICP-MS.....	66

List of Figures

Figure 1.1. Map illustrating the location of Pelee within Lake Erie, relative to the Leamington area.....	2
Figure 1.2. Paleozoic geology of Essex County, specifically illustrating location of the Dundee Formation (modified from Morris 1994).....	7
Figure 1.3. Arrows indicate ice flow directions over the Essex County region during the Port Bruce Stadials (modified from Morris 1994).....	10
Figure 1.4. Locations of Brookston and Toledo soils on Pelee Island (modified from Essex Region Conservation Authority Interactive Mapping 2011).....	15
Figure 2.1. Locations of soil samples, bedrock samples, and glacial till samples on Pelee Island.....	25
Figure 2.2. Images of the soil sampling kit used to extract soil cores on Pelee Island.....	28
Figure 3.1. Organic matter content versus soil pH of Pelee Island soil samples.	41
Figure 3.2. Carbonate content versus soil pH of Pelee Island soil samples.....	41
Figure 3.3. Comparison of grain size between Brookston and Toledo soils at each of the four sampling depths on Pelee Island.	43
Figure 3.4. Harker diagrams showing major oxide concentrations of each soil sample (%; y-axis) plotted against concentrations of Al ₂ O ₃ for each soil sample on Pelee Island.....	47
Figure 3.5. Harker diagrams illustrating major oxide differences between Brookston (triangles) and Toledo (circles) soils on Pelee Island	49
Figure 3.6. Average oxide concentrations (%; x-axis) of Pelee Island soils plotted against mean sampling depths	52
Figure 3.7. Incompatible element diagram of averaged minor and trace element depth values for comparing elemental field concentrations on Pelee Island.....	57
Figure 3.8. Incompatible element diagram of minor and trace element averaged field values at each depth to compare elemental depth concentrations on Pelee Island.	58
Figure 3.9a. Averaged REE depth values for comparing REE concentrations among fields on Pelee Island.	59
Figure 3.9b. Averaged REE field values for comparing REE concentrations among depths on Pelee Island.....	59
Figure 3.10. REE concentrations of six bedrock samples from Pelee Island.	60

Figure 3.11a. Comparison of REE concentrations between bedrock sample PI-18-5 and section 4 soil samples of nearby Toledo fields (27GM318, 27CS, 26CF, and 27GW).....	61
Figure 3.11b. Comparison of REE concentrations between bedrock sample PI-18-7 and section 4 soil sample of the adjacent Brookston field (5GM318).	61
Figure 3.12. Comparison of REE concentrations between till (averaged values) and soil (averaged section 4 soil values).	62
Figure 3.13. Incompatible element diagram of minor and trace element concentrations of Pelee Island fertilizers.....	64
Figure 3.14. REE diagram comparing Pelee Island fertilizers and soils.....	65
Figure 3.15. Average elemental concentrations (ppm and ppb only for Mo; y-axis) of plant extractable nutrients in soils plotted against mean sampling depths on Pelee Island	68
Figure 4.1. Ternary diagram illustrating weathering patterns at four soil depths across Pelee Island	71
Figure 4.2. PC1 scores and loadings, illustrating elemental variations at depth and among field locations on Pelee Island	81
Figure 4.3. Depth versus concentration graphs comparing concentration differences with depth of Sr, CaO, MgO, MnO, Al ₂ O ₃ , and SiO ₂	82
Figure 4.4. Bubble plots for PC1 provide spatial representation of the element data on Pelee Island and are to be used together with the element loadings plot from PC1	84
Figure 4.5. Depth versus concentration graphs comparing concentration differences with depth of Al, Ca, Mg, and Sr between Brookston and Toledo soils.....	85
Figure 4.6. Depth versus concentration graphs comparing concentration differences with depth of MnO and Fe ₂ O ₃ between Brookston and Toledo soils.	87
Figure 4.7. Silicon oxide versus Al ₂ O ₃ concentrations in Pelee Island soils.	88
Figure 4.8. Organic matter content versus pH values in Brookston and Toledo soils at sections 1 and 2.....	88
Figure 4.9. Depth versus concentration graphs comparing concentration differences with depth of P ₂ O ₅ between sampling dates (August and October).	89
Figure 4.10. PC2 scores and loadings, illustrating elemental variations at depth and among field locations on Pelee Island	92

Figure 4.11. Bubble plots for PC2. These graphs provide spatial representation of the element data on Pelee Island.....	93
Figure 4.12. Soil sample depth of each soil sample plotted against oxide and elemental concentrations (Na ₂ O, P ₂ O ₅ , SiO ₂ , and Pb) of each soil sample.....	94
Figure 4.13. Soil sample depth of each soil sample plotted against oxide and elemental concentrations (Mo, Sb, Co, Ni, MnO, MgO, Fe ₂ O ₃) of each soil sample.....	95
Figure 4.14. PC3 scores and loadings, illustrating elemental variations at depth and among field locations on Pelee Island	100
Figure 4.15. Bubble plots for PC3. These graphs provide spatial representation of the element data on Pelee Island.....	101
Figure 4.16. Depth versus concentration graphs comparing concentration differences with depth of Cd, Pb and U.....	102
Figure 4.17. PC4 scores and loadings, illustrating elemental variations at depth and among field locations on Pelee Island	105
Figure 4.18. Bubble plots for PC4. These graphs provide spatial representation of the element data on Pelee Island.....	107
Figure 4.19. PC5 scores and loadings, illustrating elemental variations at depth and among field locations on Pelee Island	109
Figure 4.20. Bubble plots for PC5. These graphs provide spatial representation of the element data on Pelee Island.....	110
Figure 4.21. Depth versus concentration graphs comparing concentration differences of Cu in surface soils between fields that grow grapes compared to fields without grapes.	112
Figure 4.22. Depth versus concentration graphs comparing concentration differences with depth of Cd between fertilized and unfertilized soils.	113
Figure 4.23. PC1 scores and loadings, illustrating nutrient element variations at depth and among field locations on Pelee Island.....	118
Figure 4.24. Depth versus extractable nutrient concentration graphs comparing concentration differences with depth of Mg, Mn, Mo and U.	120
Figure 4.25. Bubble plots for PC1. These graphs provide spatial representation of the nutrient element data on Pelee Island	121

Figure 4.26. PC2 scores and loadings, illustrating nutrient element variations at depth and among field locations on Pelee Island.....	125
Figure 4.27. Depth versus concentration graphs comparing concentration differences with depth of Li between Brookston and Toledo soils.	126
Figure 4.28. Bubble plots for PC2. These graphs provide spatial representation of the nutrient element data on Pelee Island	127
Figure 4.29. Depth versus concentration graph showing concentrations of Ba increasing with soil depth.....	128
Figure 4.30. Depth versus concentration graphs comparing average concentration differences with depth of Mg and Mn between the mineralogical components (green circles) and the PEN components (red triangles) of the Pelee Island soils.....	130

List of Appendices (where applicable)

Appendix A: Mineral Element Soil Profile Graphs	152
Appendix B: Plant Extractable Nutrients Element Soil Profile Graphs	163
Appendix C: Seismic Refraction Figures	167
Appendix D: Soil Profile Descriptions	electronic
Appendix E: Trace Element Concentrations of Bedrock Samples	electronic
Appendix F: Soil Moisture, Organic Matter, and CO ₃ ⁻ Content.....	electronic
Appendix G: R ² and Slope Values.....	electronic
Appendix H: Major Oxide and Trace Element Soil Concentrations	electronic
Appendix I: Major Oxide and Trace Element Till Concentrations.....	electronic
Appendix J: Major Oxide and Trace Element Fertilizer Concentrations	electronic
Appendix K: PEN Major and Trace Element Concentrations	electronic
Appendix L: Soil and Bedrock Mineral Composition	electronic
Appendix M: Pelee Island Seismic Survey.....	electronic

Chapter 1

1 Introduction

Soil composition plays an important role in grapevine productivity and research suggests that soil composition can also influence grape composition, ultimately affecting the taste of the wine (Fraga 2014; Burns & Retallack 2015). Soil composition is influenced by many factors such as climate and geomorphology, but it is also largely influenced by parent material, such as bedrock (Weil & Brady 2017). This means that the region where grapes are grown produce wines that may have a distinct flavour (Atkin & Johnson 2010). One of the aims of this study is therefore to understand the deep subsurface mineralogy and geochemistry of bedrock and soils on Pelee Island, which is a grape-growing region in Canada. An additional aim of this study is to understand how soil and bedrock composition affect changes in soil nutrient availability with depth on Pelee Island. This will assist in improving grape quality and enable Pelee Island Winery to enhance their soil management practices to produce quality wines.

1.1 Literature Review

Pelee Island is the southernmost part of Canada and is located approximately 25km south of the northern shoreline of Lake Erie (Figure 1.1). The island has 225 hectares of vineyard growing 17 different grape varieties including Chardonnay, Pinot Gris, Riesling, Gewürztraminer, GM318 (Geisenheim), Cabernet Sauvignon, Cabernet Franc, Merlot and Pinot Noir (VAQ Ontario 2017). The island has the longest growing and frost-free season in Canada (two weeks longer than the adjacent mainland) due to its location in Lake Erie. The warm breezes coming from the shallow waters of the lake, low levels of precipitation, and high number of sunny days throughout the growing season make the island ideal for grape production. In addition to the optimal climate conditions, the clay-rich soils provide excellent growing conditions for the grapes (Pelee Island Winery 2019).



Figure 1.1. Map illustrating the location of Pelee within Lake Erie, relative to the Leamington area.

The Canadian wine industry is important for the Canadian economy and creates a variety of employment opportunities in agricultural production, manufacturing, and tourism (Wade & Pun 2009). For example, in 2012, the wine industry generated \$1.1 billion and employed over 3,700 people. There are 476 wineries across Canada, with the majority (234) located in Ontario. Over the last two decades, the wine industry in Canada has grown. For example, from 2004-2012, sales of Canadian wine increased by 31.2%, generating an increase of one-billion dollars. In addition, Canada's employment in the wine industry during the period of 2004-2012 grew from 2,828 to 3,719 (Agriculture and Agri-Food Canada 2016). It is expected that future growth in the wine industry will occur through Vintners Quality Alliance (VQA) wines (Doloreux & Lord-Tarte 2012; Azcarate et al. 2015). The VQA is a regulatory system that has been employed in Canada to ensure authenticity and quality of Canadian wines (VQA Ontario 2019).

Canadian vineyards are typically located between $41^{\circ}00'00''\text{N}$ and $51^{\circ}00'00''\text{N}$, a latitude similar to many other acclaimed wine regions of the world (Wines of Canada 2016). In addition, many Canadian wine regions thrive in soils derived from glacial

deposits and also benefit from temperature-moderating effects of nearby bodies of water (Wines of Canada 2016). Although Canada has been producing wines for 150 years, Canadian wines have only recently become internationally recognized, shortly after the establishment of the VQA in 1988 (Canadian Vintners Association 2017a). In addition to the establishment of the VQA, there are several other reasons for global recognition of Canadian wines. One, Canada is known to consistently produce the best ice wine worldwide (Pope 2016). Selling ice wine through the VQA regulatory system is a marketing tool used to promote Canadian wines and gain global recognition in hopes that other types of wine will increase in popularity and become recognized worldwide (Wines of Canada 2016). Two, Canada has more geographic diversity compared to many other countries, and thus Canadian climates can support a wide variety of grapes, and winemakers are able to experiment with new styles and blends of wine (Pope 2016). Three, Canada has, on average, cooler temperatures compared to other wine regions and is becoming globally recognized for being one of the world's finest producers of premium cool-climate wines (Canadian Vintners Association 2017b).

The VQA recognizes eight acclaimed wine regions; three in Ontario and five in British Columbia (Pope 2016). The three designated VQA regions in Ontario are: Niagara Peninsula, Lake Erie North Shore, and Prince Edward County. Each of these regions has their own microclimate but contain subregions. Currently, Pelee Island is one of the subregions of the Lake Erie North Shore region called the South Islands (VQA Ontario 2019). Until 2013, Pelee Island was designated by the VQA as its own appellation. An appellation is a region defined by unique soil, geology, climate, and topography where grapes are grown to give wine a unique place name (Atkin & Johnson 2010). Pelee Island lost its appellation status in 2013 because the Pelee Island Winery, located on the mainland, sources grapes from both Pelee Island and Essex County (Phillips 2017).

Pelee Island is one of Canada's oldest grape growing regions with the first grapes harvested in the 1860s (Wines of Canada 2016). The Vin Villa, one of the early wineries, was built on the island in 1866 and opened in 1871. This winery was internationally recognized and won many awards for its Catawba wine. By the 1900s, grape growing was well established, Pelee Island was a significant producer of wine, and was

recognized for this at the 1900 Paris Wine Exposition (Wines of Canada 2016). However, during WWI there was a major decline in the wine market, and Pelee Island stopped producing wine and growing grapes (Pelee Island Winery 2019). The lack of interest in Pelee Island wines was perhaps related to cheap imports and/or the development of the Niagara wine district. Then, in 1935, a fire on the island destroyed the wine house and it wasn't until the 1980s that vineyards on Pelee Island and wine production restarted (Wines of Canada 2016). In 1979, grapes were reintroduced to the island and Pelee Island produced Canada's first commercial ice wine (Pelee Island Winery 2019).

Many studies have found that the region where the grapes are grown strongly influences the composition and quality of wine grapes (MacNeil 2001; Orth et al. 2005; Zhao 2005). Mackenzie and Christy (2005) analyzed major elements and 27 trace elements in soils and found that grape juice properties, such as acidity, correlated with plant-available trace elements in the soil. This suggests that soil chemistry has an influence on grape composition. By analyzing trace elements in soil and grape juice, Almeida & Vasconcelos (2003) proved that compositional soil differences are incorporated into the grapes. Other studies further suggest that soil chemistry can affect the taste of the wine (Fraga 2014). The nutrients in soils in different regions depend on soil formation processes. One of the most important controls on grape composition is the geographic region in which the grapes are grown (Greenough et al. 2005). This is because different regions of the world have different climates and different soil compositions, which will alter the production and quality of grapes (Fraga 2014). It has been suggested that the type and amount of major and trace extractable elements in the soil affect the grape quality and production, and ultimately affect the taste of the wine (Acuna-Avila et al. 2016).

The relationship between sensory attributes of the wine and its origin are referred to as terroir and are affected by several physical elements of the vineyard growing habitat, such as soils and climate (van Leeuwen et al. 2018). The concept of terroir was first developed by French winemakers when they noticed that wines coming from different regions or vineyards developed characteristic tastes and flavours (McCarthy & Ewing-Mulligan 2001). The concept of terroir remains unclear because the meaning of terroir is

not universally understood. As a result, this has become an area of increasing interest for research (Jones 2014).

Over the last twenty years, scientists have been trying to identify the most important aspects of terroir. However, chemical processes that occur in the production of wines make it difficult to discern if differences in the taste and aromas of these wines are related to the vineyard. Nonetheless, there are several factors that have an indirect impact on wines, such as climate, topography, grape type, vinification (converting grape juice to wine by fermentation), and soil (Jones 2014). Arguably one of the most important factors contributing to terroir is the soil and clay mineralogy, soil composition and permeability and porosity, and related aspects such as geology of the bedrock (Fraga 2014; Burns & Retallack 2015).

Many agricultural and viticulture practices assess the nutrient availability in only the top 40 cm of soil where approximately 60% of grape plant roots are found (Smart et al. 2006). This is the case for two main reasons. First, sampling closer to the soil surface increases the chances of detecting soil changes because mineral breakdown and dissolution are most intense in surface soils, thus releasing the majority of nutrients utilized by plant roots (Staben et al. 2003). Second, nutrients applied to the soil, via fertilizers, will be more concentrated at the surface (Anderson et al. 2010). Although most of the nutrients are contained in the first few cm of soil, deep root activity plays an important role in supplying water to grape plants (Smart et al. 2006). Because grape-vine roots can access nutrients in the soil down to approximately 6 m, it is important to compare nutrient availability at different depths (Staben et al. 2003; Smart et al. 2006).

1.2 Background

1.2.1 Geological History of Pelee Island

Numerous studies, including those conducted by Vestin et al. (2006), Vestin et al. (2013), and Myrvang et al. (2016), have suggested that bedrock geology plays an important role in determining the composition and geochemistry of overlying soils. These studies found that there was a distinct geochemical signature from the underlying carbonate bedrock throughout the overlying soil horizons in Norway. In addition, a report on Pelee Island

written by John Slack (2015) suggested that sulfur-rich ground waters traveling through porous limestones of bordering sedimentary basins potentially mobilize trace metals that contribute to soil geochemistry on Pelee Island. Therefore, in order to explore soil formation and geochemistry of soils on Pelee Island, it is important to understand the geology of Southwestern Ontario.

Ontario is underlain by Precambrian rock of the Canadian Shield (Thurston 1991). The Canadian Shield is divided into three geological provinces from oldest in the northwest to youngest in the southeast: the Superior Province, composed of a variety of metamorphic rock types ranging from subgreenschist to granulite facies (Percival et al. 2012); the Grenville Province, composed of mainly of high-grade metamorphic gneisses (Slagstad et al. 2004); and the Southern Province, composed of metasedimentary and metavolcanic rocks of the Huronian Supergroup (Raharimahefa et al. 2014). Southern Ontario is underlain by the Grenville and Southern Province (Earle 2019). The Canadian Shield is made up of remnants of mountains that were created from continental collisions that occurred during the Precambrian Eon. The end of these mountain-building events is marked by the Grenville Orogeny, which occurred between 1141 – 1152 Ma (Mezger et al. 1993). During the Grenville Orogeny, five northeast trending ridges were created (Gao 2011). Pelee Island is located on the western flank of one of these ridges called the Finlay Algonquin Ridge and lies within the Grenville Front Tectonic Zone (GFTZ) (Eyles 1997). Although there is no evidence that the Proterozoic basement bedrock of the Grenville Front Finlay-Algonquin Arch was the source of Pelee Island sediment, the topography of the arch had an important role in deposition patterns of overlying sediment deposition on Pelee Island. Differences in topography within the Canadian Shield ensured that the area that is now Pelee Island, would become a marine shelf (Earle 2019).

During the Paleozoic Era, shallow marine seas covered lowlands surrounding the mountains of the Grenville Orogeny. Ancient sea conditions were well suited to reef growth and resulted in an accumulation of limestone deposits (Earle 2019). Some deposits were altered to dolostone during contact with magnesium-rich water upon burial and these limestone and dolostone deposits can be seen outcropping in various places on Pelee Island (Morris 1994). Limestone outcrops on Pelee Island are part of the Dundee

Formation, which extends west of Port Stanley to east of Port Dover on Lake Erie, northwest to Lake Huron where it crops out from southwest of Grand Bend to north of Goderich, and crops out in Essex County (Hewitt 1972). The limestone unit has a thickness of 18-50 m (Hewitt 1972). It consists of brown, cherty crinoidal limestone but the weathered surface appears as massive, brown bioclastic limestone in outcrop locations on the Island (Morris 1994). It is underlain by the older Detroit River Group and overlain by the younger Hamilton Group (Hewitt 1972). The Detroit River Group consists of limestone and dolostone, whereas the Hamilton Formation consists of grey shales with interbeds of crystalline cherty limestone (Hewitt 1972). These Middle Devonian aged groups form northwest trending bands and have southwest dipping strata (Hewitt 1972). The relative locations of these units are displayed in Figure 1.2.

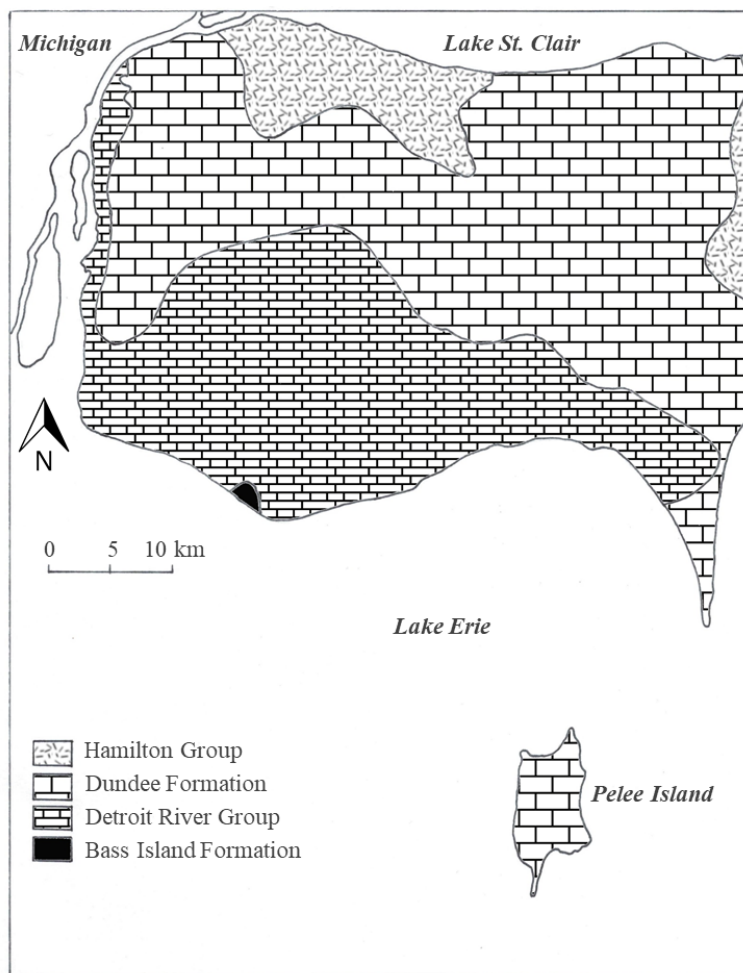


Figure 1.2. Paleozoic geology of Essex County, specifically illustrating location of the Dundee Formation (modified from Morris 1994).

1.2.2 Glacial History of Pelee Island

During the Late Wisconsinan substage (approximately 23 000 years BP), Southern Ontario was covered by large ice sheets including the Laurentide Ice Sheet that advanced and carved out the bedrock directly beneath it (Morris 2008). The Great Lakes system, including the Lake Erie basin, is one of the features produced from the advancement of the ice sheet and glacial erosion. Differences in bedrock composition controlled the extent of glacial erosion in that the softer, less resistant shale was preferentially removed while harder, more resistant limestone remained, thereby creating a group of islands within Lake Erie (Morris 2008). These islands are called the Archipelagic Islands and Pelee Island is included within this group (Figure 1.1). Glacial erosion also produced changes in bedrock topography. Limestone pinnacles at the northwest and southwest edges of Pelee island allowed the glacier to carve out soft sediment in the middle of the island, creating a bowl-shaped bedrock topography; higher near the edges and deeper in the middle (Chapman & Putnam 1951).

As the Laurentide Ice Sheet advanced and carved out the bedrock beneath it, glacial tills were deposited (Meyer & Eyles 2007). The overburden material (till) in the region was formed as a result of several successive major glaciation events during the Late Wisconsin Glaciation that occurred in the northern hemisphere (Fulton and Prest, 1987). The drift thickness (thickness of material deposited by glaciers) on Pelee Island varies between 0 to 29 m, with about 75% of the island covered by drift that is 3 m deep. The till extends down to 15 m and 29 m below the surface in the western and northwestern sides of the island, respectively (Chapman and Putnam, 1984).

During the Port Bruce stadial (15 000 – 14 000 BP) a southward ice advance over the Lake Huron basin occurred and the Huron ice lobe deposited the Tavistock till (Figure 1.3) (Morris 1994; Morris & Kelly 1996; Morris 2008). Tavistock till is in the silt to clay range and has a low stone content (<5-10%), although in moraines it can be sandy and stony with a carbonate content of around 20% (Karrow 1968; Cowan 1976; Sado 1980). In addition, the Tavistock till contains sedimentary clasts that were sourced from the Huronian Supergroup (Morris & Kelly 1996).

A later westward flow of the Erie lobe through the Lake Erie basin deposited the Port Stanley till along the north shore of Lake Erie in Kent County and on the northeastern shore of Point Pelee (Morris & Kelly 1996). This till was derived from material from the Grenville Province (Morris & Kelly 1996). During the late stages of the Port Bruce Stade (15 000 – 14 000 BP), ice flow from the Lake Huron basin slowed (Huron lobe) and ice flow from the Lake Erie basin increased (Erie lobe), resulting in a westward ice shift in the Lake Erie basin (Morris 1994; Morris 2008). The shift in flow direction, from south to southwest, caused mixing of sediment derived from the Lake Huron basin ice, with materials carried by ice from the Lake Erie basin. This formed the Port Stanley – Tavistock hybrid till found on Pelee Island (Figure 1.3) (Morris 1994).

The Port Stanley – Tavistock till on Pelee Island is a fine-grained and almost stone-free till with large quantities of glaciolacustrine silt and clay (de Vries and Dreimanis 1960; Karrow 1984). The grain size of the Port Stanley – Tavistock till is in the silt to clay range and on Pelee Island this till underlies glaciolacustrine silty clay. Cowan (1976) considered this till to be formed at the same time as the Tavistock till. The carbonate content in the Port Stanley – Tavistock till is lower than in the Tavistock till (only 3% carbonate), but this likely reflects surface weathering and leaching of carbonate because the till was sampled near surface (Morris 1994). In addition, Richards et al. (1949) suggested that the tills deposited on Pelee Island contained limestone fragments that were glacially derived from the limestone bedrock.

During the Mackinaw Interstade (14 000 -13 000 BP), the glaciers began to melt and retreat, causing the Laurentide ice sheet to break into lobes (Morris, 1994; Morris 2008). These lobes retreated and advanced interchangeably in an approximate east-west direction, creating a north-south trending end moraine east of Pelee Island called the Pelee-Lorraine Ridge (Figure 1.3) (Morris, 1994; Holcombe 1997; Morris 2008). This ridge is also correlated with the formation of a proglacial lake (Lake Maumee), likely responsible for the deposition of glaciolacustrine deposits and lacustrine sediment on Pelee Island (Morris 2008; NOAA n.d.) In addition, a series of coarse-grained glaciolacustrine materials and recessional moraines were deposited by the Huron lobe as it retreated north and are capped by fine-grained glaciolacustrine deposits in the

Leamington area, on the north shore of Lake Erie (Morris & Kelly 1996). These moraines have a significant impact on Quaternary history of the area because they controlled the flow of meltwater, thereby forming many glacial lakes and depositing glaciolacustrine sediment in the Essex County region (Morris 1994). As a result, the overburden stratigraphy in the Essex region consists of tills, lacustrine sediments, fine-grained glaciolacustrine silt and clay, and coarse-grained glaciolacustrine sand. These deposits laid down by glacial streams and lakes have strongly influenced soil development on Pelee Island (Thompson 2000; Strynarka et al., 2004).

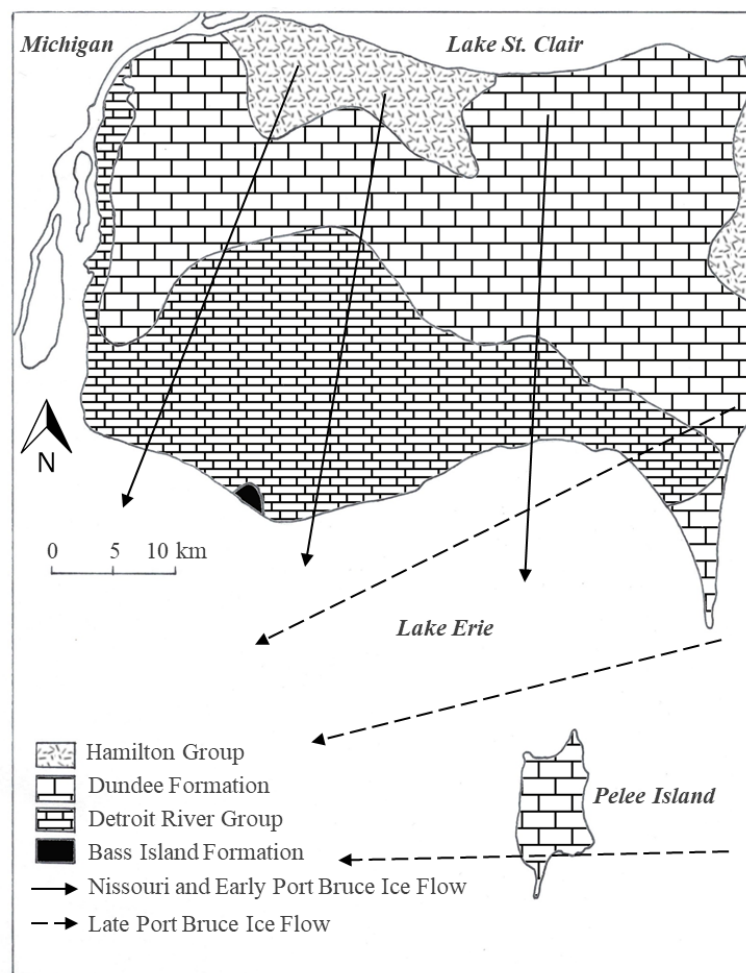


Figure 1.3. Arrows indicate ice flow directions over the Essex County region during the Port Bruce Stadials (modified from Morris 1994).

1.3 Soil Formation Processes

1.3.1 Weathering

Weathering is a process that breaks apart rocks and minerals to form soils. There are three types of weathering: physical, chemical, and biological. Physical weathering breaks material down into smaller pieces but does not alter the chemical composition.

Breakdown of minerals by changes in temperature and erosion by wind, water, and ice are examples of physical weathering. Chemical weathering changes the composition of the original material during complex chemical reactions. Examples of some chemical reactions that occur during chemical weathering are hydrolysis (reaction with water), dissolution (reaction with acid) and oxidation-reduction reactions. Biological weathering is the breakdown of materials by plants, animals, and microbes. All three of these weathering processes are interdependent and work together to break down material (Weil & Brady 2017).

Over time, weathering of minerals and degradation of organic material creates soil horizons. There are four main horizons from top to bottom: O, A, B, and C (Berner & Berner 2012). The O horizon is formed from an accumulation of partially decomposed organic material and is usually only about 5 cm thick. It is dark brown to black and is slightly more acidic than other soil horizons (Weil and Brady 2017). The A horizon, sometimes referred to as topsoil, is directly below the O horizon and is composed mostly of mineral particles, but is dark brown to black due to the leaching of organic matter from the layer above (Berner & Berner 2012). The A horizon is usually 10-25 cm thick and the majority of plants roots are found in this horizon. The B horizon, sometimes referred to as subsoil, is lighter in colour than the A horizon because it contains much less organic matter and has various amounts of accumulated materials that have been leached from the horizons above or have been precipitated in place (Weil and Brady 2017). Thus, the B horizon is a zone of accumulation, especially for silicate clay minerals (illite, kaolinite, chlorite, vermiculite), iron and aluminum oxides, and/or calcium carbonate.

Carbonic acid and other acids formed from the decay of organic matter near the surface are carried by percolating waters through the soil where they stimulate weathering

reactions. Acid-charged waters dissolve minerals and leach soluble products from upper horizons to lower horizons where pH is higher, and they can precipitate and/or adsorb to mineral surfaces. Dissolved substances include positively charged cations (e.g., Ca^{2+}) and negatively charged anions (e.g., CO_3^{2-} and SO_4^{2-}). These processes create a zone of depletion in upper layers and a zone of accumulation in lower layers. The C horizon is the deepest and therefore the least weathered part of the soil horizon (Berner & Berner 2012). This horizon is often made of material from the biochemical weathering of the regolith. Together, the A, B, and C horizons make the soil profile (Weil & Brady 2017). It should be noted that this description of soil horizons has been generalized and there is much variability within each of the horizons. Horizon formation and variability is dependent on parent material, climate, geomorphology, and time (Weil & Brady 2017). Pelee Island soils were formed from calcareous glacial till producing soils that have high carbonate content (National Cooperative Soil Survey 2012; National Cooperative Soil Survey 2014). The temperate humid climate of Pelee Island favours the accumulation of organic matter in the A horizon, ultimately affecting distributions and accumulation of elements in the B horizon (Weil and Brady 2017).

Soil horizon and profile development are dependent on many factors such as climate (temperature and precipitation), topography, vegetation, time, and parent material. Under favourable conditions (i.e. warm, humid, high relief topography that promotes drainage), organic matter accumulation and formation of the A horizon can occur in 10-20 years and structural alteration and colouring by accumulation of iron in the B horizon can develop within a few hundred years. However, under less favourable conditions (i.e. dry, cold, flat), the formation of silicate clay minerals and of blocky structure in the B horizon can take a few thousand years (Weil & Brady 2017). Soil formation on Pelee Island is favourable because of its warm humid summers followed by cold winters and equable distribution of precipitation throughout the year (Shaw 2001). Total precipitation ranges from 880 mm – 902 mm and two-thirds of it is received throughout the 7-month growing season (Shaw 2001). In addition, vineyard managers have been adding locally grown compost to island soils, which has increased soil organic matter content and enhances soil development.

1.3.2 Parent Material – Effect on Soil Formation

The parent material of the soil determines the nutrient supply of elements that are released by weathering (Anderson 1988). Weathering of parent material affects soil texture and composition, which in turn affects soil properties such as water and nutrient retention, chemical weathering and soil acidity (Weil & Brady 2017). For example, soils forming from soft rock or unconsolidated material, such as limestone or glacial till will produce fine grained clayey soils, such as those seen on Pelee Island. Soils with high clay content hold moisture more effectively than sandier soils and prevent nutrient leaching (Jenny 1941). In addition, calcareous soils, such as those on Pelee Island are easily weathered by the process of dissolution, which increases the pH of the soil.

1.3.3 Using REE to Trace Parent Materials in Soils

Rare Earth Elements (REE) have been used in numerous studies to trace the origin of soil parent materials and track pedogenic processes (Laveuf & Cornu 2009) because REE have low mobility and solubility in the soil profile due to their 3+ valence state (Laveuf & Cornu 2009). The REE are a group of 17 elements with similar chemical and physical properties and include the elements Ce, Dy, Er, Eu, Gd, Ho, La, Lu, Nd, Pr, Pm, Sm, Sc, Tb, Tm, Yb, Y (Hu et al. 2006). Although REE concentrations can be different between parent material and soil, the processes of soil formation rarely influence relative abundance, or distribution, of REE in soil horizons. This means that absolute concentrations of REE may be different between parent material and soil and even within soil horizons, however: REE distribution patterns (concentrations of REE relative to each other) should be the same between parent material and soil (Bryanin & Sorokina 2014).

1.3.4 Soil Drainage on Pelee Island and Implications for Pedogenetic Processes

Because of the saucer-shaped and low topography of Pelee Island, the center of the island was once mostly submerged. The Pelee Island soils in the center of the island were waterlogged until drainage systems were implemented in the 1890s and the island was drained by a series of dykes and pumping schemes (Taylor et al. 1961). Thus, soils on Pelee Island are young, around 100-200 years, and only started to develop a soil profile

following drainage of the island in the 1890s. Prior to drainage, when the island was a low-lying wetland, aeration and drainage were restricted and created anaerobic conditions. The weathering of minerals and decomposition of organic matter were therefore slowed (Leyton & Yadav 1960). Artificial drainage systems implemented on the island produced arable land, which led to greater productivity and growth because of improved oxygen supply and enhanced rooting depth (Leyton & Yadav 1960).

Although the island has a relief of 175-182 m above sea level, it is only 10 m above Lake Erie's mean water level at its apex. This means that the water table on the island is high, probably ranging between 1-10 m, which is typical of soils in humid regions (Chapman and Putnam 1984). In areas with shallow groundwater, water removed from soil by plants can be replaced by upward capillary movement from a shallow water table. The zone of wetting by capillary movement is known as capillary fringe. The capillary rise can supply plants with water during periods of low rainfall and it can also bring a steady supply of dissolved ions to the surface (Weil & Brady 2017). Lateral movement of groundwater can also transport elements through porous bedrock (aquifers) until they eventually precipitate out of solution (Weil & Brady 2017).

A theory proposed by Slack (2015) suggested that groundwater carrying dissolved metals (specifically Pb and Zn) from bordering carbonate-rich sedimentary basins (e.g. Michigan Basin) could be contributing to the metal content of Pelee Island soils (Slack 2015). Lead and Zn are dissolved in hot fluids and transported via salty groundwater. Groundwater containing Cl^- can form aqueous complexes with metals. When these fluids are diluted with fresh water and/or encounter H_2S produced by sulfide reducing bacteria in organic rich rocks or sediment, the metals can be deposited within the cavities of carbonate rocks (Fowler 1993). Therefore, Slack (2015) predicted that soils on Pelee Island would have increased amounts of Zn and Pb, and perhaps other anomalous element signatures.

1.3.5 Pelee Island Soils

Brookston and Toledo are the two most abundant soil types on Pelee Island. Figure 1.4 illustrates spatial distributions of these two soil types. Both were glacially derived and are classified as gleysols (Sposito et al. 2008). Gleysolic soils occur in poorly drained areas

surrounding Lake Erie and are developed on flat, calcareous tills, lacustrine deposits, and slowly permeable clay plains. Both soil types are naturally poorly drained and may be water-saturated within 50 cm of surface for long periods of time (Sposito et al. 2008). However, since the implementation of artificial drainage on Pelee Island, these soils can successfully support agriculture. In addition, both of these soil types are clay rich in clay minerals such as: illite, kaolinite, and chlorite (Tolo 2019).

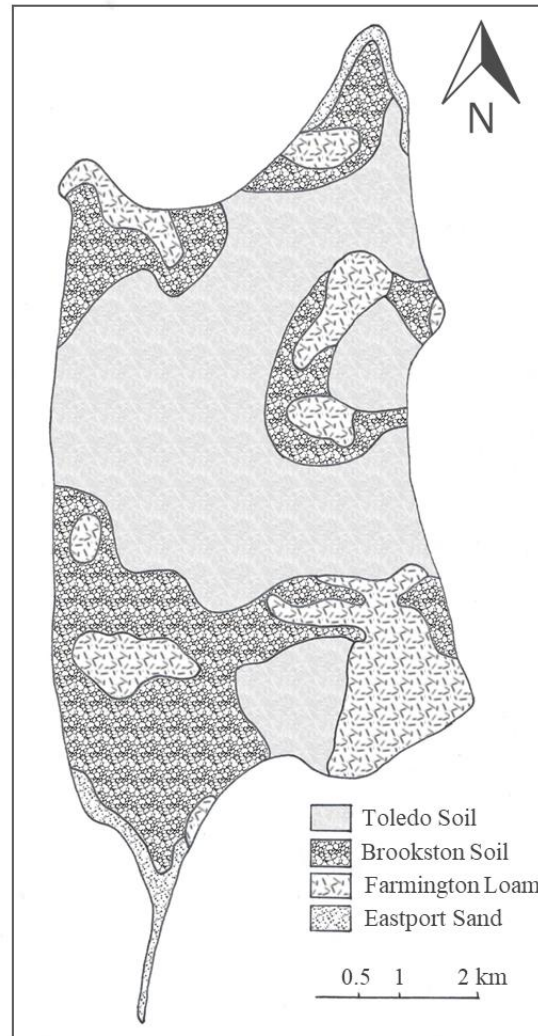


Figure 1.4. Locations of Brookston and Toledo soils on Pelee Island (modified from Essex Region Conservation Authority Interactive Mapping 2011).

Toledo clay is the most abundant soil type on the island followed by Brookston clay. Toledo clay is most abundant at the center of the island where the bedrock surface is deep. The Toledo soil was formed in clayey glaciolacustrine sediment (Government of

Canada 2013a). The A horizon of Toledo clay is typically 0-30 cm thick, is composed of dark grey clay and silt, and is stone free. The B horizon is approximately 30-80 cm thick, is composed of dark brown clay, has high Fe and Mn oxide content throughout, and contains pebbles of black shale and granite. The C horizon is 80+ cm, contains gritty sand, shale, and granite pebbles and is strongly calcareous (Chapman and Putman 1951).

Brookston clay is more abundant along the edges of the island where bedrock surface is shallow. Brookston soils were formed from moraine material (till) and are composed of a mixture of boulders, sand, silt, and/or clay (Government of Canada, 2013b). The A horizon is approximately 15 cm thick, is composed of clay, and is mostly stone free. The B horizon is 75 cm thick and is composed of clay. The C horizon is 90 cm thick and is composed of clayey till and is highly calcareous (Richards et al. 1949).

Bruno Friesen, the Pelee Island vineyard manager, noted that vines on different regions of the island had different productivity and growth rates and also noted that areas of the island where soils were shallower had less grape production and growth compared to plants in deeper soils towards the middle of the island. Slack (2015) suggested that this observation may be a function of grape rooting depth. Shaw (2001) suggested that because precipitation is at a minimum throughout the months of July and August, vines that grow on shallow soils on the island are more likely to experience stress during this time compared to deep and well drained soils, which provide vines with steady moisture throughout the Pelee Island growing season. Shaw's reasoning suggests that differences in grape productivity on the island could result from different soil types. Toledo soils are typically deeper and have higher clay content and therefore, have a higher water-holding capacity compared to Brookston soils. Brookston soils are shallower and have larger grain sizes, and thus have a lesser ability to retain moisture compared to Toledo soil. There is a tendency for vines growing in deep Toledo soils to be more productive than vines growing in shallow Brookston soils.

1.3.6 Plant Nutrition – Macro and Micronutrients and Trace Elements

There are several essential elements for plant nutrition and growth, and they can be divided into two categories: macronutrients and micronutrients. Essential macronutrients include Ca, N, K, Mg, C, H, O, P, and S. These macronutrients are >0.1% of dried plant tissue. Carbon, hydrogen, and oxygen are taken up by the plants from air and water and the remainder of the macronutrients are taken up by the plant through the soils. The macronutrients can then be further divided into primary and secondary nutrients. The primary, and most important nutrients are N, P, and K. The N content of Pelee Island soils was assessed in a separate study. Jiang (2018) found elevated levels of $\delta^{15}\text{N}$ in Pelee Island surface soils that could result from either the application of N-rich fertilizers and/or faster N-cycling. This indicates that the N cycle is more open in surface soils; thus, N is more available to plants in surface soils compared to deep soils on Pelee Island.

Secondary plant nutrients include Ca, Mg, and S. Essential micronutrients making up <0.1% of dried plant tissue include Cu, Fe, Mn, Ni, Zn, B, Cl, and Mo. These nutrients are termed essential because they play important roles in plant growth and reproduction. These elements enhance root growth and development, form amino acids and proteins, and activate enzymes that are responsible for energy metabolism such as photosynthesis (Weil & Brady 2017). Deficiencies in essential elements can inhibit plant growth, which causes browning or yellowing of leaves, and inhibits or decreases fruit production.

A trace element is defined as an element that is present in a rock in concentrations of <0.1% and they commonly substitute for elements in rock-forming minerals (Rollinson 1993). Incompatible elements and REE are subgroups within the trace element group. Incompatible elements are incompatible in most mineral structures and are among the first to weather out of minerals (Rollinson 1993). Examples include the elements Rb, Ba, U, and La. Trace and REE are taken up by plants in small concentrations of <100 ppm, but there are no conclusive studies stating that these elements are essential for plant growth and reproduction (Alloway 2010). However, studies show that soils with high concentrations of trace and REE (>1000 ppm) can produce plants with high and sometimes toxic concentrations of these elements (Wuana & Okieimen 2011). In

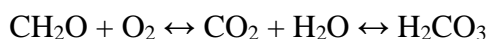
addition, some consumers suggest that minerals from the vineyard soils can be tasted in the wine. The sensation of tasting minerals in wine is referred to as “minerality”. However, there have been no conclusive studies to verify the taste of “minerality” in wines (Howell & Swinchatt 2000; Parr et al. 2018).

1.3.7 Reactions in Soil Horizons and soil pH, HCO_3^- Content, and Organic Matter

Nutrients are released into the soils originally by mineral weathering; however, the bioavailability of these nutrients is dependent on many factors. Bioavailability is a term used to describe nutrients that are available to the plant, and these nutrients are termed plant extractable nutrients (PEN) (Alloway 2013). The PEN are either bound to soil particle surfaces or organic matter where they are available for exchange with other ions or are present in soil solution (Alloway 2013). The PEN are strongly affected by soil characteristics such as pH, organic matter content and clay mineral content (which control cation exchange capacity; CEC), and fertilizer application (Semple et al. 2003).

Soil organic matter is approximately 50% carbon and is made from the decay of organic substances – often plant material. Plant tissue is decomposed to organic matter by microbes in the soil. The stable organic matter that is resistant to further degradation is called humus and accounts for approximately 5% of soils (Weil & Brady 2017). The role of organic matter is very important within the soil profile. It improves the ability of a soil to hold nutrients, decreases pH, and increases the soil’s water holding capacity. Organic matter particles have both positive and negative surface charges enabling them to hold both cations and anions in surface soils and thus providing important nutrients to the soil available for plant root uptake (Weil & Brady 2017). Humus particles, also referred to as soil colloids, have many H^+ binding sites in acidic soils, but can also release H^+ ions from their binding sites in basic soils, therefore acting as an important pH buffer for soil solution. Although organic matter works as a buffer, in the long-term, microbial decomposition of organic matter produces organic acids that decrease soil pH and enhance dissolution weathering reactions (Weil & Brady 2017).

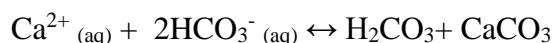
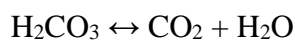
Soil pH is one of the most important factors controlling nutrient availability in soils and the optimal pH range for plant growth is 5.5-7 (Weil & Brady 2017). Soils are often more acidic near the surface because of accumulation and degradation of organic matter. The H^+ ions can be lost from organic matter, which decreases the pH of soil. This also creates a negative charge on the humic molecules, which can bind with positive cations (Berner & Berner 2012). In addition, decayed organic matter (humus) in the O horizon reacts with oxygen from the atmosphere and rainwater to produce carbonic acid, from the reaction:



Carbonic and organic acids produced in the O horizon percolate into the A horizon, where dissolution reactions occur. Dissolution is the reaction of acid with minerals to produce ions in solution (including cations and bicarbonates), and secondary silicate clay minerals (i.e. clays) (Berner & Berner 2012). Soil in the A horizon is close to the surface and reacts with the atmosphere and rainwater through oxidation and hydrolysis reactions. Oxidation is important for the decomposition of ferromagnesium minerals and hydrolysis releases cations from mineral structures (Berner & Berner 2012). All of these reactions cause ions to be leached from the A horizon, thus termed the zone of leaching (Weil & Brady 2017). Specifically, Ca, Fe, and Mg are leached from this horizon because they are part of silicate structures that are easily weathered and so are susceptible to dissolution from organic acids (Berner & Berner 2012).

Ions and clay particles leached from the A horizon will accumulate in the B horizon. This is the zone of accumulation and precipitation of new minerals occurs in this horizon. Iron and Mn will precipitate out of solution to produce Fe and Mn oxides and hydroxides, which gives the B horizon its characteristic reddish hue. In addition, an increase in pH results in the adsorption of ions onto mineral phases in the B horizon such as clay minerals, oxides and hydroxides. Minerals will precipitate out of soil solution in the B horizon because pH is high (Weil & Brady 2017). The pH is higher in the B horizon because the dissolution of calcite (see reaction below) utilizes H^+ ions to produce Ca^{2+} and bicarbonate. Reduced carbon dioxide in deep soils causes the breakdown of carbonic acid to produce carbon dioxide and water. Further, this causes a decrease in carbonic acid

so that cations (such as Ca^{2+}) and bicarbonate ions that were leached from the A horizon combine to produce carbonic acid and calcite (calcium carbonate). These reactions occur because the soil system must always maintain a state of equilibrium and reactions will shift to achieve equilibrium and reduce changes within the soil profile (Berner & Berner 2012). This happens via the following reactions:



Availability of nutrients for plants is dependent on the cation exchange capacity (CEC) of the soil. The CEC is a measure of the number of cations that can be retained on negatively charged surfaces in the soil and determines the ability of a soil to exchange positive cations with the soil solution (Weil & Brady 2017). Particles that are small, such as clay minerals and soil colloids, have larger surface area and will have a greater CEC compared to particles that are larger and have less surface area, such as sand. Materials with larger surface areas can bind more cations because they have a greater number of negatively charged sites. In addition, clay mineral surfaces have a negative charge as a result of their layered structure. They are arranged in sheets of negatively charged oxygen and hydroxyl groups with an interlayer of positively charged cations. Cations of similar charge and radius can replace cations in the interlayers of clay minerals. If the replacement cation has a lesser charge than the original cation, the clay mineral will carry an extra negative charge and higher negatively charged clay minerals have greater exchange rates. This negative charge attracts positively charged cations in the soil solution that can loosely bind to the negative clay surface to equalize the charge. These cations are loosely bound to clay mineral surfaces and are not part of the clay mineral structure and therefore, they can then be exchanged for other cations in the soil solution (Weil & Brady 2017).

1.3.8 Distribution of Elements in the Soil Profile

Distributions of elements in the soil profile are affected by soil processes such as weathering, leaching, accumulation, precipitation, and adsorption. Upon breakdown of

organic matter, acids are released into the soil, which lowers the pH and breaks down easily weathered minerals in surface soils, such as calcite (Berner & Berner 2012). Concentrations of elements found in easily weathered minerals, such as Ca, are readily released from surface soils and form ions (Ca^{2+}) in solution that are leached into deep soils. Thus, the process of mineral weathering creates a soil profile in which concentrations of Ca are low in surface soils and high in deep soils (Weil & Brady 2017). Conversely, elements such as Al and Si, that are in minerals that are more resistant to weathering (quartz and feldspars) become more concentrated in surface soils because they remain in residual minerals formed in upper horizons during mineral weathering (Weil & Brady 2017).

The B horizon is where ions that have been released in the A horizon will accumulate. Elements leached from the A horizon that accumulate in the B horizon commonly include Ca, Fe, and Mn. The pH is higher in the B horizon, thereby causing Ca^{+2} to precipitate as calcite. In addition, elements with similar ionic radii to Ca, such as Mg and Sr, can substitute for Ca in the mineral structure and are therefore, more abundant in deep soils (Thorpe et al. 2012; Xiaolei et al. 2012). Iron and Mn leached from the A horizon also accumulate in the B horizon and form Fe and Mn oxides and hydroxides. Fine clay particles formed in the A horizon can also be transported to the B horizon through the process of eluviation (Stonehouse & Arnaud 1971). Many metals have a high charge to size ratio and will adsorb to negatively charged clay mineral surfaces and also to Fe and Mn oxides and hydroxides in the B horizon (Uddin 2016; Ugwu & Igbokwe 2019). In addition, Mo has a notably higher charge (+6) relative to other metals and is mostly present in soils as the oxyanion MoO_4^{2-} . It is least available in acidic soils, most available in soils with pH above 6.5, and is most strongly adsorbed by Fe hydroxides. Thus, Mo is leached more easily from surface soils compared to other metal elements, leading to higher abundances in deep soils (Alloway 2010).

Adsorption of plant extractable nutrients is highest in surface soils because weathering is most intense and organic matter accumulation high. This is because organic matter has a higher CEC compared to clay minerals with a measured CEC ranging from 150-500 cmol_c/kg compared to clay minerals ranging from 2-170 cmol_c/kg (both measured at pH

of 7) (Weil & Brady 2017). Thus, ions released by weathering are adsorbed to organic matter particles in surface soils. Plant extractable metals tend to accumulate in surface soils because soil organic matter has many negatively charged surfaces on which positively charged metal ions can adsorb. However, there are some exceptions; Mo and U are more available in deeper soils. Both Mo and U have relatively higher charges (+6) compared to other metals and thus are strongly sorbed by Fe hydroxides and oxides, respectively in the B horizon (Alloway 2010). Plants can also cause enrichment of some extractable elements in surface soils. When plant litter starts to decompose at the soil's surface it releases elements into solution, which are taken up by negatively charged surfaces of organic matter particles (Aide 1999).

In agricultural soils, fertilizers also affect the distribution of elements throughout the soil profile. Fertilizers are added to surface soils and can increase concentrations of elements in surface soils. The main components of fertilizers are P, K, N, but they also contain small amounts of trace elements, which can add to the elemental content of surface soils (Otero et al. 2005; Laveuf & Cornu 2009; Zhang et al. 2019). Anthropogenic influences can also increase amounts of elements in the soil profile. Elements such as Pb and Cd can have higher concentrations in surface soils as a result of airborne pollution (e.g. from automotive gasoline) and soil additives (Sheppard et al. 2009).

Element distribution in the soil profile depends on many factors such as parent material, climate, and anthropogenic influences, and is affected by soil processes such as weathering, leaching, accumulation, precipitation, and adsorption. These factors and processes are crucial to understand and assess soils on Pelee Island.

1.4 Purpose and Objectives

Wine terroir is in part influenced by soil composition and the nutrients that are available to the plants (Slack 2015). The first objective of this study is to determine whether the chemistry of the bedrock affects the soil composition on Pelee Island. The second objective is to determine how mineralogy and soil chemistry on Pelee Island vary between the Brookston and Toledo soils, which are both used for vineyards. The final objective is to assess if soil depth, type, or agricultural treatment affect the availability of

nutrients in the soils on Pelee Island. The results of this study will provide Pelee Island winery with an understanding of the variability in soil chemistry among the vineyard fields, which may allow them to tailor their soil management strategies to improve grape quality. In addition, identifying unique soil characteristics may enable the Pelee Island Winery to apply to be re-instated as its own appellation, thereby increasing the marketability of their wine. This study will determine the main controls on soil geochemistry in calcareous vineyard soils throughout the top 2 m of the soil profile. This approach could be applied to other vineyards and other crop types to develop or further enhance crop management practices.

Chapter 2

2 Methodology

This chapter outlines the following: sample locations and collection methods, sample descriptions and preparation, methods used for soil sample analysis, and methods used to determine soil depth on Pelee Island.

2.1 Location and Climate of Pelee Island

Pelee Island is located approximately 20 km off the north shore of Lake Erie at 41.7745°N/82.6591°W. Pelee Island has warm summers, cold winters, and evenly distributed precipitation throughout the year (Shaw 2001). Throughout the growing season, which generally starts late May and ends mid-October, average temperatures range from 18°C during the day to 8.6°C at night, with an average rainfall of 81.1 mm (Weather Atlas 2020). Growing season ends when autumn frost commences, with earliest reports of frost on October 5 and latest on December 2 (Shaw 2001). Table 2.1 summarizes average monthly temperatures and precipitation on the island from 2002 – 2019.

Table 1.1. Reported average monthly daily high and overnight low temperatures and precipitation on Pelee Island from 2002-2019 (Weather Atlas 2020).

Month	Temp. High	Temp. Low	Rainfall (mm)
Jan	-2	-8.1	24.2
Feb	-0.3	-7	23
Mar	5.1	-1.9	58.7
Apr	11.3	3.4	79.9
May	18	9.7	86.4
Jun	24.2	15.5	92.2
Jul	27.5	18.9	78.9
Aug	26.3	18.1	87.4
Sep	22.7	14.2	86
Oct	16.2	8.6	55.5
Nov	8.1	2.5	79.3
Dec	1.8	-3.7	64.5

2.2 Sample Collection

Nineteen soil profiles were sampled throughout the island at the locations illustrated in Figure 2.1. The sites were chosen based on depth to bedrock, soil type (Brookston or

Toledo), and fertilization strategy. Table 2.2 summarizes the soil sampling locations and sampling information of each soil core and Table 2.3 includes weather information during sampling days (Government of Canada 2019).

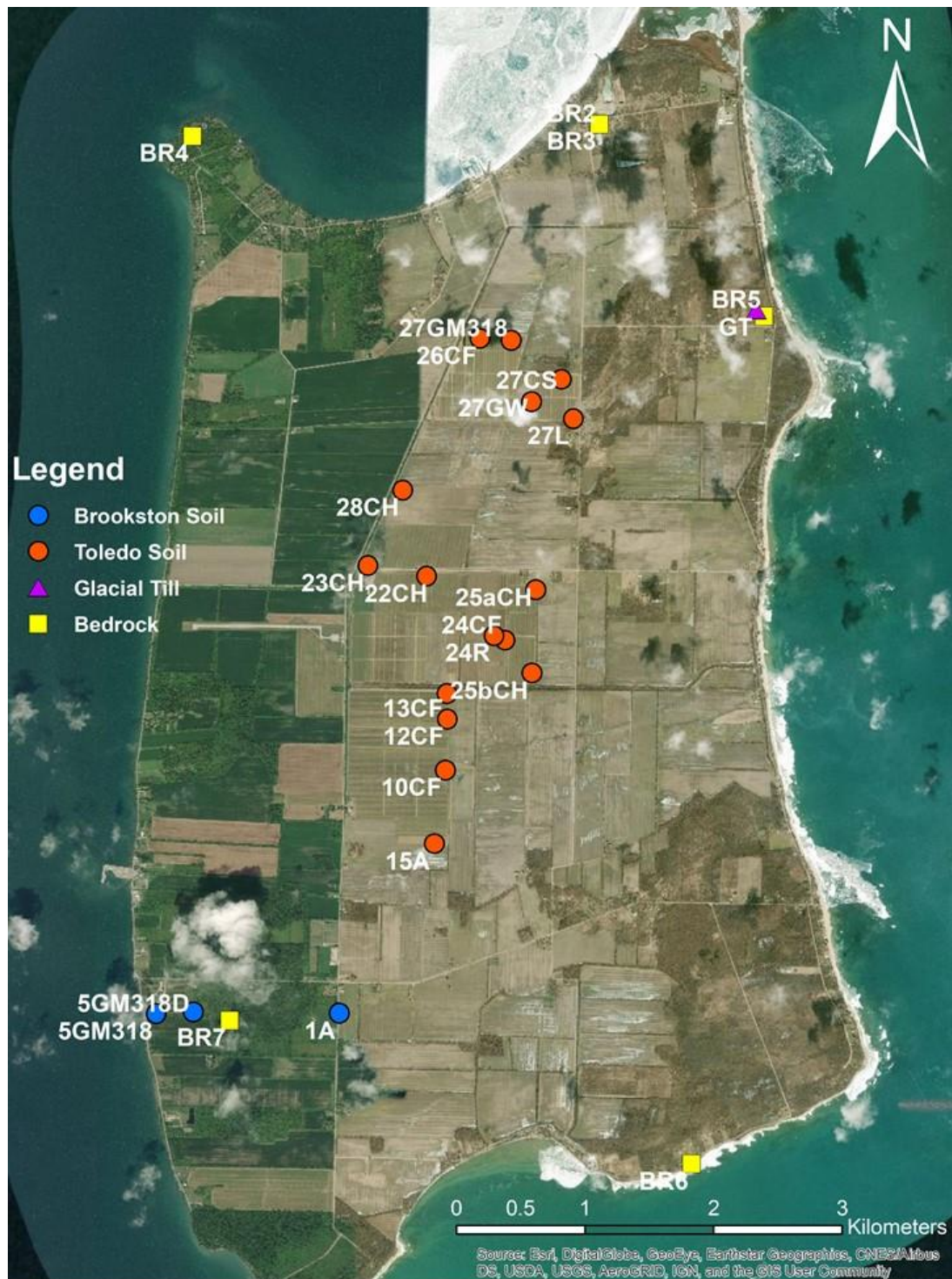


Figure 2.1. Locations of soil samples, bedrock samples, and glacial till samples on Pelee Island.

Table 2.2. Summary table of sampling information for Pelee Island. Table includes field number, grape/plant type, sample identification (soil and grape), GPS locations (decimal degrees), soil type, soil depth to bedrock (m) from seismic survey, and soil coring depth (m) of soil cores extracted and grapes collected. Note that the coring tool only sampled to a depth of 2.44 m, and thus coring depths of <2 m in fields with no seismic data indicate the soil depth at respective locations. EL: elevation above sea level.

Field #	Grape / Plant Type	Soil Sample ID	Date Sampled	Grape Sample ID	Location (decimal degrees)			Soil Type	Bedrock Depth (m)	Coring Depth (m)
					Easting	Northing	EL (m)			
1	Alfalfa	1A	15-Oct-17	-	-82.6696	41.7537	178	Brookston	-	1.52
5	Geisenheim	5GM318	15-Oct-17	-	-82.6867	41.7531	178	Brookston	2	1.45
5	Geisenheim	5GM318D	28-Aug-17	-	-82.6833	41.7536	178	Brookston	-	1.83
10	Cabernet Franc	10CF	17-Oct-17	PI-GRAPE-10CF	-82.6601	41.7708	174	Toledo	18-21	2.39
12	Cabernet Franc	12CF	17-Oct-17	PI-GRAPE-12CF	-82.6600	41.7744	174	Toledo	-	2.36
13	Cabernet Franc	13CF	17-Oct-17	PI-GRAPE-13CF	-82.6601	41.7761	174	Toledo	13-22	2.17
15	Alfalfa	15A	17-Oct-17	-	-82.6610	41.7657	175	Toledo	17-19	2.26
22	Chardonnay	22CH	16-Oct-17	PI-GRAPE-22CH	-82.6622	41.7843	173	Toledo	25	2.36
23	Chardonnay	23CH	28-Aug-17	PI-GRAPE-23CH	-82.6677	41.7850	173	Toledo	20-30	2.08
24	Cabernet Franc	24CF	17-Oct-17	PI-GRAPE-24CF	-82.6547	41.7800	174	Toledo	13-19	2.32
24	Wheat	24R	17-Oct-17	-	-82.6558	41.7803	174	Toledo	-	2.34
25	Chardonnay	25aCH	16-Oct-17	PI-GRAPE-25aCH	-82.6520	41.7836	174	Toledo	-	1.52
25	Chardonnay	25bCH	16-Oct-17	PI-GRAPE-25bCH	-82.6522	41.7777	174	Toledo	-	1.71
26	Cabernet Franc	26CF	17-Oct-17	PI-GRAPE-26CF	-82.6576	41.8010	173	Toledo	18-25	1.57
27	Cabernet Sauvignon	27CS	29-Aug-17	PI-GRAPE-27CS	-82.6499	41.7983	174	Toledo	5	1.40
27	Geisenheim	27GM318	29-Aug-17	PI-GRAPE-27GM318	-82.6547	41.8009	173	Toledo	-	2.24
27	Gewürztraminer	27GW	29-Aug-17	PI-GRAPE-27GW	-82.6527	41.7967	174	Toledo	-	2.10
27	Lavender	27L	29-Aug-17	-	-82.6488	41.7956	176	Toledo	0.6	0.63
28	Chardonnay	28CH	16-Oct-17	PI-GRAPE-28CH	-82.6646	41.7903	173	Toledo	22-27	2.69

Table 2.3. Weather on Pelee Island on sampling days. Data retrieved from Environment Canada: Climate ID: 6134190, Kingsville, 42°02'35.064"N/82°40'26.088"W, 200.0m. Note that on August 28, 26mm of precipitation occurred after sampling (Government of Canada 2019).

Date (2017)	Mean Temperature (°C)	Total Precipitation (mm)
28-Aug	20.5	26
29-Aug	20.5	2
15-Oct	19.5	-
16-Oct	9.8	0
17-Oct	13.3	0

Soil core samples were extracted using a gas-powered core sampling kit along with the REDI Boss Hammer - part # 360.01, both purchased from AMS Inc. The metal sampling rod was assembled and 3.8 x 61 cm PVC plastic tube liners (5006.423) were inserted into the stainless-steel coring tool. The hammer was placed on top of the rod while operators held onto the handles and applied a downward force assisting it into the ground. As the corer was pushed into the ground, soil entered the plastic tube liners. The rod was then removed by a foot pedal or fork-lift, and once fully removed, the PVC tubes were removed from the corer, capped, and put into a cooler. At each location, this process was completed twice, four feet at a time to retrieve one core with a total length of 2.44 m. Once the first 1.22 m of soil core was removed from the ground, another metal sampling rod was attached to the original rod and assembled into a 2.44 m metal rod. The 2.44 m rod was reinserted into the existing hole, and the REDI Boss Hammer was used to push the remainder of the rod into the ground to obtain the remaining 1.22 m of soil core. Figure 2.2a displays all parts of the sampling kit. Figure 2.2b shows how the parts are assembled and Figure 2.2c shows the sampling kit in use. An instructive video on how to use the gas-powered core sampling kit can be found on the AMS website at: <https://www.ams-samplers.com/gas-powered-core-sampling-kit.html>.



Figure 2.2. Images of the soil sampling kit used to extract soil cores on Pelee Island. A) Disassembled components of the sampling kit; B) assembly of the sampling kit; C) operation of the sampling kit. Figures retrieved from the AMS website (AMS 2019).

In addition to soil samples, bedrock, grape, till, and fertilizer samples were also collected. Six bedrock samples were collected from areas on the island where bedrock was exposed. Three till samples were collected from the bottom of a freshly dug well approximately 3 m deep. The locations of these bedrock and till samples are listed in Table 2.4 and are illustrated in Figure 2.1. Approximately 10-30 grapes from the same vine were picked from each of the fields where soil was sampled and frozen upon return to the university. However, because sampling was done following the harvest, grapes were not collected

from every field where soil was sampled because some vines had no grapes. Table 2.2 indicates fields where grapes were sampled. The vineyard manager, Bruno Friesen, supplied nine fertilizer and compost samples that had been applied to the vineyard fields during the 2017 growing season. Table 2.5 indicates types of fertilizers used and their sample identification. UAN is a urea ammonium nitrate fertilizer and AGRIS (Agricultural Innovation and Solutions) is the company that produces fertilizer containing N, P, K, S, Mg, Zn, Fe, Mn, Cu, and B.

Table 2.4. Sample identification and GPS locations of bedrock and till samples. Note that glacial tills were sampled from one location and on Figure 2.1 are labeled as GT.

Sample ID	Location	
	Northing	Easting
PI-18-2	41.8162	-82.6468
PI-18-3	41.8162	-82.6468
PI-18-4	41.8148	-82.6849
PI-18-5	41.803	-82.631
PI-18-6	41.7436	-82.6363
PI-18-7	41.7531	-82.6798
GT1	41.8034	-82.6318
GT2	41.8034	-82.6318
GT3	41.8034	-82.6318

Table 2.5. Types of fertilizers used on Pelee Island and their sample identification. UAN is a urea ammonium nitrate fertilizer, and AGRIS (Agricultural Innovation and Solutions) and Thompsons are fertilizer companies.

Sample ID	Type
FERT1	Liquid Fish
FERT3	Molasses
FERT3	UAN 25% (liquid fertilizer)
FERT4	AGRIS (chemical fertilizer)
FERT5	Thompsons (chemical fertilizer)
FERT6	Compost 2017
FERT7	Old Compost
FERT8	Young Compost
FERT9	Compost

2.3 Sample Description and Preparation

Each soil core was logged by indicating key features such as colour and texture. Soil colour was identified using a Munsell soil colour book. Full descriptions of each soil core

are included in Appendix D. After each core was described, four samples were taken from each, with the exception of 5GM318D and 27L, where three and two samples were taken, respectively. Fewer samples were taken from these cores because core 27L was a short soil core due to proximity to bedrock, and during extraction from a PVC tube, soil was lost from soil core 5GM318D. It is important to note that throughout this paper, unless otherwise specified, sampling depths will be referred to as sections 1, 2, 3, and 4 in each core; one is the shallowest sampling section (soil depth sampling range of 0-46 cm), followed by section 2 (soil depth sampling range of 29-110 cm), section 3 (soil depth sampling range of 73-188 cm), and section 4 (soil depth sampling range of 110-269 cm). True sampling depths for each soil sampled are provided in Appendix H. The samples taken from each core were sampled at different depths and chosen based on soil horizon. Thus, the sampling depth labeling scheme (i.e. section 1, 2, 3 and 4) is used to indicate relative sampling depths among soil cores. The soil horizons were distinguished primarily by colour and texture; A horizons were dark brown with almost no rock fragments, whereas B horizons were often light brown and locally contained rock fragments. At least one sample was taken from each horizon, section 1 soil samples indicate samples taken from the A horizon while sections 2, 3, and 4 indicate samples taken from the B horizon. A total of 73 soil samples were collected from all soil cores. Soil samples were dried in an oven at 105°C for 48 hours. After 48 hours in the oven, 100 g of each dried soil sample was pulverised to a grain size of 90 µm using the vibratory pulveriser - ring and puck mill at Western University. The ring and puck pulverising mill contained a steel grinding bowl (complete with a lid, metal ring and puck) into which soil samples were placed. The motor in the mill vibrated and rotated both the bowl and its contents (soil sample, metal ring and puck), which pulverized the samples. After the samples were pulverized, they were sent to Geoscience Laboratories (Willet Green Miller Ctr Level A4 & A5, 933 Ramsey Lake Rd., Sudbury, ON P3E 6B5) for geochemical analysis. Another 100 g of each dried soil sample was crushed with a porcelain mortar and pestle, sieved to a size of <2 mm, and sent to Activation Laboratories (41 Bittern St., Ancaster, ON L9G 4V5) for plant extractable nutrient analysis. Another 50 g of soil from cores 5GM318 (Brookston soil) and 26CF (Toledo soil) were rehydrated and wet sieved through 106 µm, 90 µm, 53 µm, 20 µm sieves to measure grain size.

Bedrock samples were described (full descriptions are included in Appendix E) and 50 g of each sample were pulverised using the vibratory pulveriser - ring and puck mill at Western University to a grain size of 90 μm and sent to Geoscience Laboratories for geochemical analysis. Till samples were also sent to Geoscience Laboratories for sample preparation (pulverising - SAM-SPG) and geochemical analysis. The frozen grapes were washed by hand with distilled water and phosphate-free soap and frozen grapes were sent to Activation Laboratories for analyses.

2.4 Sample Analysis

2.4.1 Soil Mineralogy, Geochemistry, and Plant Extractable Nutrients

X-ray diffraction (XRD) was used to determine the mineralogy of all bedrock samples and six soil profiles: 22CH, 24CF, 25aCH, 25bCH, 5GM318, and 5GM318D. The six soil profiles were chosen to compare the difference in mineralogy between: deep and shallow soils; Brookston and Toledo soils; and fertilized and unfertilized soils. The XRD analysis was performed using a Rigaku rotating-anode X-ray diffractometer with $\text{CoK}\alpha$ radiation source at Western University in the Laboratory for Stable Isotope Science (LSIS).

Major elements in the soil were analyzed by Geoscience Laboratories using x-ray fluorescence (XRF-M01). First, soil samples went through a three-step loss on ignition program (LOI-3ST) to determine water, organic, and carbonate content within the soils. This three-step process involved heating samples at: 105°C in a nitrogen atmosphere; 500°C in an oxygen atmosphere; and 1000°C in an oxygen atmosphere. This produced a total LOI at 1000°C. The amount of time each sample remained in the oven varied from 30 minutes to 3 hours and was dependent on sample consistency. This means that each sample (1 g or 2 g) remains at each temperature until there is equal or less than 0.03% (± 0.003 g or ± 0.006 g respectively) variation in weight for three consecutive weighings (each about 4 minutes apart). Sample consistency is a more reliable measure than length of time in the oven because consistency indicates that a sample has completed all processes at each specific temperature. After each step, the soil was cooled and

reweighed to determine amount of material lost during the ignition process. The LOI lower limit weight percent is accurate to ± 0.05 percent. Following the LOI program, the soil samples were fused with a borate flux to produce a glass bead for XRF analysis. Each analyte was expressed as its oxide: Al_2O_3 , BaO , CaO , Cr_2O_3 , Fe_2O_3 , K_2O , MgO , MnO , Na_2O , P_2O_5 , SiO_2 , and TiO_2 (Ontario Ministry of Northern Development and Mines 2018). Appendix F includes LOI raw data.

Minor, trace, and rare earth elements were analyzed by Geoscience Laboratories using inductively coupled plasma – mass spectroscopy (ICP-MS) custom analysis (IMX-CUS). Prior to analysis, the soil samples were pretreated with a custom closed multi-vessel acid digest SOL-CUS. This solution was used for complete dissolution of silicates in samples. Unlike regular pre-treatments (SOL-CAIO), and regular ICP-MS (IMC-100), both the pre-treatment and ICP-MS analyses were custom. This is because the soils contained abundant organic matter (high graphite content) and needed to be oxidized prior to digestion to prevent dangerous reactions between the organic component and perchloric acid used in digestions (Ontario Ministry of Northern Development and Mines 2018). The elements analysed by ICP-MS were: Ba, Be, Bi, Cd, Ce, Co, Cr, Cs, Cu, Dy, Er, Eu, Ga, Gd, Hf, Ho, In, La, Li, Lu, Mo, Nb, Nd, Ni, Pb, Pr, Rb, Sb, Sc, Sm, Sn, Sr, Ta, Tb, Th, Ti, Tl, Tm, U, V, W, Y, Yb, Zn, and Zr.

Plant extractable nutrients were analysed by Activation Laboratories (Actlabs). Actlabs performed a calcium chloride leach on 73 soil samples. Twenty mL of 0.01 mol/L CaCl_2 solution was added to 20 g of each soil sample. The solution was placed on a mechanical shaker for 2 hours. After the solution was filtered, each sample solution was analyzed by ICP-MS for the following elements: Si, Ti, Al, Mn, Mg, Na, K, B, Ba, Co, Cr, Cs, Cu, Li, Mo, Nb, Ni, Pb, Rb, Sc, Se, Sr, Th, U, V, Zn, and Zr and by inductively coupled plasma atomic emission spectroscopy (ICP-OES) for: Fe, P, and S.

Houba et al. (2008) and Van Raij (2008) examined numerous types of soil nutrient extraction methods and concluded that the CaCl_2 leach was one of the best at determining nutrient bioavailability in soils. This leach has been suggested to more accurately mimic cation exchange that would occur at the plant root interface because Ca from the CaCl_2

solution would exchange with cations attached to soil particle surfaces, thereby releasing them into solution, which can later be measured by ICP-MS (Houba et al. 1986). Houba et al. (1986) also suggested that this method was quick and could be used to analyze many elements in the soil, while still being cost effective. For these reasons, the CaCl_2 leach was chosen over the more frequently used soil extraction methods such as Olsen sodium bicarbonate, ammonium acetate, diethylene triamine penta-acetic acid – DTPA, and/or, ethylene diamine tetra-acid – EDTA, phosphoric acid to measure the bioavailability of the soils.

2.4.2 Bedrock Geochemistry

The bedrock samples were analysed by Geoscience Laboratories for minor, trace, and REE. They were analysed by ICP-MS (IMC-100) and were pretreated with a closed multi-vessel acid digest (SOL-CAIO). The elements analysed were: Ba, Be, Bi, Cd, Ce, Co, Cr, Cs, Cu, Dy, Er, Eu, Ga, Gd, Hf, Ho, In, La, Li, Lu, Mo, Nb, Nd, Ni, Pb, Pr, Rb, Sb, Sc, Sm, Sn, Sr, Ta, Tb, Th, Ti, Tl, Tm, U, V, W, Y, Yb, Zn, and Zr (Ontario Ministry of Northern Development and Mines 2018). The elements from the bedrock were used to compare similarities and differences among soil samples and bedrock.

2.4.3 Glacial Till Geochemistry

Till samples were analysed by Geoscience Laboratories for major, minor, trace, and REE. Major elements were analysed by XRF (XRF-M01) and each analyte was expressed as its oxide: Al_2O_3 , BaO , CaO , Cr_2O_3 , Fe_2O_3 , K_2O , MgO , MnO , Na_2O , P_2O_5 , SiO_2 , and TiO_2 . Minor, trace, and REE were analysed by ICP-MS (IMC-100) and were pretreated with a closed multi-vessel acid digest (SOL-CAIO). Elements analysed were: Ba, Be, Bi, Cd, Ce, Co, Cr, Cs, Cu, Dy, Er, Eu, Ga, Gd, Hf, Ho, In, La, Li, Lu, Mo, Nb, Nd, Ni, Pb, Pr, Rb, Sb, Sc, Sm, Sn, Sr, Ta, Tb, Th, Ti, Tl, Tm, U, V, W, Y, Yb, Zn, and Zr (Ontario Ministry of Northern Development and Mines 2018). Elements from the tills were used to compare similarities and differences among soil samples and tills.

2.4.4 Grapes and Fertilizer Geochemistry

Fertilizers applied to vineyards were analyzed for trace and REE. Analysis was performed by ActLabs, using ICP-MS. Prior to ICP-MS analysis, fertilizer samples were digested using an acid matrix containing HCl and HNO₃. Elements analysed were: Li, B, Na, Mg, Al, Si, P, S, K, Ca, Sc, Ti, V, Cr, Mn, Fe, Co, Ni, Cu, Zn, Se, Rb, Sr, Zr, Nb, Mo, Cs, Ba, La, Ce, Pr, Nd, Sm, Eu, Gd, Tb, Dy, Ho, Er, Tm, Yb, Lu, Pb, Th, and U. Grapes were also analysed for trace elements. Analysis was performed by ActLabs, using ICP-MS. Prior to analysis, grape samples were pretreated with a microwave digestion method using HNO₃, H₂O₂, and HCl. Elements analysed were: Li, B, Na, Mg, Al, Si, P, S, K, Ca, Sc, Ti, V, Cr, Mn, Fe, Co, Ni, Cu, Zn, Se, Rb, Sr, Zr, Nb, Mo, Cs, Ba, Pb, Th, and U.

2.5 Soil Depth Seismic Survey

Seismic refraction is a geophysical method commonly used to detect compositional differences among subsurface layers. This is performed using an energy source (hammer) to produce vibrational waves and a seismograph and geophones to measure vibrations. Seismic waves travel at different velocities in different types of soil or rock and are refracted at different angles when they cross the interface boundary between different rock or soil types. The velocities of compressive waves (P-waves) in each layer can be calculated from first-arrival picking of direct and critically refracted waves. The depth to each interface can then be calculated to determine layer thickness. Thus, a geophysical survey was conducted by Kukovica and Pratt (2018) to measure depth to bedrock at twelve locations throughout the island. The results of this survey are included in the Pelee Island Survey Report in Appendix M. The locations of each survey were taken within a few meters of soil sampling locations in fields 5GM318, 10CF, 13CF, 15A, 22CH, 23CH, 24CF, 26CF, 27CS, and 27GM318. This survey used refraction seismology to measure thicknesses of soil layers and depth of soil. The signals sent and received by geophones measure the velocities of each layer, to identify different compositions and thicknesses of each layer. The geodes were spaced at optimal and equal distances from each other so they could receive return velocities of output signals; most often the optimal geophone spacing was 4 m. Geodes were set up 1, 4, 5, or 10 m apart from each

other. One m spacing was too narrow for sensors to detect reflections from the bedrock, and therefore geode spacing was increased. The velocities of the seismic waves indicated the type of material. Dense material, such as bedrock, had higher velocities than less dense material such as soils. The survey detected three layers: soil, clay, and bedrock (Kukovica & Pratt 2018). Because Pelee Island has a history of glaciation and has known glacial till deposits, the clay layer from the geophysical report will be referred to throughout this paper as glacial till.

Chapter 3

3 Results

This chapter provides depth and profile descriptions of Pelee Island soils and identify important soil properties such as soil organic matter content, carbonate content, and soil pH. Soil, bedrock, glacial till, plant extractable nutrient, and fertilizer geochemical data are also provided in this chapter.

3.1 Depth to Bedrock

The thicknesses of soil and till from ground surface to bedrock surface are included in Table 3.1. The results from the geophysical survey show that Brookston soil in field 5GM318 is very shallow; it is 2 m deep and lies directly over bedrock. The seismic survey results show that Toledo soil in field 27CS is shallow; it is 1 m deep followed by 4 m of till, which directly overlies bedrock. Soil is very shallow in field 27L because during soil core sampling bedrock was reached at 0.6 m. The remainder of the fields with Toledo soils are deep; soils are 1-3 m deep followed by till layers ranging from 14-22 m thick, which directly overlie bedrock (Table 3.1). Images of the subsurface produced from seismic refraction surveys can be found in Appendix C. The images illustrate the thicknesses of layers in each field.

Table 3.1. Average thicknesses of soil, till, and depth to bedrock on Pelee Island determined by the seismic survey. Note that the topography of underlying bedrock is variable, so that maximum and minimum depth to bedrock are provided in the table as ranges.

Field	Soil Thickness (m)	Average Till Thickness (m)	Depth to Bedrock Range (m)
5GM318	2	0	2
10CF	3	15	18-21
13CF	1	16	13-22
15A	1	17	17-19
22CH	2	20	25
23CH	2	22	20-30
24CF	1	14	13-19
26CF	1	20	18-25
27CS	1	4	5
28CH	1	22	22-27

3.2 Soil Properties

3.2.1 Profile Description, Organic Matter and CO₃⁻ Content

Of the nineteen soil cores extracted, each were logged in detail, and the logs can be found in Appendix D. The A horizon of each soil core is dark brown due to the presence of abundant organic matter. Average organic matter content in surface soils is 5.24% by weight, whereas average organic matter content in deep soils is 2.24% by weight (Table 3.2). Fields 1A and 15A have the lowest organic matter content with weight percentages of 3.05% and 3.95% respectively, whereas field 27L has the highest organic matter content with a weight percent of 8.15% (Table 3.2). The A horizon is on average approximately 30 cm deep. The soils here have a crumbly texture and contain abundant root hairs. The B horizons are characterized by soil that has a sticky consistency and smaller particle size compared to the A horizons. In deeper soils, the B horizons range in colour from a greenish grey to a reddish-brown and many contain lithic fragments, which constitute <1% of this horizon. The lithic fragments are 0.5-1 cm, black, and sub-angular to angular or white, 0.5-3 cm and angular. In addition, blebs of yellowish silty sand are located in some of the deeper soils of the B horizon. The thickness of the B horizon varies and is dependent on soil depth to bedrock. The B horizon is thicker in deeper soils, and thinner in shallower soils. In the deeper soils, such as 24CF, 10CF, 13CF, 12CF, 22CH, 24R, 28CH, 27GW, 5GM318D, 23CH, 27GM318, 15A, 26CF, and 25bCH, this layer constitutes the whole lower portion of the core and thus could be >2 m. In shallower soils, the thickness of the B horizon averages about 50 cm. The C horizon is only present in shallow soils, such as 5GM318, 27CS, 1A, 27L, and 25aCH and has the same reddish-brown colour as the B horizon. However, it contains a greater abundance of lithic fragments compared to the B horizon, which comprise 2-5% of the soil. These lithic fragments are white, angular and range in size from 0.5-3 cm. Lithic fragments are found in soils that are near bedrock and some of the lithic fragments could originate from the underlying carbonate bedrock.

Carbonate content in section 4 soils is high with an average of 11.19% and standard deviation of 1.83%, whereas carbonate content in shallow soils is low with an average of 0.99% and standard deviation of 0.18% (Table 3.3). In section 1 soils, fields 1A and

27CS have the lowest carbonate content with values of 0.7% and 0.8%, respectively whereas fields 25aCH and 15A have the highest carbonate content in section 1 soils with values of 1.38% and 1.24%, respectively. In section 4 soils, fields 26CF and 27CS have the lowest carbonate content with values of 7.83% and 6.26%, respectively whereas field 24CF has the highest carbonate content in section 4 soils with a value of 13.03%. Fields 26CF and 27CS have low carbonate content at all depths. Sampling section 1 and 4 soils have the lowest and highest carbonate content averages respectively, but also have the lowest standard deviations. This indicates that the variability of carbonate content at these depths is low. In comparison, sampling section 2 and 3 soils have the largest standard deviations (3.85% and 3.17% respectively) and indicates high variability of carbonate content (carbonate content ranges from 0.8 – 13.68%).

Table 3.2. Organic matter content, measured in weight percent (dry), of each soil sample arranged by field and sampling depth on Pelee Island as determined by LOI. Average organic matter content as well as standard deviations for each depth are included.

Field ID	OM:	Section 1	Section 2	Section 3	Section 4
1A		3.05	2.44	1.99	2.49
5GM318		4.13	3.13	2.35	2.68
5GM318D		4.22	2.55	2.05	-
10CF		5.73	3.05	2.12	2.13
12CF		4.99	2.24	2.39	1.98
13CF		4.28	3.08	2.68	2.20
15A		3.95	3.20	3.81	2.22
22CH		5.96	3.25	2.19	1.91
23CH		6.47	2.89	2.98	2.60
24CF		4.43	2.80	2.02	2.11
24R		4.65	2.97	2.54	2.01
25aCH		4.55	3.57	2.14	2.08
25bCH		5.21	3.39	2.33	2.37
26CF		6.97	3.65	3.15	3.51
27CS		5.86	3.35	3.04	2.97
27GM318		4.92	3.04	2.40	2.97
27GW		5.92	2.39	2.48	1.91
27L		8.15	4.24	-	-
28CH		6.06	3.75	2.29	2.08
Average		5.24	3.10	2.50	2.37
St. Dev.		1.21	0.50	0.48	0.45

Table 3.3. Carbonate content, measured in weight percent, of each soil sample arranged by field and sampling depth on Pelee Island as determined by LOI. Average carbonate content as well as standard deviations for each depth are included.

Field ID	CO ₃ :	Section 1	Section 2	Section 3	Section 4
1A		0.70	11.78	12.75	10.63
5GM318		0.64	6.43	11.97	11.83
5GM318D		0.91	10.12	13.42	-
10CF		1.18	8.27	12.24	12.72
12CF		0.95	12.49	10.37	12.02
13CF		1.08	5.40	10.65	11.24
15A		1.24	2.03	3.82	10.79
22CH		1.04	2.20	12.09	12.46
23CH		1.12	6.45	8.10	10.34
24CF		0.87	3.72	12.51	13.03
24R		0.94	1.18	10.17	11.65
25aCH		1.38	1.94	13.68	12.37
25bCH		1.02	1.04	11.31	12.13
26CF		0.87	0.80	7.75	7.83
27CS		0.80	1.03	2.05	6.26
27GM318		1.04	2.26	11.66	9.80
27GW		0.95	6.50	9.39	12.38
27L		0.97	3.27	-	-
28CH		1.07	9.36	12.32	12.80
Average		0.99	5.07	10.35	11.19
St. Dev.		0.18	3.85	3.17	1.83

3.2.2 Soil pH

Lower pH values were measured in surface soils and higher pH values in deeper soils (Table 3.4). In section 1 soils, pH values range from 5.37 – 7.34 with an average of 6.52 and standard deviation of 0.57. Section 2, 3 and 4 soils range from a pH of 7.00 – 8.27 with an average of 7.93 and standard deviation of 0.30. This indicates that pH in the A horizon is more variable than in deep soils. Section 1 soils of fields 24CF, 24R, and 25bCH had comparatively low pH values of 5.37, 5.63, and 5.76, respectively, whereas section 1 soils of fields 1A, 10CF, and 25aCH had comparatively high pH values of 7.34, 7.21, and 7.31, respectively. In addition, although they are located near each other, the pH values of section 1 soils in fields 25aCH and 25bCH are very different, with values of 7.31% and 5.76%, respectively. Table 3.4 displays the pH values of all soil samples.

Figure 3.1 illustrates the relationship between organic matter content and soil pH. Organic matter content of soils and soil pH have a negative relationship, meaning that as organic matter content decreases, soil pH increases. Figure 3.1 shows that soil samples taken in section 1 have high organic matter content and low pH, whereas soil samples taken in section 2, 3, and 4 soils have low organic matter content and high soil pH. Figure 3.2 illustrates the relationship between carbonate content and soil pH and shows that carbonate content and soil pH have a positive exponential relationship. This means that as soil pH increases, soil carbonate content increases exponentially. Figure 3.2 shows that carbonate content only starts to increase when soil pH is above 7.5. Further, a few observations should be noted: section 1 soils always have low carbonate content (average of 0.99%); carbonate content of section 2 soils is highly variable (0.8-12.49% with a standard deviation of 3.85%); and section 3 and 4 soils have high carbonate content (average of 10.35 and 11.19% respectively).

Table 3.4. pH values of each soil sample arranged by field and sampling depth on Pelee Island. Average soil pH as well as standard deviations for each depth are included.

Sample ID	pH:	Section 1	Section 2	Section 3	Section 4
1A		7.34	7.83	7.92	7.68
5GM318		6.65	8.20	8.02	7.94
5GM318D		6.33	8.23	8.22	-
10CF		7.21	8.07	8.22	8.19
12CF		6.04	8.17	7.99	8.25
13CF		6.90	7.83	8.09	8.19
15A		6.83	7.62	7.56	8.08
22CH		6.16	7.91	8.06	8.27
23CH		6.98	7.68	7.74	7.91
24CF		5.37	8.00	8.25	8.18
24R		5.63	7.52	8.20	8.26
25aCH		7.31	7.00	8.27	8.17
25bCH		5.76	7.07	8.12	8.19
26CF		6.69	7.28	8.05	7.93
27CS		6.54	7.35	7.82	7.87
27GM318		6.43	7.59	7.99	7.94
27GW		6.03	7.77	7.96	8.27
27L		6.76	7.76	-	-
28CH		6.86	7.77	7.88	7.81
Average		6.52	7.72	8.02	8.07
St. Dev.		0.57	0.36	0.19	0.19

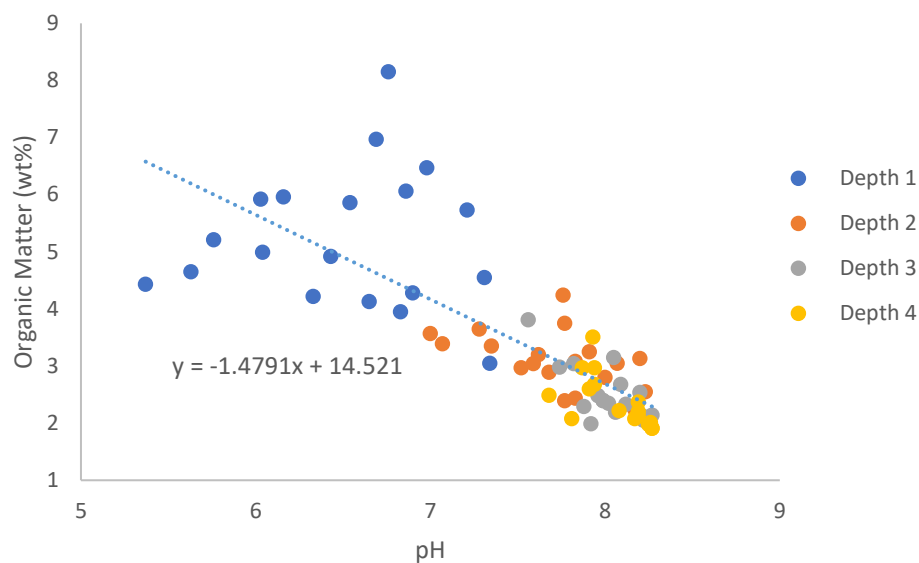


Figure 3.1. Organic matter content versus soil pH of Pelee Island soil samples. This graph shows a linear causation between organic matter content and soil pH with an R^2 value of 0.62 and a 95% confidence interval. This graph shows that as pH increases, organic matter decreases. Error bars are all <0.1 and smaller than the data symbols.

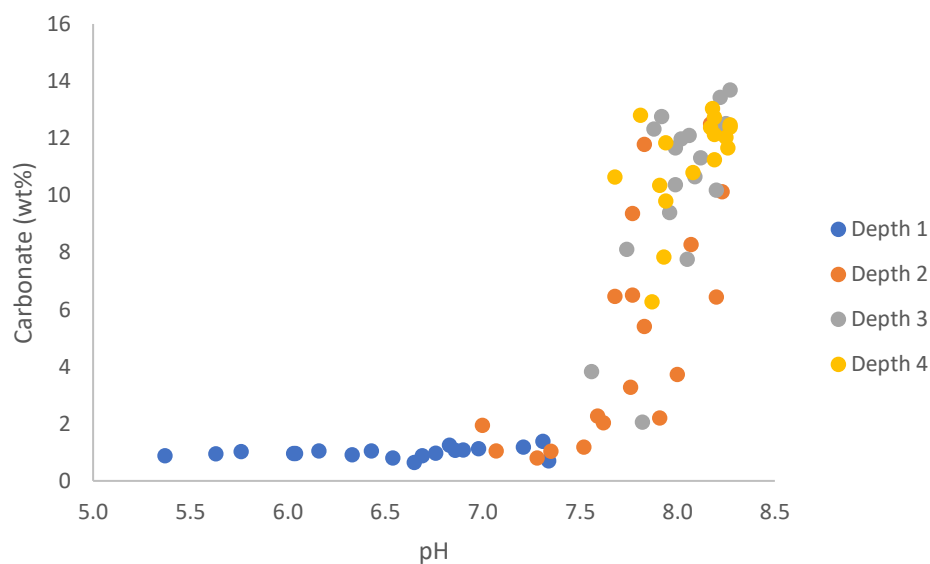
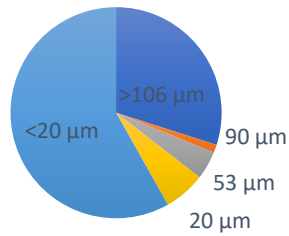


Figure 3.2. Carbonate content versus soil pH of Pelee Island soil samples. The trend of this graph shows that as pH increases, carbonate content increases exponentially, indicating that there is higher carbonate content in the deeper soils. Error bars are all <0.1 and smaller than the data symbols.

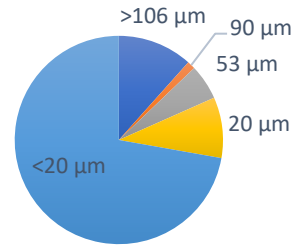
3.2.3 Grain Size

Grain size was compared between Brookston and Toledo soils. Field 5GM318 was used to represent grain size in Brookston soils and field 26CF was used to represent grain size in Toledo soils (Figure 3.3). Grain sizes of: $>106\ \mu\text{m}$ are fine sand and coarser; $90\text{-}106\ \mu\text{m}$ are very fine sand; $53\text{-}90\ \mu\text{m}$ are coarse silt and very fine sand; $20\text{-}53\ \mu\text{m}$ are medium to coarse silt; and $<20\ \mu\text{m}$ are fine silt and finer. Brookston soils had a higher sand fraction in section 1 and 2 soils compared to Toledo soils. However, in section 3 Toledo soils had a higher sand fraction and in section 4 the sand fraction was the same in both soils. Toledo soils had a greater fraction of medium silt and finer in sections 1 and 2 compared to Brookston soils. However, in section 3 Brookston soils had a greater fraction of medium silt and finer and in section 4 the very finest was the same.

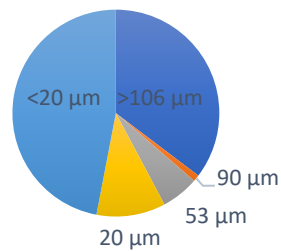
Brookston - Section 1



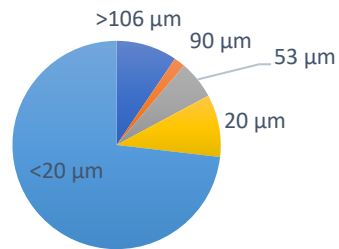
Toledo - Section 1



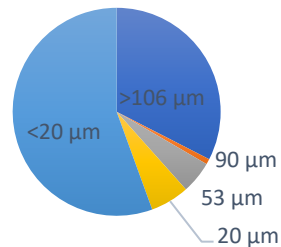
Brookston - Section 2



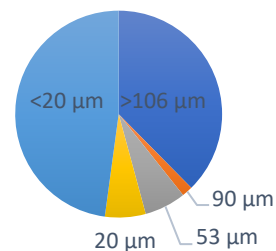
Toledo - Section 2



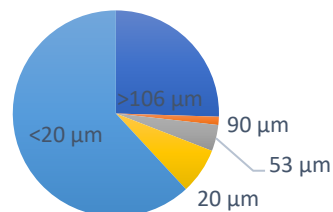
Brookston - Section 3



Toledo - Section 3



Brookston - Section 4



Toledo - Section 4

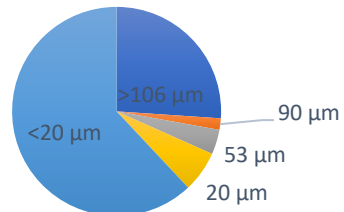


Figure 3.3. Comparison of grain size between Brookston and Toledo soils at each of the four sampling depths on Pelee Island. Brookston soils are represented by field 5GM318 and Toledo soils are represented by field 26CF. Note fractions labeled: 90 μm range in grainsize from 90-106 μm ; 53 μm range in grainsize 53-90 μm ; and 20 m range in grainsize 20-53 μm .

3.3 Soil and Bedrock Mineralogy

Mineralogical components of the soil are listed in Table 3.5 and are listed as either major (> 50%), intermediate (15-50%), or minor (<15%) components of the soil. Mineral abundances were estimated using XRD diffraction patterns. The major mineralogical component of all soils was quartz and the minor component of all soils was illite. Calcite was always found in the deepest soils but ranged from being a minor component to a major component. Conversely, calcite was almost always absent in the XRD patterns of the surface soils except for field 5GM318, where it made up a minor component of the soil. Although LOI results (Table 3.3) showed some carbonate in surface soils, abundance was low in all surface samples (<2%) and was not detected by XRD. Dolomite and mica were minor components in the soils and were present at varying soil sampling depths. Albite was a minor component of the soils and was found in all soil samples except 5GM318 in section 4.

Table 3.5. Relative mineralogical abundance results from XRD of select fields at each of the soil sampling depths on Pelee Island.

Soil Sample ID	Depth	Mineral & Abundances					
		Quartz	Calcite	Albite (Feldspar)	Illite	Dolomite	Mica
5GM318	1	Major	Minor	Intermediate	Minor	-	-
5GM318	2	Major	Minor	Minor	Minor	-	-
5GM318	3	Major	Major	Minor	Minor	Minor	-
5GM318	4	Major	Major	-	Minor	Minor	-
5GM318D	1	Major	-	Minor	Minor	-	-
5GM318D	2	Major	Intermediate	Intermediate	Minor	-	-
5GM318D	3	Major	Major	Minor	Minor	Minor	-
22CH	1	Major	-	Minor	Minor	-	Minor
22CH	2	Major	Major	Minor	Minor	Minor	-
22CH	3	Major	-	Minor	Minor	Minor	-
22CH	4	Major	Major	Minor	Minor	Minor	Minor
24CF	1	Major	-	Minor	Minor	Minor	-
24CF	2	Major	Minor	Intermediate	Minor	Minor	Minor
24CF	3	Major	Intermediate	Minor	Minor	Minor	Minor
24CF	4	Major	Intermediate	Minor	Minor	Minor	-
25aCH	1	Major	-	Minor	Minor	Minor	-
25aCH	2	Major	Minor	Minor	Minor	Minor	-
25aCH	3	Major	Intermediate	Minor	Minor	Minor	Minor
25aCH	4	Major	Intermediate	Minor	Minor	Minor	-
25bCH	1	Major	-	Minor	Minor	-	-
25bCH	2	Major	Minor	Intermediate	Minor	-	-
25bCH	3	Major	Intermediate	Minor	Minor	Minor	-
25bCH	4	Major	Minor	Minor	Minor	-	-

The bedrock mineralogy, unlike the soil mineralogy, was predominantly composed of calcite and dolomite, whereas quartz made up a minor component of the bedrock. Calcite is the major component of the bedrock, followed by dolomite in four of the samples and dolomite is the major component followed by calcite in the remaining two bedrock samples (Table 3.6).

Table 3.6. Relative mineralogical abundances in bedrock samples from Pelee Island.

Bedrock Sample ID	Mineral & Abundances		
	Calcite	Dolomite	Quartz
PI-18-2	Major	Intermediate	Minor
PI-18-3	Intermediate	Major	-
PI-18-4	Intermediate	Major	-
PI-18-5	Major	Minor	-
PI-18-6	Major	Minor	-
PI-18-7	Major	Intermediate	-

3.4 Geochemistry of Pelee Island Soils, Till, and Bedrock

3.4.1 Major Element Soil Composition

The oxide contents of each soil sample were plotted against Al_2O_3 abundance (Figure 3.4). Samples were plotted against Al_2O_3 because Al_2O_3 has a large spread in concentrations and is relatively less mobile during weathering compared to other oxides. Aluminum oxide concentrations decrease with depth, and thus oxides that are positively correlated with Al_2O_3 also decrease in abundance with depth. In contrast, oxides that are negatively correlated with Al_2O_3 increase in abundance with depth. Appendix G provides the R^2 and slope values for each oxide at each depth, displayed on the graphs in Figure 3.4. The Harker diagrams show a general decrease in CaO and general increases in Fe_2O_3 , K_2O , and SiO_2 with increasing Al_2O_3 content. Abundances of MgO, MnO, Na_2O , and P_2O_5 show less association with Al_2O_3 content. In addition, section 1 samples of each soil core generally have higher Al_2O_3 concentrations.

Harker diagrams of major and minor oxide versus Al_2O_3 show differences in the behavior of oxide abundances between the section 1 soil samples and the other three soil sampling depths. For example, CaO abundances in section 1 have no association with Al_2O_3 content, evident from the 0.04 R^2 value. However, section 2, 3, and 4 soils show a strong

negative relationship between CaO and Al₂O₃ (R² values of 0.93, 0.92, 0.76 and slope values of -2.93, -2.61, -2.69, respectively). There is no association between Fe₂O₃ and Al₂O₃ in section 1 (0.18 R²); however, there is a weak positive relationship between Fe₂O₃ and Al₂O₃ in deeper layers (0.58, 0.26, 0.60 R² values and 0.32, 0.24, 0.48 slope values). Although MgO vs Al₂O₃ concentrations are negatively correlated in sections 2, 3, and 4 soils, there is a strong positive correlation between MgO vs Al₂O₃ in section 1 soils (although the MgO content is much lower near the surface). Abundances of SiO₂ in the soils show the opposite trend; where there is a positive relationship between SiO₂ and Al₂O₃ in sections 2, 3, and 4 soils, there is a negative relationship in section 1 soils where Si contents are highest. Na₂O content has a slight negative relationship with Al₂O₃ in section 1 soils and almost no relationship with Al₂O₃ content in the deeper soils. K₂O vs Al₂O₃ displays a strong positive relationship at all depths. These graphs demonstrate that the topsoils (section 1 soils) on Pelee Island have distinctly different oxide concentrations compared to the underlying soils for most oxides.

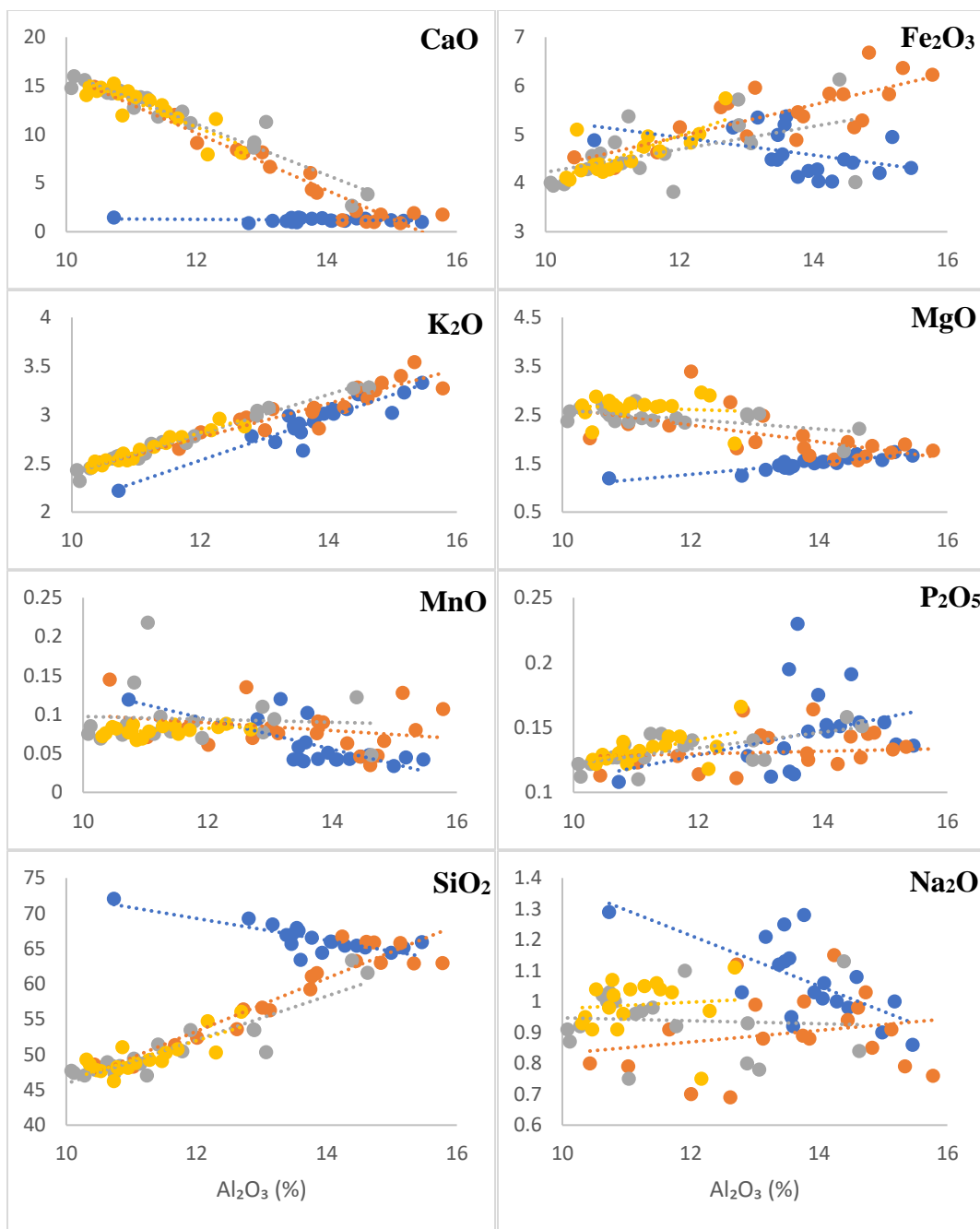


Figure 3.4. Harker diagrams showing major oxide concentrations of each soil sample (%; y-axis) plotted against concentrations of Al_2O_3 for each soil sample on Pelee Island. Colours indicate sampling depth: blue represents soils sampled in section 1; orange represents soils sampled in section 2; grey represents soils sampled in section 3; yellow represents soils sampled in section 4. The coloured lines are the corresponding trendlines of the coloured data points. The slopes of the trendline are listed in Appendix G. Error bars are all <0.1 and smaller than the data symbols.

The Harker diagrams in Figure 3.5 compare average oxide content (averaged over all four depths) of Brookston and Toledo soils. The R^2 values and the slopes for each of these lines are included in Appendix G. Therefore, Figure 3.5 displays a comparison among fields and not among depths. CaO vs Al_2O_3 trends are similar in Brookston and Toledo soil; as Al_2O_3 increases CaO decreases. However, Brookston soils have a higher CaO: Al_2O_3 ratio compared to Toledo soils, which means that Brookston soils have more CaO and less Al_2O_3 than Toledo soils. This suggests that Toledo soils are more leached. Further, XRD data show that Brookston soils contain more calcite in surface soils compared to Toledo soils, indicating that leaching is less intensive in Brookston soils. The trends of Fe_2O_3 vs. Al_2O_3 are similar in both Brookston and Toledo soils. Trends of K_2O vs. Al_2O_3 are also similar in both soil types, but K_2O abundances are much higher in Toledo soils. Trends for P_2O_5 vs. Al_2O_3 are similar in both soils when field 25aCH is excluded in Brookston soils, and field 27L is excluded in Toledo soils, showing a slight positive correlation (R^2 value of 0.97 in Brookston, and R^2 value of 0.25 in Toledo). However, even when these 2 fields are removed, P_2O_5 contents of Toledo soils do not have a strong association with Al_2O_3 (R^2 value of 0.25). MgO and MnO in both Brookston and Toledo soils show little association with Al_2O_3 ; the trends are weak with very low R^2 values of 0.26 and 0.02 for Mg in Toledo and Brookston soils, and 0.0089 and 0.022 for Mn in Toledo and Brookston soils, respectively.

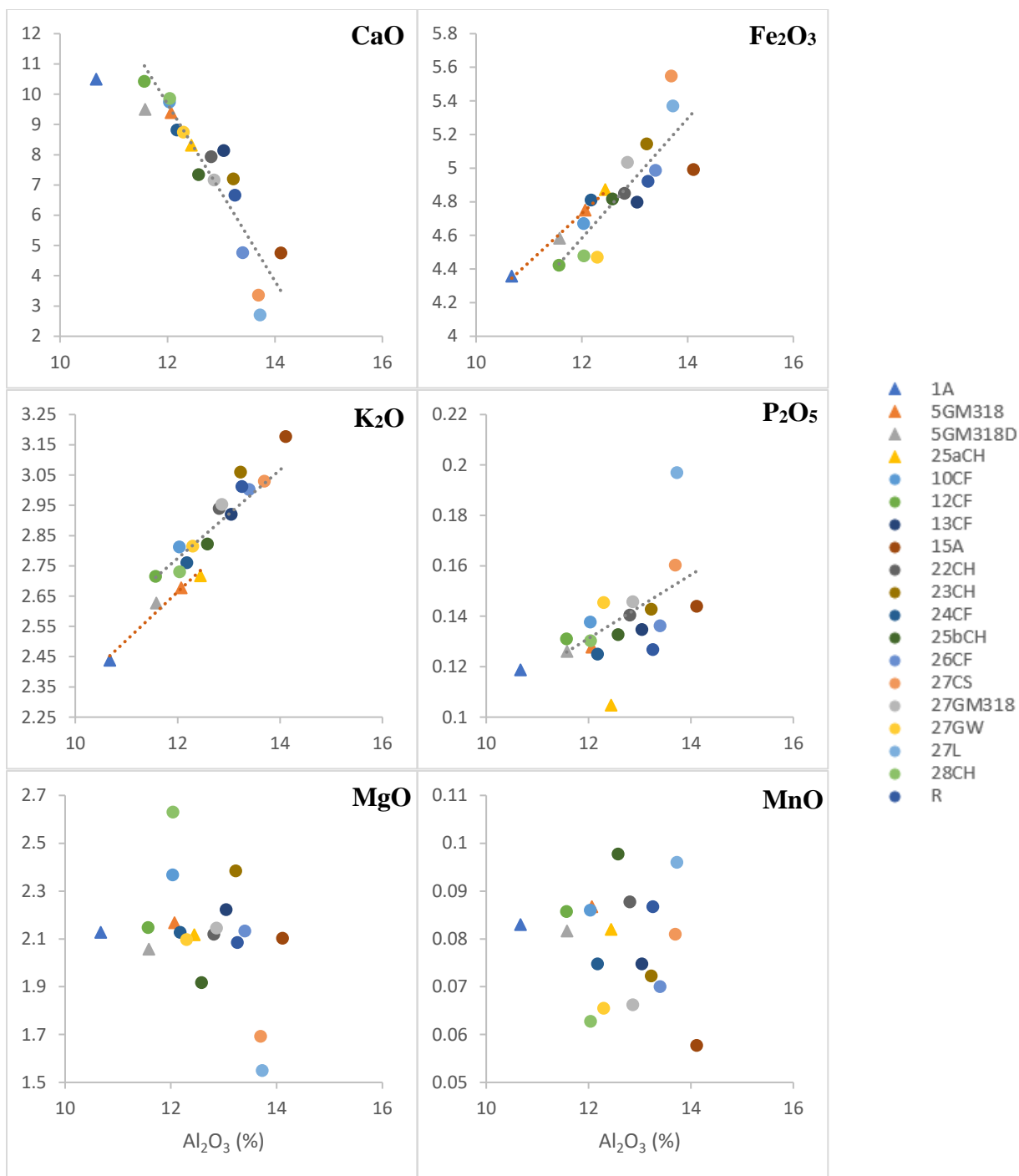


Figure 3.5. Harker diagrams illustrating major oxide differences between Brookston (triangles) and Toledo (circles) soils on Pelee Island. Major average oxide concentrations of each soil sample (%) plotted against average oxide concentrations of Al_2O_3 for each soil sample. The grey line and circles indicate trends for Toledo soils and the red line and triangles indicate trends for Brookston soils. Average concentration values in each field are represented by a different colour marker (see annotated legend). Error bars are all <0.1 and smaller than the data symbols.

Although there was some variability in oxide abundances among soils sampled at the same depth from different fields and different soil types (Brookston and Toledo), a one-way ANOVA (performed using Excel) determined that the variability among fields was insignificant (p-values >0.05) for all oxides with the exception of P₂O₅ (p-values <0.05; Table 3.7). Figure 3.4 illustrates that soils from different fields sampled at the same depth behave in a similar manner relative to Al₂O₃. However, a one-way ANOVA among soil sampling depths determined that there is oxide variability among soil sampling depths. Since element concentration differences among sampling depths are greater than elemental concentration differences among fields, oxide values from each field at the same depth were averaged together to get one value for each oxide at each soil sampling depth for all 19 profiles. These values are reported in Table 3.7 and are illustrated in Figure 3.6. Individual oxide values for each soil sample are reported in Appendix H and depth versus major oxide concentration graphs of each soil sample are illustrated in Appendix A.

Also included in Table 3.7 are the maximum and minimum oxide abundances of each major element for all soil samples. Where average soil oxide concentrations are reported, average sampling depths will also be assumed; the following numbers are average values calculated from true sampling depths from shallowest (section 1 soils) to deepest (section 4 soils): 18 cm, 71 cm, 138 cm, 191 cm. True sampling depths for each soil sampled are provided in Appendix H. The abundances of Al₂O₃, Na₂O, P₂O₄ and SiO₂ are greater at the surface and decrease with depth. Potassium oxide and Fe₂O₃ have highest concentrations in section 2 soils, as opposed to section 1 soils, and their abundances decrease in deeper soils. The abundances of CaO, MnO, and MgO have the opposite trend; these oxides are less abundant in surface soils, and more abundant in deep soils. In a study conducted by Schöenberger et al. (2012), seven soil samples were collected from eastern Ontario at depths between 0.2 m and 0.8 m, and major oxide concentrations of these soils were analyzed by XRF. The average concentrations of major oxides resulting from this study are included in Table 3.7. There are limited major oxide soil data reported in Ontario, and for this reason, data from the Schöenberger et al. (2012) study were compared to Pelee Island soil data because soils were sampled within the same general region. This means that these soils experience similar climates throughout

formation and in some areas, soils of eastern Ontario were formed over carbonate rock (Seguin 1984). Major oxide concentration values of soil samples collected from Pelee Island are comparable to samples within Ontario, as is outlined in Table 3.7, although, slightly lower concentrations of Na₂O and P₂O₅ are found in Pelee Island soils compared with other Ontario soils (about 2% less Na₂O and 0.1% less P₂O₅).

Table 3.7. Calculated average major oxide concentrations (%) at each soil sampling depth on Pelee Island as determined by XRF. Standard deviation, standard error, maximum and minimum, and p-values determined from a one-way ANOVA among sampling fields and p-values from a one-way ANOVA among sampling depths are also included. The last column includes average major elemental values from a study conducted by Schöenberger et al. (2012) for Ontario soils.

Element	Depth	Avg. Conc.	St. Dev.	St. Error	Max	Min	p-value (fields)	p-value (depths)	Averages (Schöenberger et al.)
Al ₂ O ₃	1	13.82	1.03	0.24	15.78	10.08	0.40	4.E-10	14.11
	2	13.53	1.50	0.34					
	3	11.65	1.38	0.33					
	4	11.18	0.71	0.17					
CaO	1	1.21	0.18	0.04	15.97	0.89	0.94	2.E-18	3.20
	2	5.65	4.55	1.04					
	3	11.97	3.77	0.89					
	4	12.97	2.18	0.53					
Fe ₂ O ₃	1	4.61	0.44	0.10	6.68	3.82	0.75	4.E-06	5.02
	2	5.46	0.64	0.15					
	3	4.61	0.64	0.15					
	4	4.58	0.44	0.11					
K ₂ O	1	2.94	0.25	0.06	3.54	2.22	0.09	3.E-05	2.56
	2	3.03	0.28	0.06					
	3	2.73	0.28	0.07					
	4	2.65	0.15	0.04					
MgO	1	1.49	0.14	0.03	3.39	1.19	0.97	5.E-18	1.81
	2	2.03	0.46	0.10					
	3	2.44	0.22	0.05					
	4	2.64	0.26	0.06					
MnO	1	0.06	0.03	0.01	0.22	0.03	0.97	3.E-03	0.10
	2	0.08	0.03	0.01					
	3	0.09	0.04	0.01					
	4	0.08	0.01	0.00					
Na ₂ O	1	1.07	0.13	0.03	1.29	0.69	0.07	2.E-04	3.17
	2	0.90	0.13	0.03					
	3	0.94	0.10	0.02					
	4	0.99	0.09	0.02					
P ₂ O ₅	1	0.15	0.03	0.01	0.23	0.09	4.E-03	1.E-01	0.24
	2	0.13	0.02	0.00					
	3	0.13	0.01	0.00					
	4	0.13	0.01	0.00					
SiO ₂	1	66.46	2.00	0.46	72.07	46.22	0.99	7.E-20	66.94
	2	59.03	6.02	1.38					
	3	51.00	4.71	1.11					
	4	49.65	2.49	0.60					

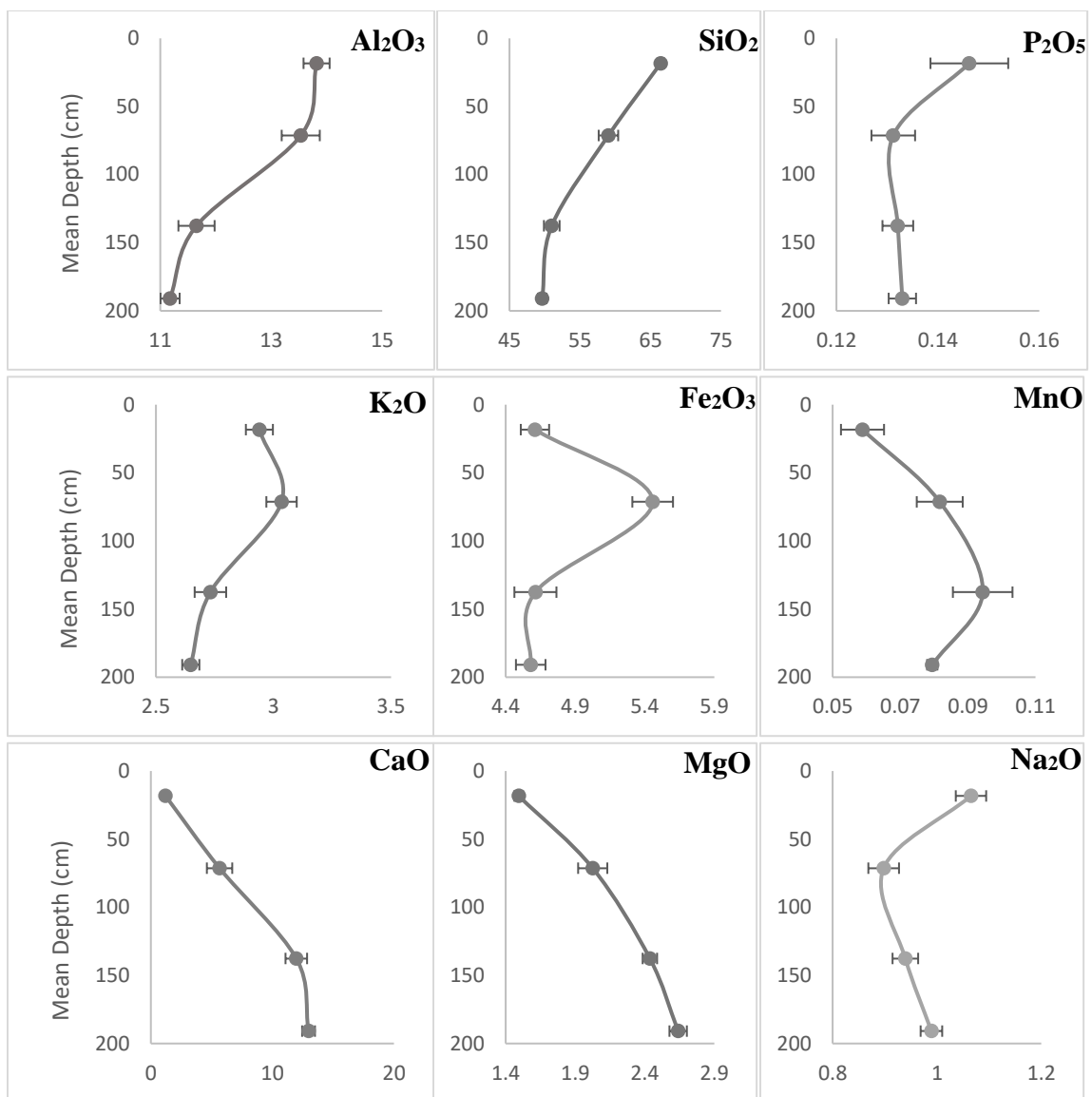


Figure 3.6. Average oxide concentrations (%; x-axis) of Pelee Island soils plotted against mean sampling depths. The spline curves on these graphs are meant to illustrate element concentration trends and do not imply vertical connectivity among soils samples, because markers on the graphs represent averages of soil samples selected from different locations on the island.

3.4.2 Soil, Bedrock, and Till Trace Elements

Averages and ranges of trace element compositions of soil, till, and bedrock are summarized in Table 3.8 and data are included in Appendix H, I, E respectively. The concentrations of trace elements in soils and tills are similar. Both concentrations, however, are very different from bedrock. Trace element concentrations in bedrock are

always lower than soils and tills. Bedrock samples have, on average lower elemental concentrations relative to soils for most elements with the exception of Cd and Zn. The concentrations of Cd and Zn are almost twice as high in the bedrock compared to the soils. In addition, Table 3.9 compares the average concentrations of some trace elements in Pelee soils to the mean trace element concentrations of other Ontario soils. In a study conducted by Sheppard et al. (2009), 59 agricultural soils were sampled in Ontario at depths from 0-60 cm and analyzed for trace element concentration. This table shows that Pelee Island soils always have higher concentrations of trace elements compared to other Ontario agricultural soils. Note that for Table 3.9 Pelee Island averaged elemental concentration values were obtained by averaging soil sections 1 and 2 (average 18.3 cm and 71.3 cm respectively) so comparison between Pelee Island values and Sheppard et al. (2009) values were equitable.

Table 3.8. Average, maximum, and minimum trace and REE values of soils, tills, and bedrock on Pelee Island as determined by ICP-MS. Note that all values are in ppm and all soil values are represented by averaged section 4 soil samples (sampling sections 1, 2, 3 soil values were not included in these calculations). x = soil/till is the number of times greater the concentrations of Pelee Island soils are than Pelee Island tills and x = soil/bedrock is the number of times greater the concentrations of Pelee Island soils are than Pelee Island bedrock concentrations.

Element	Soil			Till			Bedrock				
	Avg. Conc.	Max	Min	Avg. Conc.	Max	Min	x = soil/till	Avg. Conc.	Max	Min	x = soil/bedrock
Ba	421.11	468.90	366.72	409.27	444.70	391.30	1.03	9.12	20.60	3.90	46.19
Be	1.60	1.81	1.46	1.55	1.71	1.32	1.03	0.06	0.07	0.04	27.57
Bi	0.17	0.24	0.15	<DL	0.00	0.00	-	<DL	0.00	0.00	-
Cd	0.18	0.47	0.12	0.20	0.25	0.15	0.93	0.43	2.02	0.02	0.42
Ce	58.85	66.19	53.70	63.03	67.85	54.84	0.93	1.57	2.96	0.22	37.49
Co	12.41	14.94	10.65	12.56	13.60	11.57	0.99	0.26	0.56	0.16	48.37
Cr	54.90	65.64	49.69	67.33	74.00	59.00	0.82	5.00	7.00	3.00	10.98
Cs	4.25	5.58	3.85	4.88	5.54	3.66	0.87	0.09	0.17	0.03	49.57
Cu	29.14	51.09	24.77	24.67	25.10	23.90	1.18	4.70	17.70	1.70	6.20
Dy	4.40	5.07	4.12	4.45	4.79	4.11	0.99	0.29	0.48	0.05	15.06
Er	2.57	2.93	2.42	2.60	2.80	2.35	0.99	0.18	0.32	0.02	14.24
Eu	1.17	1.37	1.09	1.16	1.25	1.07	1.01	0.06	0.10	0.01	20.79
Ga	14.64	16.78	13.49	16.20	18.03	13.21	0.90	0.34	0.58	0.11	43.49
Gd	4.80	5.55	4.48	4.88	5.22	4.44	0.99	0.31	0.47	0.06	15.59
Hf	3.90	4.45	3.55	4.50	5.08	4.15	0.87	0.27	0.43	0.17	14.45
Ho	0.89	1.02	0.84	0.88	0.94	0.82	1.01	0.07	0.10	0.01	13.60
In	0.05	0.06	0.05	0.05	0.06	0.04	1.02	0.00	0.01	0.00	14.30
La	29.13	32.43	26.69	29.67	32.50	26.60	0.98	1.47	2.30	0.40	19.86
Li	34.09	38.84	31.11	35.10	41.90	27.50	0.97	1.12	1.60	0.50	30.53
Lu	0.37	0.44	0.33	0.37	0.41	0.35	0.98	0.03	0.04	0.02	12.43
Mo	4.75	8.34	3.22	3.58	5.50	2.07	1.33	0.52	0.64	0.42	9.07
Nb	10.14	11.50	9.27	11.13	13.41	8.98	0.91	0.36	0.90	0.06	28.10
Nd	27.96	31.79	26.10	27.93	30.82	24.44	1.00	1.22	1.91	0.36	23.01
Ni	31.53	40.90	27.21	36.37	41.20	29.70	0.87	3.88	6.80	2.60	8.12
Pb	13.32	17.69	11.05	13.77	16.28	11.44	0.97	1.59	3.26	0.89	8.38
Pr	7.35	8.42	6.83	7.48	8.07	6.67	0.98	0.28	0.48	0.06	26.48
Rb	92.14	107.72	83.55	98.87	110.29	79.86	0.93	2.09	3.89	0.76	44.01
Sb	0.55	1.12	0.42	0.56	0.65	0.43	0.99	0.10	0.15	0.07	5.52
Sc	10.37	11.81	9.63	10.97	12.70	8.90	0.95	<DL	0.00	0.00	-
Sm	5.46	6.23	5.07	5.46	6.03	4.84	1.00	0.23	0.35	0.03	23.92
Sn	1.95	2.49	1.65	1.81	2.01	1.46	1.08	0.23	0.32	0.18	8.49

Element	Soil			Till			Bedrock				
	Avg. Conc.	Max	Min	Avg. Conc.	Max	Min	x = soil/till	Avg. Conc.	Max	Min	x = soil/bedrock
Sr	220.76	247.86	133.31	163.17	210.40	137.10	1.35	82.58	92.30	73.10	2.67
Ta	0.67	0.79	0.58	0.72	0.87	0.57	0.93	0.03	0.05	0.01	23.88
Tb	0.73	0.85	0.68	0.73	0.78	0.67	1.00	0.04	0.08	0.01	17.55
Th	7.67	9.20	6.83	8.11	9.36	6.58	0.95	0.08	0.21	0.03	90.48
Ti	3442.19	3805.86	3172.80	3623.33	4031.00	3171.00	0.95	76.17	168.00	14.00	45.19
Tl	0.14	0.52	0.06	0.80	0.99	0.63	0.17	0.04	0.07	0.02	3.28
Tm	0.38	0.42	0.35	0.37	0.40	0.34	1.01	0.02	0.04	0.00	15.98
U	3.06	4.24	2.64	3.25	3.59	2.85	0.94	2.89	4.45	2.11	1.06
V	91.90	124.74	76.53	96.97	107.30	80.30	0.95	7.65	13.20	4.00	12.01
W	0.94	1.20	0.83	1.05	1.26	0.77	0.89	1.63	6.62	0.11	0.58
Y	24.43	28.25	23.38	23.63	26.81	20.99	1.03	2.63	5.34	0.14	9.28
Yb	2.45	2.82	2.29	2.51	2.70	2.28	0.98	0.15	0.23	0.02	15.96
Zn	68.68	83.79	62.47	68.17	77.20	59.40	1.01	118.73	671.60	4.00	0.58
Zr	146.33	172.01	131.42	168.67	194.00	155.00	0.87	10.67	18.00	6.00	13.72

Table 3.9. Comparison of average trace element concentrations for sections 1 and 2 of Pelee Island soils and in Ontario soils analyzed by Sheppard et al. (2009). $x = \text{soil}/\text{avg}$ is the number of times greater that averaged Pelee Island soil concentrations are than averaged Sheppard et al. (2009) soil concentrations. Element concentrations are in ppm and standard error of both Pelee Island soils and Ontario soils from Sheppard et al. (2009) are included.

Element	Average (Sheppard 2009)	St. Error	Average Pelee Soils	St. Error	$x = \text{soil}/\text{avg}$. (Sheppard 2009)
Ba	116.67	3.33	461.38	4.96	3.95
Cd	0.19	0.03	0.32	0.01	1.72
Ce	54.00	2.08	68.66	0.83	1.27
Co	9.30	0.44	14.31	0.23	1.54
Cr	33.00	1.00	68.60	1.07	2.08
Cs	1.33	0.07	5.59	0.11	4.19
Cu	18.67	0.67	33.41	0.67	1.79
La	24.33	1.20	33.54	0.39	1.38
Mo	0.70	0.01	4.28	0.26	6.12
Nb	0.90	0.10	12.77	0.19	14.13
Nd	25.33	1.20	32.89	0.40	1.30
Ni	22.33	0.88	39.53	0.73	1.77
Pb	11.43	1.11	18.63	0.40	1.63
Sb	0.12	0.01	0.76	0.02	6.50
Sm	5.07	0.30	6.46	0.08	1.28
Sr	37.33	6.57	138.27	5.23	3.70
Tb	0.55	0.03	0.88	0.01	1.61
Th	3.27	0.64	9.43	0.15	2.89
U	1.10	0.06	3.96	0.08	3.60
V	46.67	1.86	117.44	2.24	2.52
Y	15.67	0.88	29.53	0.38	1.88
Zn	61.33	2.33	91.33	1.66	1.49

Minor and trace elements in soils were normalized to the North American Shale Composite (NASC) using Rudnick & Gao (2017). The NASC has been used as a standard comparison in a number of geochemical studies (Gromet et al. 1984). Trace element data for soil samples are provided in Appendix H. Normalized concentrations of all four depths in each field were averaged and plotted on an incompatible element graph. Incompatible elements are unsuitable in size or charge to the cation sites of the minerals in which they are included and are often replaced by other more suitable cations (Ridley 1998).

Figure 3.7 displays the minor and trace element concentration values averaged over 4 depths in each field. All fields have a depletion of Ba and Sr and an enrichment in U compared to NASC. In addition, all fields show the same general trends and show no major differences in minor and trace elemental values among fields.

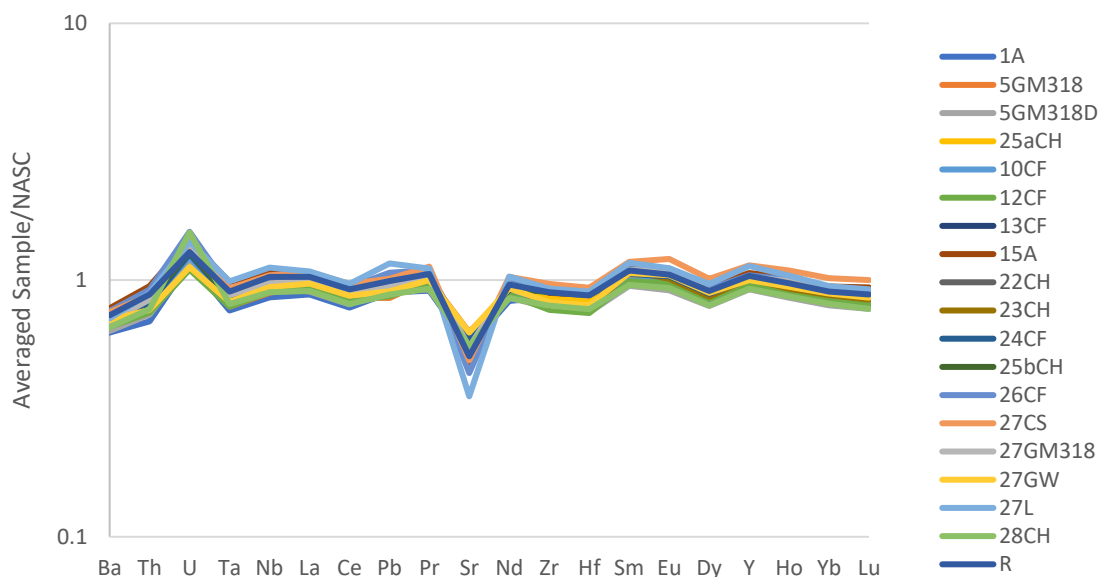


Figure 3.7. Incompatible element diagram of averaged minor and trace element depth values for comparing elemental field concentrations on Pelee Island. Element values are normalized to NASC using Rudnick & Gao (2017). Note that the purpose of plotting all fields on the same graph is to show that all fields have very similar trace element concentrations, thus distinguishing line colours that represent fields is not necessary.

Next, the same data were used, but normalized concentrations of nineteen fields at each depth were averaged and plotted on an incompatible element diagram to compare elemental differences among all four soil depths (Figure 3.8). In soil sampling sections 3 and 4, with the exception of U, all elements are more depleted compared to the NASC standard. In soil sampling sections 1 and 2, elements are closer to standard values and are only slightly enriched or depleted (with the exception of Sr, U, Pb, and Ba, which have values that are further from the standard). In general, Figure 3.8 displays higher abundances of minor and trace elements in surface soils and lower abundances in deeper soils. However, there are two exceptions: Sr is most depleted at section 1 and becomes more enriched in deeper soils; and in section 1 soils, Pb does not follow the trends of the soil samples at other depths and is more enriched compared to the other soil samples and compared to the standard.

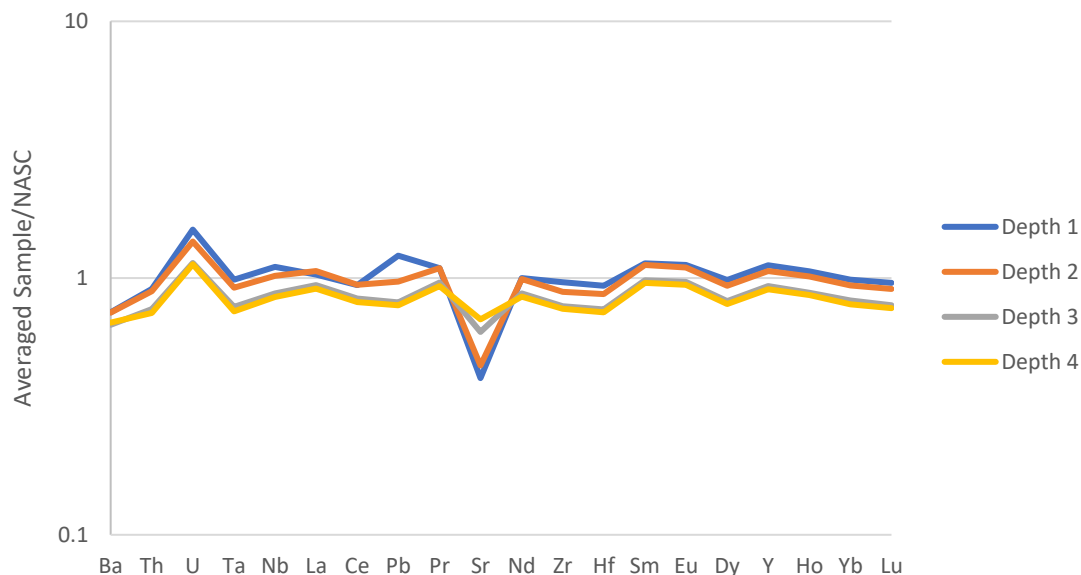


Figure 3.8. Incompatible element diagram of minor and trace element averaged field values at each depth to compare elemental depth concentrations on Pelee Island. Element values are normalized to NASC using Rudnick & Gao (2017).

3.4.3 Soil and Bedrock REE Patterns

The REE can be used to identify the source materials for mixtures of minerals. The REE are used for this purpose because they become incorporated into common minerals at very low concentrations and are relatively immobile within mineral structures. Rare earth element diagrams display patterns that can be used to determine source material of a soil (Wen et al. 2014). The REE data for soil and bedrock of Pelee Island were normalized to NASC using Haskin et al. (1968) for all REE except Dy, which was normalized using Gromet et al. (1984). Data was normalized to NASC so Pelee Island soils can be compared to other studies, since NASC has been used as a standard comparison in a number of geochemical studies (Gromet et al. 1984). REE data for soils are included Appendix H.

Figure 3.9 compares the REE patterns in soil in different fields on Pelee Island (Figure 3.9a) and for different soil depths (Figure 3.9b). Data for different soil depths represent the average elemental concentration values of all 19 soil sample locations (Figure 3.9a), whereas the data for different fields represents averaged elemental concentration values for each element from all four soil sampling depths (Figure 3.9b). There is little

difference in REE abundances and patterns among sites, whereas REE concentrations are typically higher in the surface soils and lower in deeper soils. For example, the concentrations of La in field 10CF decrease from 36.3 ppm to 26.7 ppm and concentrations of Nd in field 22CH decrease from 35.43 ppm to 27.76 ppm in section 1 to 4 soils (Appendix H). The similar patterns on both Figure 3.9a and Figure 3.9b indicate that the soils from all locations and all depths are derived from the same source material. In addition, the patterns show that the REE concentrations are similar to the NASC standard.

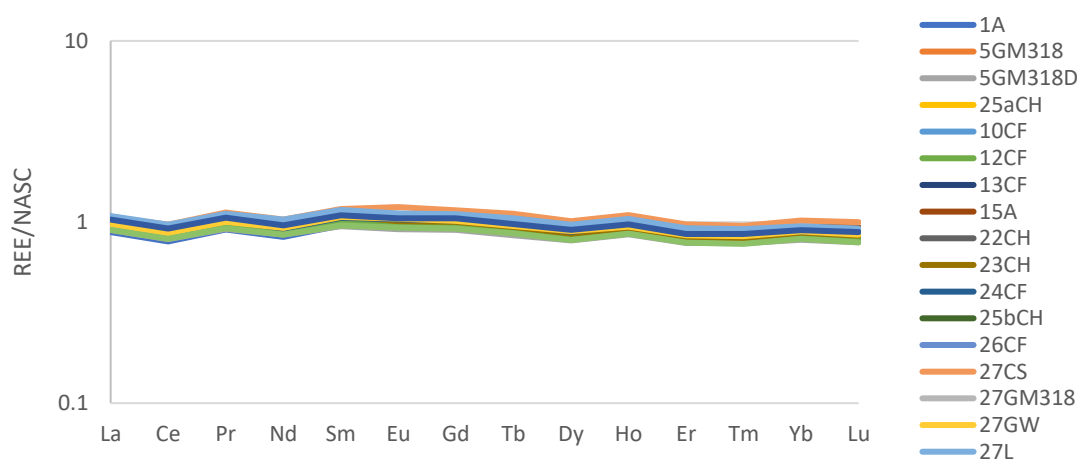


Figure 3.9a. Averaged REE depth values for comparing REE concentrations among fields on Pelee Island. Element values are normalized to NASC using Haskin et al. (1968).

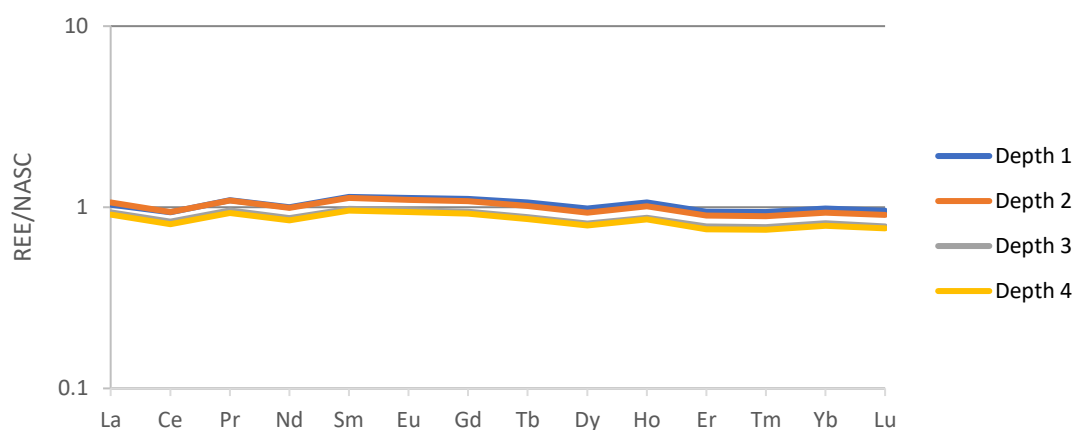


Figure 3.9b. Averaged REE field values for comparing REE concentrations among depths on Pelee Island. Element values are normalized to NASC using Haskin et al. (1968).

The normalized REE contents of the bedrock samples are plotted on Figure 3.10. The data represent elemental concentration values for each element from each bedrock sample. Pelee Island bedrock samples PI-18-2, PI-18-3, PI-18-4, PI-18-5 all show the same pattern for REE content, indicating the same rock type. However, PI-18-6 and PI-18-7 have a different REE pattern, which indicates a different rock type. Based on geological maps, bedrock samples 2 to 5 represent limestone bedrock from the Lucas Formation of the Detroit River Group, whereas samples 6 and 7 represent bedrock from the younger Dundee Formation (Hewitt 1972). Both formations have similar mineralogy based on XRD analyses (Section 3.3 above).

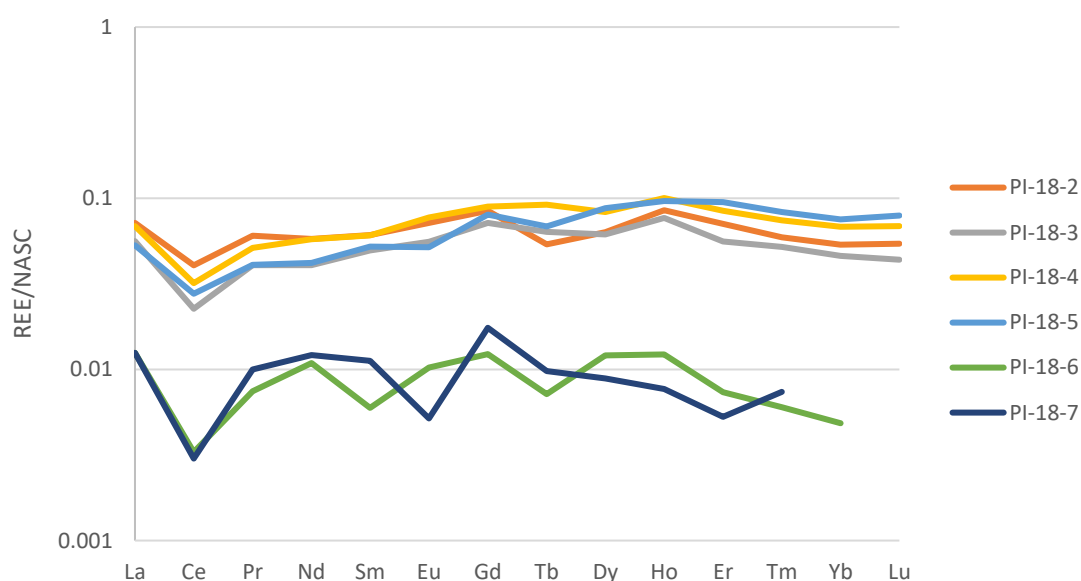


Figure 3.10. REE concentrations of six bedrock samples from Pelee Island. Element values were normalized to NASC using Haskin et al. (1968), except Dy which was normalized using Gromet et al. (1984).

The REE concentrations of samples from bedrock and the nearest soils were compared to determine if the bedrock is a major contributor of elements to the overlying soil (Figure 3.11a, b). There is very little similarity between the basement and the Toledo and Brookston soils. The REE concentrations of the soil were also compared to the concentrations in the till (Figure 3.12). The results show that the soil contains elements that are very similar to the underlying till.

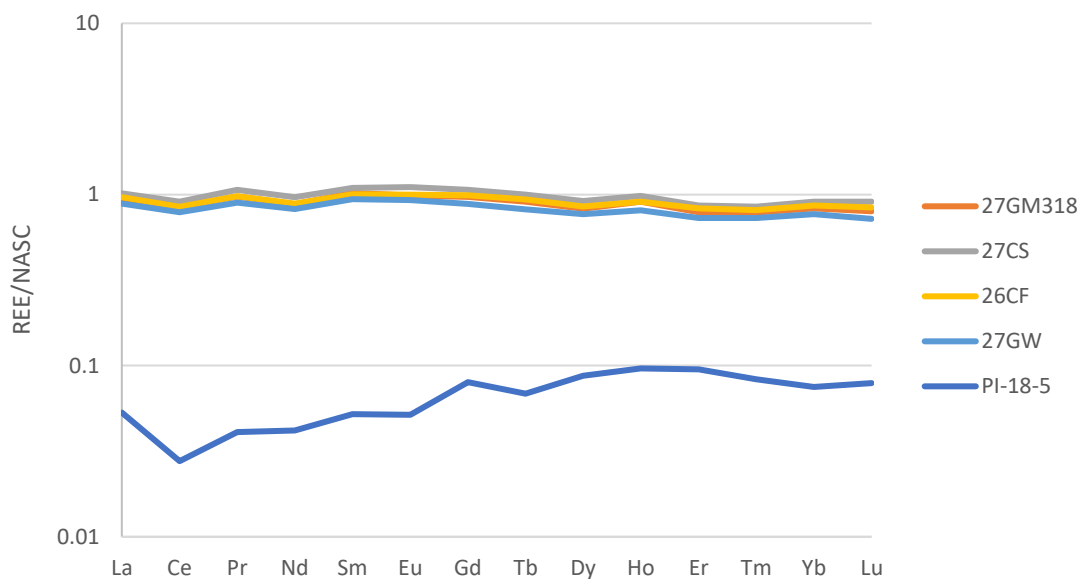


Figure 3.11a. Comparison of REE concentrations between bedrock sample PI-18-5 and section 4 soil samples of nearby Toledo fields (27GM318, 27CS, 26CF, and 27GW). Element values were normalized to NASC using Haskin et al. (1968).

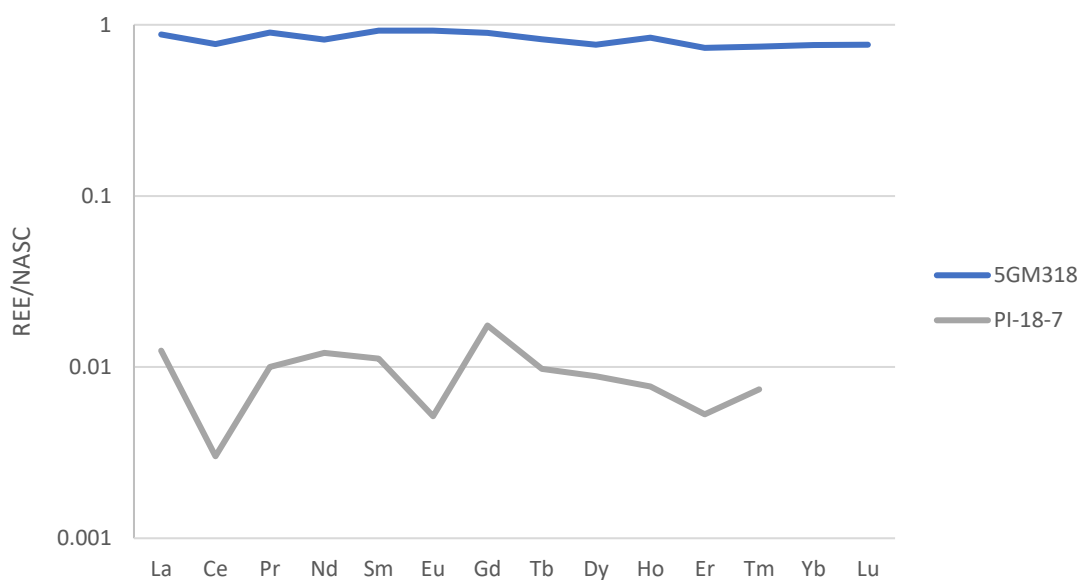


Figure 3.11b. Comparison of REE concentrations between bedrock sample PI-18-7 and section 4 soil sample of the adjacent Brookston field (5GM318). Element values were normalized to NASC using Haskin et al. (1968).

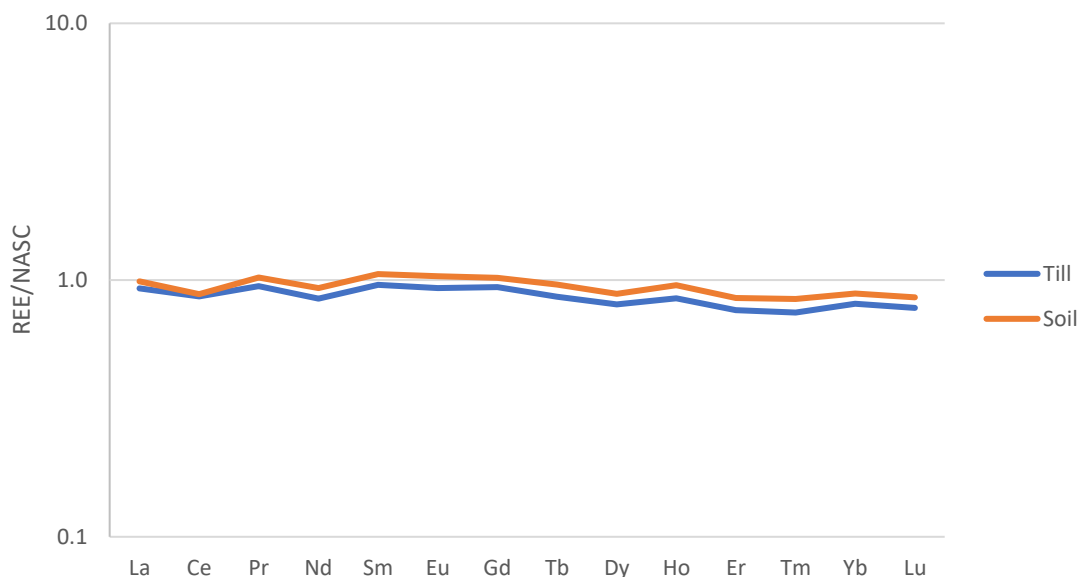


Figure 3.12. Comparison of REE concentrations between till (averaged values) and soil (averaged section 4 soil values). Element values were normalized to NASC using Haskin et al. (1968).

3.4.4 Pelee Island Fertilizers

Major element and trace element concentrations in fertilizers are included in Tables 3.10 and 3.11, respectively. Since only essential trace elements and elements that could be compared to PEN data were included in Table 3.11, additional trace element data can be found in Appendix J. Fertilizer sample IDs and descriptions are included in Table 3.12. Figure 3.13 illustrates trace element concentrations of the fertilizers. This graph shows that chemical fertilizers (FERT4, FERT5) are depleted of Ba, but enriched in U, Pb, and Sr relative to NASC. Pelee Island composts (FERT6, FERT7, FERT8, FERT9) are depleted of Zr and Nb, but are enriched in U and Sr. The liquid fish (FERT1), molasses (FERT2), and UAN 25% (FERT3) are not plotted on Figure 3.13 because most element concentrations were below detection limits.

Table 3.10. Major element concentration values (weight %) of fertilizers used on Pelee Island as determined by ICP-MS. Element columns containing < indicate that the element was less than the detection limit for each fertilizer sample.

Sample ID	Al	Ca	Fe	K	Mg	Mn	Na	P	Si
FERT1	<0.00040	0.15950	<0.00200	0.19574	0.03500	0.00003	0.26200	1.97267	<0.04000
FERT2	0.00107	0.90733	0.00948	3.71278	0.29300	0.00118	0.06528	0.05559	0.07072
FERT3	<0.00040	<0.01000	<0.00200	<0.00600	0.00167	<0.00002	0.00121	<0.01000	<0.04000
FERT4	0.11	0.23	0.14	26.50	4.38	1.69	0.42	2.74	0.08
FERT5	0.11	1.41	0.42	31.90	2.91	0.06	0.17	2.71	0.06
FERT6	1.75	3.88	0.79	3.98	0.76	0.02	0.06	0.54	0.22
FERT7	2.24	2.42	1.06	2.47	0.80	0.02	0.03	0.56	0.23
FERT8	0.51	2.33	0.23	4.18	0.57	0.01	0.01	0.25	0.25
FERT9	0.08	2.16	0.97	1.06	0.23	0.01	0.40	2.12	0.10

Table 3.11. Trace element concentration values (ppm) of fertilizers used on Pelee Island as determined by ICP-MS. Element columns containing < indicate that the element was less than the detection limit for each fertilizer sample.

Sample ID	Ba	Co	Cu	Mo	Ni	Pb	Sr	U	Zn
FERT1	<0.2	0.01	<0.4	<0.2	<0.6	0.02	9.12	0.002	5
FERT2	4.3	0.13	10.7	1.0	<0.6	0.11	63.8	0.016	9
FERT3	<0.2	<0.01	<0.4	2.1	<0.6	<0.02	<0.08	<0.002	<1
FERT4	6.7	3.76	0.4	1.6	4.7	0.49	29.1	14.4	12900
FERT5	10.3	0.82	31.0	1.8	7.1	6.11	45.9	17.6	5510
FERT6	120.6	4.27	31.1	7.1	13.1	8.11	138	1.27	100
FERT7	147.2	5.10	33.7	5.4	14.6	8.46	86.4	1.08	119
FERT8	36.5	2.06	21.2	25.4	21.9	2.09	29.9	0.379	48
FERT9	11.6	0.84	99.8	3.2	10.2	0.63	34.3	0.889	382

Table 3.12. Pelee Island fertilizer sample IDs and descriptions.

Sample ID	Type
FERT1	Liquid Fish
FERT2	Molasses
FERT3	UAN 25%
FERT4	AGRIS (chemical fertilizer)
FERT5	Thompsons (chemical fertilizer)
FERT6	Compost 2017
FERT7	Old Compost
FERT8	Young compost
FERT9	Compost

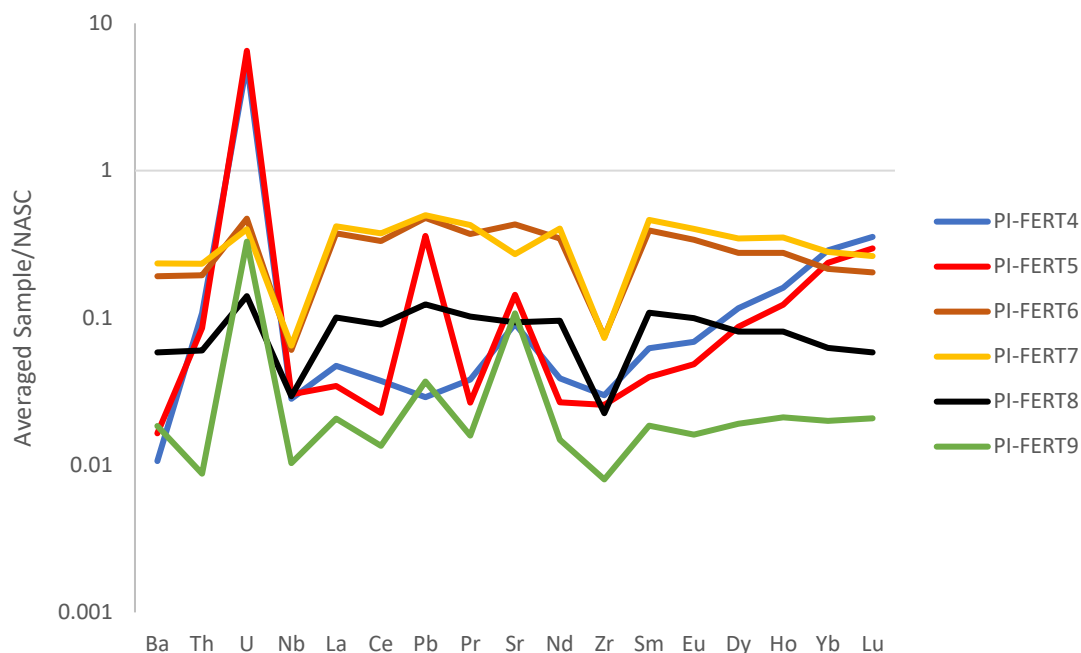


Figure 3.13. Incompatible element diagram of minor and trace element concentrations of Pelee Island fertilizers. Element values are normalized to NASC using Rudnick & Gao (2017).

Figure 3.14 compares the REE composition of fertilizers to soils on Pelee Island. Both fertilizers and soils were normalized to the NASC standard using Haskin et al. (1968). Note that soil REE concentrations displayed in the figure represent the average values of all soil samples. This diagram illustrates that the trend of the liquid (FERT2) and chemical fertilizers (FERT4, FERT5) do not match REE trends of the soils. However, REE trends of compost fertilizers are similar to REE trends of the soils; in particular, compost 2017 (FERT6) and old compost (FERT7) are similar to the soil samples. The compost is made from plants grown on the island, and thus the similarities in REE distribution between soils and compost is not surprising.

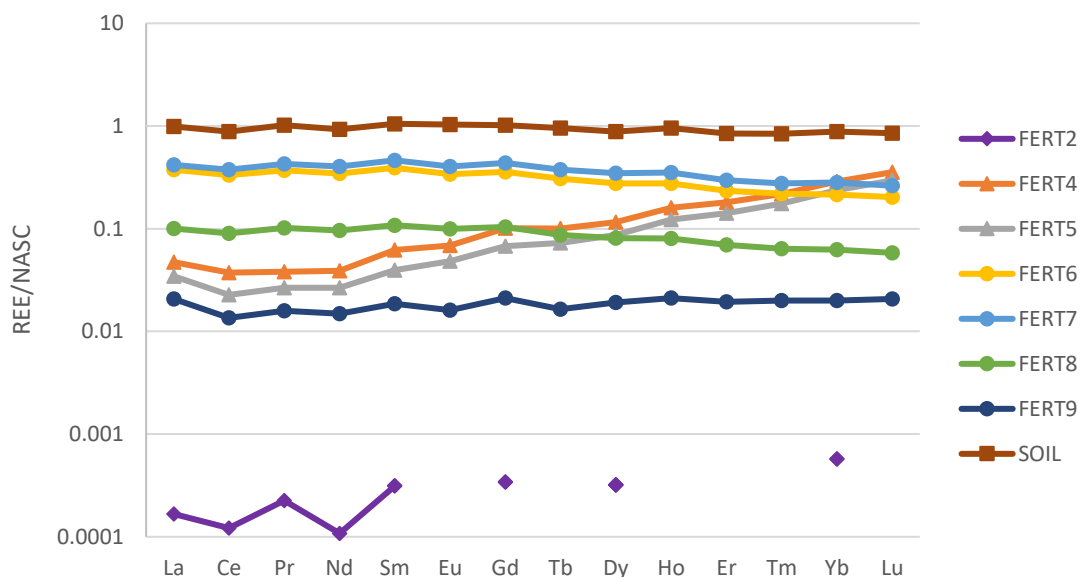


Figure 3.14. REE diagram comparing Pelee Island fertilizers and soils. Soil values are represented by the average of all soil samples. Note FERT1 and FERT3 are not displayed on the graph because values were below REE detection limits. REE values have been standardized to NASC using Haskin et al. (1968).

3.4.5 Plant Extractable Nutrients

Plant extractable nutrients are elements that are loosely bound to soil particles and so are available for uptake by plant roots (Weil & Brady 2017). The average plant extractable nutrient concentrations, standard deviations, and the maximum and minimums are summarized in Table 3.13. Figure 3.15 displays how average elemental concentrations of plant extractable nutrients across different fields change at each depth. Silicon, Mg, Zr, Sc, B, Rb and Mn concentrations are high at surface and decrease with depth.

Molybdenum, Na, Li, Sr, and U generally have low concentrations at surface and increase with depth. Comparing total elemental concentrations of the soil minerals (Figure 3.6) to plant available concentrations in the soil (Figure 3.15), Mg and Mn have the opposite trends; total soil elemental concentrations of Mg and Mn are generally low at the surface and increase with depth, while plant extractable nutrient concentrations of Mg and Mn are generally high at the surface and decrease with depth. In section 4 soils of field 13CF, the Na concentration of plant extractable nutrients is very high. It is important to note that for many elements, the analyzed concentrations were below detection limits (Al, Fe, K, P, S, Ni, Ti, Co, Cr, Cs, Cu, Pb, Se, Nb, Th, V, and Zn). The concentrations of

all PEN for each sample are included in Appendix K and depth versus PEN concentration graphs of each soil sample are illustrated in Appendix B. Because many plant extractable nutrient values were below detection limits, these were not able to be compared to fertilizer elemental concentrations.

Table 3.13. Average plant extractable nutrient concentrations at each soil sampling depth on Pelee Island as determined by ICP-MS. Standard deviations, standard errors, maximum, minimum, and average concentrations of plant extractable nutrients are also included. Note that the outlier for Na in section 4 (concentration of 284.70 ppm in field 13CF) was omitted when calculating the standard deviation, standard error, and average concentration.

Element	Units	Depth	Avg. Conc.	St. Dev.	St. Error	Max	Min
Si	ppm	1	25.50	5.61	1.29	34.01	14.52
		2	19.87	3.27	0.75		
		3	21.03	2.79	0.66		
		4	22.60	3.04	0.74		
Mg	ppm	1	221.07	50.73	11.64	289.81	36.62
		2	159.00	65.85	15.11		
		3	123.82	55.47	13.08		
		4	116.20	32.57	7.90		
Mn	ppm	1	4.91	2.94	0.68	12.74	0.10
		2	0.31	0.25	0.07		
		3	0.34	0.18	0.06		
		4	0.31	0.23	0.07		
Na	ppm	1	18.89	2.64	0.73	284.70	15.12
		2	22.29	4.06	0.98		
		3	20.73	4.60	1.12		
		4	23.27	4.08	1.09		
Mo	ppb	1	21.08	15.75	5.57	206.49	12.26
		2	38.95	33.13	9.56		
		3	65.00	33.33	7.86		
		4	96.11	40.24	9.76		
B	ppm	1	0.35	0.10	0.02	0.63	0.20
		2	0.24	0.04	0.02		
		3	0.20	0.00	0.00		
		4	0.23	0.05	0.03		
Ba	ppm	1	1.43	0.35	0.08	4.77	0.64
		2	1.18	0.62	0.14		
		3	1.33	0.59	0.14		
		4	2.09	1.05	0.25		
Sr	ppm	1	4.90	1.27	0.29	13.25	1.24
		2	4.66	1.55	0.36		
		3	5.09	2.36	0.56		
		4	5.96	2.49	0.60		
Li	ppb	1	196.31	84.62	19.41	489.94	22.63
		2	246.38	82.14	18.84		
		3	240.27	77.44	18.25		
		4	279.86	98.39	23.86		

Element	Units	Depth	Avg. Conc.	St. Dev.	St. Error	Max	Min
Sc	ppb	1	16.59	3.56	0.82	23.70	9.14
		2	12.16	1.96	0.45		
		3	12.96	1.96	0.46		
		4	13.84	2.09	0.51		
U	ppb	1	0.99	0.38	0.11	12.55	0.60
		2	4.48	2.82	0.75		
		3	4.61	2.16	0.51		
		4	4.95	2.27	0.55		
Zr	ppb	1	10.17	7.53	1.73	24.27	0.53
		2	0.80	0.27	0.10		
		3	1.73	0.92	0.53		
		4	1.35	1.36	0.68		
Rb	ppb	1	24.73	9.36	2.15	42.35	5.80
		2	11.45	3.94	0.90		
		3	15.48	4.99	1.18		
		4	18.87	7.41	1.80		

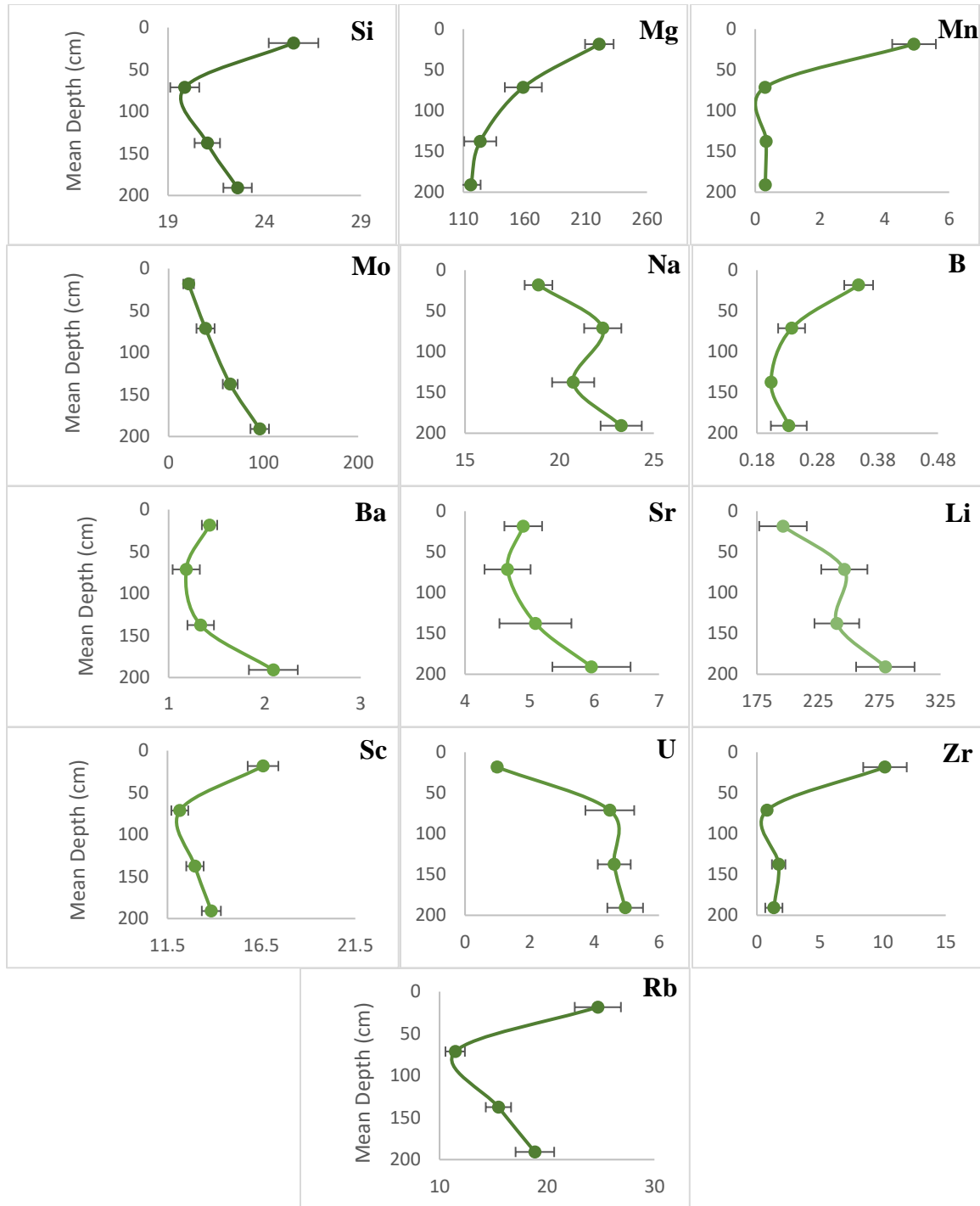


Figure 3.15. Average elemental concentrations (ppm and ppb only for Mo; y-axis) of plant extractable nutrients in soils plotted against mean sampling depths on Pelee Island. The spline curves on these graphs are meant to illustrate element concentration trends and do not imply vertical connectivity among soils samples, because markers on the graphs represent averages of soil samples selected from different locations on the island.

3.4.6 Grape Elemental Contents

We intended to compare elemental concentrations of grapes to the plant extractable nutrient data. However, the data returned from plant extractable nutrients was limited and therefore comparisons were not useful. In addition, comparing soil mineral elemental values to grape elemental values is not a good representation or indication of available elements in soils because of selective nutrient uptake and distribution in plants (Peuke 2009).

Chapter 4

4 Discussion

This chapter discusses interpretations drawn from the bedrock and soil geochemical data outlined in the results section. Further, these interpretations are used to explain whether the geology and geochemistry of the bedrock affects soil composition on Pelee Island and how the mineralogy and soil chemistry vary for Brookston and Toledo soils. In addition, soil nutrient data interpretations are used to explain how the availability of nutrients on Pelee Island varies depending on soil depth, type, or agricultural treatment.

4.1 Soil Weathering Profile

Leaching of soils on Pelee Island is most intense at the surface and decreases with depth, as has been observed in other studies (Rollinson 1993). This is evident from increasing amounts of Ca as soil depth increases and a larger relative proportion of Al in shallower soils (Figure 3.6, Table 3.7). As calcite weathers it releases Ca, which is leached into deep soils, while more resistant minerals containing Al remain in surface soils causing a relative enrichment of Al in shallow soils and enrichment of Ca in deep soils. The distribution of all soils along one trendline on an Al-K-Ca+Na ternary diagram (Figure 4.1) suggests that all soils on Pelee Island have similar source materials, but have been differentiated into highly weathered surface soils (rich in Al, depleted of Ca) and less-weathered soils (rich in Ca, depleted of Al) at depth.

Based on soil mineralogy determined from XRD analyses, Ca in the Pelee Island soils is found in the mineral calcite. Organic matter in the A-horizon creates acids that encourage the dissolution of carbonate minerals like calcite according the reaction:



Ca^{2+} ions are leached to deeper soils where pH increases and ions precipitate out of soil solution as calcite, the reverse of the reaction above (Weil and Brady 2017). Other minerals also weather in the A horizon (albeit at a much slower rate) and ions released in solution are transported via gravitational water flow to deeper soil horizons. This leaves

surface soils relatively more enriched in residual minerals, such as quartz and feldspar, that contain elements such as aluminum and silicon. The changes in mineralogy of the Pelee Island soils that result from this weathering can be observed in the XRD results (Table 3.5). The predominant mineral in soils on Pelee Island was quartz (Table 3.5), which is common in highly weathered soils. There are more feldspars in soils sampled in sections 1 and 2 than sections 3 and 4. Quartz, along with muscovite and K-feldspar, are the minerals most resistant to weathering relative to calcite and dolomite and are therefore more abundant in weathered soils (Wilson 2004). In deep soils on Pelee Island, the more easily weathered minerals, specifically calcite and dolomite, are present in greater abundance than less easily weathered minerals such as quartz, mica and feldspar. The change in mineral abundance with depth in the Pelee Island soil profile can be attributed to soil weathering, but there may also be a contribution of calcite from bedrock to overlying soils, given the increased number of stones observed in the deeper samples (Zhang et al. 2019). Mineral distributions in the Pelee Island soil profiles are typical of soils that have been forming for at least 100 years. They have a distinct A horizon, with minerals that are resistant to weathering accumulating at the surface, and deep soils that are enriched in calcite (Weil & Brady 2017).

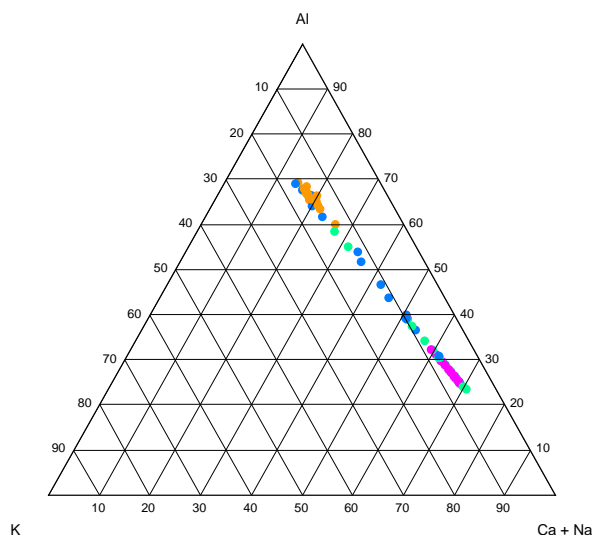


Figure 4.1. Ternary diagram illustrating weathering patterns at four soil depths across Pelee Island. Sampling depths are distinguished by colour: Section 1 soils = orange, section 2 soils = blue, section 3 soils = green and section 4 soils= purple. Surface soils (orange) are relatively enriched in Al and deep soils (purple) are relatively enriched in Ca.

4.2 Relationship Between Soil and Bedrock

The Dundee Formation and Detroit River Group are predominantly limestone formations that comprise the bedrock of Pelee Island (Hewitt 1972). The XRD results confirm that the major mineralogical components of Pelee Island bedrock are calcite and dolomite (Table 3.6). Soils derived from limestone bedrock have high carbonate content, such as those on Pelee Island, suggesting that the bedrock on Pelee Island may contribute to or influence the source material from which the soils were formed (Weil & Brady 2017). In addition, Slack (2015), suggested that sulfur-rich ground waters on Pelee Island might leach elements from the bedrock into the overlying soils and further contribute to their geochemistry. Bruno Friesen, the vineyard manager at Pelee Island, noticed that shallow soils were less productive compared to deep soils and hypothesized that bedrock may be altering the chemistry of the shallower soils. However, in areas where glacial drift is more than 60 cm thick, limestone bedrock should have little contribution to soil chemistry. Where soils are < 30 cm thick, bedrock dominates soil formation and controls REE concentration patterns (Hornung 1971). Thus, one of the objectives of this study was to determine the influence of bedrock on the chemistry of the soils on Pelee Island. To this end, REE were used to determine the extent to which the limestone bedrock on Pelee Island contributes to the overlying soil composition.

4.2.1 Rare Earth Elements

Rare earth elements are good indicators of geochemical processes and soil development (Zhang 2019) and are used to identify parent material of soil and track pedogenic processes (Laveuf & Cornu 2009). The low solubility and mobility of REE due to their high valence state (+3) makes it more difficult for REE to be released into solution (Laveuf & Cornu 2009). Thus, REE content in soil profiles can be used to identify the source rocks of soil minerals that have been changed by weathering (Martin et al. 1978; Gromet & Silver 1983). Studies show that because REE are released during soil weathering, weathering processes control the levels of element concentrations in the soil (Nesbitt 1979, 1996; Nesbitt et al. 1980; Middelburg et al. 1988; Nesbitt and Markovics 1997; Aubert et al. 2001; Aubert et al. 2004). However, Bryanin & Sorokina (2014) found that the processes of soil formation do not influence relative abundance, or

distribution, of REE in soil horizons. This means that concentrations of REE may be different between soil and bedrock and even between soil horizons. However, REE distribution patterns should be the same between soil and bedrock if the bedrock was the parent material for the soils.

In a study conducted by Schilling et al. (2014), REE were used to compare soil and bedrock composition in Norway, where normalized REE concentration values of soil and bedrock samples were plotted to compare anomalies and element concentrations. The authors found that bedrock and soil had similar REE anomalies and concentrations, indicating an in-situ formation of the soils. A study done by Gouveia et al. (1993) concerning the behavior of REE and other trace elements during the weathering of granitic rocks found that the REE distribution patterns were the same in soil and the underlying bedrock, indicating that soil REE signatures were inherited from the host rock. In contrast, Zhang et al. (2019), in their study of the distribution, fractionation, and controlling factors of REE in 8 soil profiles in China found that distribution patterns of REE in soils and bedrock were not the same and they concluded that the source of the soils was not the bedrock. Concentrations of REE in both soil and bedrock on Pelee Island are reported in Table 3.8. The different distribution of REE in soils versus bedrock on Pelee Island confirms that Pelee Island soils were not formed from Pelee Island bedrock nor does bedrock have any influence on the overlying soils (Figure 3.11a, 3.11b and 3.12).

The parent material of the soils on Pelee Island is the underlying glacial tills. Both Brookston and Toledo soils were formed from glacial activity (Sposito et al. 2008). These soils are widely distributed and are found in southern parts of Ontario, such as the Essex and Kent County regions, and in some of the northeastern states such as Wisconsin, Indiana, Michigan, and Ohio (Evans & Cameron 1983; National Cooperative Soil Survey 2012; National Cooperative Soil Survey 2014). Brookston soils formed from loamy till, which is found in depressions on till plains and from moraine material of Wisconsinan age (National Cooperative Soil Survey 2014), whereas Toledo soils formed from clayey glaciolacustrine sediment deposited on Wisconsinan age lake plains (National

Cooperative Soil Survey 2012). Similar patterns and concentrations of REE in the tills and soils on Pelee Island (Figure 3.12) confirm that the soils are formed from glacial till.

The REE concentrations are not significantly different among fields, as indicated by p-values >0.05 determined by a one-way ANOVA. However, differences in REE abundances were observed among soil depths. Many studies have found that in natural soils, REE concentrations increase with depth. For example, in a study conducted by Prudencio et al. (1993) determining REE mobilization, fractionation, and precipitation during weathering of basalts, found REE concentrations were greater in deep soils as a result of weathering and low pH at the surface. Thus, surface soil horizons become depleted of REE as a result of leaching and surficial erosion and accumulated in deeper horizons (Aide 2012). However, we observe the opposite trend in Pelee Island soils. Pelee Island soil REE concentrations are enriched in surface soils and decrease with depth (Figure 3.9b). Other studies that report REE concentrations in agricultural soils also found higher concentrations of REE in surface soils relative to deeper soils (Volokh et al. 1990; Tyler 2004; Germund & Tommy 2005; Hu et al. 2006). It has been suggested that this pattern is attributed to the addition of fertilizers to surface soils. Phosphate is a main component of fertilizers and it easily incorporates REE into its structure (Otero et al. 2005; Laveuf & Cornu 2009; Zhang et al. 2019). Hu et al. (2006) estimate that if an application of $300 \text{ kg ha}^{-1} \text{ year}^{-1}$ of phosphate fertilizers containing 30 to 170 g ha^{-1} REE are added to soils each year, the REE content of the soils will double over the span of about 160 years (Laveuf & Cornu 2009). On Pelee Island however, REE distribution patterns of the soils and chemical fertilizers are not the same (Figure 3.14). In addition, the organic field (24CF) and field 5GM318, receive no chemical fertilizers but have the same REE distribution patterns as the fertilized fields (Figure 3.9a). Further, fertilizers are applied to surface soils, however, Pelee Island soils display the same REE distribution patterns at all depths within the soil profile (Figure 3.9b). Both observations indicate that the source of REE in Pelee Island surface soils is not the chemical fertilizers.

Some studies offer alternative explanations for enrichment of REE at the surface of agricultural soils (Aide et al. 1999; Aide and Smith 2001; Ohta & Kawabe 2001; Stille et al. 2009; Galbarczyk-Gasiorowska 2010; Zhang et al. 2019). One suggestion is that when

plant litter starts to decompose at the surface, it releases elements into solution. These elements, particularly REE that have a small ionic radius and high positive charge, are taken up by the negatively charged surfaces of organic matter particles and cause a slight accumulation of REE in surface soils. Further, studies found that the main soil parameters influencing concentrations of REE within the soil profile were total phosphorous (TP) content, metal hydroxide content (namely Fe and Mn), pH, CEC, clay mineral content, and soil organic matter content (Laveuf & Cornu 2009). During weathering, when minerals such as calcite dissolve, organic matter, phosphates and hydroxides can incorporate residual REE into their structures or adsorb REE onto their surfaces. Mineral weathering releases REE thus resulting in formation of phosphate and organic complexes with REE and adsorption of REE onto clay minerals coated with both Fe and Mn oxides and hydroxides. The organic matter is negatively charged, thus has a high capacity to complex and adsorb highly positively charged REE (Cantrell & Byrne 1987; Lee & Byrne 1993; Johannesson et al. 1996; Aide et al. 1999; Taunton et al. 2000; Ohta & Kawabe 2001; Schijf & Byrne 2001; Aide and Smith 2001; Laveuf & Cornu 2009). This is likely the cause of high REE in surface soils on Pelee Island, as the surface soils are rich in organic matter (3.05 to 8.15%, Table 3.2). Additionally, locally grown compost is added to the surface soils on Pelee Island. Figure 3.14 shows that the REE distribution patterns of soils and compost are the same, although, the absolute REE concentrations are higher in the soil, and display no fractionations among REE, suggesting enrichment in surface soils is a result of plant recycling. Adding compost increases organic matter content in surface soils on Pelee Island resulting in formation of organic complexes with REE, thus holding them in surface soils. The compost is locally grown and thus any REE taken up by plants used for compost (alfalfa and grasses) will be recycled to surface soils, causing an enrichment of REE near surface (Laveuf & Cornu 2009). Jowitt et al. (2017) also suggested that intense weathering in surface soils dissolves easily weathered minerals such as calcite, while resistant heavy minerals (minerals with density $>2.9 \text{ g/cm}^3$) with relatively higher concentrations of REE remain in surface soils (Jowitt et al. 2017).

4.3 Using PCA to Identify Controls on Pelee Island Soil Geochemistry

Initially, this study was undertaken to assess whether bedrock was affecting the chemistry and fertility of soils on Pelee Island. Vineyard management had for years noticed differences in productivity among fields and suspected the trend was related to depth of the soils (i.e. depth to bedrock) or was related to contribution of bedrock elements to the soils from percolating groundwater. However, our study has demonstrated that bedrock geochemistry has no influence on soil chemistry at Pelee Island. In order to better understand the causes and amount of variation in soil chemistry across the vineyard, principal component analyses (PCA) was used to assess all elemental data for 19 soil profiles with 4 depths each. The PCA identifies patterns in variations among the element concentration data. By examining which elements vary in a similar (or opposite) manner and identifying at which depths and locations these variations are most extreme, we can determine which processes cause the variations. Possible controls on variations of elemental concentrations in soil include weathering, agricultural practices (e.g. fertilizers), organic matter or clay mineral content and soil depth to bedrock. Although we have already shown that the bedrock does not control soil chemistry, the depth to bedrock may affect water movement or retention in the soils, which in turn affects drainage, organic matter preservation and mineral weathering.

Principal component analysis (PCA) is a well-established statistical technique that is used to identify variations among large data sets with multiple variables. For this study, PCA was used to identify common variations in elemental concentrations among soil samples. These variations are called principal components (PC) and are derived using a series of mathematical equations. The software used to run the PCA was PLS Toolbox Version 8.0.1 from Eigenvector Research running on Matlab R2015a. This software is preprogrammed with PCA equations and uses statistical analysis to assign numerical values to soil samples and elemental variables defined by each PC. All data was auto scaled prior to analysis. In this procedure, the data are first mean-centered. This is done by subtracting the column mean from each column, thus forming a matrix where each column has a mean of zero. Each mean-centered variable is then divided by its standard

deviation, resulting in variables with unit variance. This procedure puts all variables on an equal basis in the analysis. Thus, the less abundant and trace elemental species receive the same level of consideration as bulk constituents. The principal component analysis model is then applied to the data.

The first principal component (PC1) describes the most variation in the data.

Subsequently, the variation explained by PC1 is mathematically removed from the data set and the same statistical analysis is used to identify variance explained by the second principal component (PC2). This process of removing each subsequent PC after variance has been explained is repeated until most of the variance can be explained by several PCs. Each subsequent PC accounts for a lesser amount of variance within the data set. Eigenvalues assigned to each PC are used to indicate the significance of each, and where eigenvalues are >1 , the corresponding PC's are significant.

To interpret variation among the data, the PCA program assigns numerical "scores" to each individual sample (soil samples) and "loadings" to each variable (elements).

Seventy-three soil samples, represented by 73 scores, and 54 elements, represented by 54 loadings are present for each principal component (PC). These scores and loadings are plotted on two separate bar graphs and must be used together for interpretations. The PC loadings describe correlations among variables, in this case, among elemental concentrations. Two or more elements with large positive loadings have concentrations that are positively correlated with each other. Two or more elements with large negative loadings have concentrations that correlate positively with each other. Elements with large positive loadings have concentrations that correlate negatively with elements with large negative loadings. In contrast, the concentrations of elements with small loadings (positive or negative) are not well correlated with other elements. Because correlations improve when there is a greater variation (spread) in the data (element concentrations), the magnitude of each loading also indicates which elements have a stronger influence on the variation identified by that principal component. Larger loadings (positive or negative) mean that those elements have a stronger influence on the PC than elements with smaller loadings.

For each PC, soil samples are given scores that indicate how much that soil sample contributes to the variation of the element concentrations described by that PC. If we were to consider only two variables that are positively correlated, for example Si vs. Al concentrations among our soils, the amount of variation (i.e. the spread in concentrations) would be defined by the soils with highest and lowest concentrations and these values would have higher magnitude scores (positive and negative, respectively). It is more complicated when considering 54 variables (elements) at once. In simple terms, the score is based on the sum of all element concentrations weighted by their contribution to the total variation (spread). Hence in our PCA, soils with high relative concentrations for the elements that have high positive loadings are given high positive scores and soils with low relative concentrations of the same elements (and/or high concentrations of elements that have negative loadings) are given very negative scores. The magnitude and direction of the scores indicate how similar, or different, soil samples are to one another. Two or more soils with high positive scores have similar elemental concentrations. Two or more soils with large negative scores have similar elemental concentrations. Soils with small scores (positive or negative) do not have element concentrations that strongly influence the variation of that PC. Note that soil samples, shown on the scores bar-graphs, are grouped by depth: yellow = section 1 soils; blue = section 2 soils; green = section 3 soils; and orange = section 4 soils. Within these depth groupings, soil samples are ordered according to location; samples listed from left to right on the bar graph represent locations from south to north on the island.

In addition to the scores and loadings bar graphs, bubble plots are included to provide a spatial representation of the data. The size of the bubble represents the score of a soil sample and each sub-graph shows samples from the same soil layer; sections 1, 2, 3, and 4 soils. The x-y coordinate of the bubbles on the graphs represent their locations on the island. The x-axis represents the easting and the y-axis represents the northing, both in decimal degrees. The blue bubbles represent positive scores and the white bubbles represent negative scores. The size of the bubble represents the score magnitude; larger bubbles have larger positive/negative scores and smaller bubbles have smaller positive/negative scores. The loadings must also be used together with the bubble plots for elemental distribution interpretations.

4.4 Mineral Principal Components

4.4.1 Mineral PC1

Principal component 1, illustrated in Figure 4.2, accounts for 72.09% of variance within the data and has an eigenvalue of 39.00. The sample scores bar-graph shows that there is a major difference between soils from sections 1 and 2 versus soils from sections 3 and 4. Soils from sections 1 and 2 show positive scores, whereas sample sections 3 and 4 show negative scores. This indicates that there is a strong difference in elemental concentrations between topsoil and subsoil. Although PCA is useful for identifying variations in large data sets, knowledge of soil chemistry must be applied to explain the observed variations.

Most of the loadings for PC1 have high positive values, with a few elements (Ca, Mg, Sr) having very low negative values. All of the elements with tall positive bars are positively correlated with each other, but negatively correlated with the behavior of elements like Ca, Mg, and Sr. For example, there are strong positive correlations between element concentrations of K versus Al and Si versus Al in the Harker diagrams, but negative correlations for Ca versus Al (Figure 3.4). The two shallower soil sampling depths (1 and 2) have positive scores that are associated with positive loadings of most elements (Figure 4.2). Associations between scores and loadings indicate connections and causalities; meaning, for example, changes in independent variables (e.g. soil weathering, organic matter, clay mineral content) will cause changes in dependent variables (elemental abundances) (Altman & Krzywinski 2015). In depth versus elemental concentration graphs (Figure 4.3) these elements (with positive loadings) are more abundant in shallow soils and decrease in concentration with depth. Hence, the positive scores and loadings reflect the higher concentrations of these elements in soil layers 1 and 2. Note that the spline curves on these graphs (and all depth versus element concentration graphs in section 4.4) are meant to illustrate element concentration trends and do not imply vertical connectivity among soils samples, because markers on the graphs represent individual soils samples selected from different locations on the island. For example, Figure 4.2 illustrates that Al and Si are most abundant in section 1 and 2 soils and their abundance decreases in section 3 and 4 soils. Conversely, soils from sections 3 and 4

have negative scores indicating that they are more enriched in Ca, Mg, and Sr (Figure 4.2). Abundances of Ca, Mg, and Sr are low at the surface and increase in abundance with increasing depth. Hence the negative loadings for these elements means that they are negatively correlated with elements such as Al and Si, whereas the negative scores for soils in sections 3 and 4 mean that they have high concentrations of Ca, Mg, and Sr. Variation of elemental abundances versus depth that explain most other elements in PC1 do not explain variation for Na and Mo concentrations, hence loadings and scores are low.

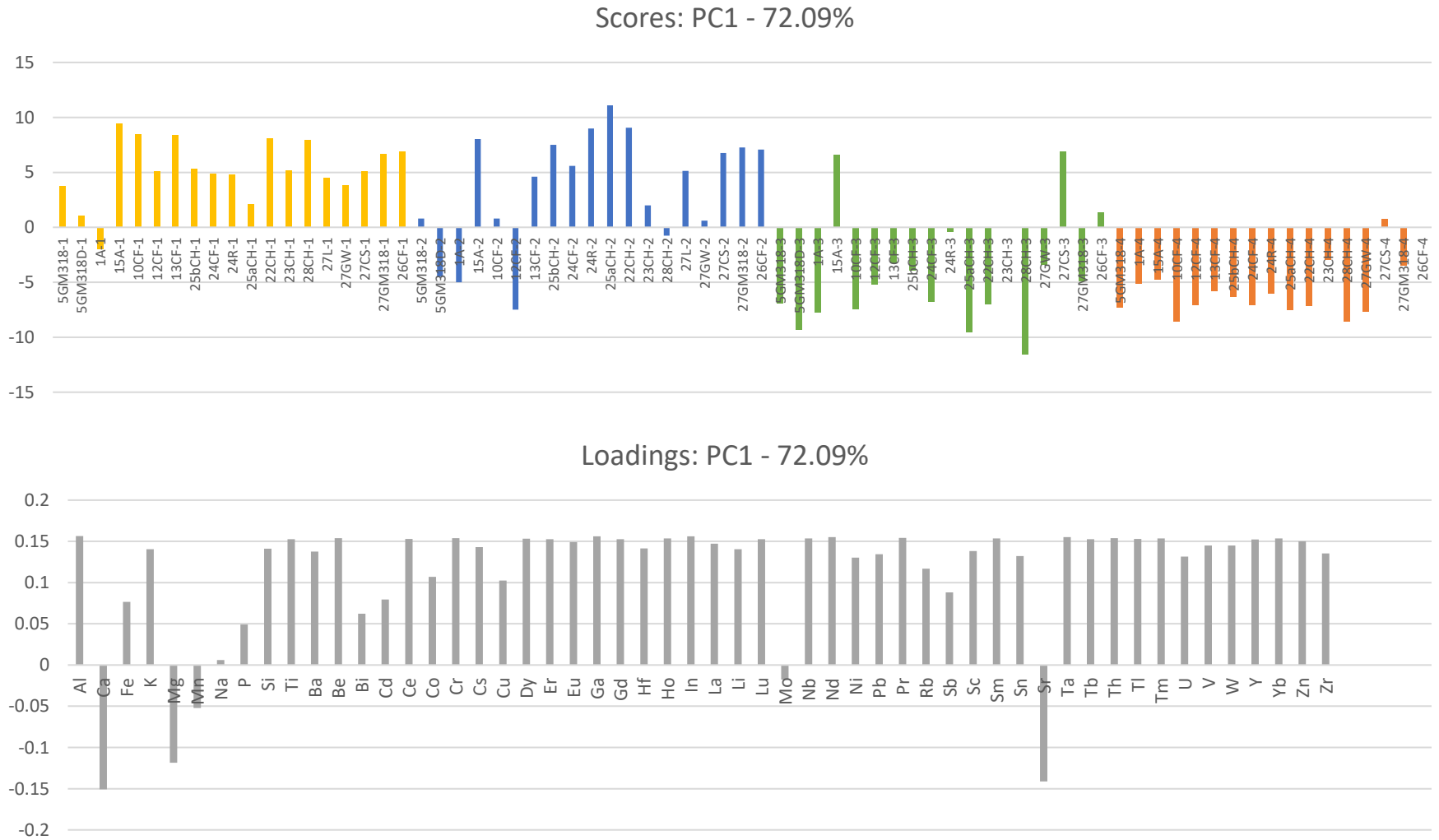


Figure 4.2. PC1 scores and loadings, illustrating elemental variations at depth and among field locations on Pelee Island. Scores in this figure are arranged by location (left to right on the graph represents south to north on the island) and by depth (yellow = section 1 soils, blue = section 2 soils, green = section 3 soils, and orange = section 4 soils). The magnitude of the bars on each graph indicate the strength of the correlations between scores (soil samples) and loadings (elements).

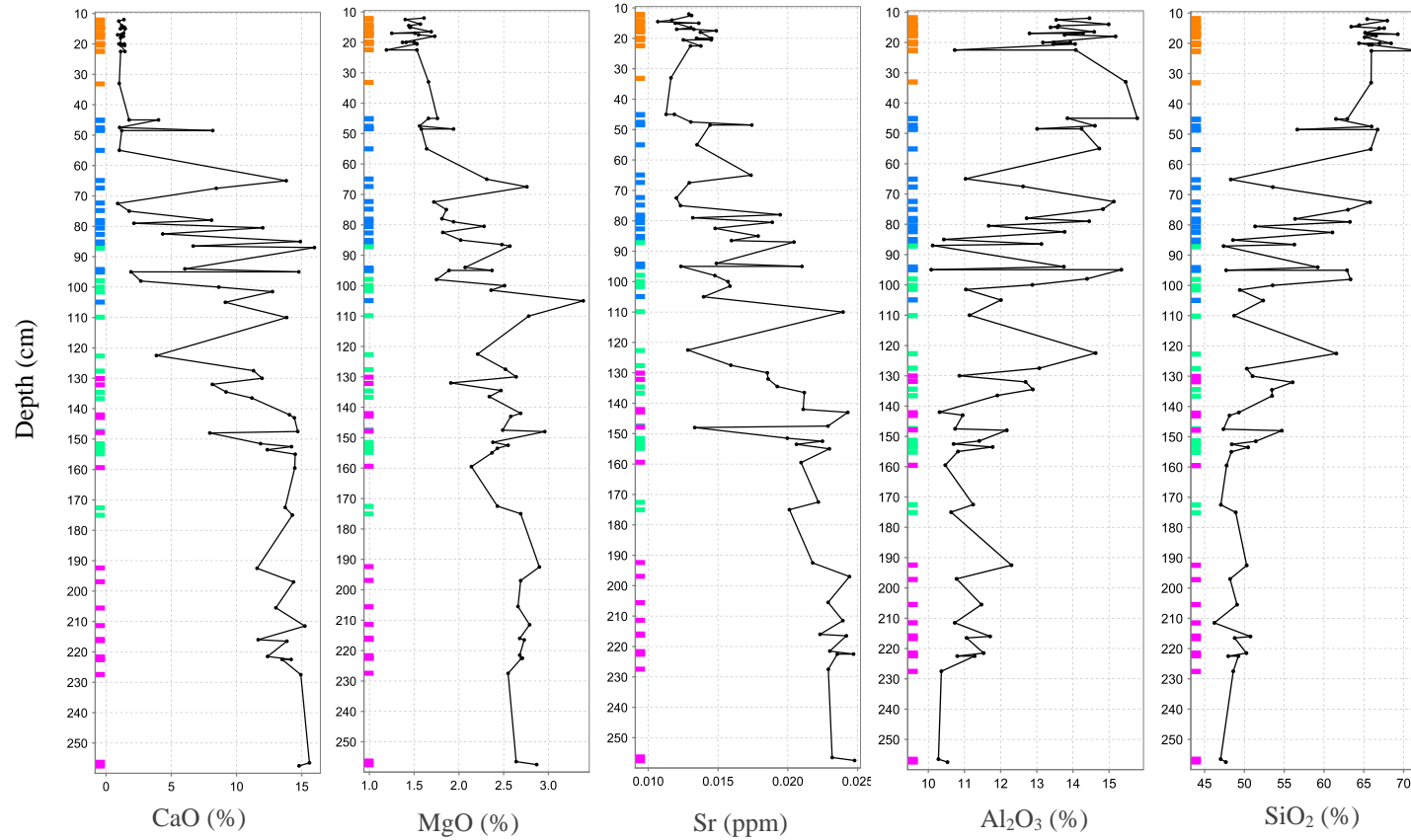


Figure 4.3. Depth versus concentration graphs comparing concentration differences with depth of Sr, CaO, MgO, MnO, Al₂O₃, and SiO₂. Soil sample depth of each soil sample plotted against concentrations (Sr, CaO, MgO, MnO, Al₂O₃, SiO₂) of each soil sample. Data is compiled from all 19 soil profiles. Soil sampling depths are distinguished by colour on the left side of the graph: Section 1 = orange, section 2 = blue, section 3 = green, and section 4 = purple.

The results indicate that PC1 describes the variation in relative elemental concentration with depth in the soils. Considering that PC1 accounts for 72% of the variation in the data, this means that the variation in elemental concentration with depth in one profile is greater than the variation between different fields. Additionally, bubble graphs shown in Figure 4.4 provide spatial representation of soil scores. Soil samples taken in section 1 and 2 have mostly positive scores (blue bubbles) whereas graphs representing soil samples taken in sections 3 and 4 have mostly negative scores (white bubbles). This figure can be used to see how well soils across the island are described by PC1. For example, no trends are observed in scores (e.g. size or colour of bubbles) from the east to the west side of the island as depth to bedrock increases. However, for the three Brookston soils (the 3 most southern sites), the scores switch from positive values in layer 1 to negative values in layer 2. This reflects the fact that the Brookston soils are not as depleted of elements like Ca, Mg and Sr in section 2 as was observed for most Toledo soils, and that in section 1 and 2, Brookston soils have lower concentrations of Al compared to Toledo soils. In section 1, Brookston soils have Al concentrations ranging from 10.5-13% whereas in Toledo soils, the concentrations are between 13-15.5%. In section 2, Brookston soils have Al concentrations ranging from 11-13% whereas Toledo soils have Al concentrations ranging from 10-16% (Figure 4.5).

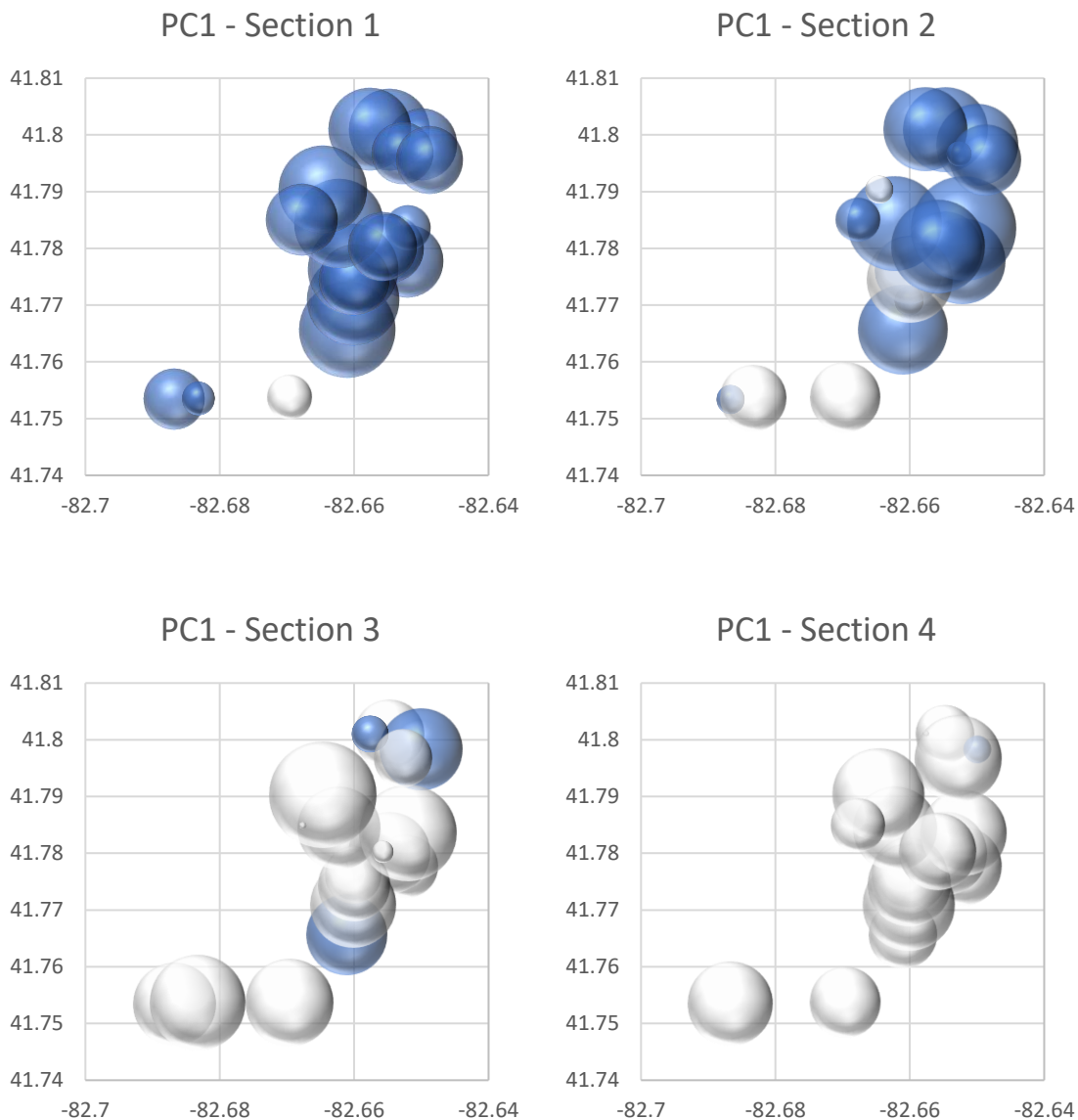


Figure 4.4. Bubble plots for PC1 provide spatial representation of the element data on Pelee Island and are to be used together with the element loadings plot from PC1. Each graph represents element loadings at sections 1, 2, 3, and 4. The x-y coordinates of the bubbles on the graphs represent their locations on the island in decimal degrees (easting; x-axis, northing; y-axis). Colour indicates positive or negative scores; blue is positive and white is negative. Size of the bubbles indicates magnitude of correlations between scores (soil samples) and loadings (elements).

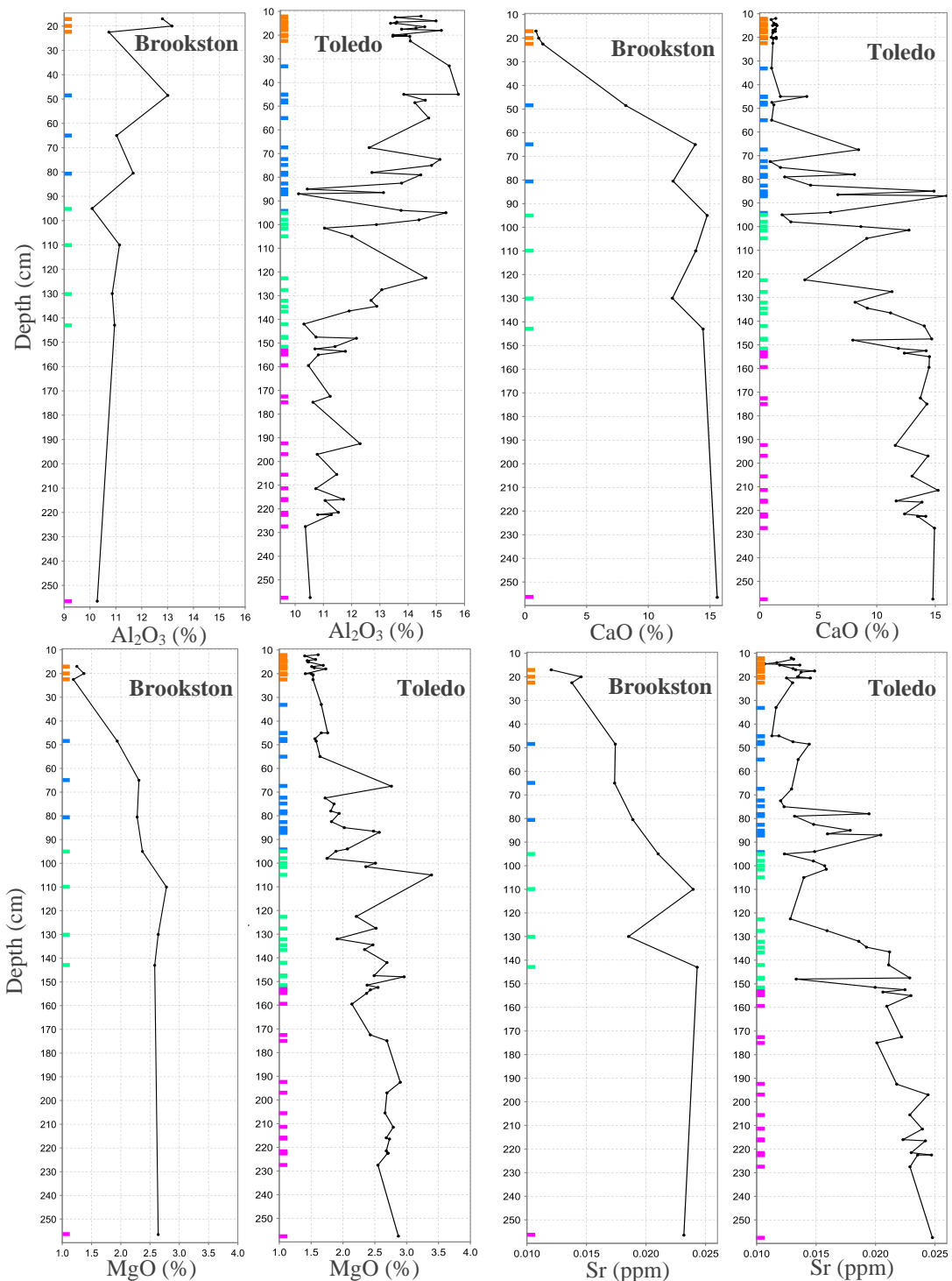


Figure 4.5. Depth versus concentration graphs comparing concentration differences with depth of Al, Ca, Mg, and Sr between Brookston and Toledo soils. Soil sample depth of each soil sample plotted against elemental concentrations (Al, Ca, Mg, Sr) of each soil sample. Soils sampling depths are distinguished by colour on the left side of the graph: Section 1 = orange, section 2 = blue, section 3 = green, and section 4 = purple.

A survey conducted by Sheppard et al. (2009) examined 59 agricultural soil profiles in southern Ontario, and analysed 50 elements at three soil depths from 0-60 m. Sheppard et al. (2009) also found that surface soils were depleted of Ca, Mg, and Sr and subsoils were enriched in these elements. Magnesium and Sr are associated with calcite because their similar ionic radius allows them to readily substitute for Ca, and because Mg and Sr are geochemically similar, these elements correlate positively with Ca in the PCA (Thorpe et al. 2012; Xiaolei et al. 2012). Sheppard et al. (2009) found that in deep soils Mg and Sr are adsorbed onto mineral surfaces and/or are absorbed within mineral structures. Conversely, shallow soils have a higher abundance of almost all other elements relative to deep soils. For example, major elements Si and Al and most trace elements are highly concentrated in the surface soils and their concentrations decrease in the deeper soils. Si and Al are concentrated in the surface soils because they remain in residual minerals left behind in upper horizons during mineral weathering (Weil & Brady 2017).

The loadings of elements Mn and Fe are smaller compared to most other elements in PC1, probably because there is a different behaviour for these elements between Brookston and Toledo soils. An accumulation of oxides (particularly Mn and Fe) at depth in a soil is an indication of a well-developed B horizon (Weil and Brady, 2017). Brookston soils don't show accumulation of Mn and Fe oxides in section 2, unlike Toledo soils (Figure 4.6). The absence of accumulation of Mn and Fe at depth in Brookston soils may indicate that the zone of accumulation (B horizon) is less developed in the Brookston compared to the Toledo soils. In addition, CO_3^{2-} content in section 2 and 3 is lower in Toledo soils with average values of 4.25 and 9.87% respectively compared to CO_3^{2-} in sections 2 and 3 in Brookston soils with average values of 9.44 and 12.71%, respectively (Table 3.3). The higher carbonate content in sections 1 and 2, and the higher Ca and Sr content in section 2 in Brookston soils relative to Toledo soils suggest there is less leaching in the A horizon of Brookston soils. In addition, more highly leached soils will have a lower Si:Al ratio (Weil and Brady, 2017). Figure 4.7 compares silicon versus aluminum concentrations at all four depths in Brookston and Toledo soils. In section 1, Brookston soils have a higher Si:Al ratio compared to Toledo soils because they are less leached and this is consistent with lower clay particle content of section 1 in Brookston soils (shown in grain size diagram Figure 3.3). Figure 4.7 also

shows that Brookston soils have less Al content in section 1 and 2 soils compared to Toledo soils, thus indicating that Brookston soils are less leached than Toledo soils. Although the pH values are comparable, Toledo soils are slightly more acidic than Brookston soils (Figure 4.8), which would result in greater dissolution and leaching. Organic matter likely contributes to the higher acidity of the Toledo soils. The soil organic matter content is higher in Toledo soils in sections 1, 2, and 3 with average values of 5.5, 3.2, and 2.6%, respectively, compared to Brookston soils with average organic matter contents at depth 1, 2, and 3 of 3.8, 2.7, and 2.1%, respectively (Table 3.2).

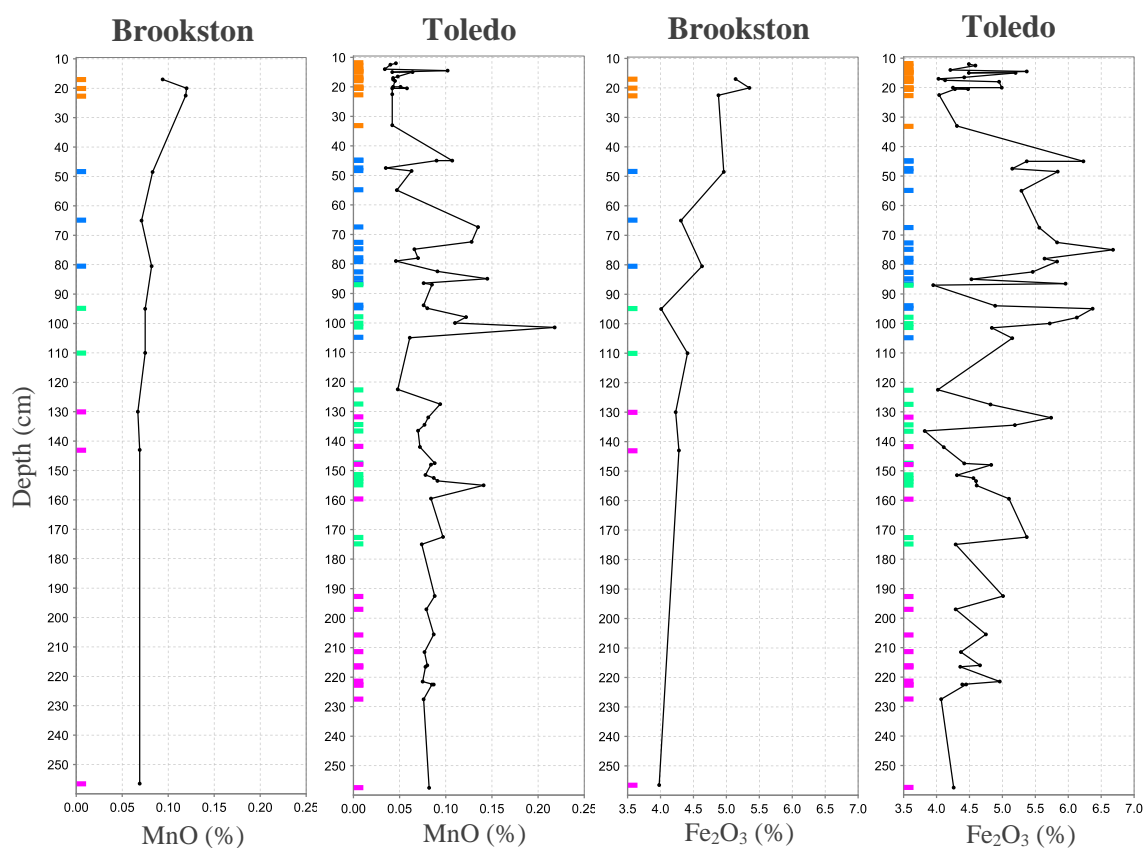


Figure 4.6. Depth versus concentration graphs comparing concentration differences with depth of MnO and Fe₂O₃ between Brookston and Toledo soils. Soil sample depth of each soil sample plotted against elemental concentrations (Mn, Fe) of each soil sample. Soils sampling depths are distinguished by colour on the left side of the graph: Section 1 = orange, section 2 = blue, section 3 = green, and section 4 = purple.

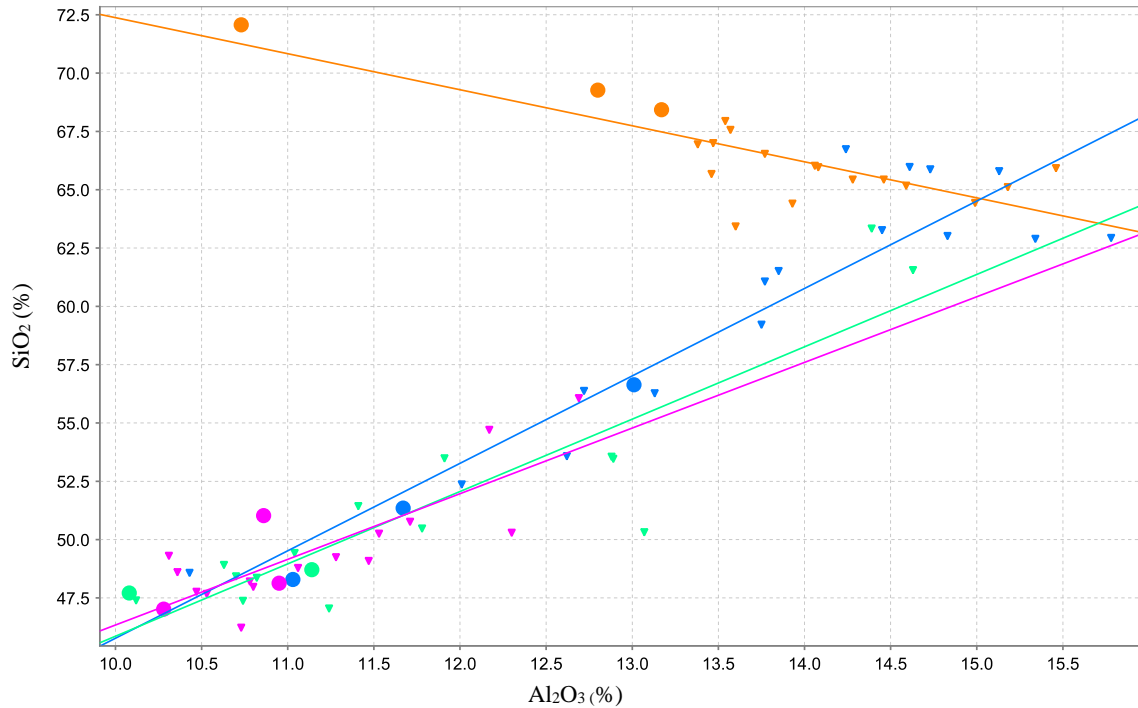


Figure 4.7. Silicon oxide versus Al_2O_3 concentrations in Pelee Island soils. Soil type is indicated by size and shape: Brookston = large circles, Toledo = small triangles. Soil sampling depths are distinguished by colour: Section 1 = orange, section 2 = blue, section 3 = green, and section 4 = purple.

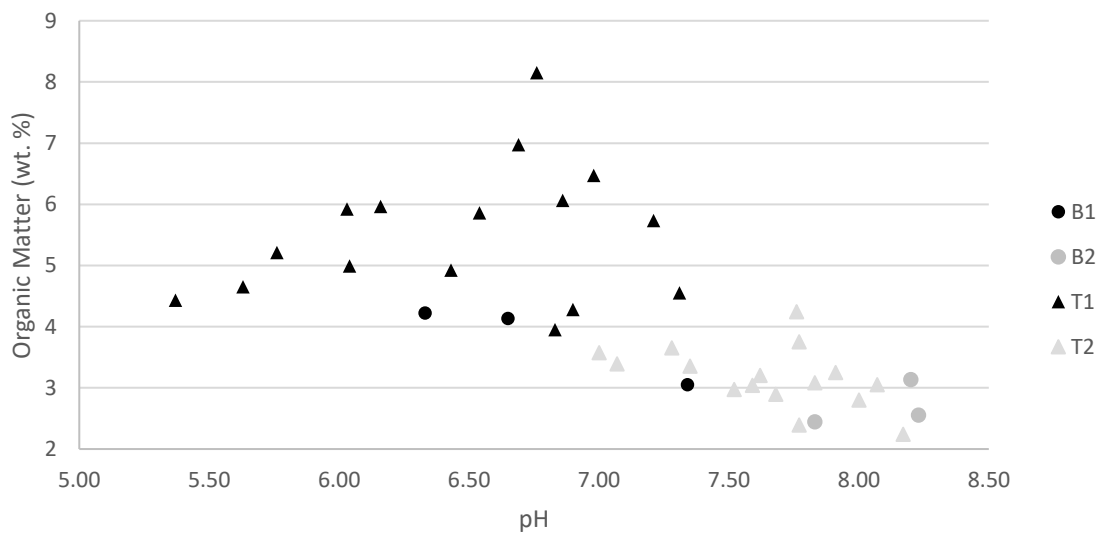


Figure 4.8. Organic matter content versus pH values in Brookston and Toledo soils in sections 1 and 2. Each point on the graph represents one soil sample. In sections 1 and 2 Toledo soils have lower pH and higher organic matter content than Brookston soils. B1 = Brookston soil sampled in section 1, B2 = Brookston soil sampled in section 2, T1 = Toledo sampled in section 1, T2 = Toledo sampled in section 2.

The loading value for P is smaller than for other elements. The P content of the soils is only weakly affected by leaching. Phosphorous was the only oxide that showed variation in concentration among fields ($p < 0.05$), with most of the variation occurring in section 1 soils. However, unlike elements Mn and Fe, P concentrations are likely affected by fertilizer strategies on different fields. A one-way ANOVA proved that most variation among elemental P_2O_5 concentrations was dependent on the month the soil was sampled. For example, P_2O_5 concentrations were greater in fields that were sampled in August and lower in fields that were sampled in October (Figure 4.9). This is likely because of the timing of fertilizer application. The variation in P_2O_5 across fields is not related to weathering as also shown by the poor correlation with Al_2O_3 in the Harker diagrams (R^2 values of 0.09, 0.01, 0.43, and 0.35 in sections 1, 2, 3, and 4 soils respectively) (Figure 3.4).

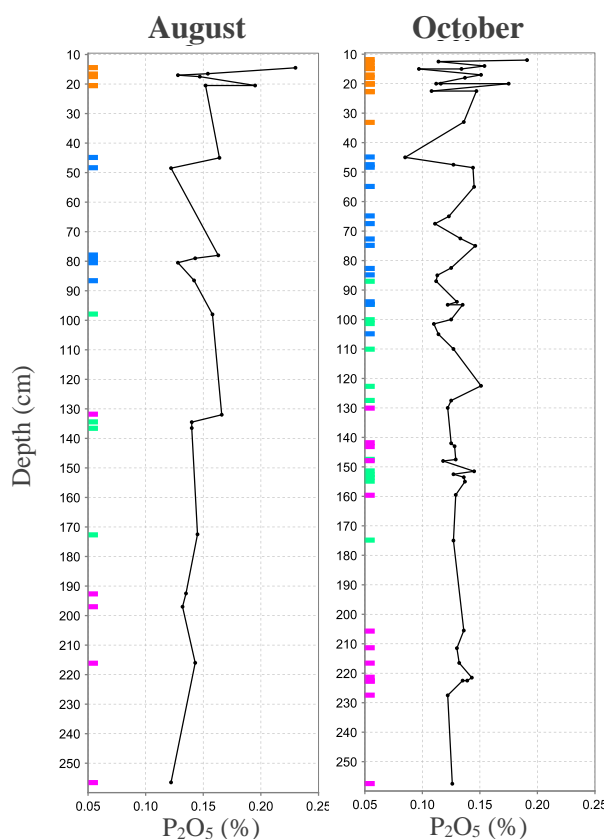


Figure 4.9. Depth versus concentration graphs comparing concentration differences with depth of P_2O_5 between sampling dates (August and October). Data is compiled from all 19 soil profiles. Soil sampling depths are distinguished by colour on the left side of the graph: Section 1 = orange, section 2 = blue, section 3 = green, and section 4 = purple.

Principal component 1 highlights the elemental differences among depths, but elemental differences among fields can also be observed. Some of the differences in scores among fields at the same depths can be attributed to the variability in depth at which each layer was sampled in different fields. For example, field 12CF in section 2 is behaving more like soils sampled in section 3 from other locations. The soil core for field 12CF was very long and therefore, to sample equally throughout the length of the core, the second sample was taken from deeper in the soil. Hence, field 12CF section 2 was sampled at 85-100 cm, which is deeper than section 2 in most other soil profiles (45-105 cm). As a result, the section 2 soils from field 12CF had low Al_2O_3 contents (10.43% compared to the average of $13.53\% \pm 1.50\%$) and high CaO contents (14.90% compared to the average of $5.65\% \pm 4.55\%$), which is often seen in section 3 and 4 soil samples from other locations. Likewise, sampling sections 3 in profiles 15A and 27CS are quite shallow, with depths of 122.5 cm and 98 cm respectively, compared to the average sampling depth of 137.6 cm. For this reason, they behave like section 2 soil samples seen in most other profiles (depleted of Ca and enriched in Al relative to other soil samples sampled in section 2). See Appendix H for CaO and Al_2O_3 values of fields 15A and 27CS.

The three Brookston soils (5GM318, 5GM318D and 1A) have smaller scores than the Toledo soils. This is because the weathering profiles are not as well developed (e.g. less leaching of calcite in the A-horizon). Notably, field 1A behaves differently from most other soils in sections 1 and 2 soils. In section 1 soils, field 1A does not contribute significantly to the variation described by PC1. The score for field 1A in section 2 soils is more associated with elements Ca, Mg, and Sr because it contains higher abundances of Ca, Mg, and Sr and lower abundances of most other elements relative to other fields at the same depth (see Appendix H for additional elemental concentrations in field 1A). In particular, Al_2O_3 is quite low in section 1 soils of field 1A, with a concentration value of 10.73% compared to the average of 13.81%. Field 1A is quite shallow (<1 m deep) and although records are not available, we speculate that this alfalfa field was tilled in the past, which would result in mixing of soil horizons. Alternatively, broadcast fertilizers (applied to surfaces of soils over large areas) may have introduced higher amounts of nutrient and trace elements to the surface of this field, resulting in poor correlations

between elements whose concentrations are determined by weathering processes. For example, field 1A has high abundances of MnO at the surface, which is one of the fertilizers applied when herbicides like Round-up are used.

4.4.2 Mineral PC2

Principal component 2, illustrated in Figure 4.10, accounts for 8.72% of the variance in the data and has an eigenvalue of 4.80. The element loadings show that there is a moderate positive correlation between the concentrations of major elements Ca, Fe, K, Mg, and Mn and minor elements Co, Cs, Mo, Ni, Rb, Sb, and Sc. There is also a moderate positive correlation between the concentrations of major elements Na, P, Si, and Pb. When concentrations of, for example, Na are high, so are concentrations of P, Si, and Pb. The strongest negative correlation is between the amounts of Na and Mo. Concentrations of Na are lower when nutrients like Mo, Ca, K and Mg are abundant. Bubble plots show that the spatial distribution of elements on the island is not well described by PC2 (Figure 4.11).

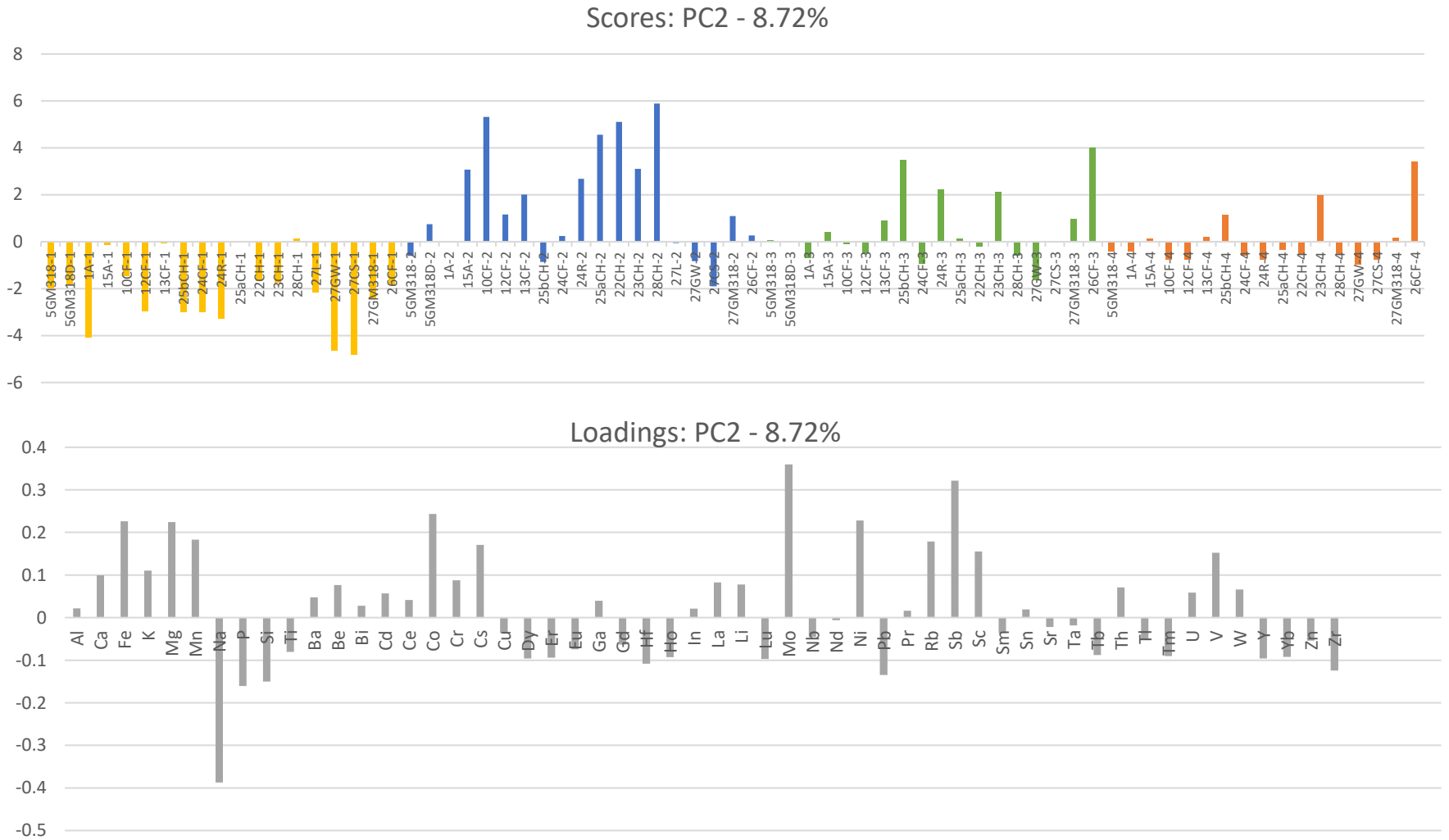


Figure 4.10. PC2 scores and loadings, illustrating elemental variations at depth and among field locations on Pelee Island. Scores are arranged by location (left to right on the graph represents south to north on the island) and by depth (yellow = section 1, blue = section 2, green = section 3, and orange = section 4). The magnitude of the bars on each graph indicate the strength of the correlations between scores (soil samples) and loadings (elements).

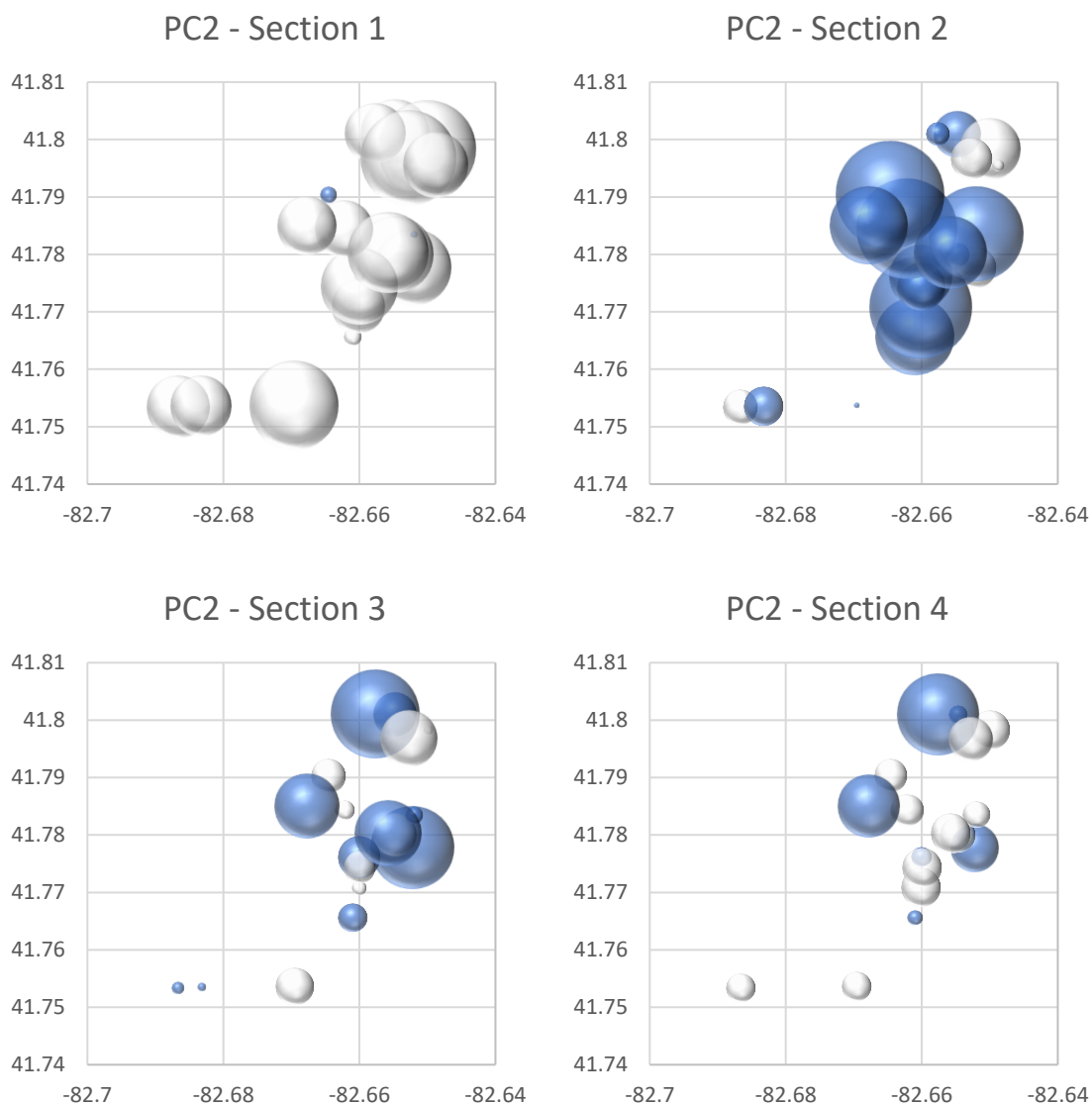


Figure 4.11. Bubble plots for PC2. These graphs provide spatial representation of the element data on Pelee Island. Each graph represents element loadings at sections 1, 2, 3, and 4. The x-y coordinate of the bubbles on the graphs represent their locations on the island in decimal degrees (easting; x-axis, northing; y-axis). These graphs are to be used together with the loadings plot for PC2. Colour indicates positive or negative scores; blue is positive and white is negative. Size of the bubbles indicates magnitude of correlations between scores (soil samples) and loadings (elements).

The most dramatic difference among soil sample scores for PC2 is between soils in section 1 versus 2 soils. The results of PC2 indicate higher elemental abundances in soil depths where there are both high positive loadings and score bars and high negative loadings and score bars. These trends can be verified by examining changes in oxide and

element concentrations with depth in soils but note that the trends in these figures primarily reflect weathering processes described by PC1 except for elements like Na and Mo that contributed very little to the variation in in PC1. The PC2 results indicate that soil samples taken from section 1 have higher concentrations of Na, P, Si, and Pb (Figure 4.12), whereas samples taken from section 2 have a stronger influence and greater abundance of Mo and Sb and to a lesser extent Fe, Mg, Mn, Co, and Ni (Fig 4.13). The change in concentrations of Si and Pb with depth (illustrated in Figure 4.12) are mostly explained by PC1. Trends for Na, however, do not decrease steadily with depth and therefore, are not described by the trend in PC1.

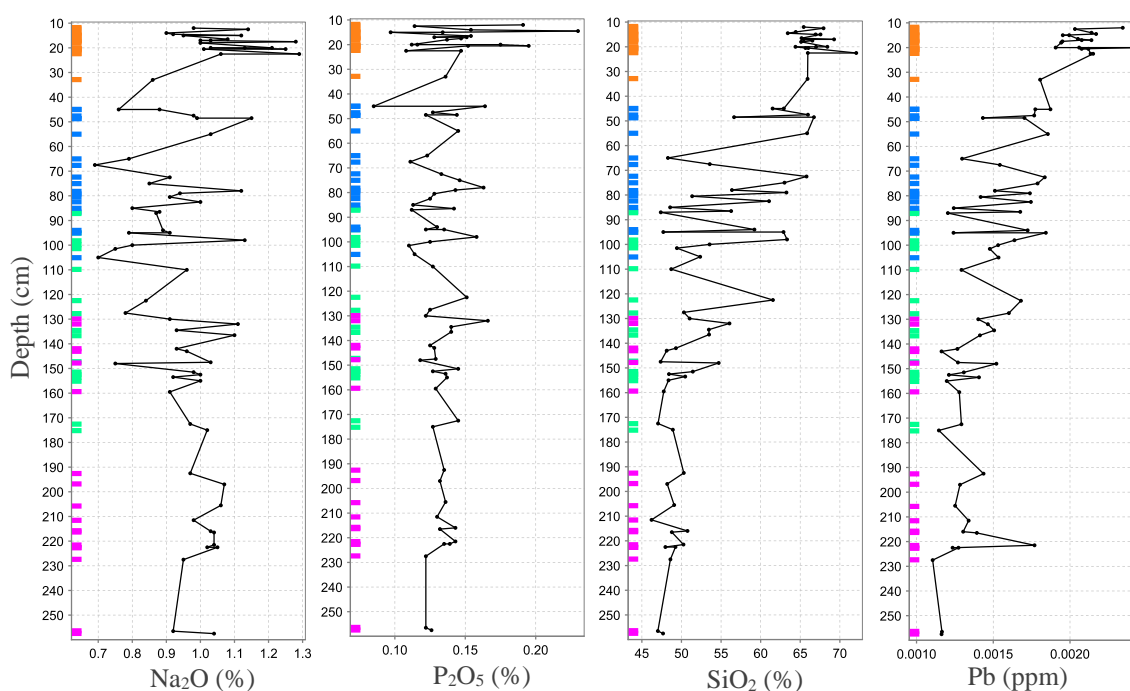


Figure 4.12. Soil sample depth of each soil sample plotted against oxide and elemental concentrations (Na₂O, P₂O₅, SiO₂, and Pb) of each soil sample. Soil sampling depths are distinguished by colour on the left side of the graph: Section 1 = orange, section 2 = blue, section 3 = green, and section 4 = purple.

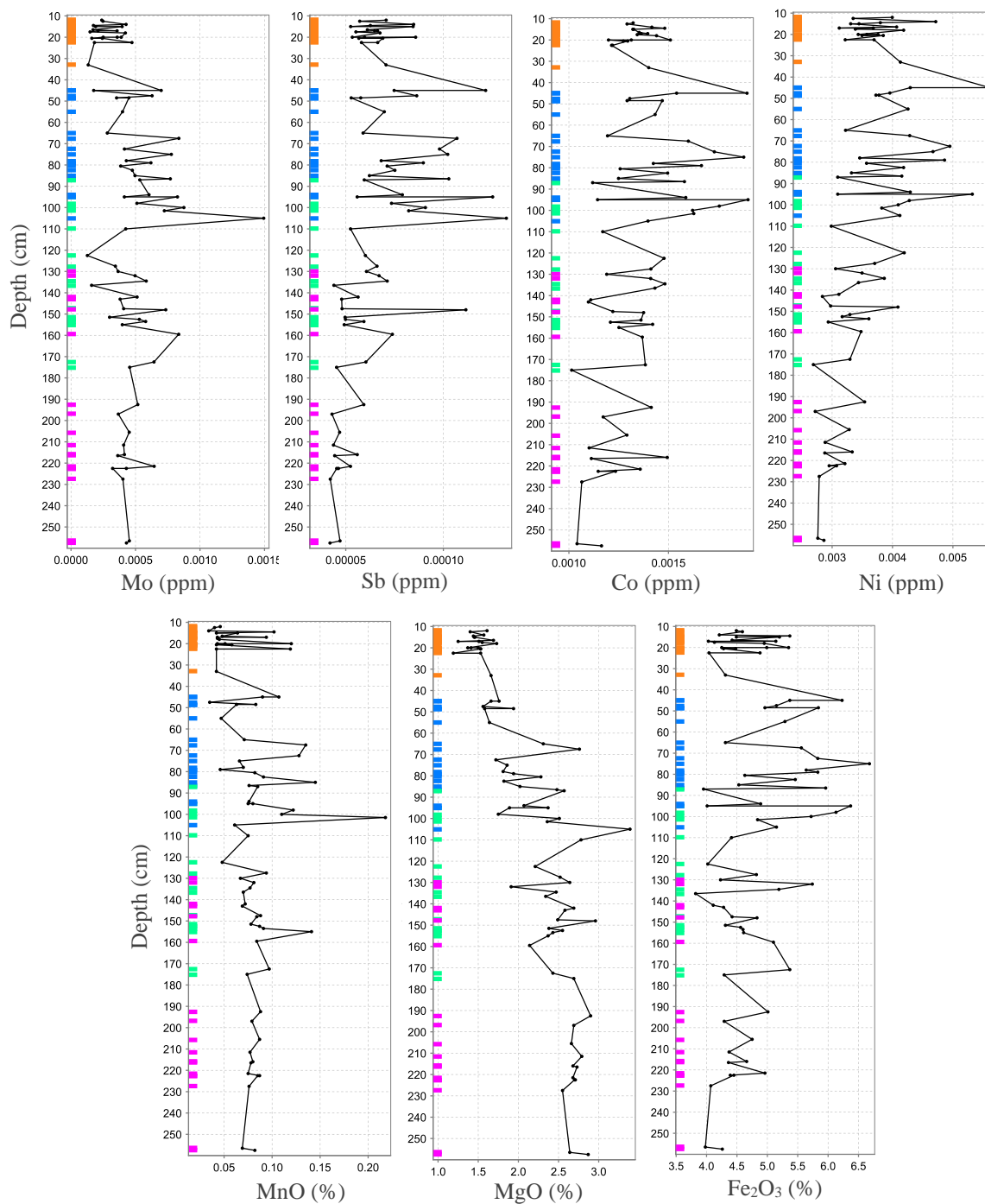


Figure 4.13. Soil sample depth of each soil sample plotted against oxide and elemental concentrations (Mo, Sb, Co, Ni, MnO, MgO, Fe₂O₃) of each soil sample. Sampling depths are distinguished by colour on the left side of the graph: Section 1 = orange, section 2 = blue, section 3 = green, and section 4 = purple.

Sodium oxide abundances are greatest in section 1 soil samples, but do not show any increasing or decreasing trend with depth. This is evident from the Na₂O data, which shows that average Na₂O concentrations in section 1, 2, 3, and 4 soils are 1.07% ($\pm 0.13\%$), 0.90% ($\pm 0.13\%$), 0.94% ($\pm 0.11\%$), 0.99% ($\pm 0.08\%$), respectively. Eimers et al. (2015) suggest that because of its positive charge, Na⁺ is often retained by negatively charged organic matter and is abundant in low pH soils where it displaces acidic cations (H⁺) on mineral surfaces. Soils on Pelee Island have high organic matter content and lower pH in section 1. Eimers et al. (2015) also found that Na is negatively associated with Ca, Mg, and K and soils derived from calcium-rich parent materials are less vulnerable to Na enrichment. This is because Na is unable to displace Ca from soil exchange sites and as a result, Na is more effectively transported through calcareous soil profiles. Shallow soils on Pelee Island have high Na concentrations because Na is more readily adsorbed when Ca contents are low (as seen in PC2). In addition, Na will accumulate in surface soils if there is insufficient drainage resulting from compaction and high clay mineral content, both of which inhibit leaching. This results in an accumulation of salts near the surface because Na cannot be leached downwards, water is evaporated from the surface, and plant roots remove water and leave behind Na, which accumulates in the root zone (Netzer et al. 2014). Fields with shallow soils like 27CS and 1A have very negative scores, which indicates high Na₂O concentrations and suggests this could be related to poor drainage. Vineyard management reports that fields 26 and 27 have lower elevation than the other fields and are more susceptible to flooding.

Iron oxide and MnO concentrations are greatest in section 2 for most soil profiles on Pelee Island (Figure 4.13). The accumulation of iron oxides in the B horizons of soils, where pH values increase, gives this horizon its characteristic reddish-brown hue (see soil core descriptions in Appendix D). In a study of the distribution of Fe, clay minerals, and extractable Fe in Saskatchewan soils, Stonehouse & Arnaud (1971) found that maximum Fe accumulation was in the upper portion of the B horizon, and that clay mineral content was generally positively correlated with Fe content. The authors suggest that this results from a comigration of fine clay minerals and Fe as small weathered particles migrate from the surface into deeper soils. This is also true for Pelee Island soils where clay particle content increases with depth from 12-22% in section 1 and 27-33% in section 2,

3 and 4 soils (Tolo 2019). High clay particle content in the deep soils on Pelee Island thus correlates well with high abundances of Fe in the B horizon. Manganese oxide is also positively associated with high clay particle content found in Pelee Island subsoils and forms in the B horizon. This is because the adsorption capacity for Mn increases with increasing pH (Kabata-Pendias & Mukherjee 2007).

Molybdenum did not correlate with any elements in PC1 and is most abundant in section 2 soils because it is highly soluble, which makes it susceptible to leaching from the A horizon. However, in deep soils, where pH increases, Mo can bind to Fe oxides and organic matter, which explains why Mo is abundant in the B horizon. Similarly, Sb is more abundant where Fe and Al are abundant as a result of adsorption. In a study of sorption and mobility of Sb in calcareous soils of Spain, Martínez-Lladó et al. (2011) also found organic matter content to affect the sorption of Sb in soils, which was mainly a result of the Fe and Al contents. Magnesium oxide, Co, and Ni also have high concentrations in section 2 soils (Figure 4.13) for similar reasons similar to the high concentration of Mo. Low soil pH, seen in the A horizon on Pelee Island (values as low as 5.37), cause leaching of elements such as Mg, Co, and Ni. Increasing pH and clay mineral content in deeper soils results in adsorption of these metals onto clay minerals and hydroxides in the B horizon. Lang et al. (2016) found that Co is mostly bound to Mn oxides, which are abundant in the B horizon. In a study of magnesium mobility in soils Gransee & Fühns (2013) found that soil acidity caused leaching of Mg, but high amounts of clay minerals (such as those found in subsoils on Pelee Island) helped prevent leaching. In a study of Ni adsorption by soils in relation to pH, organic matter, and Fe oxides, da Cruz & Casagrande (2004) found that Ni adsorption was most strongly affected by pH, but Ni was also affected by other factors such as clay mineral content and Fe and Mn oxides. Adsorption of Ni increases with increasing pH and in the presence of Fe oxides and high clay particle content found in the B horizons of Pelee Island soils.

Similar to PC1, PC2 mainly outlines the elemental differences among depths, but elemental differences among fields are also observed. For example, fields 25bCH, 23CH, and 26CF are the only fields that have high positive loadings in sections 3 and 4 soils. Some of the inconsistent or minor differences in elemental compositions among fields at

the same depths can be attributed to the variability among sampling depths resulting in the B-horizon spanning different sampling layers. However, the more consistent elemental differences among fields may require a different explanation. For example, in section 3 and 4 soils, most fields have very low magnitude scores, which means there is little variance in elemental abundance. The high positive scores for fields 25bCH, 23CH, and 26CF in section 3 and 4 soils indicate higher abundances of Mo, Sb, Fe₂O₃, MnO, MgO, Co, and/or Ni, compared with other fields. Field 26CF has very low CO₃ contents in section 2, 3, and 4 soils of 0.8, 7.75, and 7.83%, respectively, compared to average values of 5.07, 10.35, and 11.19% for section 2, 3, and 4 soils, respectively (Table 3.3). This suggests that acid leaching has been extensive. In their study of decalcification of periodically waterlogged soils, Van Den Berg & Loch (2008) found that low CO₃²⁻ content, or decalcification, occurred in soils that were subject to periodic waterlogging. They suggested that increased CO₂ pressure combined with continuous drainage of pore-water solutes during periods of waterlogging contributed to the decalcification of soils (Van Den Berg & Loch 2008). In addition, waterlogged soils usually exhibit greater organic matter accumulation (Luisa 1984) and organic matter is abundant in fields 25bCH, 26CF, and 23CH. These three fields have high organic matter content in section 1 and 2 soils, with values of 5.21% and 3.39% in field 25bCH, 6.97% and 3.65% in field 26CF, and 6.47% and 2.89% in field 23CH compared to average values of 5.24% and 3.10%, respectively (Table 3.2). Although there is high organic matter in these fields in section 1 and 2 soils, periods of waterlogging slow organic matter decomposition and reduce the ability of organic matter to bind metals to particle surfaces (Luisa 1984), and organic matter is slightly acidic and increases the mobility of metals. This means that the metals that are leached from surface soils because of low pH and inability to bind to organic matter, will accumulate in deep soils where clay content and pH are high (Rajmohan et al. 2014; Caporale & Violante 2016). These observations indicate that fields 26CF, 25bCH, and 23CH have experienced periods of poor drainage and/or waterlogged conditions, which caused accumulations of heavy metals in deep soils on Pelee Island.

4.4.3 Mineral PC3

Principal component 3, illustrated in Figure 4.14, accounts for 3.91% of the variance in the data and has an eigenvalue of 2.17. There are very few elements with either strong positive or negative loadings. The highest positive loadings belong to Cd, Bi, U, Si, Pb, Zr and Sb, whereas the highest negative loadings belong to most of the major elements and Sr, and some REE like Nd and Sc. The loadings suggest that when the concentrations of major oxides are low, there is a relatively higher concentration of heavy metals like Cd, Pb, Sb and U. The variation in PC3 can mostly be attributed to these heavy metals as they have the highest loadings. Bubble plots show that the spatial distribution of elements on the island is not well described by PC3 (Figure 4.15).

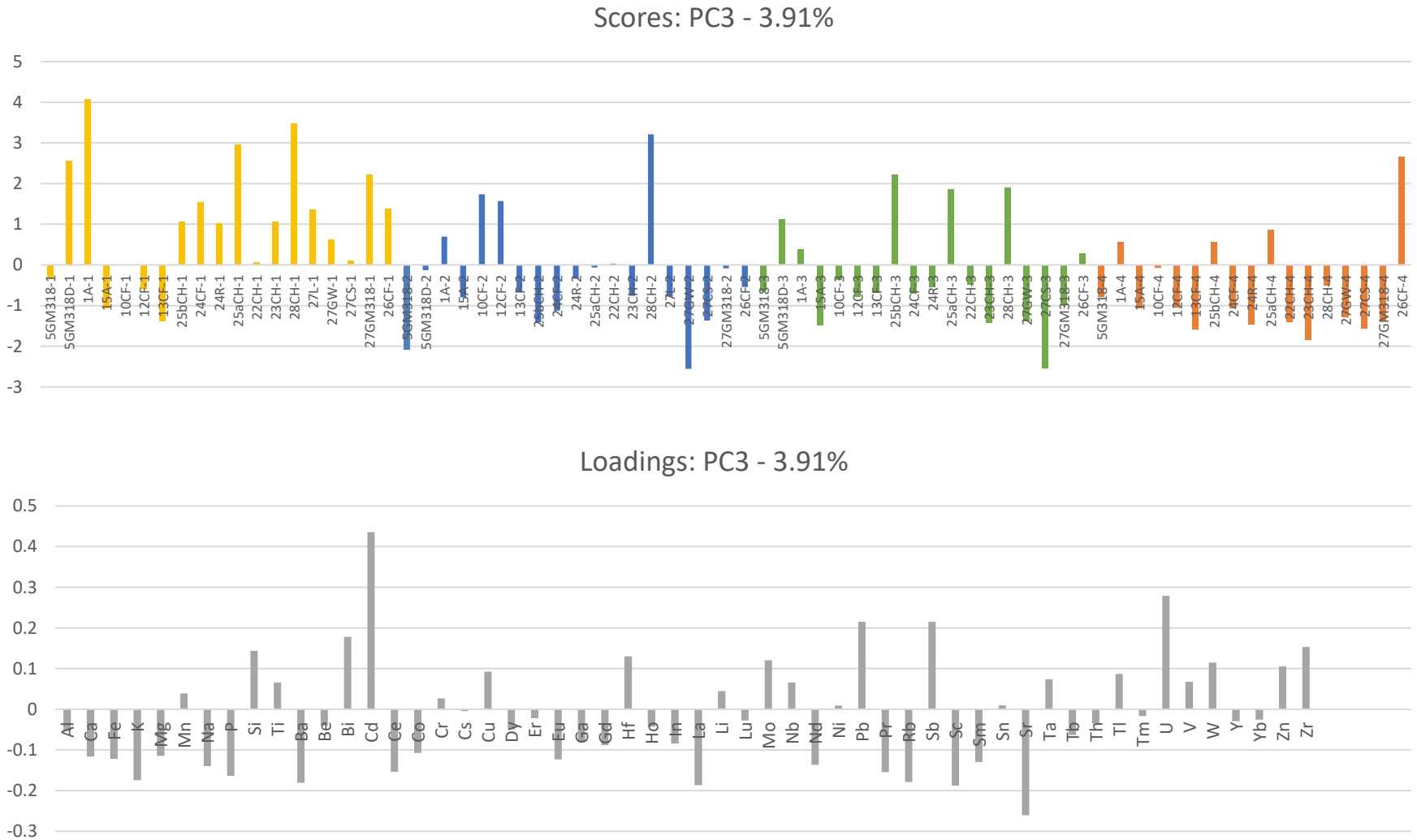


Figure 4.14. PC3 scores and loadings, illustrating elemental variations at depth and among field locations on Pelee Island. Scores are arranged by location (left to right on the graph represents south to north on the island) and by depth (yellow = section 1, blue = section 2, green = section 3, and orange = section 4). The magnitude of the bars on each graph indicate the strength of the correlations between scores (soil samples) and loadings (elements).

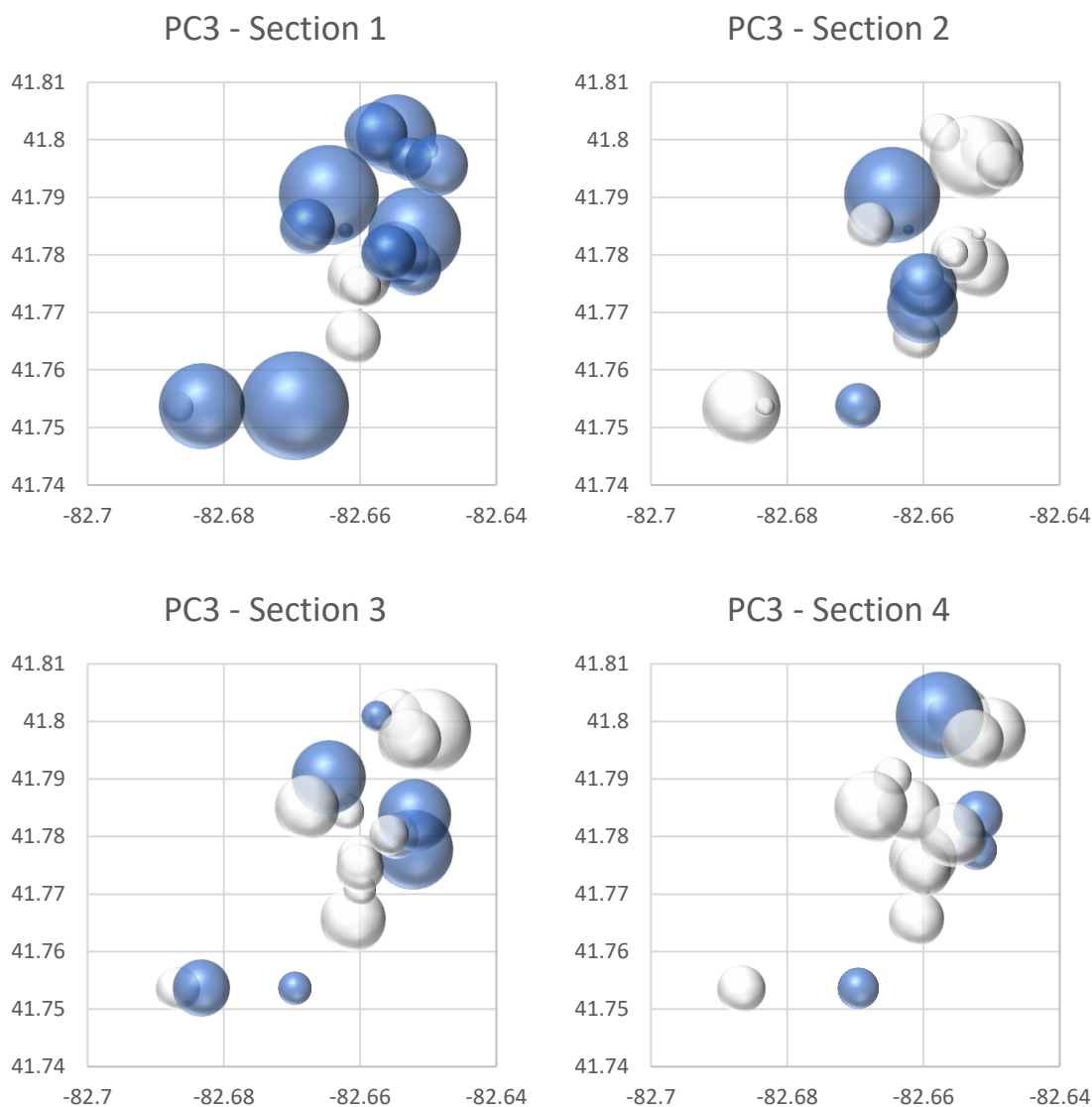


Figure 4.15. Bubble plots for PC3. These graphs provide spatial representation of the element data on Pelee Island. Each graph represents element loadings at sections 1, 2, 3, and 4. The x-y coordinate of the bubbles on the graphs represent their locations on the island in decimal degrees (easting; x-axis, northing; y-axis). These graphs are to be used together with the loadings plot form PC3. Colour indicates positive or negative scores; blue is positive and white is negative. Size of the bubbles indicates magnitude of correlations between scores (soil samples) and loadings (elements).

Most positive scores for PC3 occur for sampling section 1 soils, which means that samples taken from section 1 contain higher amounts of Cd, Pb, Sb, U (Figure 4.16), whereas samples taken from other depths (with some exceptions) are more weakly driven by Sr concentrations. The variation described by PC3 is dominated by high

concentrations of some heavy metals at the surface. This can result from both natural and anthropogenic processes. For example, Cd and Pb are enriched in Ontario agricultural surface soils as a result of airborne pollution and soil additives (Sheppard et al. 2009). Lead was widely distributed in soils when it was used in automotive gasoline (Sheppard et al. 2009). This is consistent with Figure 3.8, which shows an enrichment of Pb in section 1 in Pelee Island soils relative to the NASC standard. Sheppard et al. (2009) found that increased concentrations of U in surface soils could be a result of biocycling by plants. As the solubility of U increases with increasing pH in deeper soils, plant roots accessing the B horizon may encounter more U ions, which would be transported into the plant and later deposited in surface soils when the plant dies. Alternatively, Pelee Island chemical fertilizers (FERT4 and FERT5) were enriched in U compared to the NASC standard (Figure 3.13). Thus, increased U concentrations observed in Pelee Island surface soils could be attributed to addition of U from chemical fertilizers.

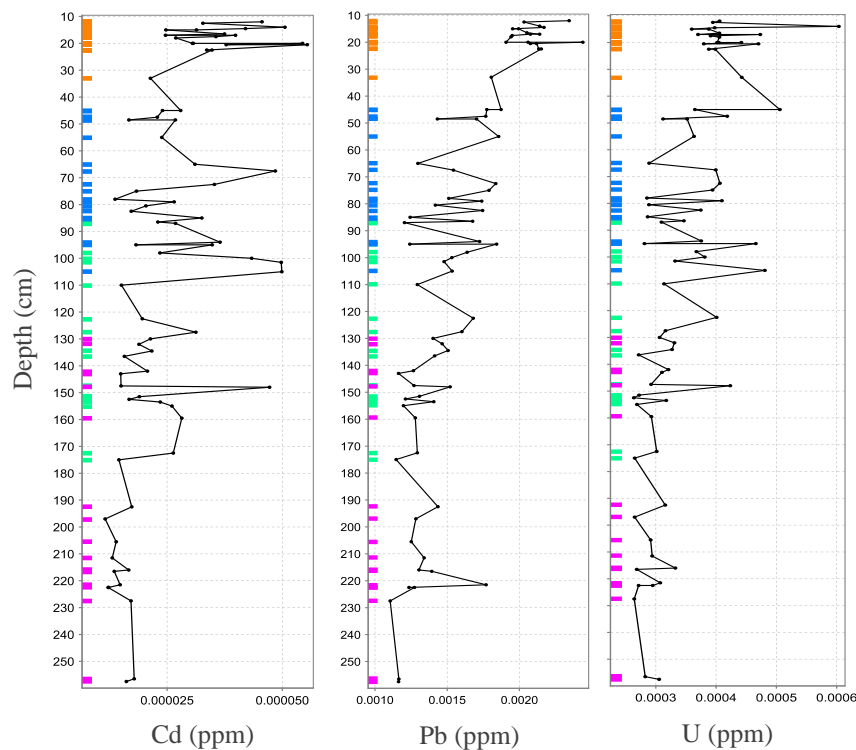


Figure 4.16. Depth versus concentration graphs comparing concentration differences with depth of Cd, Pb and U. Soil sample depth of each soil sample plotted against elemental concentrations (Cd, Pb, U) of each soil sample. Data is compiled from all 19 soil profiles. Sampling depths are distinguished by colour on the left side of the graph: Section 1 = orange, section 2 = blue, section 3 = green, and section 4 = purple.

Cadmium, Pb, Sb, U are nonessential heavy metals and although these metals occur naturally in all soils from weathering of parent material, they are toxic to plants in excessive amounts. Generally, heavy metals are regarded as trace and are rarely toxic at <1000 ppm (Wuana & Okieimen 2011). In Pelee island soils, the concentrations of U, Sb, Cs, and Pb are all well below toxic levels: the average concentration of Cd is 0.26ppm with a maximum of 0.29ppm in 27CS section 2 soils; average concentration of Pb is 16.71ppm with a maximum of 24.39ppm in field 26CF section 1 soils; average concentration of Sb is 0.669ppm with a maximum of 1.32ppm in field 28CH section 2 soils; and average concentration of U is 3.53ppm with a maximum of 6.04ppm in field 28CH section 1 soils.

Principal component 3 demonstrates that some heavy metals are concentrated in the surface soils on Pelee Island and to a greater extent than can be explained by the distribution expected from leaching (PC1) and adsorption (PC2) processes. Principal component 3 also highlights a few differences in elemental behavior among fields. For example, 28CH section 2 soils and 26CF section 4 soils are more associated with Cd, Pb, Sb, U, and 27GW section 2 soils and 27CS section 3 soils are more associated with Sr than other soils at similar depths. The soils in section 3 of 27CS has the lowest carbonate content among all other fields at this depth with a CO₃ value of 2.05%, with most other samples in the 10-13% range (Table 3.3). The reasons for these anomalies are unknown, but further studies could explore whether plant growth is affected by the occurrence of these metals at depth.

4.4.4 Mineral PC4

Principal component 4, illustrated in Figure 4.17, accounts for 3.43% of the variance in the data and has an eigenvalue of 1.84. The variations described by PC4 through PC6 are quite small. It is not possible to see these variations in the raw data without eliminating variation from PC1 through PC3. As such, it can be challenging to understand the causes of very small variations in soil chemistry. Here, variations observed in the data will be described and probable causes will be suggested where possible. Nevertheless, observations can be made about which fields differ from others and can possibly provide insight into differences in plant productivity in different soils.

For PC4, the elements with the highest positive loadings are Fe, Mn, Na, Co, Mo, and Zr and these elements are positively correlated with each other. Elements with highest negative loadings are K, Mg, P, Bi, Cs, Cu, Li, Rb, and Sn and these elements are positively correlated with each other, but negatively correlated to the previous group (i.e. elements with high positive loadings). These loadings suggest that some soils have an abundance of the major oxides Fe_2O_3 , MnO , Na_2O and extra trace elements Co and Mo, both of which are not described by the previous principal components.

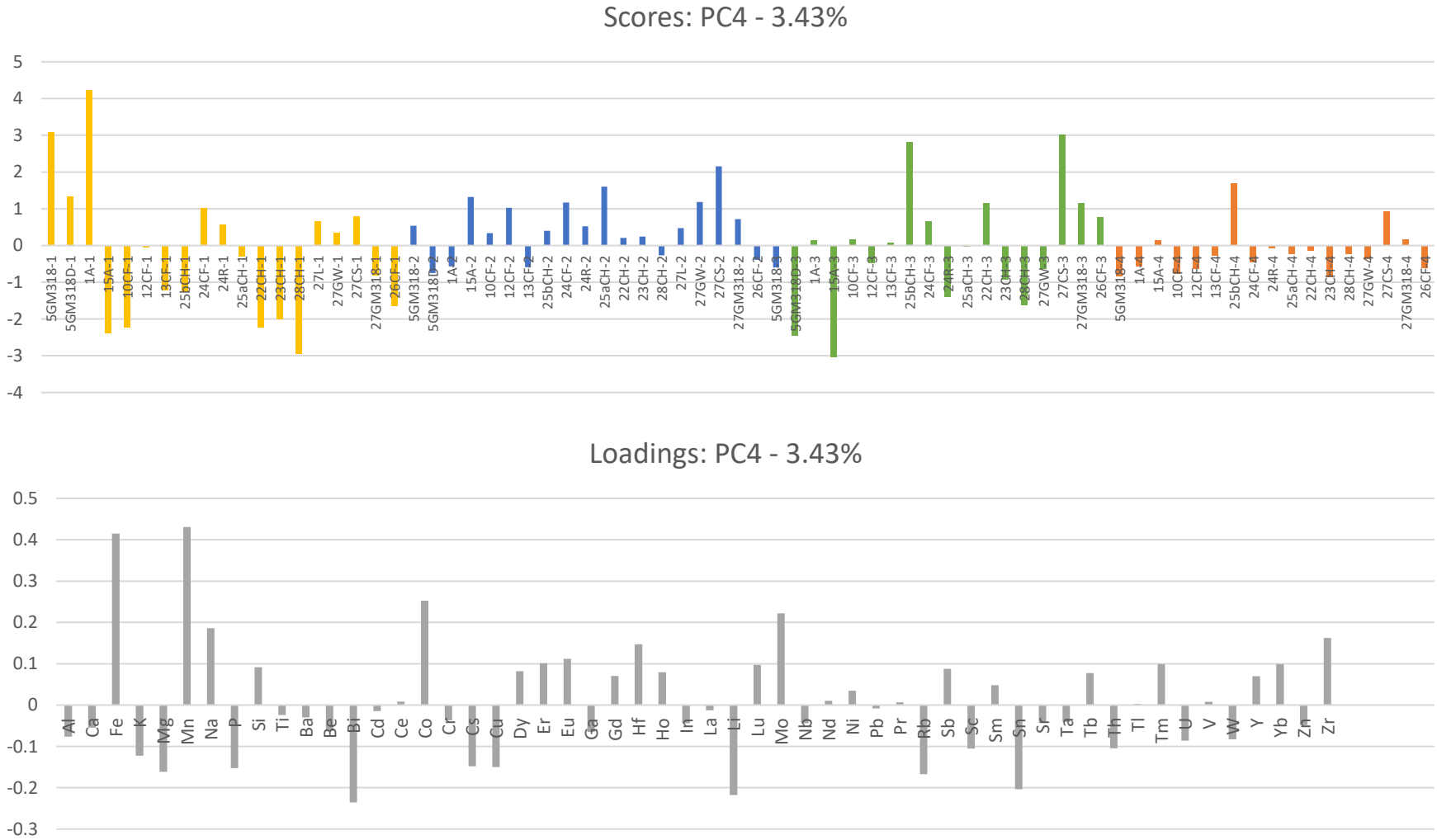


Figure 4.17. PC4 scores and loadings, illustrating elemental variations at depth and among field locations on Pelee Island. Scores are arranged by location (left to right on the graph represents south to north on the island) and by depth (yellow = section 1, blue = section 2, green = section 3, and orange = section 4). The magnitude of the bars on each graph indicate the strength of the correlations between scores (soil samples) and loadings (elements).

In Toledo soils, most samples taken from section 1 are enriched in Bi, Li, and Sn (negative scores), whereas soils from section 2 are enriched in Fe, Mn, Co, and Mo (positive scores). The opposite is true for Brookston soils and the scores for PC4 in Brookston soils (5GM318, 5GM318D and 1A) are quite high in section 1 soils.

Conversely, Toledo soils have higher positive scores than the Brookston soils in section 2 soils. This indicates that there is a greater abundance of Fe, Mn, Na, Co and Mo in Brookston surface soils relative to Toledo surface soils. However, in deeper horizons, the abundances of these elements in Brookston soils are similar or lower than observed for Toledo soils. The bubble plots (Figure 4.18), show that samples on the west side of the island are typically more associated with Bi, Li, and Sn and samples on the east side of the island are more associated with Fe, Mn, Co, and Mo.

The causes for these variations are unknown. The shift in oxide content and element abundance from the west to the east side of the island might indicate that depth of the soil causes some variation. Depth to bedrock changes from about 5 m in fields 25bCH and 27CS in the east to more than 30 m under the rest of the Toledo soils to the west (Table 3.1). Brookston soils are quite shallow (about 2 m in fields 5GM318 and 1A) and lie directly over bedrock, which is evident from the coring depths listed in Table 2.2. Field 25bCH has high positive scores for section 3 and 4 soils and the vineyard manager suspects this corner of field 25 is Brookston clay. For these reasons, variation for PC4 may be driven by differences between Brookston and Toledo soils. Alternately, positive scores (indicating lower values of P, K, Bi, Li, and Sn) were determined for Brookston soils in section 1 and in field 24CF (organic field) and 24R (reference field), and both fields 24CF and 24R do not receive commercial fertilizers. Two of the main constituents of fertilizers are P and K, which are in low concentrations in section 1 Brookston soils and in fields 24CF and 24R. However, when trace element concentrations in soils were compared to trace element concentrations in fertilizers, Li was only found in one out of three of the chemical fertilizers and Bi and Sn were not at all analyzed in any fertilizer samples. Thus, trace element data do not provide any indication that variations observed in PC4 between Brookston and Toledo soils is from fertilizer application and causes for variation of PC4 data remain unclear.

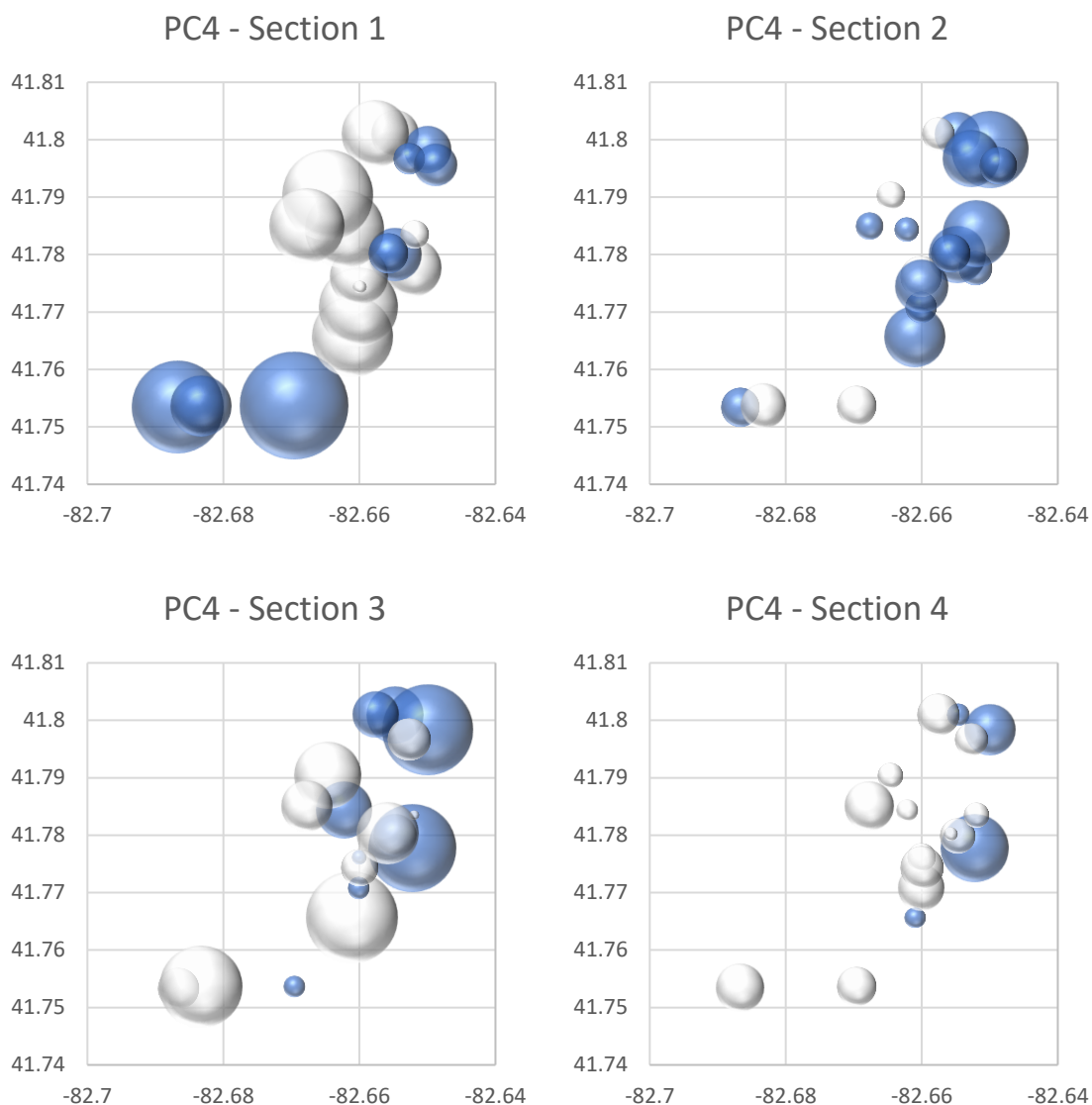


Figure 4.18. Bubble plots for PC4. These graphs provide spatial representation of the element data on Pelee Island. Each graph represents element loadings at sections 1, 2, 3, and 4. The x-y coordinate of the bubbles on the graphs represent their locations on the island in decimal degrees (easting; x-axis, northing; y-axis). These graphs are to be used together with the loadings plot form PC4. Colour indicates positive or negative scores; blue is positive and white is negative. Size of the bubbles indicates magnitude of correlations between scores (soil samples) and loadings (elements).

4.4.5 Mineral PC5

Principal component 5, illustrated in Figure 4.19 accounts for 2.07% of variation in the data and has an eigenvalue of 1.10. This variation is driven by the loadings for just a few elements. Potassium, Mn, Cd and Cu have high positive loadings. These elements are positively correlated with each other and negatively correlated with Bi, and to a lesser extent Si. Although exceptions occur (e.g. section 4 soils of 27CS), the general pattern of variation will be described. Fields 10CF and other Toledo surface soils at the north end of the island (27L, 27GW, 27 GM318, 27CS, and 26CF) have higher concentrations of P, Cd, and Cu. Fields 5GM318D and 25aCH (section 1 soils), 5GM318D and 28CH (section 3 soils), and 27CS (section 4 soils) are enriched in Bi. The scores shown on the bubble plots (Figure 4.20) demonstrate that there are smaller variations in the concentrations of these elements in the deep soils (smaller scores = smaller bubbles), and greater variation between samples and elements in the shallow soils. This trend might indicate that the variation highlighted by PC5 is related to surface application of fertilizers or pesticides.

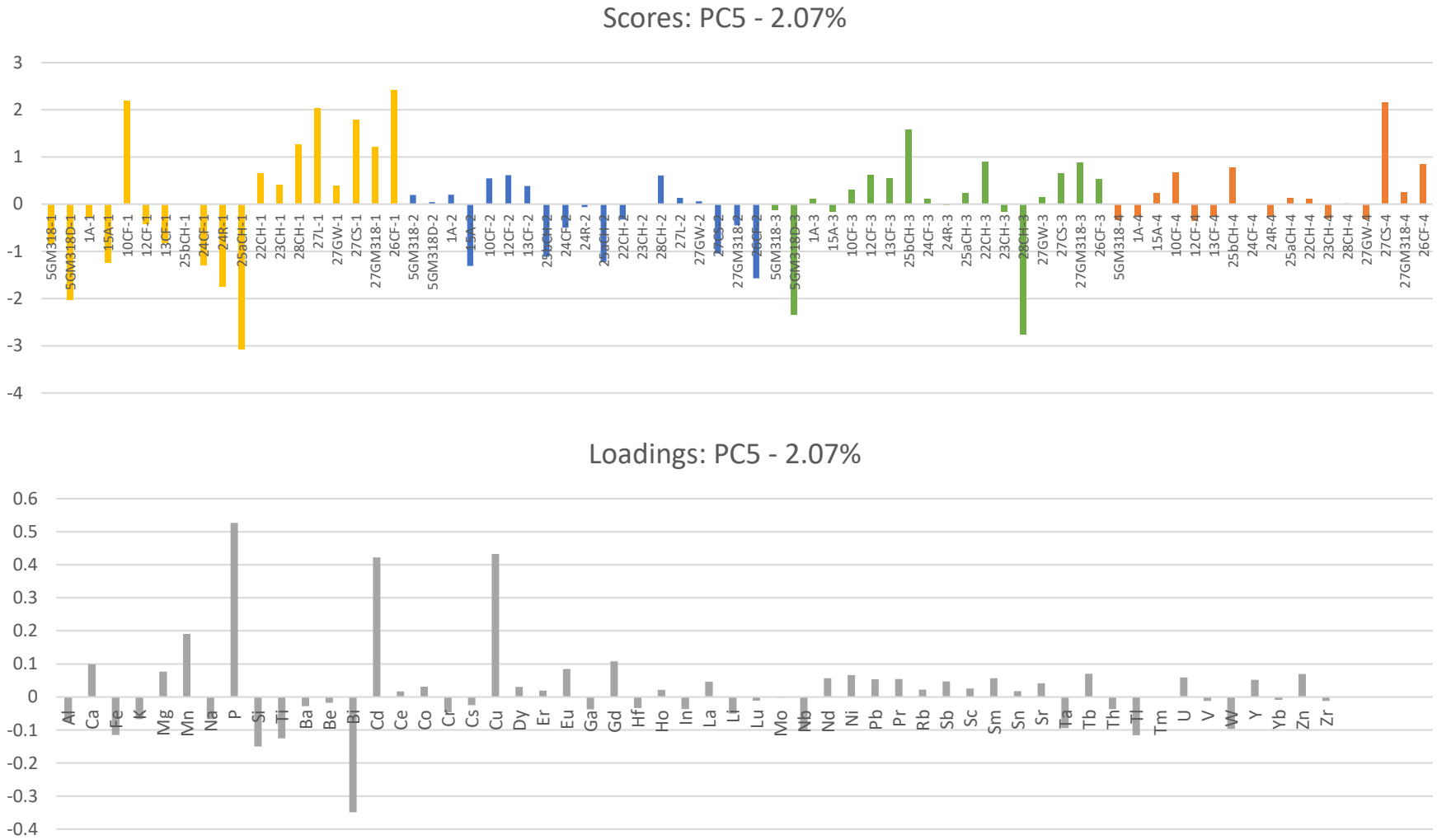


Figure 4.19. PC5 scores and loadings, illustrating elemental variations at depth and among field locations on Pelee Island. Scores are arranged by location (left to right on the graph represents south to north on the island) and by depth (yellow = section 1, blue = section 2, green = section 3, and orange = section 4). The magnitude of the bars on each graph indicate the strength of the correlations between scores (soil samples) and loadings (elements).

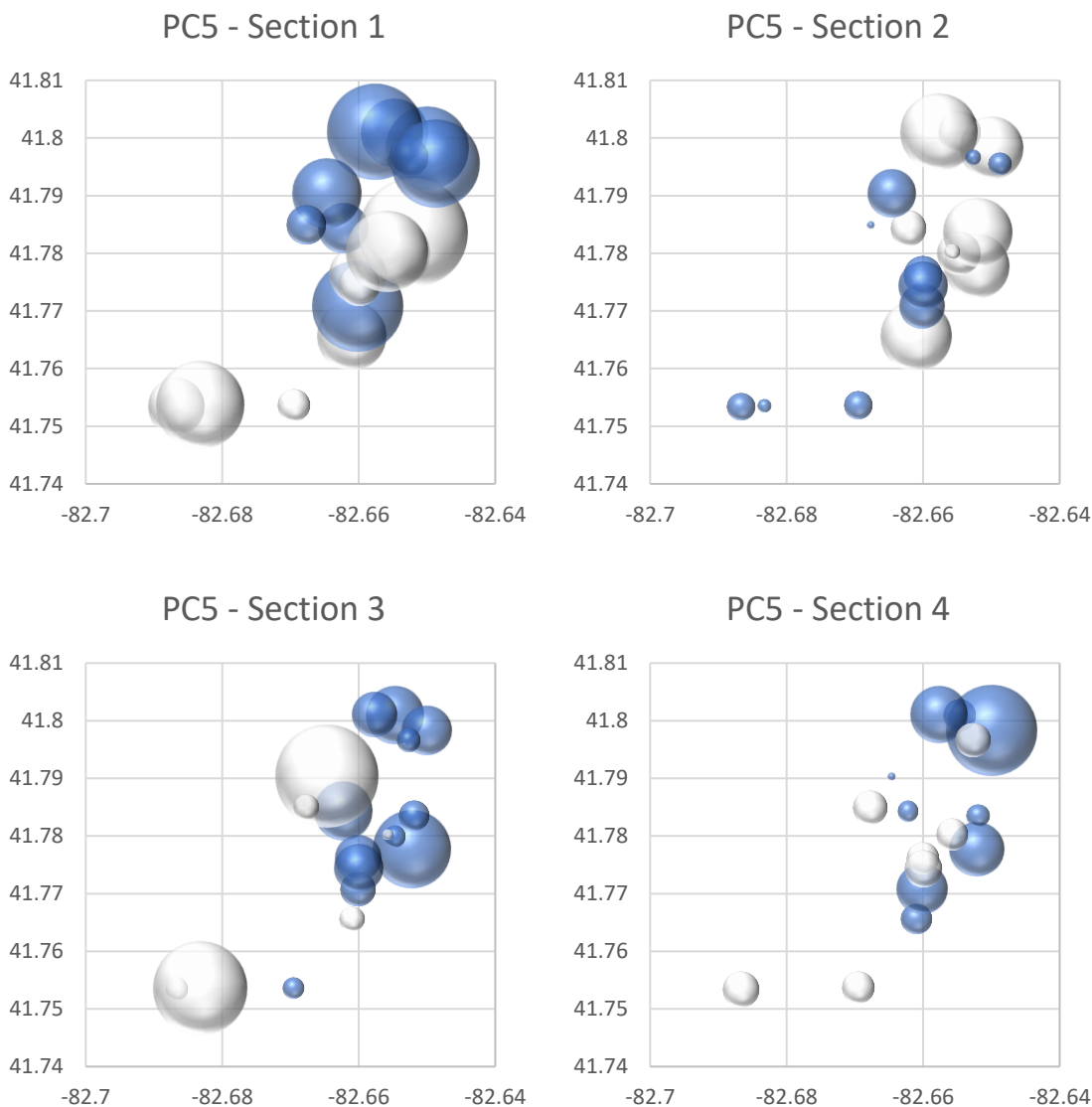


Figure 4.20. Bubble plots for PC5. These graphs provide spatial representation of the element data on Pelee Island. Each graph represents element loadings at sections 1, 2, 3, and 4. The x-y coordinate of the bubbles on the graphs represent their locations on the island in decimal degrees (easting; x-axis, northing; y-axis). These graphs are to be used together with the loadings plot form PC5. Colour indicates positive or negative scores; blue is positive and white is negative. Size of the bubbles indicates magnitude of correlations between scores (soil samples) and loadings (elements).

Copper is adsorbed by Mn, Al, and Fe oxides and also organic matter. The adsorption potential becomes stronger for Cu with soil depth as pH increases (Romić et al. 2014), which should result in higher levels of Cu in section 2 soils (as observed with other metals for PC2). However, elevated levels of Cu are observed in surface soils, especially

in surface soils of fields that have grapes (as opposed to fields without grapes such as 27L, 24R, 1A, 15A) (Figure 4.21). The most common elevated levels of Cu in agricultural soils is the use of Cu-containing compounds to control plant disease and most of the Cu that is accumulated on the leaves and in the soils from spraying will be retained in topsoil (Deluisa 1996). It is important to note however, that toxic levels of Cu are uncommon in calcareous soils, as the bioavailability of Cu has been reported to decrease as pH and CEC increase (Romić et al. 2014). Alloway (2010) suggests that elevated concentrations of Cd in topsoils are from anthropogenic inputs and particularly from application of phosphate fertilizers. This association suggested by Alloway (2010) is highlighted in PC5 data, which shows that P and Cd are positively correlated, indicating that Cd could be sourced from fertilizers added to topsoils on Pelee Island. Figure 4.22 illustrates the concentrations of Cd in surface soils on Pelee Island between fertilized and unfertilized fields. The average Cd in unfertilized fields is 0.262 ppm compared to the average Cd of fertilized fields of 0.391 ppm. Further, soils that are unfertilized, such as fields 24CH and 24R have negative scores, indicating these fields have low P and Cd.

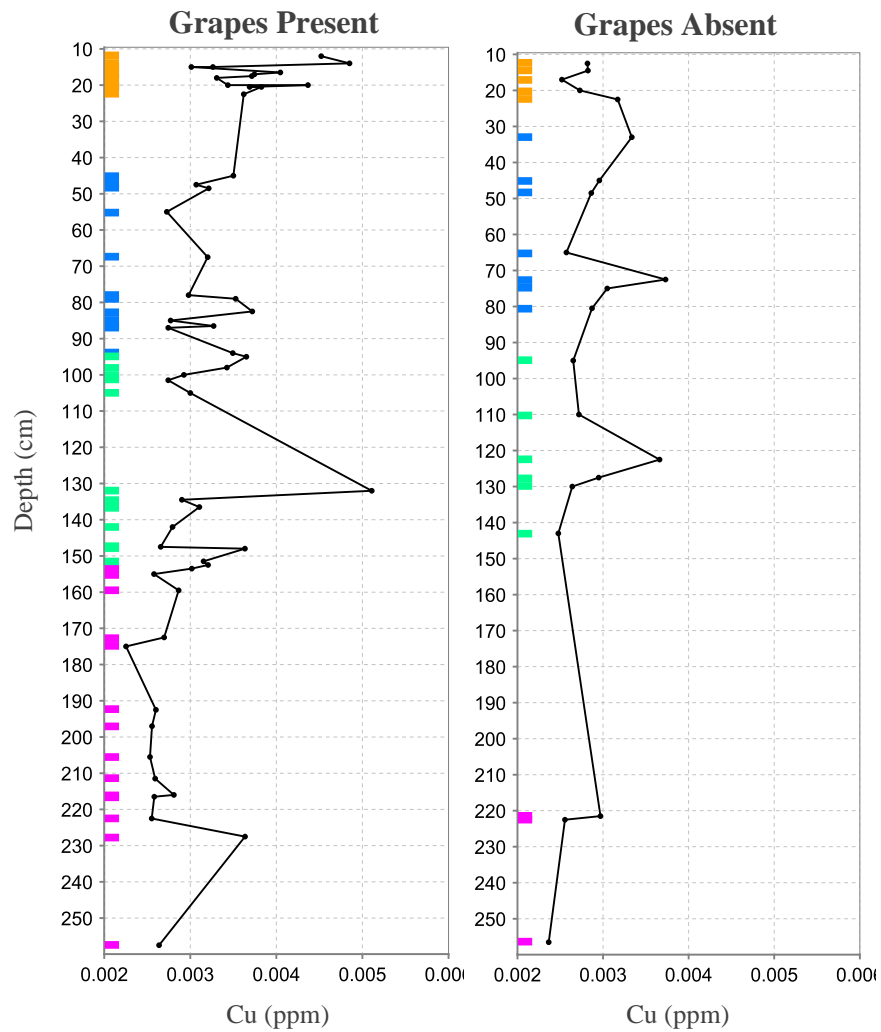


Figure 4.21. Depth versus concentration graphs comparing concentration differences of Cu in surface soils between fields that grow grapes compared to fields without grapes. Soil sample depth of each soil sample from all 19 soil profiles plotted against elemental concentrations (Cu) of each soil sample. Soil sampling depths are distinguished by colour on the left side of the graph: Section 1 = orange, section 2 = blue, section 3 = green, and section 4 = purple.

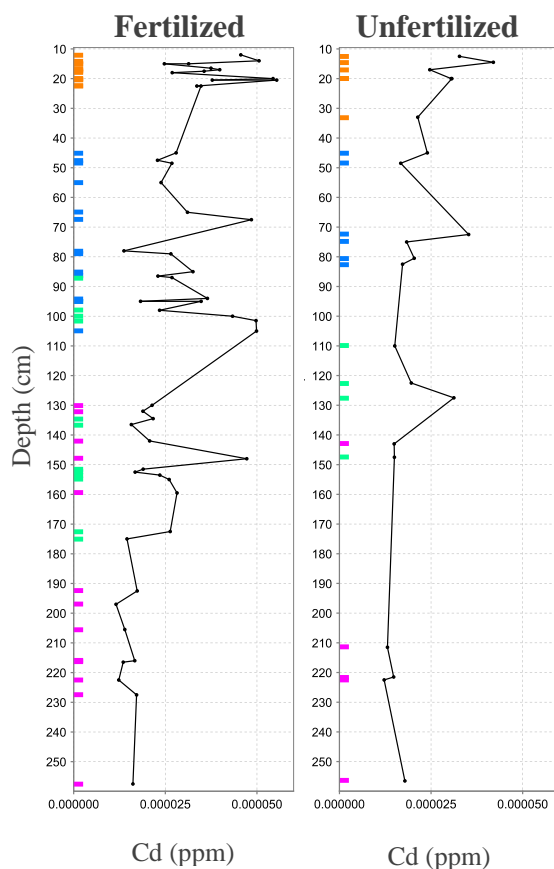


Figure 4.22. Depth versus concentration graphs comparing concentration differences with depth of Cd between fertilized and unfertilized soils. Soil sample depth of each soil sample plotted against elemental concentrations of Cd of each soil sample. Data is compiled from all 19 soil profiles. Sampling depths are distinguished by colour on the left side of the graph: Section 1 = orange, section 2 = blue, section 3 = green, and section 4 = purple.

4.5 Plant Extractable Nutrient Principal Components

4.5.1 Measuring Bioavailability in Soil

Plant extractable nutrients (PEN) are those that are loosely bound to mineral surfaces and are available for plant uptake (Reid & Hayes 2003). Exchangeable ions are held by negatively charged soil particle surfaces through relatively weak electrostatic interactions. Therefore, exchangeable ions are defined as the measure of ions that are removed from the soil by a solution containing a neutral salt, such as CaCl_2 (Dauer & Perakis 2013). Unlike plant extractable nutrients, the majority of soil elements studied in the previous PCA are locked up in crystalline form within primary and secondary minerals that weather too slowly to replenish nutrients required for highly productive

plant growth (Reid & Hayes 2003). Thus, assessing plant extractable nutrient concentrations will provide a better understanding of elements in the soil that are accessible for uptake or adsorption by plants, also termed bioavailability (Semple et al. 2004). The uptake of nutrients by plant roots can only proceed when the elements are in solution. The factors that can affect the concentrations of plant available nutrients in the soil include weathering rates, agricultural practices (e.g. fertilizers), and organic matter or clay mineral content. Understanding the relative influence of these factors on different fields can guide crop management practices.

Another PCA was performed to identify patterns in concentrations of plant extractable nutrients. The PCA results allow for identification of variations among some major and trace elements among fields. However, the ability to interpret the cause of these variations are limited because the CaCl_2 extraction method produced solutions with low element concentrations and many elements were below detection limits. Thus, element values below detection limits were assigned very small concentration values prior to the PCA (since the PCA will not work with values of zero). This means that the PCA after PC1 and PC2 detected mostly outliers in the data. Outliers were given too much weight during the autoscaling weighting preprocessing and did not provide useful information to detect processes that control nutrient variability in Pelee Island soils.

It was surprising that some essential elements such as Ca, P, K, Fe, S, Cu, and Zn and those that are abundant in fertilizers (namely P and K) were not released to solution by the CaCl_2 treatment. Thus, it was difficult to assess the causes of the observed variations when some of the key elements (e.g. K from fertilizers) were missing. Alternate extraction methods (e.g. Olsen sodium bicarbonate, ammonium acetate, diethylene triamine penta-acetic acid – DTPA, ethylene diamine tetra-acid – EDTA, phosphoric acid, mobile metal ion – MMI etc.) likely could have yielded higher concentrations of plant extractable nutrients because these methods dissolve some minerals, such as iron-oxides and overestimate the amount of available nutrients to the plants (Houba et al. 2000). However, these methods only provide an index of nutrient availability that must then be interpreted and calibrated against actual measurements of crop response in the field (Munroe 2018). These methods do not provide absolute nutrient concentration

values, in contrast to the CaCl_2 extraction method, and therefore, they were not selected for this study. In addition, the CaCl_2 extraction method was chosen over alternate extraction methods because many of these extraction methods only analyze a few nutrients in the soil at a time. For example, the Olsen sodium bicarbonate is used to assess extractable P, ammonium acetate is used to measure extractable Ca, Mg, K and Na, and chelating agents such as DTPA and EDTA are used to assess extractable micronutrients - except Fe, Cu, and B, which don't have any associated accredited tests (Munroe 2018). Thus, CaCl_2 was chosen because it imitates nutrient availability, it detected multiple elements at once, it is cost and time efficient, and results are reproducible (Houba et al. 1986).

Another study conducted by Société Générale de Surveillance (SGS) on Pelee Island in 2019 analysed nutrient availability in soils using the mobile metal ion (MMI) method. Values produced from the MMI extraction method are compared to other MMI soil data from around the world. This means that the values produced from the MMI extraction method are not absolute plant extractable nutrient concentrations, and values are interpreted using other MMI standards. Soils sampled for the SGS study were from fields 27L, 27GM318, 27GW, 27CS, 26CF, 24GM318 (organic fields – 24CF), 26CF and 5GM318 on Pelee Island. The results show high Ca concentrations in all fields; K concentrations are similar to other reference fields but are low in the organic field; Cd concentrations are especially high in Toledo soils; Cu concentrations are high in all fields except in the organic field (24CF); Mg concentrations are high and are greatest in the organic field (24CF); and P concentrations are low in all fields relative to MMI reference sites (SGS 2019).

Low concentrations of some elements could be the result of plant uptake resulting in limited bioavailable nutrients on soil particle surfaces. Many studies suggest that the season of soil sampling has an effect on available nutrients in soils and affects soil fertility testing (Franzen 2018; Omer et al. 2018). Société Générale de Surveillance (SGS) laboratories suggest that nutrients are lowest in soils from July through to August, when crops are fully grown and beginning to mature because crops deplete the soil nutrient supply. They further suggest that spring is the best time to sample because it

provides the best representation of nutrients in the soil that will be available to plants for that crop year. However, soil amendments applied to crops can affect nutrient concentrations in soil samples. Therefore, the most popular time to sample is in the fall because soil depletion can be observed, and management strategies can be adjusted to increase soil fertility for the next season (Omer et al. 2018). In addition, clayey soils, such as those on Pelee Island, are more apt to seasonal element variability than sandier soils because of higher CEC. Soil pH, Zn and P concentrations are stable throughout the year, however low K values are usually seen in the fall after harvesting due to plant uptake (Franzen 2018). Pelee Island soils were sampled in late August (August 28-29) and again in mid-October (October 16-18). Because the soils were sampled in the fall, it is possible that the CaCl_2 extraction method produced low plant extractable nutrient concentrations because of plant uptake. The SGS study on Pelee Island found that the season did not affect nutrient content in Pelee Island soils; however, they used a different extraction method, and so our results are not directly comparable.

Another possible reason the elements were below detection limits could be that they were not soluble in the CaCl_2 solution that was used for nutrient extraction. Equilibrium reactions drive the capacity of soil particle surfaces (organic matter and clay colloids) to exchange cations and equilibrium must be achieved between ions on soil particle surfaces and ions in solution (Weil & Brady 2017). Soils on Pelee Island are highly calcareous and perhaps many of the exchange sites on soil particle surfaces were already occupied by Ca^{2+} ions, thus limiting the ability of Ca^{2+} in the CaCl_2 salt solution to exchange with other cations (Munroe 2018). Thus, equilibrium would easily be achieved between soil particle surfaces and the CaCl_2 solution without need for additional cation exchange, and concentrations in the CaCl_2 solution would have to be much higher for cation exchange to achieve equilibrium (Munroe 2008). It does seem however, that the CaCl_2 solution was strong enough to replace some cations (e.g. Mn^{2+} , Mg^{2+}), but with a strong preference, as follows: first, Ca^{2+} should replace cations with large ionic radii and low positive charges, such as K^+ ; next, Ca^{2+} should replace cations that are more difficult to remove from soil particle surfaces (small ionic radius and high positive charge, such as Al^{3+} and Mo^{4+}), but can be removed because they are in greater abundances on soil particle surfaces than in solution (Weil & Brady 2017). Therefore, two conclusions can be drawn from the CaCl_2

extraction method. (1) Considering that K^+ has a lower positive charge and larger ionic radius than Ca^{2+} , it should easily exchange with Ca^{2+} in the extraction solution. However, K^+ concentration values were all below detection limits. This suggests that K^+ ions are in very low abundance on exchange sites. Consequently, Ca^{2+} will start to exchange with ions such as Al^{3+} and Mo^{4+} that are more difficult for Ca^{2+} to remove but are abundant on exchange sites relative to the $CaCl_2$ solution. Therefore, the elements Al, B, Bi, Co, Li, Mo, Nb, Ni, Rb, Sc, Si, Ti, U, and Zr are relatively more abundant on exchange sites compared to easily removed cations, such as K^+ . Reasons for higher abundances of these elements on exchange sites include, but are not limited to, composition of parent material, weathering rates, fertilizer application, organic matter content, clay content, and carbonate content. These are expanded upon in the PCA analysis below.

4.5.2 Plant Extractable Nutrients PC1

Principal component 1, illustrated in Figure 4.23, accounts for 33.82% of the variance in the data and has an eigenvalue of 6.08. The sample scores show that there is a major difference between soils from section 1 versus soils from sections 2, 3, and 4. Sample section 1 has high positive scores, whereas sample sections 2, 3, and 4 show low-magnitude, negative scores. This indicates that there is a strong difference in elemental concentrations between topsoil and subsoil for plant extractable nutrients. Soils from sections 2, 3 and 4 do not contribute much to the variation in PC1.

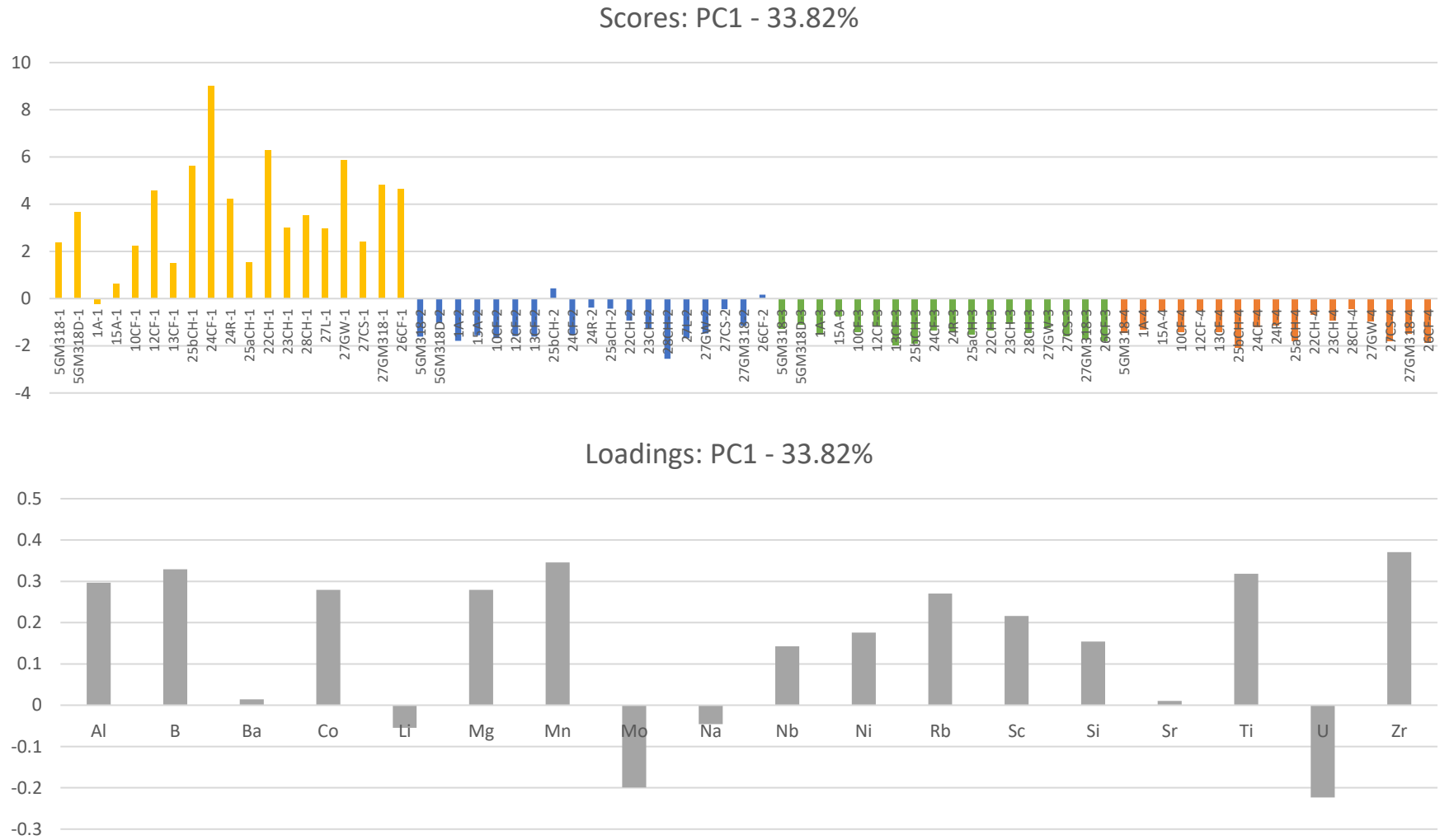


Figure 4.23. PC1 scores and loadings, illustrating nutrient element variations at depth and among field locations on Pelee Island. Scores are arranged by location (left to right on the graph represents south to north on the island) and by depth (yellow = section 1, blue = section 2, green = section 3, and orange = section 4). The magnitude of the bars on each graph indicate the strength of the correlations between scores (soil samples) and loadings (elements).

Most of the loadings for PC1 have high positive values, whereas two elements (Mo and U) have low negative values. All of the elements with tall positive bars are positively correlated with each other, but negatively correlate with the behaviour of Mo and U. Because only the section 1 soil samples have high scores, PC1 reflects the negative correlation between the concentration of most elements versus Mo and U in surface soils, meaning that there are lower concentrations of Mo and U at the surface. In graphs that plot depth versus plant extractable nutrient concentration (Appendix B) the majority of elements, such as Al, B, Mn, Mg, Zr, and Ti, are more abundant in section 1 soils and decrease in concentration with depth. Hence, the positive scores and loadings reflect the higher concentrations of these elements in section 1 soil samples. For example, Mg and Mn are abundant in surface soils and decrease in concentration with depth as is illustrated in Figure 4.24. Note that the spline curves on these graphs (and all depth versus element concentration graphs in section 4.5) are meant to illustrate element concentration trends and do not imply vertical connectivity among soils samples, because markers on the graphs represent individual soils samples selected from different locations on the island. Soils from sections 2, 3, and 4 have small-magnitude negative scores indicating that they do not have as great of an effect on variation in PC1 as section 1 soils and are also more enriched in Mo and U. Abundances of Mo and U are low at the surface and increase in abundance with increasing depth (Figure 4.24). Barium, Li, Na, and Sr have very small loadings (either positive or negative), indicating that the contribution of these elements to variation of PC1 is negligible. Principal component 1 is therefore describing the variation in plant extractable nutrient concentrations in section 1 in the soils. Bubble graphs shown in Figure 4.25 provide spatial representation of soil scores. Soil samples taken from section 1 have mostly positive scores (blue bubbles) whereas graphs representing soil samples taken from sections 2, 3, and 4 have mostly negative scores (white bubbles). This figure shows that there is no spatial variation for PC1.

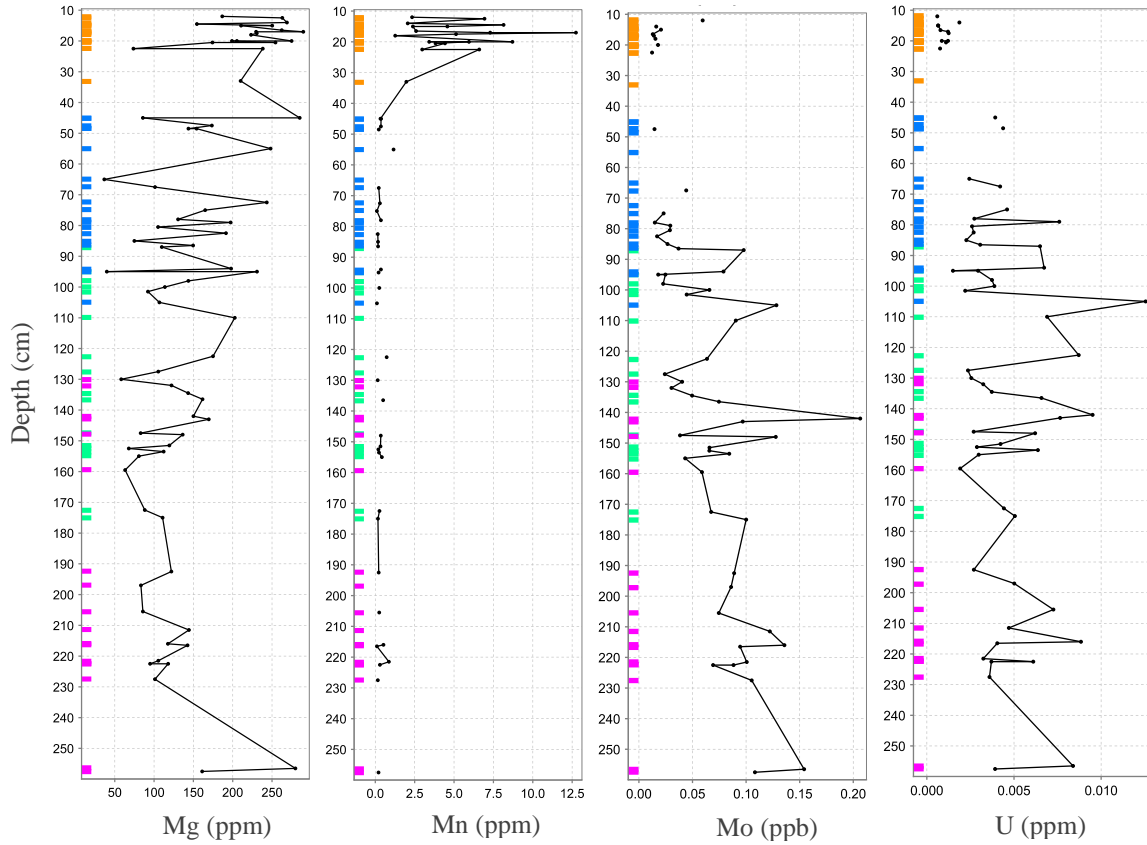


Figure 4.24. Depth versus extractable nutrient concentration graphs comparing concentration differences with depth of Mg, Mn, Mo and U. Soil sample depth of each soil sample plotted against elemental concentrations (Mg, Mn, Mo, U) of each soil sample. Sampling depths are distinguished by colour on the left side of the graph: Section 1 = orange, section 2 = blue, section 3 = green, and section 4 = purple.

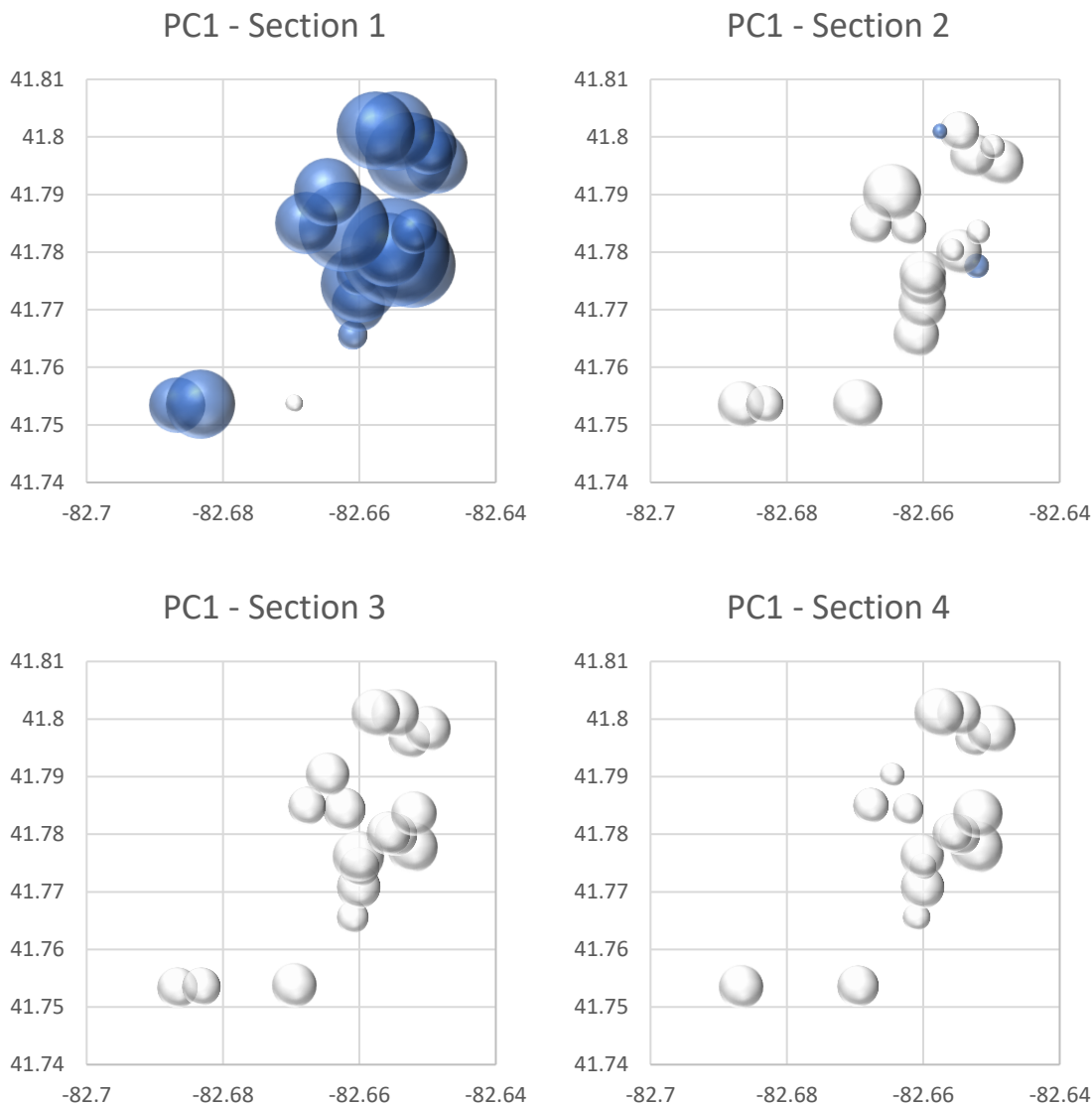


Figure 4.25. Bubble plots for PC1. These graphs provide spatial representation of the nutrient element data on Pelee Island. Each graph represents element loadings at sections 1, 2, 3, and 4. The x-y coordinate of the bubbles on the graphs represent their locations on the island in decimal degrees (easting; x-axis, northing; y-axis). These graphs are to be used together with the loadings plot form PC1. Colour indicates positive or negative scores; blue is positive and white is negative. The size of the bubbles indicates magnitude of correlations between scores (soil samples) and loadings (elements).

The highest concentrations of most plant extractable nutrients are in the A horizon (section 1 soils). It has already been demonstrated that minerals in Pelee Island soils are highly weathered at the surface and weathering decreases with depth (Figure 4.1). In addition to converting primary minerals to secondary minerals, weathering also releases ions available for plant uptake (Weil & Brady 2017). Weathering is most intense in

surface soils where there is increased organic matter content and the minerals are exposed to the atmosphere, water, and variable temperatures (changes in temperature increases weathering rates) (Weil & Brady). Since weathering is most intense in surface soils, it is not surprising that most plant extractable nutrients are found in the A horizon. In addition, soils in section 1 have the highest concentration of organic matter (with an average of 5.24 % compared to an average of 2.66% in deep soils), which has a high CEC and can adsorb nutrients that are easily released with a salt-water extraction. This indicates that complexation of nutrients with organic matter is a factor that affects the availability of nutrients in surface soils (Weil & Brady 2017).

Fertilizers are also applied to surface soils. On Pelee Island this either occurs as broadcast fertilizing to alfalfa fields (to the surface of the soil) or through injection of fertilizers along the dripline of the grape plants. Fertilizer application could therefore be contributing to the abundance of available nutrients in Pelee Island surface soils and could be influencing variation of elemental abundances in PC1. However, unfertilized fields (chemical fertilizers not applied), such as 24CF (organic field), 24R (reference field), 15A (alfalfa field), and 5GM318, do not differ from the fertilized fields in PC1 and it can be thus concluded that variation in PC1 is not caused by application of chemical fertilizers. However, it is likely that compost added to the surface of fields 24CF increases both the CEC of the soil and the amount of plant extractable nutrients. Studies using extractants that release more major plant nutrients (e.g. P and K) should be done to determine the influence of fertilizers on the availability of nutrients in Pelee Island soils.

Although there are many reasons why there are higher amounts of plant extractable nutrients in the upper soils of Pelee Island, it needs to be considered why there is a negative correlation between Mo, U and other nutrients at this depth. The mineral data shows that the abundance of Mo was low in surface soils, suggesting that smaller amounts of Mo are incorporated into mineral structures. The mineral data also show that there are higher concentrations of Mo in the B horizon. Both observations are consistent with the literature, as Alloway (2010) noted that Mo is the lowest of all essential trace elements in soils and that Mo is strongly adsorbed by hydrous Fe-oxides in the B horizon. Extractable Mo is more abundant in deep soils because in alkaline soils, such as the deep

soils on Pelee Island, it is mostly present as an oxyanion (MoO_4^{2-}). This oxyanion is leached from surface soils but sorbs onto Fe and Mn-oxides and organic matter in deeper, more alkaline soils where it can exchange with other cations (Wichard et al. 2009). In addition, Mo is most easily taken up by plants from alkaline soils with poor drainage (gleying) (Alloway 2010), which is the case for soils on Pelee Island. Plant available Mo may also be depleted of surface soils because it is an essential micronutrient used by plants and therefore is depleted in surface soils from plant uptake (Alloway 2010).

Similarly, there are low concentrations of extractable U in surface soils. Cations, such as Ca, Mg and K, can displace U ions from soil exchange sites and force them into solution. Uranium has a high positive charge, and therefore, it is strongly sorbed by soils rich in Fe and Mn-oxides and organic matter (Alloway 2010). Uranium is readily leached under oxidative and acidic conditions, which are common in Pelee Island surface soils, and will be leached deeper into the soil profile to form soluble complexes with CO_3^- ions at a higher pH. This increases the amount of available U in soil solution for plant uptake (Alloway 2010; Vodyanitskii 2011).

4.5.3 Plant Extractable Nutrients PC2

Principal component 2, illustrated in Figure 4.26, accounts for 18.31% of the variance in the plant extractable nutrient data and has an eigenvalue of 3.30. Variance can be observed among sampling depths and sampling fields. Generally, section 4 soils have higher concentrations of Ba, Li, Mo, Si, and Sr, whereas section 1, 2, and 3 soils have less. Lithium is variable among fields and the most important factor controlling Li content in soils is clay mineral content. High Li concentrations are found in soils where clay mineral content is also high and especially in humid and temperate climate conditions where it is leached down through the soil profile (Alloway 2010). Thus, Li is usually found in deeper soil horizons on Pelee Island where clay is more abundant (Figure 3.3). Brookston soils (5GM318, 5GM318D, and 1A) are mostly negatively correlated with Li in sections 1 and 2, whereas some Toledo soils are positively correlated, indicating that Brookston soils have lower Li abundance and thus lower clay abundance compared to Toledo soils (Figure 4.27). In addition, soils at sections 1 and 2 are mostly negatively correlated with Li, whereas soils at sections 3 and 4 are positively

correlated with Li. This means that there is lower Li content in surface soils and higher Li content in deep soils (Figure 4.27), thus indicating a higher clay content in deep soils. Similar findings were observed by Tolo (2019); Brookston soils contained lower clay content than Toledo soils ($23 \pm 3\%$ in Brookston and $29 \pm 3\%$ in Toledo) and surface soils had low clay content compared to deep soils (12-22% in surface soils and 27-33% in deep soils) (Tolo 2019).

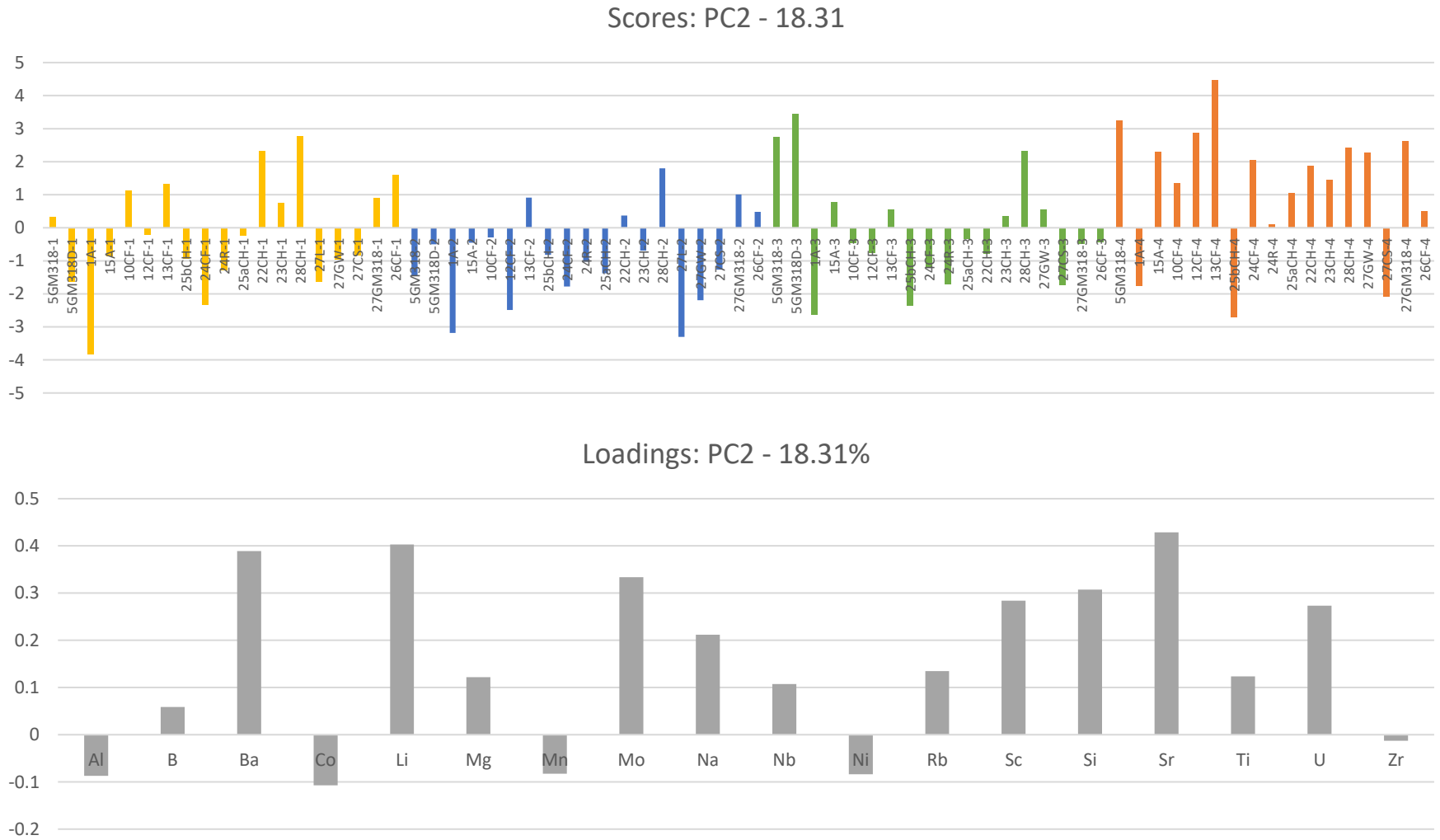


Figure 4.26. PC2 scores and loadings, illustrating nutrient element variations at depth and among field locations on Pelee Island. Scores are arranged by location (left to right on the graph represents south to north on the island) and by depth (yellow = section 1, blue = section 2, green = section 3, and orange = section 4). The magnitude of the bars on each graph indicate the strength of the correlations between scores (soil samples) and loadings (elements).

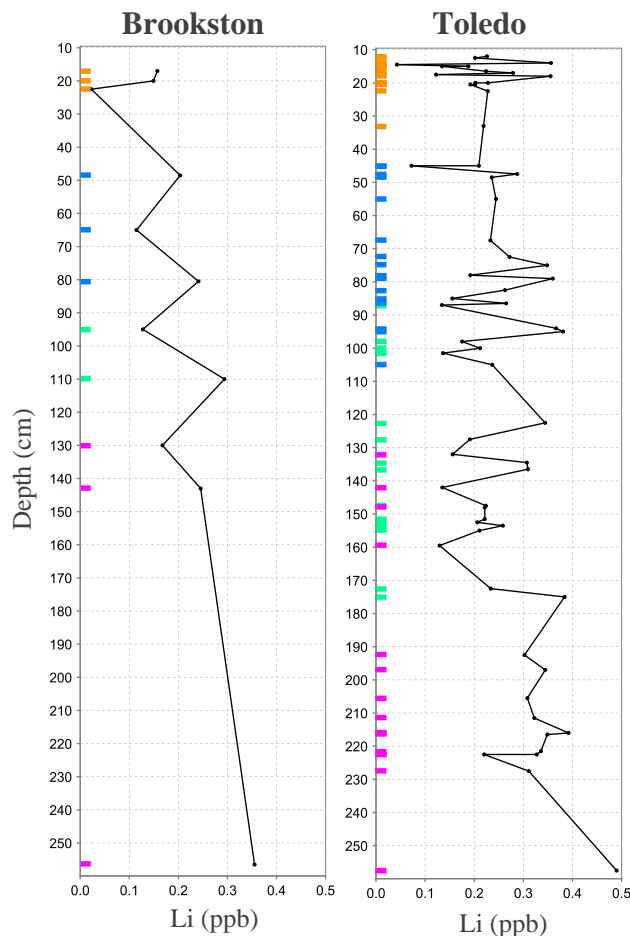


Figure 4.27. Depth versus concentration graphs comparing concentration differences with depth of Li between Brookston and Toledo soils. Soil sample depth of each soil sample plotted against elemental concentrations of Li of each soil sample. Data is compiled from all 19 soil profiles. Sampling depths are distinguished by colour on the left side of the graph: Section 1 = orange, section 2 = blue, section 3 = green, and section 4 = purple.

The bubble plots (Figure 4.28) show that the northwest side of the island is associated with low concentrations of Ba, Li, Mo, Si, and Sr, whereas the southeast side is generally associated with more Ba, Li, Mo, Si, and Sr regardless of depth. However, the reasons for this distribution is unknown. In addition, Ba is abundant in deep soils (Figure 4.29), which can be explained by the sorption of Ba by some hydroxides such as MnO and displacement from Al₂O₃ by alkaline earth metals such as Sr (Alloway 2010). Barium is not very mobile due to adsorption onto clays and because of precipitation as BaCO₃ in the presence of high carbonate content, such as in deep soils on Pelee Island (average of

11.19% CO_3 in section 4 soils). In addition, Cl^- ions increase Ba mobility (Alloway 2010) and these ions were used in the CaCl_2 extraction.

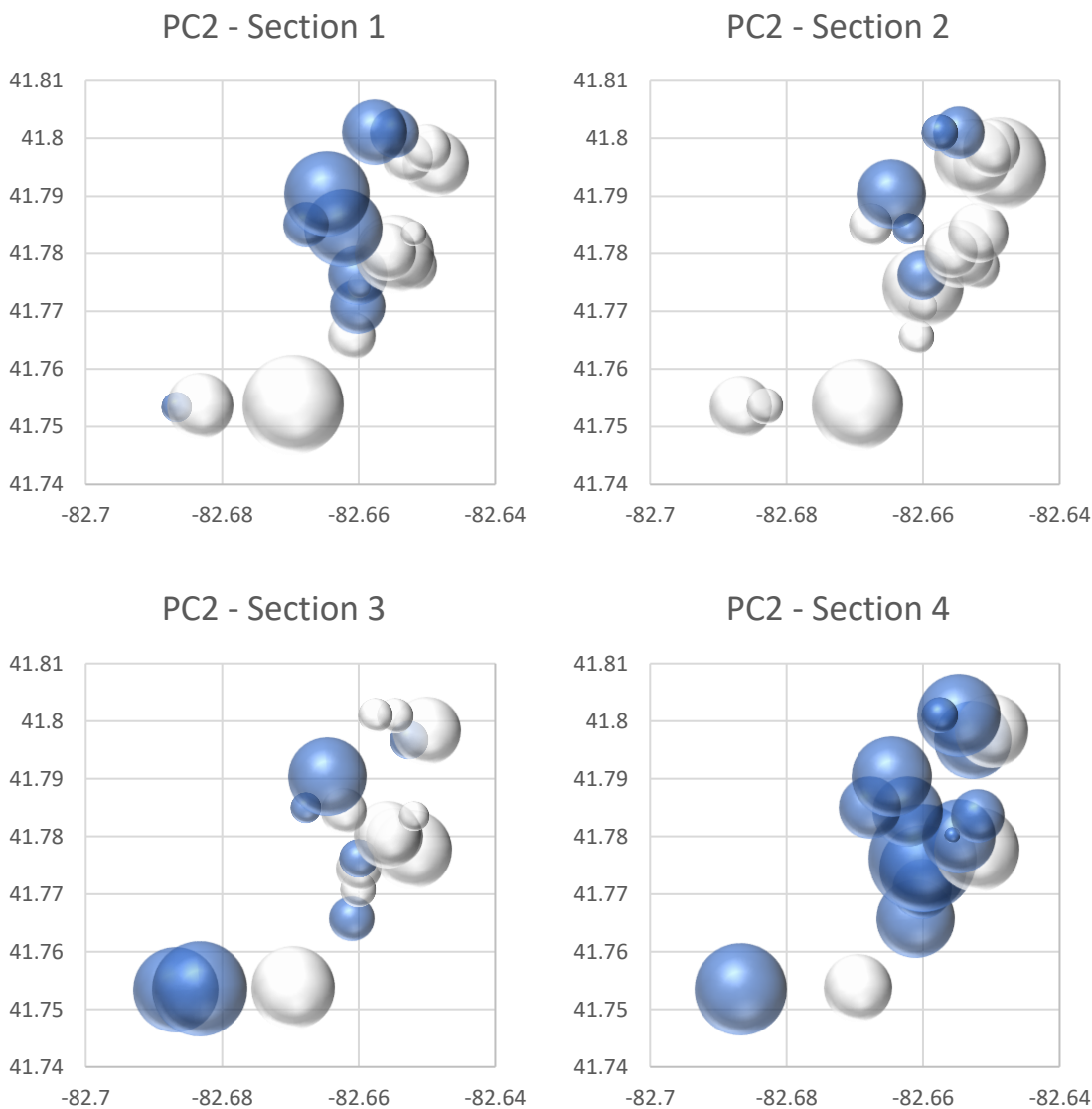


Figure 4.28. Bubble plots for PC2. These graphs provide spatial representation of the nutrient element data on Pelee Island. Each graph represents element loadings at sections 1, 2, 3, and 4. The x-y coordinate of the bubbles on the graphs represent their locations on the island in decimal degrees (easting; x-axis, northing; y-axis). These graphs are to be used together with the loadings plot from PC2. Colour indicates positive or negative scores; blue is positive and white is negative. Size of the bubbles indicates magnitude of correlations between scores (soil samples) and loadings (elements).

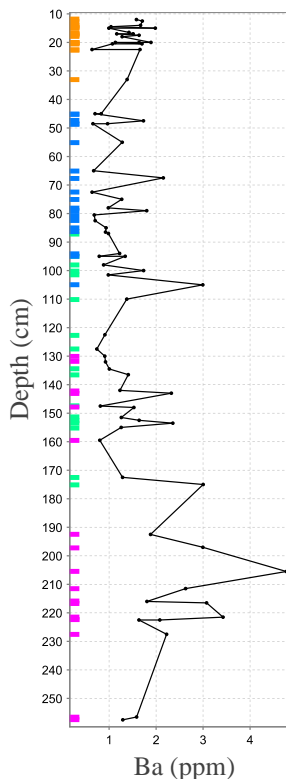


Figure 4.29. Depth versus concentration graph showing concentrations of Ba increasing with soil depth. Soil sample depth of each soil sample plotted against elemental concentrations of Ba of each soil sample. Data is compiled from all 19 soil profiles. Sampling depths are distinguished by colour on the left side of the graph: Section 1 = orange, section 2 = blue, section 3 = green, and section 4 = purple.

4.5.4 Plant Extractable Nutrients PC3, PC4, PC5

Principal component 3 has a variance of 13.53% and an eigenvalue of 2.44, PC4 has a variance of 6.92% and an eigenvalue of 1.25, and PC5 has a variance of 6.32% and an eigenvalue of 1.14. Although all these PC's have eigenvalues >1 , the ability to interpret the cause of these variations is limited due to low element concentrations and many elements being below detection limits. Thus, these principal components did not provide valuable indicators of soil processes. These components did, however, detect outliers among fields. For example, field 13CF soils in section 4 have a high amount of soluble Na, with values of 285ppm compared to the average of 26 ± 15 ppm. It is possible that the presence of Na might suggest salts had formed in the capillary fringe above the water table. Up until the late 1800s many areas on Pelee Island were covered by marshy lowlands below lake level until the implementation of drainage systems in the late 1800s

(Brown 2009). Although drainage systems have lowered the water table on the island, it would not be unreasonable that a soil sampled at a depth of 205 cm was in the capillary fringe just above the water table. Natural ponds on the east side of the island (e.g. in field 27L) indicate that the water table is quite shallow in some areas. Another outlier detected by the PCA, field 24CF, contained Al and Co whereas many other fields were below detection limits for these elements. Field 24CF soils in section 1 have the lowest pH value of all soil samples with a value of 5.37 and is likely a result of the compost fertilizer used on this field. Field 24 soils in section 1 likely have more Al, Ni and CEC from the addition of compost, making these elements present in greater concentrations compared to other fields.

4.6 Relationship of PEN to Soil Mineralogy

Plant extractable nutrient data and mineral data measure different features of the soil; mineral data measures the total elemental composition of soils (elements that make up the minerals as well as any elements that are attached to particle surfaces), whereas PEN data measure elements that are available for exchange on soil particle surfaces. Weathering is most intense in surface soils and releases many elements locked in crystalline structures and bound to organic matter. Therefore, PEN are generally highest in surface soils. The organic matter and clay mineral content of the soils prevents these elements from being leached deeper into the profile (Weil & Brady 2017). Thus, differences in abundances of elements between plant extractable nutrients and soil mineralogy in Pelee Island soils can be attributed to CEC, clay mineral abundance, and adsorption. Although soil mineralogy plays an important role in determining nutrients available to plants, the CEC, clay mineral content, and adsorption play a more important role. For example, elements such as Mn and Mg that have relatively low mineral abundances in surface soils are still abundant in PEN in surface soils (Figure 4.30). The difference in elemental composition of Mg and Mn between the soil mineral component and the plant extractable component of Pelee Island soils indicates that the controlling factor is not the mineral component but the CEC of the soil.

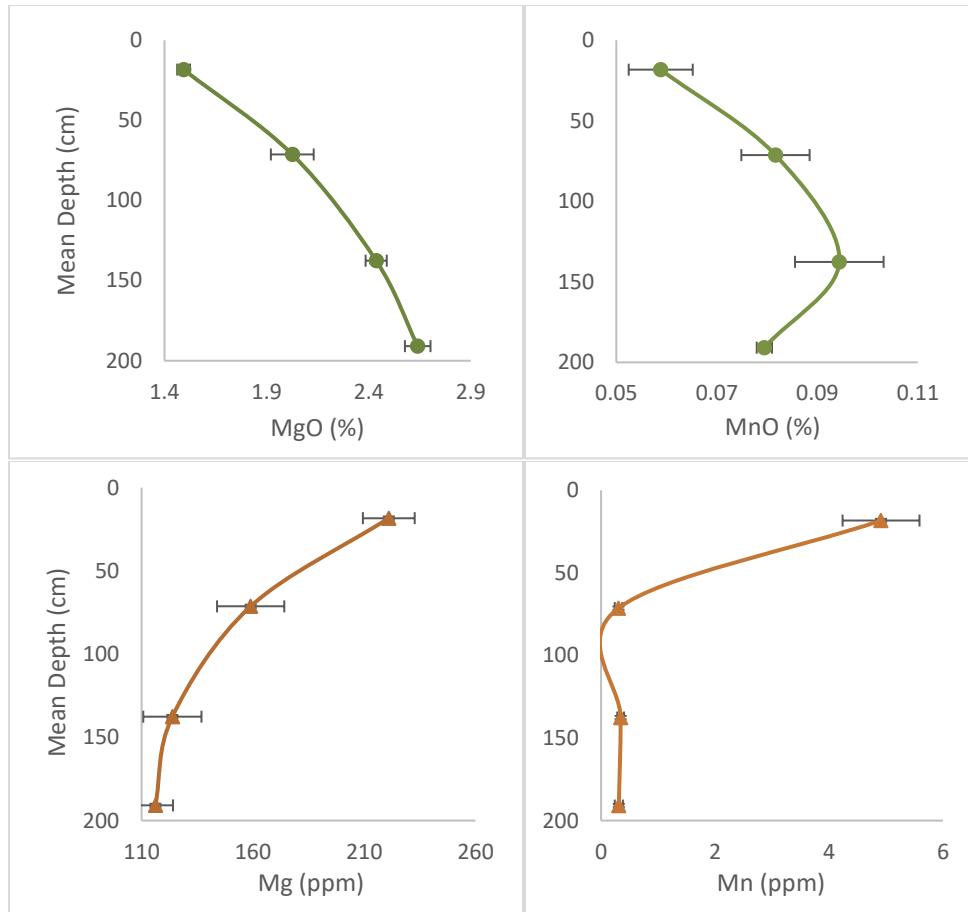


Figure 4.30. Depth versus concentration graphs comparing average concentration differences with depth of Mg and Mn between the mineralogical components (green circles) and the PEN components (red triangles) of the Pelee Island soils. Soil sample depth plotted against oxide and elemental concentrations (Mg, Mn) of averaged soil sample concentrations at each depth.

Clay mineral content of soils and adsorption onto their mineral surfaces are important factors for controlling extractable nutrients (Alloway 2010). Adsorption and CEC are higher in clay-rich soils because there are more negatively charged surface particles for cation exchange due to the smaller grain size. This is evident when comparing elemental concentrations of Li between soil mineral data and soil extractable nutrient data.

Although mineral Li is most abundant in surface soils, the extractable portion of Li is most abundant in deep soils where clay mineral contents are greater (Figure 3.3). Further, Toledo soils have higher clay mineral content relative to Brookston soils (Figure 3.3) and have greater abundances of some PEN such as Li and U. In addition, adsorption of

elements onto mineral surfaces increases PEN, and is evident from increased abundances of available Mo, Ba, and U adsorbed onto Fe and Mn oxides in the B horizon (Alloway 2010).

Mineralogy (parent material) of the soils will also affect the availability of extractable nutrients. For example, soils that are calcareous, such as Pelee Island soils, produce carbonate ions upon weathering and raise the pH of soils, which helps prevent soil acidification and leaching of elements (Weil & Brady 2017). Therefore, higher abundances of extractable nutrients will be available for plant uptake. For instance, U is more available in deep soils where it forms soluble complexes with CO_3^- (Vodyanitskii 2011). Parent material can also inhibit the availability of some elements. For example, in a study of Na accumulation in calcareous soils, Eimers et al. (2015) found that soils derived from Ca-rich parent materials are less vulnerable to Na enrichment. This is because Na is unable to displace Ca from soil exchange sites and Na is more effectively transported through calcareous soil profiles.

It is clear that CEC, clay mineral content, and adsorption are important factors that affect the PEN portion of Pelee Island soils. In addition, soil mineralogy is equally important because it controls factors such as CEC, clay mineral content, and adsorption capacity. In addition, weathering of parent material determines the original supply of nutrients and controls their distribution throughout the soil profile. Therefore, the mineralogy of the soil ultimately determines type and quantity of nutrients that will be available for plants in soil solution. Although the CaCl_2 extraction method provided essential information on nutrient availability throughout the soil profile, other extraction techniques are required to better understand Pelee Island soil fertility.

Chapter 5

5 Conclusions

This study provides an extensive overview of the geochemical composition of bedrock and soils on Pelee Island and outlines general soil processes that cause differences in elemental distribution throughout the soil profile and among different sites. This chapter draws conclusions from the research presented throughout this thesis and provides recommendations for future work.

5.1 Depth to Bedrock

Depth to bedrock in Toledo soils, in the middle area of the island, is variable with depths ranging from 0.6 m to 30 m. However, in most fields the depth to bedrock is deep (13-30 m), except in the middle northeast area of the island; field 27CS has a shallow depth to bedrock of 5 m and 27L has an even shallower depth of 0.6 m. Soil thickness in Toledo soils ranges from 1-3 m and the underlying till has a thickness of 4-22 m. Conversely, depth to bedrock in Brookston soils, in the southwest area of the island, is very shallow at approximately 2 m deep. Brookston soils directly overlie bedrock and lack the till layer that is present under the Toledo soils. Brookston soils are shallow and soil layering is different than in Toledo soils, and therefore, Brookston soils are not directly comparable to Toledo soils and depth to bedrock does not have a direct influence on the elemental composition of either soil.

5.2 Effect of Bedrock on Soil Composition of Pelee Island

The REE distribution patterns confirm that Pelee Island bedrock does not influence the composition of Pelee Island soils. Although Slack (2015) proposed that groundwater percolating through bedrock could leach elements and contribute them to Pelee Island soils, no anomalous elemental signatures are observed in the soils, disproving this theory.

The REE distribution patterns are the same among all fields and soil depths. However, concentrations of REE are different among soil depths; concentrations of REE are highest in the surface soils and decrease with depth. The high REE concentrations observed in

surface soils, however, are not from fertilizer application and the more likely cause of REE enrichment in Pelee Island surface soils is organic matter input. This could be from leaf litter of the grape vines, natural cycling of the cover crops, or the addition of compost which is locally grown on the island. The REE distributions of Pelee Island compost are the same as observed for the soil (although absolute concentrations in the soil are higher).

5.3 Using PCA to Identify Geochemical Differences Among Soil Samples

Principal component analysis is an effective tool that identifies geochemical differences among soil samples, detects anomalies within the data, and allows for concise interpretations to be made from the data, which further outline soil processes. Principal component analysis reveals significant differences in elemental concentrations between soil depths and different fields on Pelee Island.

5.3.1 Mineralogical Variability

The mineral element data include both elements that are contained within mineral structures and those adsorbed onto particle surfaces. Although the adsorbed elements may not have been released by the CaCl_2 extraction method (for reasons that are explained in the discussion), they are included in the mineral element results because the analyses did not exclude any components of the soil (i.e. mineral components, plant extractable components, and added fertilizers). Most soil oxides and elements are highest in surface soils and decrease with depth; however, there are some exceptions. Specifically, Al and Si are abundant in surface soils because these are the most common oxides that remain following mineral weathering, such as feldspars. Generally, Ca, Mg, and Sr are most abundant in deep soils. This is because calcite weathers from surface soils via the process of dissolution and precipitates in deeper soil horizons where pH is higher, such as in the deep soils on Pelee Island. The Mg and Sr abundances are greater in deep soils because they have a similar ionic radius to Ca and can substitute for Ca in mineral structures. Iron, Mn, and Mo are more abundant in the B horizon because Fe and Mn are leached from the A horizon and form oxides and hydroxides in the B horizon and Mo adsorbs onto hydroxides formed in the B horizon.

Sodium concentrations are slightly higher in surface soils; however, Na concentrations do not decrease steadily with depth. Sodium is slightly higher in surface soils because it is retained by organic matter in low pH surface soils. Additionally, in clay mineral rich soils that are not well drained, Na^+ is not effectively leached into deep soils and evaporation and removal of water by plant roots can also cause it to accumulate in surface soils.

5.3.2 PEN Variability

The abundance of plant-extractable nutrients within the soil profile is primarily affected by soil depth. Plant extractable nutrients are most abundant in surface soils, except for Mo and U, which are more readily available in deep soils. Plant extractable nutrients are generally more abundant in surface soils where organic matter is most abundant and where weathering is most intense, thus releasing most nutrients available for plant uptake.

Plant extractable Mo and U are most available in deep soils, where they can adsorb onto Fe and Mn oxides and hydroxides formed in the B horizon. Lithium is also abundant in deep soils on Pelee Island because Li is generally associated with soils that have high clay content, such as the deeper soils on Pelee Island. Thus, Li is more associated with Toledo surface soils than with Brookston surface soils because of the high clay mineral content of Toledo soils. The plant extractable nutrient data show that organic matter content, clay abundance, and adsorption are the most important factors controlling the nutrient availability in Pelee Island soils.

In this study we observe that the plant extractable nutrient contents of the Pelee Island soils do not differ between fertilized and unfertilized fields. According to our study, this finding appears to indicate that application of chemical fertilizers does not contribute to the nutrient content of Pelee Island soils. However, because the CaCl_2 extraction method produced very low concentrations of plant extractable nutrients, it is likely that the CaCl_2 extraction method was too weak to detect contributions of chemical fertilizers to Pelee Island soils and/or since PEN were measured in the fall, the soil's nutrient supply had been depleted by grapevine uptake during the summer months. Thus, further investigations using either, a higher concentration of the CaCl_2 extraction solution, or using different soil nutrient extraction methods should be performed.

5.3.3 Soil Horizon and Weathering Profiles in Brookston and Toledo Soils

The A horizons are approximately 30 cm thick and have abundant organic matter causing dark brown colouration. The B horizons in Toledo soils extend >2 m deep, but in Brookston soils are on average approximately 50 cm deep. All B horizon soils are clay mineral rich, ranging in colour from a greenish grey to reddish brown. The greenish grey colour indicates that these soils have been exposed to periods of water saturation which produces gleysols. The C horizons are only present in shallow soils such as 5GM318, 27CS, 1A, 27L, and 25aCH, and are only differentiated from B horizons by the abundance of lithic fragments.

Soil weathering is greatest in surface soils, which have high Al and low Ca content, whereas deep soils have low Al and high Ca content. Soil organic matter is highest in surface soils and organic acids produced by organic matter contribute to the low pH of surface soils. The acids released from the decay of organic matter leach elements, such as Ca, Fe, Mn into the B horizon where pH is greater, and these elements accumulate as oxides, hydroxides, and carbonates (specifically CaCO_3). Thus, carbonate content is lowest in surface soils and increased exponentially when soil pH was over 7.5.

Mineralogy and soil chemistry vary between Brookston and Toledo soils because of differences in leaching intensities. Calcium, Mg, and Sr are more abundant in Brookston surface soils compared to Toledo soils. Because calcite is an easily weathered mineral, higher concentrations of Ca in Brookston surface soils indicate that they are less leached than Toledo soils. Conversely, high concentrations of Al in Toledo soils indicate that intensive leaching has leached elements like Ca from easily weathered minerals, leaving behind minerals rich in Si and Al that are more resistant to weathering. In addition, Brookston soils don't show an accumulation of MnO or Fe_2O_3 in the B horizon, which is also an indication that Brookston soils are less leached.

5.3.4 Soil Elemental Difference Among Vineyard Fields on Pelee Island

Generally, elemental concentrations of the mineral components of the soils are similar among fields, however, there are a few fields where differences were identified by the PCA. Some differences observed among fields can be attributed to differences in soil horizon thicknesses and sampling depth that result in inconsistent element behavior when comparing all soils from the same relative depth (e.g. section 3 soils) between cores. Some fields have elemental contents that varied for other reasons.

Field 1A behaves differently from most fields with respect to element distribution with depth. Field 1A has low organic matter content, higher pH and higher Ca, Mg, and Sr content in surface soils compared to other fields. This may suggest mixing of soil horizons has occurred, which disrupts the natural weathering profile and could be a result of soil tillage. The deepest soil in field 13CF, sampled at a depth of 205 cm, has a significantly high concentration of extractable Na compared to other fields, which suggests the formation of salt above the capillary fringe of the water table on Pelee Island. Field 24CF, which is used for organic farming, contains higher concentrations of some plant extractable elements than other fields, which is likely the result of the addition of large amounts of compost fertilizer to this field, which also results in one of the lowest pH values (5.37) in surface soils on Pelee Island.

Fields 25bCH, 23CH, and 26CF in soil sampling sections 3 and 4 have higher amounts of Mo, Sb, Fe, Mn, Mg, Co and/or Ni compared to other fields at the same sampling depths. Field 26CF has a low carbonate content at all depths, demonstrating that acid leaching has been extensive and that this field may have been subject to periods of waterlogging. Further, waterlogged soils usually exhibit slowed organic matter decomposition, resulting in high accumulation of organic matter and was observed that fields 25bCH, 23CH, and 26CF have abundant organic matter in their surface soils. The acidity of organic matter increases metal mobility resulting in an accumulation of metals in deep soils where clay content and pH are high. Thus, these observations indicate that fields 25bCH, 23CH, and 26CF have experienced periods of poor drainage and/or waterlogged conditions, which cause accumulations of heavy metals in deep soils.

5.3.5 Agricultural and Anthropogenic Inputs and Effect on Soil Composition

Although this study has shown that soil additives do not affect REE composition of the soil, they do impact soil composition of other elements. For example, P concentrations are significantly different among fields that were sampled in August versus fields that had been sampled in October. This suggests that the difference in P concentrations is a result of fertilizer application. Copper is abundant in the surface of Pelee Island soils that grow grapes as a result of Cu containing compounds that are sprayed on grape leaves to control disease. Pelee Island surface soils contain greater amounts of the heavy metals Pb, Cd, and U than deep soils. Cadmium and Pb are constituents of airborne pollutants, such as automotive gasoline, which can be deposited on surface soils, and is likely responsible for increased levels of these elements. Cadmium is also a common constituent in phosphate fertilizers and elevated levels of Cd are found in topsoils of fields that are fertilized and low levels of Cd are found in unfertilized fields such as 24CH (the organic field) and 24R (the reference field). Uranium was enriched in Pelee Island chemical fertilizers, compared to the NASC standard, suggesting that increased U concentrations in Pelee Island soils could be attributed to addition of U from chemical fertilizers.

5.4 Future Work

The CaCl_2 extraction method produced low plant extractable nutrient concentrations, and many element concentrations are below detection limits. Some of the elements below detection limits are key plant nutrients such as Ca, K, P, Fe, S, Cu, and Zn, thus making interpretations of nutrient availability difficult. It would be interesting to compare the results of the CaCl_2 extraction method to other more popular extraction methods used in Ontario, such as the sodium bicarbonate extraction method (Olsen), ammonium acetate, DTPA, EDTA, and/or phosphoric acid; particularly for P and K, which are two main components of chemical fertilizers. Doing this could provide a better understanding of fertilizer influence on plant extractable nutrient composition. It would also be useful to compare concentrations of plant extractable nutrients during different seasons, as some studies have demonstrated that some nutrients are more available depending on timing of

fertilizer application and the season (Franzen 2018; Omer et al. 2018). Further, a natural fertilizer made from carbonate rocks, that contains 50% calcium carbonate, 25% biotite (increases available K), 12% apatite (increases available P), 13% trace and REE (including, but not limited to Mn, Zn, Cu, Co, Mo, B) may be added to Pelee Island soils. Since soil processes and natural distributions of elements on Pelee Island have been investigated and are now understood, it would be beneficial to test the effects such a fertilizer has on the soil.

The REE have been used to authenticate wines by comparing the REE content of soil to wine (e.g. Aceto et al. 2018). Numerous studies including those conducted by Aceto et al. (2013), Di Paola-Naranjo et al. (2011), Hopfer et al. (2015), and Taylor et al. (2003), have compared the trace and REE content between soils and wine and found that REE distribution patterns were the same in grapes and the soils in which they grew. Comparing the REE fingerprints of grapes to the soils on Pelee Island would show how the REE signature in the soils affects the REE signature of the grapes. Identifying REE fingerprints specific to grapes that grow on Pelee Island versus the Essex County mainland, could provide proof of the uniqueness of Pelee Island soils in hopes that Pelee Island may be reinstated as its own appellation.

This study provides an extensive overview of the geochemical composition of bedrock and soils on Pelee Island and also outlines general soil processes that cause differences in elemental distribution throughout the soil profile. It could be beneficial to investigate the causation of different weathering intensities between Brookston and Toledo soil profiles and to compare productivity of the grapes grown on each of these soil types so that the winery can adjust their plant management strategies accordingly. Finally, in order to identify unique soil characteristics that would enable the Pelee Island Winery to be reinstated as its own appellation, similar studies should be performed at other wineries on the North Shore of Lake Erie.

References

- Aceto, M., Musso, D., Bonello, F., Tsolakis, C. 2018. Wine traceability with rare earth elements. *Beverages*, **4**: 1-11.
- Aceto, M., Robotti, E., Oddone, M., Marengo, E. 2013. A traceability study on the Moscato wine chain. *Food Chemistry*. **138**: 1914–1922.
- Acuna-Avila, P.E., Vasquez-Murrieta, M.S., Hernandez, M.O.F., Lopez-Cortez, M.D.S. 2016. Relationship between the elemental composition of grapeyards and bioactive compounds in the Cabernet Sauvignon grapes *Vitis vinifera* harvested in Mexico. *Food Chemistry*, **203**: 79-85.
- Agriculture and Agri-Food Canada. 2016. Canada's wine industry. Available from <http://www.agr.gc.ca/eng/industry-markets-and-trade/statistics-and-marketinformation/by-product-sector/processed-food-and-beverages/canadas-wineindustry> [11 November 2017].
- Aide, M.T. & Aide, C. 2012. Rare Earth Elements: Their importance in understanding soil genesis. *Soil Science*, **2012**: 1-11.
- Aide, M.T., Herberlie, L., Statler, P. 1999. Soil genesis on felsic Rocks in the St. Francois Mountains. II. The distribution of elements and their use in understanding weathering and elemental loss rates during genesis. *Soil Science*, **164**: 946–959.
- Aide, M.T. & Smith, C. 2001. Soil genesis on peralkaline felsics in Big Bend National Park. *Soil Science*, **166**: 209–221.
- Alloway, B. J. 2013. Bioavailability of elements in soil. *Essentials of Medical Geology*, Springer Science, Berkshire, UK.
- Alloway, B. J. 2010. *Heavy metals in soil*. Springer, New York, United States.
- Altman, N. & Krzywinski M. 2015. Association, correlation and causation. *Nature Methods*, **12**: 899-900.
- AMS. 2019. Gas powered core sampling kit. Available from <https://www.ams-samplers.com/gas-powered-core-sampling-kit.html> [August 2019].
- Anderson, D. W. 1988. The effect of parent material and soils development on nutrient cycling in temperate ecosystems. *Biogeochemistry*, **5**: 71-97.
- Anderson N.P., Hart, J.M., Horneck, D.A., Sullivan, D.M., Christensen, N.W., Pirelli, G.J. 2010. *Evaluating Soil Nutrients and pH by Depth*. Oregon State University, Extension Service.

- Atkin, T. & Johnson, R. 2010. Appellation as an indicator of quality. *International Journal of Wine Business Research*, **22**: 42-61.
- Aubert, D., Stille, P., Probst, A. 2001. REE fractionation during granite weathering and removal by waters and suspended loads: Sr and Nd isotopic evidence. *Geochimica et Cosmochimica Acta*, **65**: 378-406.
- Aubert, D., Stille, P., Probst, A. 2004. Distribution and origin of major and trace elements (particularly REE, U and Th) into labile and residual phases in an acid soil profile (Vosges Mountain, France). *Applied Geochemistry*, **19**: 899-916.
- Azcarate, S.M., Martinez, L.D., Savio, M., Camina, J.M., Gil, R.A. 2015. Classification of monovarietal Argentinean white wines by their elemental profile. *Food Control*: **57**, 268-274.
- Berner, E. K. & Berner, R. A. 2012. *Global environment – water air, and geochemical cycles*. Princeton University Press, Second Edition.
- Brown, R. 2009. *The Lake Erie Shore – Ontario’s Forgotten South Coast*. Natural Heritage Books.
- Bryanin, S.V. & Sorokina, O. A. 2014. The first data on the vertical REE distribution in Taiga soils of the Russian far east. *Geochemistry*, **464**: 1053-1057.
- Burns, S. & Retallack, G.J. 2015. The effects of soil on taste of wine. *Geological Society of America Today*, **26**: 4-9.
- Canadian Vintners Association. 2017a. Industry statistics. Available from <https://www.canadianvintners.com/industry-statistics/> [March 2020].
- Canadian Vintners Association. 2017b. International market development: International export strategy from Canadian wine. Available from <http://www.canadianvintners.com/initatives/international-market-development/> [July 2019].
- Cantrell, K.J. & Byrne, R.H. 1987. Rare earth element complex by carbonate and oxalate ions. *Geochimica et Cosmochimica Acta*: **51**: 597–605.
- Caporale, A. G. & Violante, A. 2016. Chemical processes affecting the mobility of heavy metals and metalloids in soil environment. *Current Pollution Reports*, **2**: 15–27.
- Chapman, L.J. & Putnam, D.F. 1951. *Physiography of southern Ontario*. University of Toronto Press, Toronto, Ontario.

- Chen, W., Krage, N., Wu, L., Pan, G., Khosrivafard, M, Chang, A.C. 2008. Arsenic, cadmium, and lead in California cropland soils: role of phosphate and micronutrient fertilizers. *Journal of Environmental Quality*, **37**: 689-695.
- Cowan, W. R. 1976. Quaternary geology of the Orangeville area, southern Ontario. Ontario Division of Mines, Geoscience Report, **141**: 1-98.
- da Cruz, M., & Casagrande, J. (2004). Nickel adsorption by soils in relation to pH, organic matter, and iron oxides. *Scientia Agricola*, **61**: 190–195.
- Dauer, J. M. & Perakis, S. S. 2013. Contribution of calcium oxalate to soil-exchangeable calcium. *Soil Science*, **178**: 671-678.
- Deluisa, A., Aichner, M., Giandon, P., Bortolami, P. (1996). Copper pollution in Italian vineyard soils. *Communications in Soil Science and Plant Analysis*, **27**: 1537-1548.
- de Vries, H. & Dreimanis, A. 1960. Finite radiocarbon dates of the Port Talbot interstadial deposits in southern Ontario. *Science*, **131**: 1738-1739.
- Di Paola-Naranjo, R.D., Baroni, M.V., Podio, N.S., Rubinstein, H.R., Fabani, M.P., Badini, R.G., Inga, M., et al. 2011. Fingerprints for main varieties of Argentinean wines: Terroir differentiation by inorganic, organic, and stable isotopic analyses coupled to chemometrics. *Journal of Agriculture Food Chemistry*, **59**: 7854–7865.
- Doloreux, D. & Lord-Tarte, E. 2012. Context and differentiation: Development of the wine industry in three Canadian regions. *The Social Science Journal*, **49**: 519-527.
- Earle, S. 2019. Physical Geology. BC campus, Victoria, B.C. Available from <https://opentextbc.ca/physicalgeology2ed/> [May 2020].
- Eimers, C. M., Croucher, K., Raney, S.M., Morris, M.L. 2015. Sodium accumulation in roadside soils. *Urban Ecosystems*, **18**: 1213-1225.
- Essex Region Conservation Authority. 2011. Interactive mapping. Available from http://ercamaps.countyofessex.ca/?viewer=http%3A%2F%2Fgisweb.countyofessex.ca%2Fhtmlerca2112%2FIndex.html%3FconfigBase%3Dhttp%3A%2F%2Fgisweb.countyofessex.ca%2FGeocortex%2FEssentials%2FERCA%2FREST%2Fsites%2FERCA__Public%2Fviewers%2Fhtmlpublic%2Fvirtualdirectory%2FResources%2FConfig%2FDefault&image.x=53&image.y=21 [May 2020].
- Evans, L. J. & Cameron, B. H. 1983. The Brookston series in southwestern Ontario: characteristics, classification and problems in defining a soil series. *Canadian Journal of Soil Science*, **63**: 339-352.

- Eyles, N., Arnaud, E., Scheidegger, A.E., Eyles, C.H. 1997. Bedrock jointing and geomorphology in southwestern Ontario, Canada: an example of tectonic predesign. *Geomorphology*, **19**: 17-34.
- Fowler, A. D. 1993. Fluid Pathways and Drive Mechanisms of Pb-Zn Mineralizing Basinal Brines, Distal, or Proximal Geopressure Zone Sources? Contributions to an International Conference on fluid evolution, migration and interaction in rocks, Torquay, England. *Sediment-Hosted Zn-Pb Ores*, Springer, Berlin, Heidelberg.
- Fraga, H. Malheiro, A.C., Moutinho-Pereira, J., Cardoso, R.M, Soares, P.M.M., Cancela, J.J., Pinto, J.G., Santos, J.A. 2014. Integrated analysis of climate, soil, topography and vegetative growth in Iberian viticulture regions. *PLoS ONE*, **9**: 1-14.
- Franzen, D.W. 2018. Soil Sampling as a basis for fertilizer application. NDSU. Available from <https://www.ag.ndsu.edu/publications/crops/soil-sampling-as-a-basis-for-fertilizer-application> [April 2020].
- Galbarczyk-Gasiorowska, L. 2010. Rare earth element mobility in a weathering profile – a case study from the Karkonosze Massif (SW Poland). *Acta Geologica Polonica*, **60**: 599-616.
- Gao, C. 2011. Buried bedrock valleys and glacial and subglacial meltwater erosion in Southern Ontario, Canada. *Canadian Journal of Earth Science*, **48**: 801-818.
- Germund, T. & Tommy, O. 2005. Rare earth elements in forest-floor herbs as related to soil conditions and mineral nutrition. *Biological Trace Element Research*, **106**: 177–191.
- Gouveia, M.A., Prudencio, M.I., Figueiredo, M.O., Pereira, L.C.J., Waerenborgh, J.C., Morgado, I., Pena, T, Lopes, A. 1993. Behaviour of REE and other trace and minor elements during weathering of granitic rocks, Evora, Portugal. *Chemical Geology*, **107**: 293-296.
- Government of Canada. 2019. Daily data report for October 2017, Kingsville, Ontario. Available from https://climate.weather.gc.ca/climate_data/daily_data_e.html?hlyRange=%7C&dllyRange=1960-10-01%7C2020-03-29&mlyRange=1960-01-01%7C2006-12-01&StationID=4647&Prov=ON&urlExtension=_e.html&searchType=stnName&optLimit=yearRange&StartYear=1840&EndYear=2020&selRowPerPage=25&Line=31&searchMethod=contains&Month=3&Day=30&txtStationName=King&timeframe=2&Year=2020 [August 2019].
- Government of Canada. 2013a. Description of soil ONTLDC~~~~A (TOLEDO) Available from <http://sis.agr.gc.ca/cansis/soils/on/TLD/C~~~~/A/description.html> [March 2020].

- Government of Canada. 2013b. Description of soil ONBKNLY~~~A (BROOKSTON). Available from <http://sis.agr.gc.ca/cansis/soils/on/BKN/LY~~~/A/description.html> [March 2020].
- Gransee, A., Führs, H. 2013. Magnesium mobility in soils as a challenge for soil and plant analysis, magnesium fertilization and root uptake under adverse growth conditions. *Plant and Soil*, **368**: 5–21.
- Greenough, J.D., Mallory-Greenough, L.M., Fryer, B.J. 2005. Geology and wine 9: Regional trace element fingerprinting of Canadian wines. *Geoscience Canada*, **32**: 129-137.
- Gromet, L.P. & Silver, I.T., 1983. Rare earth element distribution among minerals in a granodiorite and their pedogenic implications. *Geochimica et Cosmochimica Acta*, **47**: 925-939.
- Gromet, P.L., Dymek, R.F., Haskin, L.A., Korotev, R.L. 1984. The “North American shale Composite”: Its compilation, major and trace element characteristics. *Geochimica et Cosmochimica Acta*, **48**: 2469-2482.
- Hewitt, D.F. 1972. Paleozoic geology of southern Ontario. Ontario Division of Mines Geological Report 105, Toronto, Ontario.
- Holcombe, T.L., Taylor, L.A., Warren, J.S., Vincent, P.A., Reid, D.F., Herdendorf, C.E. 1997. Lake floor geomorphology of western Lake Erie. *Journal of Great Lakes Research*, **23**: 190-201.
- Hornung, M. 1971. Unique Bedrock and Soils Associated with the Teasdale, Flora. *Nature*, **232**: 453-456.
- Houba, V.J.G., Novozamsky, I., Huybregts, A.W.M., Van Der Lee, J.J. 1986. Comparison of soil extractions by 0.01 M CaCl₂, by EUF and by some conventional extraction procedures. *Plant and Soil*, **96**: 433-437.
- Houba, V.J.G., Temminghoff, E.J.M., Gaikhorst, G.A., van Vark, W. 2008. Soil analysis procedures using 0.01 M calcium chloride as extraction reagent. *Communications in Soil Science and Plant Analysis*, **31**: 1299-1396.
- Howell, D. G., & Swinchatt, J. P. 2000. A discussion of geology, soils, wines, and history of the Napa Valley Region. *Geological Society of America Field Guide*, **2**: 415-422.
- Hu, Z., Haneklaus, S., Sparovek, G., Schnig, E. 2006. Rare Earth Elements in Soils. *Communications in Soil Science and Plant Analysis*, **37**: 1381-1420.

- Jiang, Z. 2018. The factors controlling $\delta^{15}\text{N}$ variation in grape-planting soils and the significance of $\delta^{15}\text{N}$ on Pelee Island, Ontario. M.Sc. Thesis, Department of Earth Science, The University of Western Ontario, London, Ontario.
- Jenny, H. 1941. *Factors of Soil Formation*. McGraw-Hill, New York.
- Johannesson, K.H., Stetzenback, K.J., Klaus, J., Hodge, V.F., Berry Lyons, W. 1996. Rare earth element complexation behavior in circumneutral pH groundwaters: Assessing the role of carbonate and phosphate ions. *Earth and Planetary Science Letters*: **139**: 305–319.
- Jones, G.V. 2014. Climate, terroir, and wine: What matters most in producing a great wine? *EARTH: The Science Behind the Headlines*. Available from <https://www.earthmagazine.org/article/climate-terroir-and-wine-what-matters-most-producing-great-wine> [November 2017].
- Jowitt, S.M., Wong, V.N.L., Wilson, S.A., Gore, O. 2017. Critical metals in the critical zone: controls, resources and future prospectivity of regolith-hosted rare earth elements. *Journal of Earth Sciences*, **64**: 1045-1054.
- Kabata-Pendias, A. & Mukherjee, A.B. 2007. *Trace Elements from Soil to Human*. Springer, N.Y.
- Karrow, P. F. 1984. Quaternary stratigraphy and history, Great Lakes – St. Lawrence Region; in *Quaternary stratigraphy of Canada – a Canadian contribution to IGCP Project 24*, Geological Survey of Canada, **10**: 137-153.
- Karrow, P. F. 1968. Pleistocene geology of the Guelph area, southern Ontario. Ontario Department of Mines, Geological Report **61**: 1-38.
- Kukovica, J. & Pratt, R.G. 2018. Pelee Island Survey. Internal report prepared for Professors Webb and Corcoran, at Western University.
- Lang, B., Pourret, O., Meerts, P., Jitaru, P., Cances, B., Grison, C., Faucon, M. 2016. Copper and cobalt mobility in soil and accumulation in a metallophyte as influenced by experimental manipulation of soil chemical factors. *Chemosphere*, **146**: 75–84.
- Laveuf, C., & Cornu, S. 2009. A review on the potentiality of rare earth elements to trace pedogenetic processes. *Geoderma*, **154**: 1-12.
- Leyton, L. & Yadav, J.S.P. 1960. Effect of drainage on certain physical properties of a heavy clay soil. *Journal of Soil Science*, **11**: 305-312.
- Luisa, B. 1984. *Flooding and plant growth*. Academic Press Inc., Orlando, Florida.

- Mackenzie, D.E., Christy, A.G. 2005. The role of soil chemistry in wine grape quality and sustainable soil management in vineyards. *Water Science & Technology*, **51**: 27-37.
- MacNeil, K. 2001. *The Wine Bible*. Workman Publishing Company, Inc., New York.
- McCarthy, E., Ewing-Mulligan, M. 2001. *French Wine for Dummies*. Hungry Minds Inc., New York, N.Y.
- Martin, R.F., Whitley, J.E., Woolley, A.R. 1978. An Investigation of rare earth mobility: fenitized quartzites, borralan complex, N.W. Scotland. *Contributions to Mineralogy and Petrology*, **66**: 69-73.
- Martínez-Lladó, X., Rovira, M., Valderrama, C., Marti, V. 2011. Sorption and mobility of Sb(V) in calcareous soils of Catalonia (NE Spain): Batch and column experiments. *Geoderma*, **160**: 468-476.
- Meyer, P.A. & Eyles, C.H. 2007. Nature and origin of sediments infilling poorly defined buried bedrock valleys adjacent to the Niagara Escarpment, southern Ontario, Canada. *Canadian Journal of Earth Science*, **44**: 89-105.
- Mezger, K., Essene, E.J., van der Pluijm, B.A., Halliday, A.N. 1993. U-Pb geochronology of the Grenville Orogen of Ontario and New York: constraints on ancient crustal tectonics. *Contributions to Mineralogy and Petrology*, **114**: 13-26.
- Middelburg, J.J., van der Weijden, C.H., Woittiez, J.R.W. 1988. Chemical processes affecting the mobility of major, minor and trace elements during weathering of granitic rocks. *Chemical Geology*, **68**: 253-273.
- Morris, T. F. 2008. Synthesis of information on quaternary geology in the vicinity of St. Clair River. Morris Geoscience. Available from http://iugls.org/DocStore/ProjectArchive/SED_StClairSediment/SED01_Morris_StClairQuaternaryGeologySynthesis/Reports/SED01-R1_Morris.pdf [May 2020].
- Morris, T.F. 1994. Quaternary geology of Essex County, southwestern Ontario. Ontario Geological Survey Open File Report 5886, Ministry of Northern Development and Mines, Toronto, Ontario.
- Morris, T. F. & Kelly R. I. 1996. Origin and physical and chemical characteristics of overburden in Essex and Kent counties, southwestern Ontario. *Canadian Journal of Earth Science*, **34**: 233-246.
- Munroe, J. 2018. Soil fertility handbook. Ministry of Agricultural and Rural Affairs. Available from <http://www.omafra.gov.on.ca/english/crops/pub611/pub611.pdf>

- Myrvang M.B., Hillersoy, M.H., Heim, M., Bleken, M.A., Gjengedal, E. 2016. Uptake of macro nutrients, barium, and strontium by vegetation from mineral soils on carbonatite and pyroxenite bedrock at the Lillebukt Alkaline Complex on Stjernøy, Northern Norway. *Journal of Plant Nutrition and Soil Science*, **179**: 705–716.
- National Cooperative Soil Survey. 2014. Brookston Series. U.S.A. Available from https://soilseries.sc.egov.usda.gov/OSD_Docs/B/BROOKSTON.html [March 2020].
- National Cooperative Soil Survey. 2012. Toledo Series. U.S.A. Available from https://soilseries.sc.egov.usda.gov/OSD_Docs/T/TOLEDO.html [March 2020].
- Nesbitt, H.W. 1979. Mobility and fractionation of rare earth elements of granodiorite. *Nature*, **279**: 206-210.
- Nesbitt, H.W., Markovics, G., Price, R.C. 1980. Chemical processes affecting alkalis and alkaline earths during continental weathering. *Geochimica et Cosmochimica Acta*, **44**: 1659-1666.
- Nesbitt, H.W., McLennan, S.M., Young, G., Keays, R.R. 1996. Effects of chemical weathering and sorting on petrogenesis of siliclastic sediments, with implication for provenance studies. *Journal of Geology*, **104**: 525-542.
- Nesbitt, H.W. & Markovics, G. 1997. Weathering of granodioritic crust, long-term storage in weathering profiles, and petrogenesis of siliclastic sediments. *Geochimica et Cosmochimica Acta*, **61**: 1653-1670.
- Netzer, Y., Schwartz, A., Shenker, M. 2014. Effects of irrigation using treated wastewater on table grape vineyards: dynamics of sodium accumulation in soil and plant. *Irrigation Science*, **32**: 283-294.
- NOAA. n.d. Bathymetry of Lake Erie and Lake Saint Clair. National Centers for Environmental Information. Available from https://www.ngdc.noaa.gov/mgg/greatlakes/lakeerie_cdrom/html/e_gmorph.htm#a3 [August 2019].
- Ohta, A. & Kawabe, I. 2001. REE(III) adsorption onto Mn dioxide (δ -MnO₂) and Fe oxyhydroxide: Ce (III) oxidation by δ -MnO₂. *Geochimica et Cosmochimica Acta*, **65**: 695-703.
- Omer, M., Ulery, A., Idowu, O.J., VanLeeuwen, D. 2018. Seasonal changes of soil quality indicators in selected arid cropping systems. *Agriculture*, **8**: 1-12.
- Ontario Ministry of Northern Development and Mines. 2018. Geoscience laboratories, schedule of fees and services. Issue 10, Sudbury, Ontario.

- Orth, U. R., Wolf, M. M., & Dodd, T. H. 2005. Dimensions of wine region equity and their impact on consumer preferences. *Journal of Product and Brand Management*, **14**: 88-97.
- Otero, N., Gil, A.S., Vitoria, L., Canals, A. 2005. Fertilizer characterization: Major, trace and rare earth elements. *Applied Geochemistry*. **20**: 1473-1488.
- Parr, W. V., Maltman, A.J., Easton, S., Ballester, J. 2018. Minerality in wine: Towards the reality behind the myths. *Beverages*, **4**: 77-96.
- Pelee Island Winery. 2019. About Us. Available from <https://www.peleeisland.com/about-us/> [July 2019].
- Percival, J.A., Stott, G., Skulski, T. Geology and tectonic evolution of the Superior Province, Canada. *Tectonic Styles in Canada: The Lithoprobe Perspective*, **49**: 321-378.
- Peuke, A.D. 2009. Nutrient composition of leaves and fruit juice of grapevine as affected by soil and nitrogen fertilization. *Journal of Plant Nutrition and Soil Science*, **172**: 557-564.
- Phillips, R. 2017. *The wines of Canada*. Infinite Ideas Limited, Oxford, United Kingdom.
- Pope, A. 2016. Canadian Geographic. Five reasons Canadian wines are unique. Available from <https://www.canadiangeographic.ca/article/5-reasons-canadian-wines-are-unique> [July 2019].
- Prudencio, M.I., Braga, M.A.S., Gouveia, M.A. 1993. REE mobilization, fractionation and precipitation during weathering of basalts. *Chemical Geology*, **107**: 251-254.
- Raharimahefa, T., Lafrance, B., Tinkham, D.K. 2014. New structural, metamorphic, and U-Pb geochronological constraints on the Blezardian Orogeny and Yavapai Orogeny in the Southern Province, Sudbury, Canada. *Canadian Journal of Earth Science*, **51**: 750-774.
- Rajmohan, N., Jayaprekash, M., Prathapar, S.A., Nagarajan, R. 2014. Vertical distribution of heavy metals in soil profile in a seasonally waterlogging agriculture field in Eastern Ganges Basin. *Environmental Monitoring and Assessment*, **186**: 5411-5427.
- Reid, R. & Hayes, J. 2003. Mechanisms and control of nutrient uptake by plants. *Internal Review of Cytology*, **229**: 73-114.
- Richards, N.R., Caldwell, A.G., Morwick, F.F. 1949. *Soil Survey of Essex County*. The Ontario Soil Survey Report No. 11, Guelph, Ontario.

- Ridley, W.I. 1998. Elements: Incompatible. Encyclopedia of Earth Science. Springer, Dordrecht.
- Rollinson, H. 1993. Using geochemical data: evaluation, presentation, interpretation. Longman Group, Ltd, Essex, England.
- Romić, M., Matijevic, L., Bakic, H., Romić, D. 2014. Accumulation in vineyard soils: distribution, fractionation and bioavailability assessment, environmental risk assessment of soil contamination. *IntechOpen*, **28**: 799-825.
- Schijf, J., & Byrne, R.H. 2001. Stability constants for monoand dioxalato-complexes of Y and REE, potentially important species in groundwaters and surface freshwaters. *Geochimica et Cosmochimica Acta*: **65**: 1037–1046.
- Schilling, J., Reimann, C., Roberts, D. 2014. REE potential of the Nordkinn Peninsula, North Norway: A comparison of soils and bedrock composition. *Applied Geochemistry*, **41**: 95-106.
- Schönenberger, J. 2012. Canadian field soils I. mineral composition by XRD/XRF measurements. *Springer*, **33**: 342-362.
- Seguin, M.K. 1984. Geology, geochemistry and paleomagnetism of the Cheneaux metagabbro (Helikian) of southern Quebec and Eastern Ontario. *Precambrian Research*, **26**: 307-331.
- Semple, K.T., Morriss, A.W.J., Paton, G.I. 2003. Bioavailability of hydrophobic organic contaminants in soils: fundamental concepts and techniques for analysis. *European Journal of Soil Science*, **54**: 809-818.
- Semple, K. T., Doick, K.J., Jones, K.C., Barauel, P., Craven, A., Harms, H. 2004. Defining bioavailability and bioaccessibility of contaminated soil and sediment is complicated. *Environmental Science & Technology*, **38**: 228-231.
- SGS. 2019. Mobile metal ion short report, Pelee Island Winery, Pelee Island. SGS Mineral Services, Lakefield, Ontario.
- Shaw, A. B. 2001. Pelee Island and Lake Erie North Shore, Ontario: a climatic analysis of Canada's warmest wine region. *Journal of Wine Research*, **12**: 19-37.
- Sheppard, S.C., Grant, A., Drury, C.F. 2009. Trace Elements in Ontario soils – mobility, concentration profiles, and evidence of non-point-source pollution. *Canadian Journal of Earth Science*, **89**: 489-499.
- Slack, J. 2015. Terroir of Pelee Island Vineyard: A Case for Island Appellation Designation. Boreal Agrominerals Inc. Report, 1-47.

- Slagstad, T., Culshaw, N.G., Jamieson, R.A., Ketchum, J.W.F. 2004. Early Mesoproterozoic tectonic history of the southwestern Grenville Province, Ontario: Constraints from geochemistry and geochronology of high-grade gneisses. *Geological Society of America*, **197**: 209-241
- Smart, D., Lakso, A., Schwass, E., Morano, L. 2006. Grapevine rooting patterns: A comprehensive analysis and review. *American Journal of Viticulture*, **57**: 89-104.
- Sposito G., Chesworth, W. Evans, L.J., Spaargaren, O. 2008. Gleysols. *Encyclopedia of Earth Sciences Series*. Springer, Dordrecht.
- Stille, P. Pierret, M., Steinmann, M., Chabaux, F., Rene, B., Dominique, A., Pourcelot, L., Gilles, M. 2009. Impact of atmospheric deposition, biogeochemical cycling and water mineral interaction on REE fractionation in acidic surface soils and soil water (the Strengbach case). *Chemical Geology*, **264**: 173-186.
- Staben, M.L. Ellsworth, J.W., Sullivan, D.M., Brown, B.D., Stevens, R.G. 2003. Monitoring soil nutrients using a management unit approach. Oregon State University, Extension Service.
- Stonehouse, H. B. & Arnaud, R.J. 1971. Distribution of iron, clay and extractable iron and in some Saskatchewan soils. *Canadian Journal of Earth Science*, **51**: 283-292.
- Taunton, A., Welch, S.A., Banfield, J.F. 2000. Microbial controls on phosphate and lanthanide distributions during granite weathering and soil formation. *Chemical Geology*: **169**: 371–382.
- Taylor, G.S., Goins, T., Holowaychuk, N. 1961. Drainage characteristics of Toledo and Hoytville soils. Research Bulletin 876. Ohio Agricultural Experiment Station, Wooster, Ohio.
- Taylor, V.F., Longerich, H.P., Greenough, J.D. 2003. Multielement analysis of Canadian wines by inductively coupled plasma mass spectrometry (ICP-MS) and multivariate statistics. *Journal of Agriculture Food Chemistry*, **51**: 856–860.
- Thompson, I.D. 2000. Forest vegetation of Ontario: factors influencing landscape change. *Ecology of a Managed Terrestrial Landscape: Patterns and Processes in Forest Landscapes of Ontario*. Vancouver, British Columbia: University of British Columbia Press.
- Thorpe, C.L., Lloyd, J.R., Law, G.T.W., Burke, I.T., Shaw, S., Bryan, N.D., Morris, K. 2012. Strontium sorption and precipitation behaviour during bioreduction in nitrate impacted sediments. *Chemical Geology*, **306-307**: 114-122.

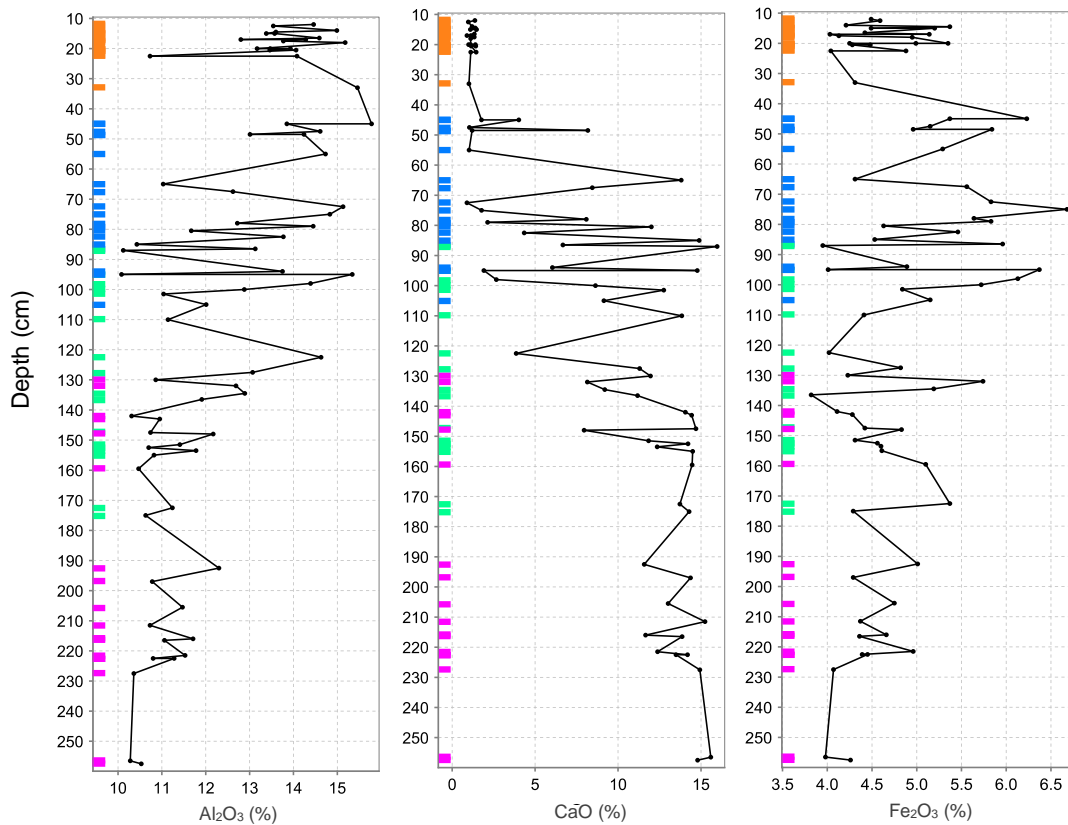
- Thurston, P.C. 1991. Geology of Ontario: Introduction. Geology of Ontario. Special Volume No. 4. Toronto, Ontario, Ontario Geological Survey: 3-26.
- Tolo, R. 2019. The role of clay in terroir (Pelee Island case study). M.Sc. Thesis, Department of Earth Science, The University of Western Ontario, London, Ontario.
- Tyler, G. 2004. Rare earth elements in soils and plant systems – A review. *Plant and Soil*, **267**: 191-206.
- Uddin, M. K. 2016. A review on the adsorption of heavy metals by clay minerals, with special focus on the past decade. *Chemical Engineering Journal*, **308**: 438-462.
- Ugwu, I.M. & Igbokwe O.A. 2019. *Advanced Sorption Process Applications*, IntechOpen, Bochum, Germany.
- Van Den Berg, G.A. & Loch, J.P.G. 2008. Decalcification of soils subject to periodic waterlogging. *European Journal of Earth Science*, **51**: 27-33.
- van Leeuwen, C., Roby, J., de Resseguier, L. 2018. Soil-related terroir factors: a review. *Vine and Wine Open Access Journal*, **52**: 173-188.
- Van Raij, B. 2008. Bioavailable tests: alternatives to standard soil extractions. *Communications in Soil Science and Plant Analysis*, **29**: 1553-1570.
- Vestin J.L.K., Bylund, D., Soderberg, U., Nambu, K. 2013. The influence of alkaline and non-alkaline parent material on Norway spruce tree chemical composition and growth rate. *Plant and Soil*, **370**: 103–113.
- Vestin J.L.K., Nambu, K., van Hees, P.A.W., Bylund, D., Lundstrom, U.S. 2006. The influence of alkaline and non-alkaline parent material on soil chemistry. *Geoderma*, **135**: 97–106.
- Vodyanitskii, Y. N. 2011. Chemical aspects of uranium behaviour in soils: A review. *Soil Chemistry*, **44**: 862-873.
- Volokh, A. A., Gorbunov, A.V., Gundorina, S.F., Revich, B.A., Frontasyeva, M.V., Pal, C.S. 1990. Phosphorus-fertilizer production as a source of rare-earth elements pollution of the environment. *The Science of the Total Environment*, **95**: 141–148.
- VQA Ontario. 2019. Ontario wine appellation authority: Lake Erie North Shore. Available from <http://www.vqaontario.ca/Appellations/LakeErieNorthShore> [July 2019].

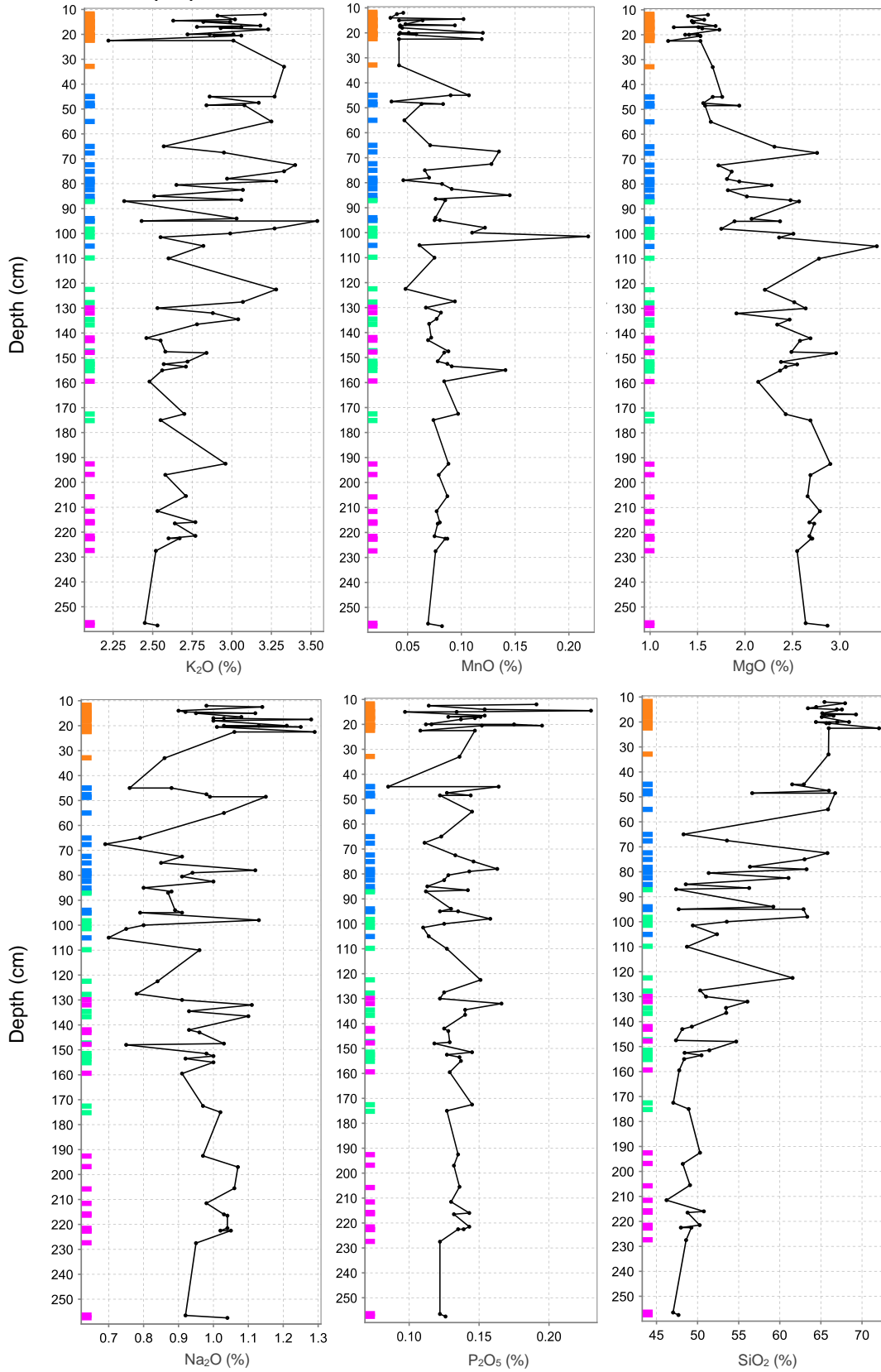
- Wade, R.I. and Pun, K. 2009. Winery visitation in the wine appellations of Pelee Island and Lake Erie North Shore. Scholar Works at The University of Massachusetts Amherst, 1-8.
- Weather Atlas. 2020. Monthly weather forecast and climate, Pelee Island, Canada. Available from <https://www.weather-ca.com/en/canada/pelee-island-climate> [August 2019].
- Weil, R., & Brady, N. 2017. The Nature and Properties of Soils. Pearson, USA.
- Wen, X., Huang, C., Tang, Y., Gong-Bo, S., et al. 2014. Rare earth elements: a potential proxy for identifying the lacustrine sediment source and soil erosion intensity on karst areas. *Journal of Soils and Sediments*, **14**: 1693-1702.
- Wichard, T., Myneni, S.C.B., Mishra, B., Bellenger, J. 2009. Storage and bioavailability of molybdenum in soils increased by organic matter complexation. *Nature Geoscience*, **2**: 625-629.
- Wilson, M.J. 2004. Weathering of the primary rock-forming minerals: processes, products and rates. *Clay Minerals*, **39**: 233-266.
- Wines of Canada. 2016. Pelee Island wine history. Available from http://www.winesofcanada.com/history_pelee_island.html [July 2019].
- Wuana, R.A. & Okieimen, F.E. 2011. Heavy metals in contaminated soils: a review of sources, chemistry, risks and best available strategies for remediation. *International Scholarly Research Notices*, **2011**: 1-20.
- Xiaolei, G., Hu, Y., Guo, T., Ye, X. 2012. Comparative study of the competitive adsorption of Mg, Ca and Sr ions onto resins. *Adsorption Science and Technology*, **31**: 45-58.
- Zhang, Q., Han, G., Man, L., Wang, L. 2019. Geochemical characteristics of rare earth elements in soils from puding karst critical zone observatory, southwest China. *Sustainability*, **11**: 4963.
- Zhao, W. 2005. Understanding classifications: empirical evidence from the American and French wine industries. *Poetics*, **33**: 179-200.

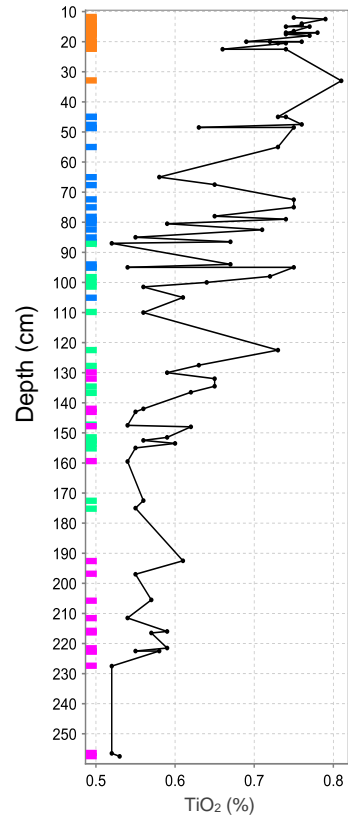
Appendices

Appendix A: Mineral Element Soil Profile Graphs

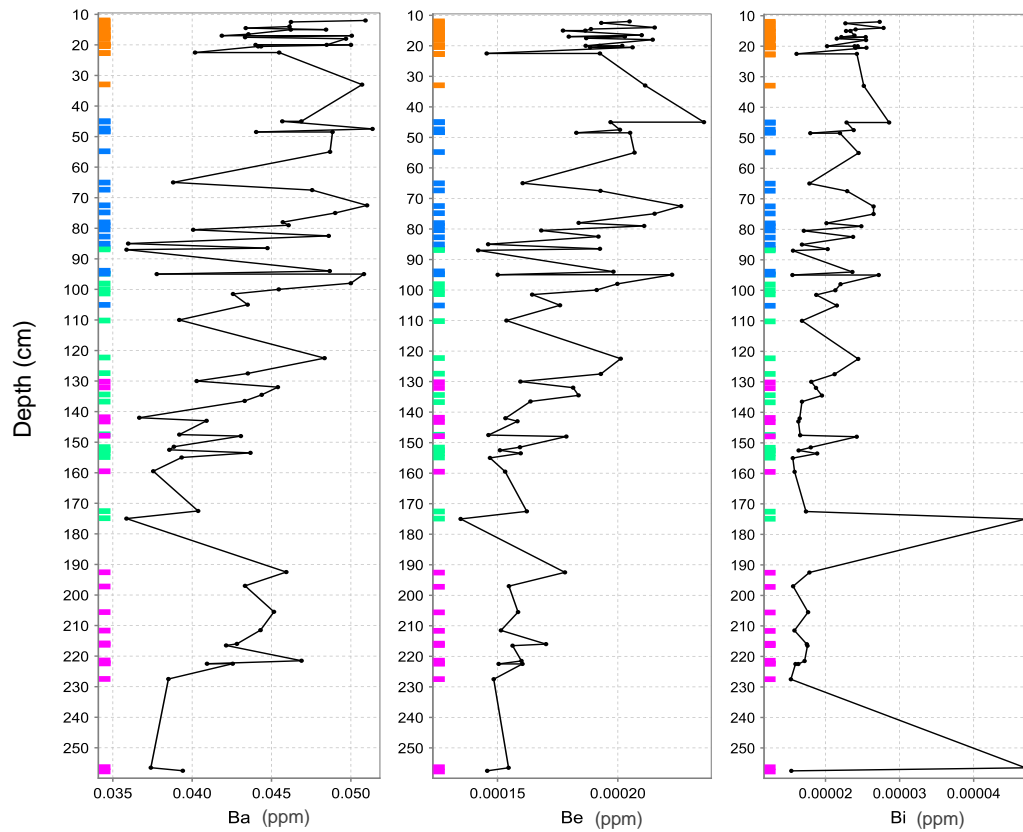
The following figures are depth versus major oxide concentration graphs. Soil sample depth of each soil sample plotted against major elemental oxide concentrations of each soil sample. Data is compiled from all 19 soil profiles. Sampling depths are distinguished by colour on the left side of the graph: Section 1 = orange, section 2 = blue, section 3 = green, and section 4 = purple. Spline curves on these graphs are meant to illustrate element concentration trends and do not imply vertical connectivity among soils samples, because markers on the graphs represent individual soils samples selected from different locations on the island.

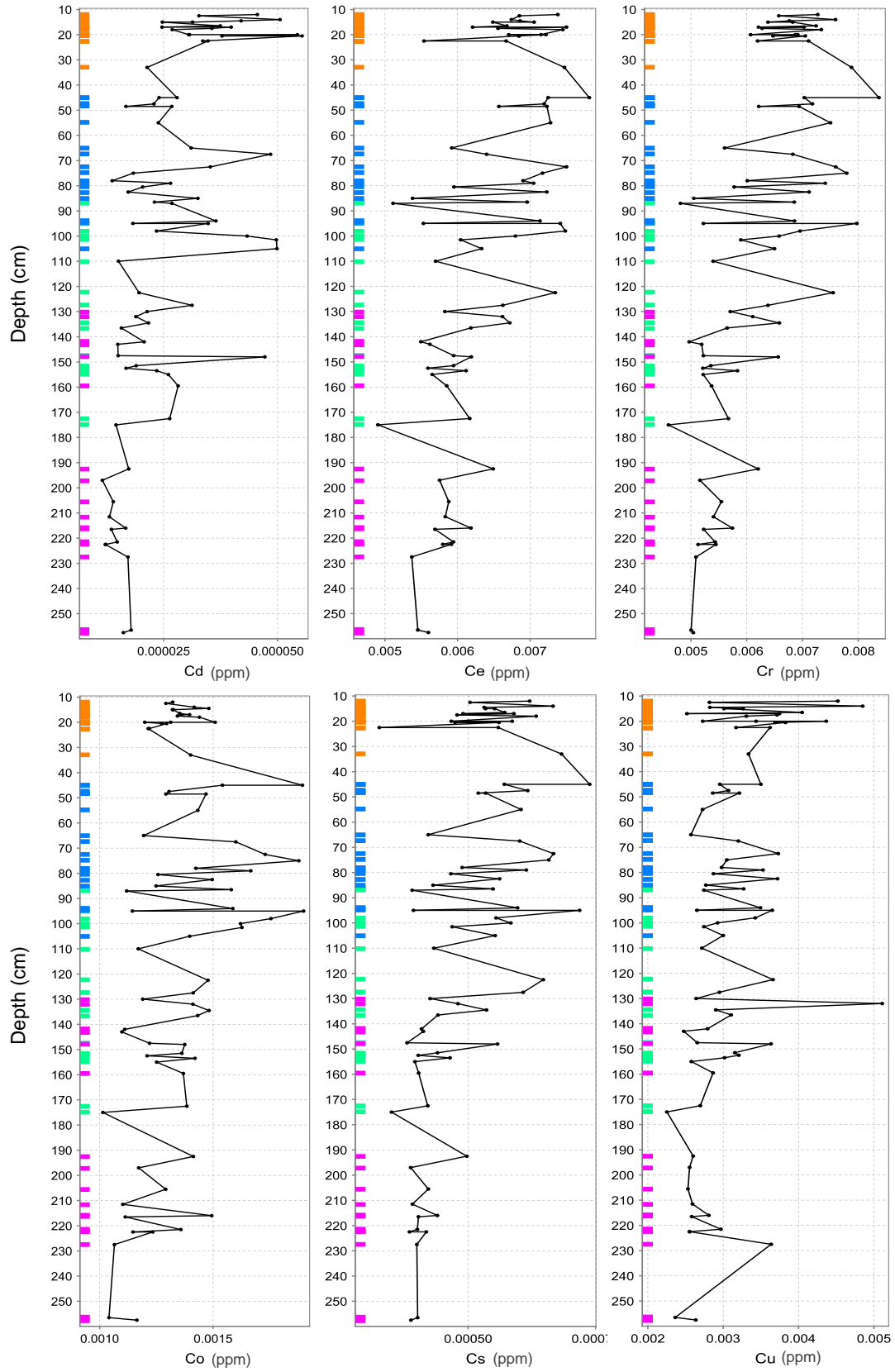


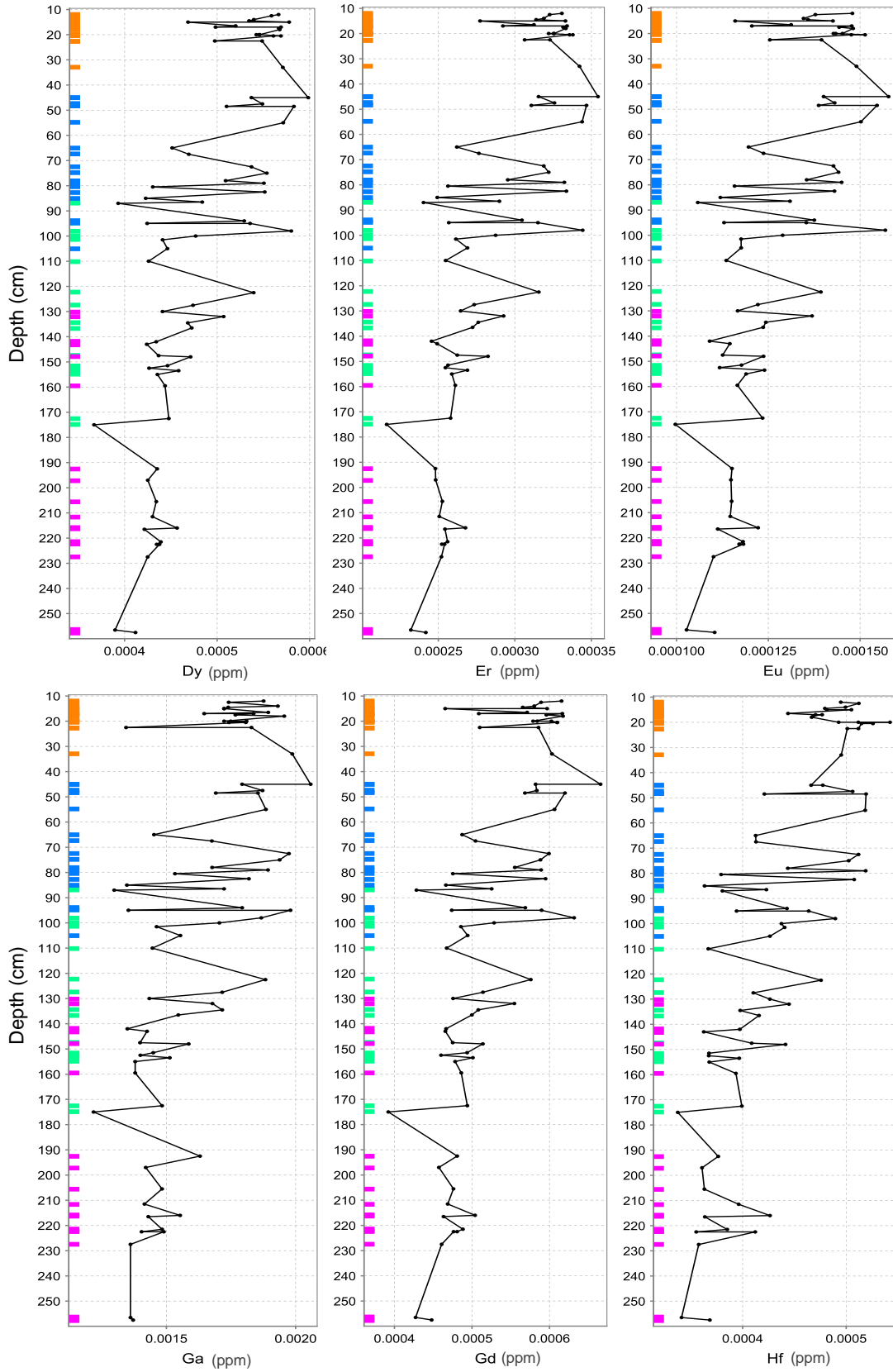


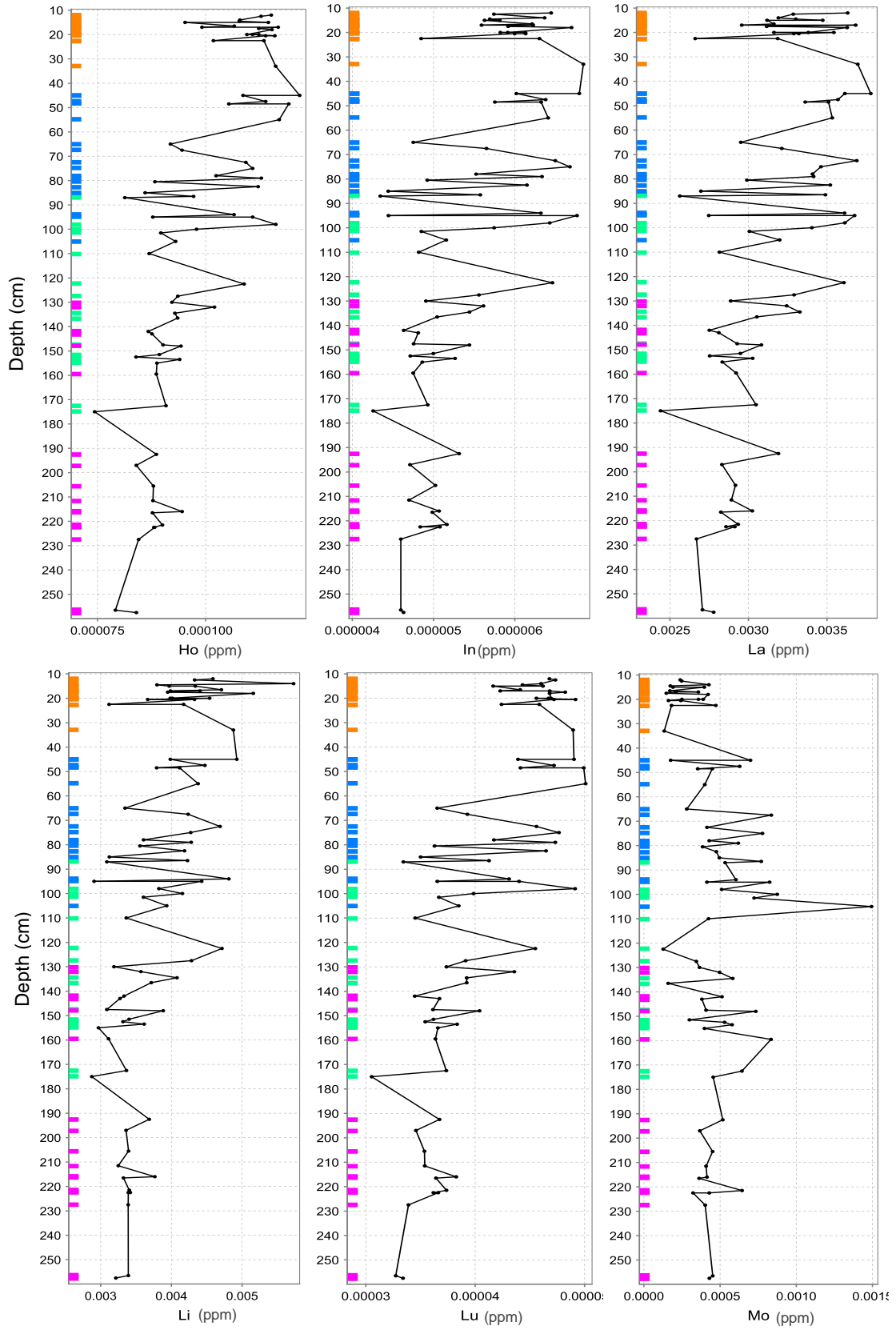


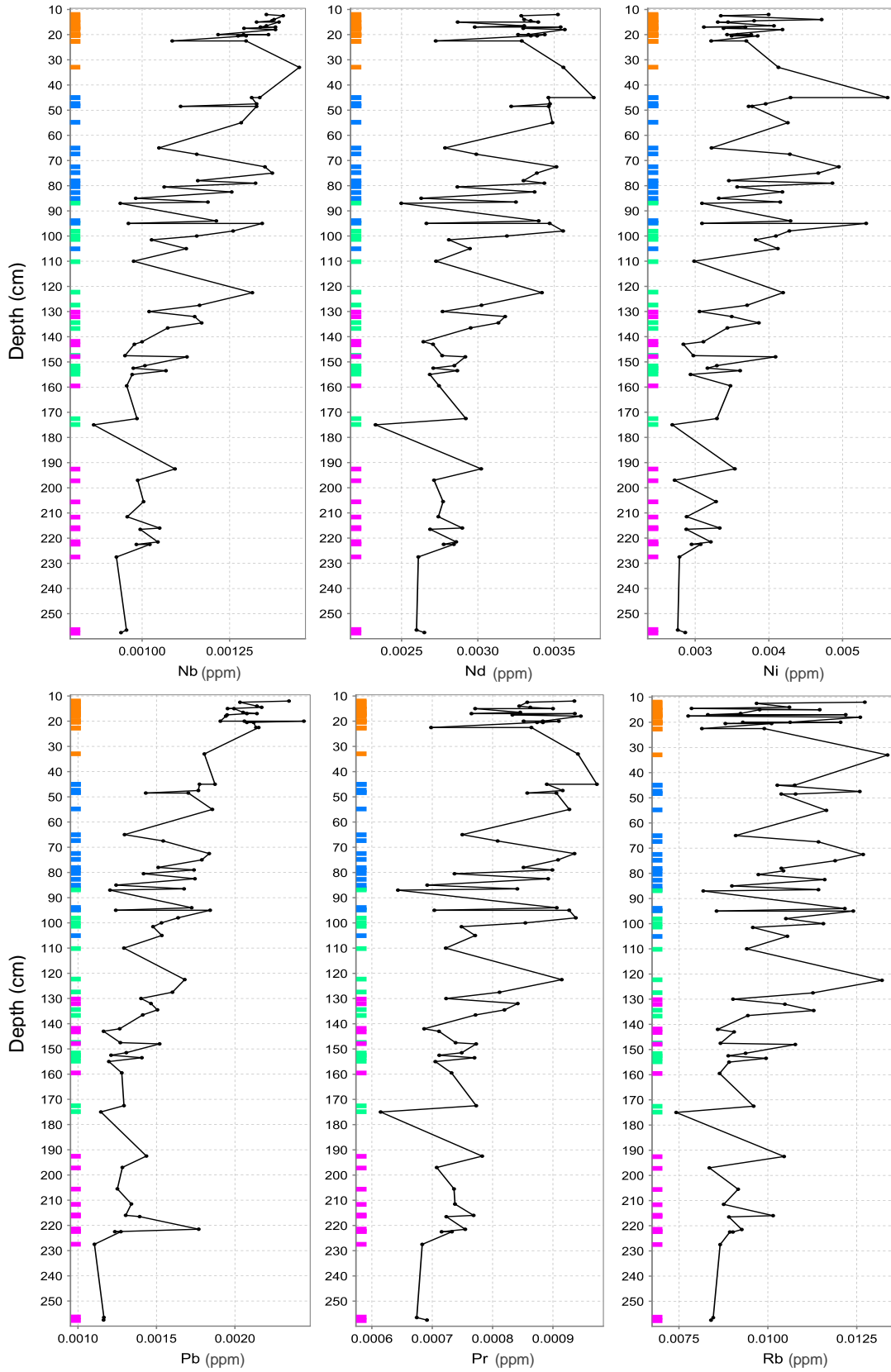
The following figures are depth versus trace element concentration graphs. Soil sample depth of each soil sample plotted against trace elemental concentrations of each soil sample. Data is compiled from all 19 soil profiles. Sampling depths are distinguished by colour on the left side of the graph: Section 1 = orange, section 2 = blue, section 3 = green, and section 4 = purple. Spline curves on these graphs are meant to illustrate element concentration trends and do not imply vertical connectivity among soils samples, because markers on the graphs represent individual soils samples selected from different locations on the island.

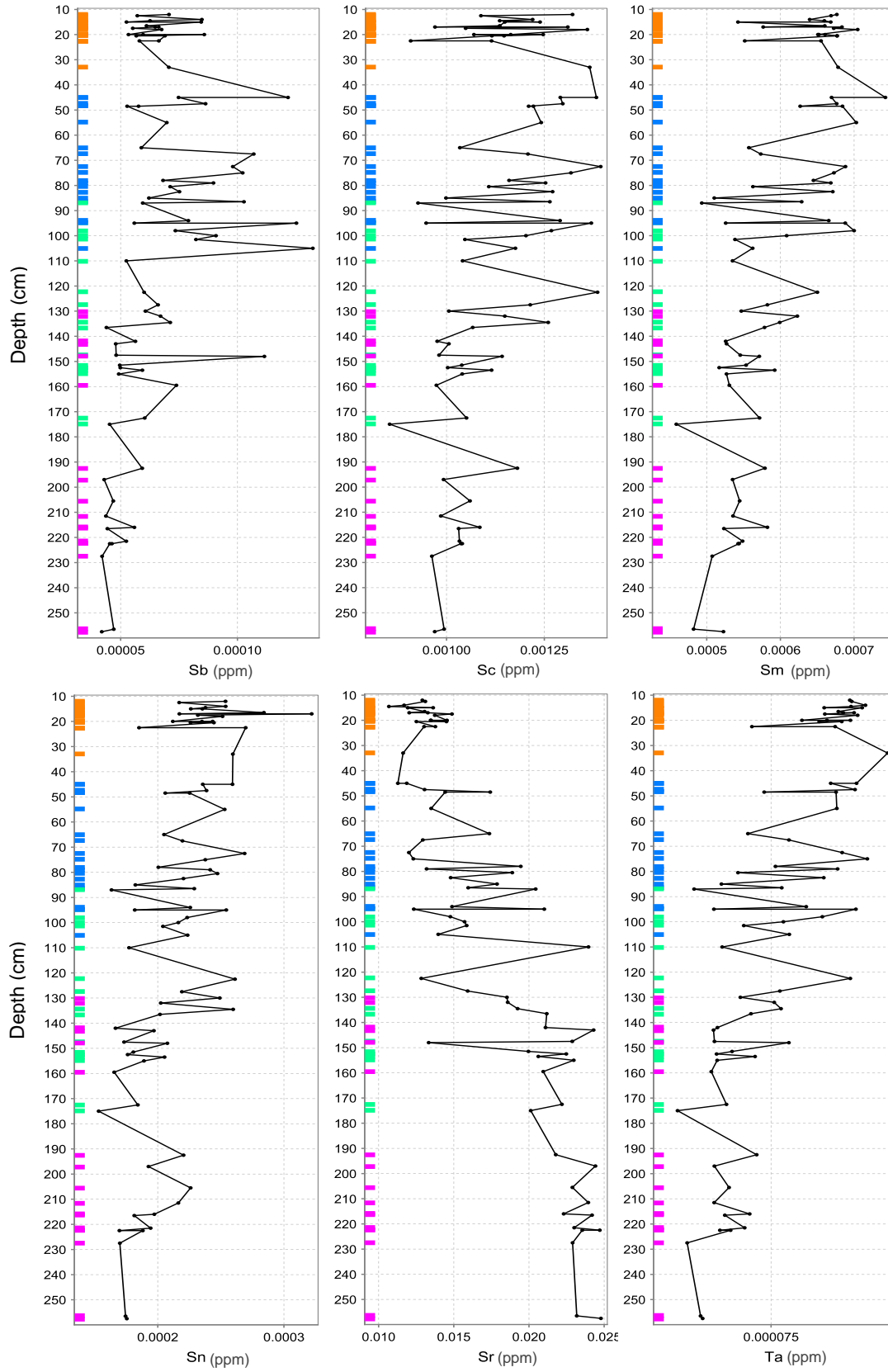


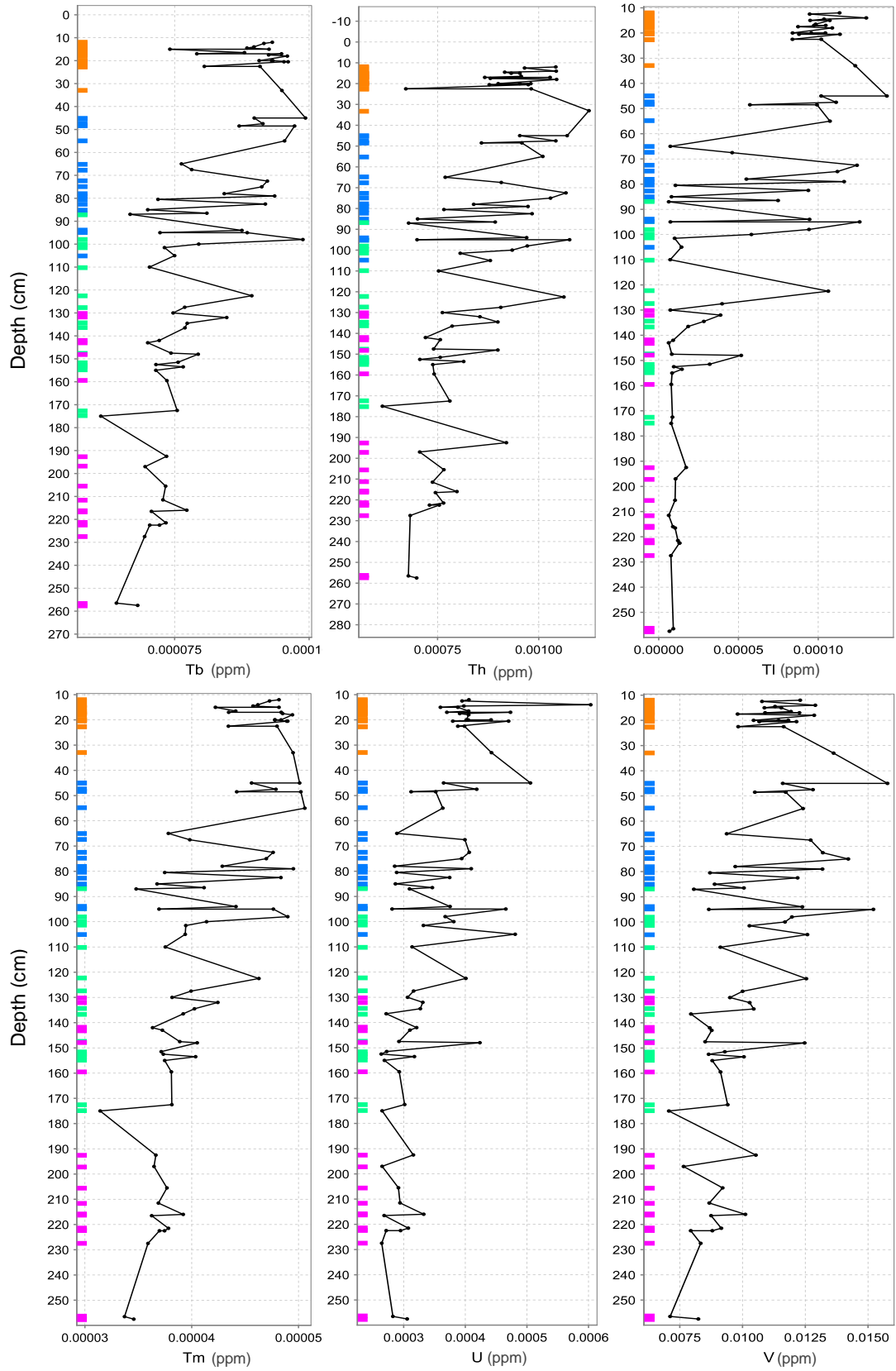


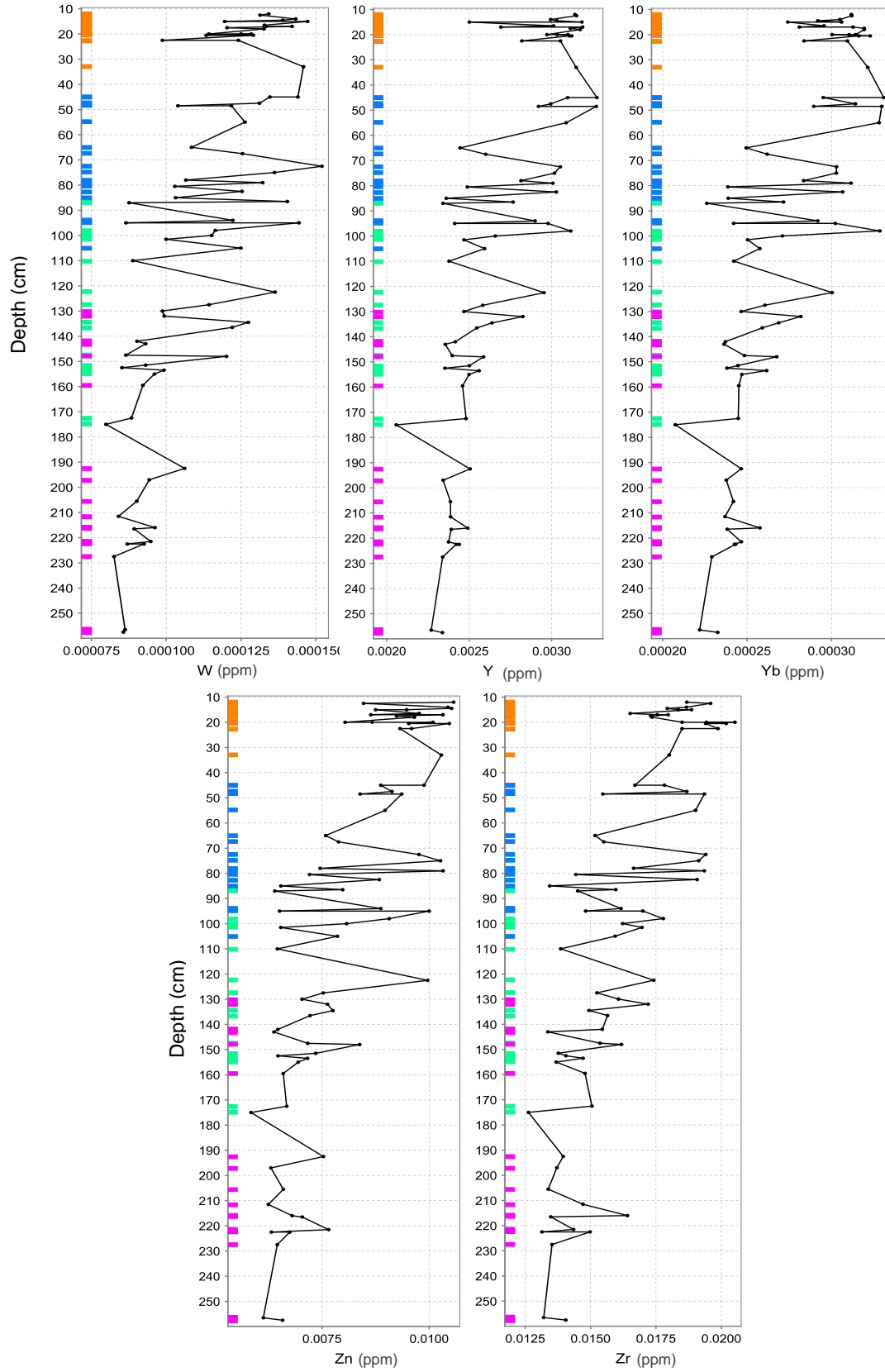






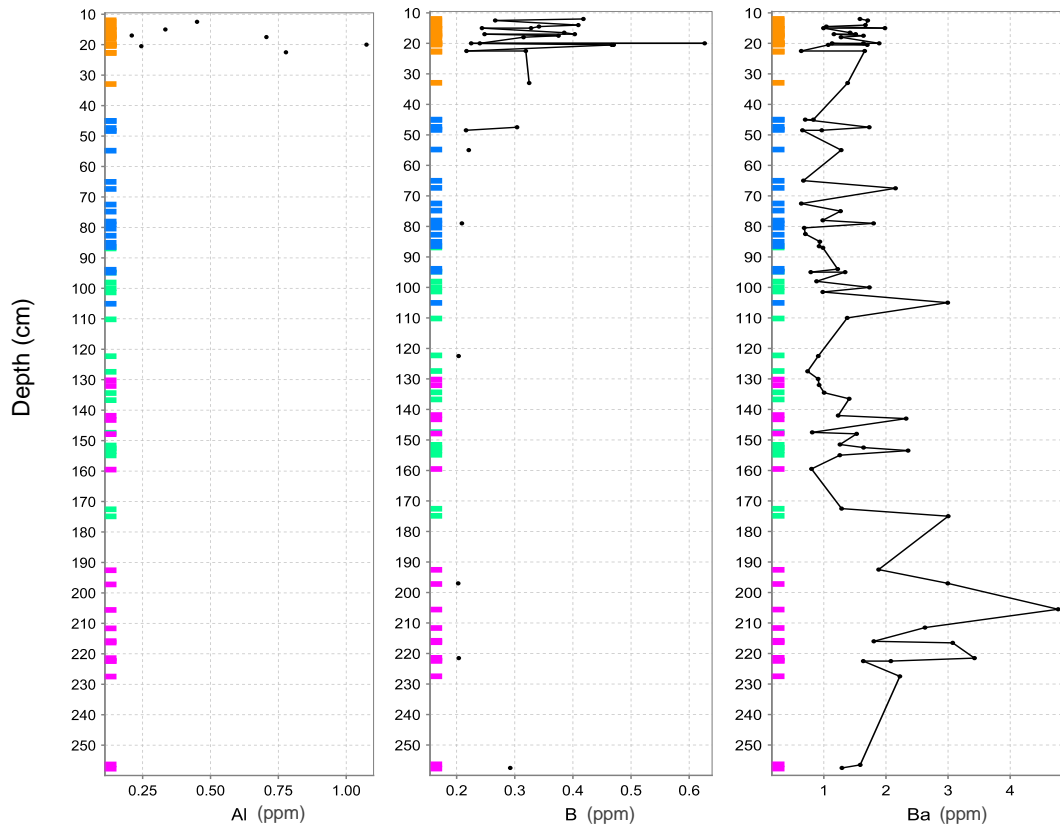


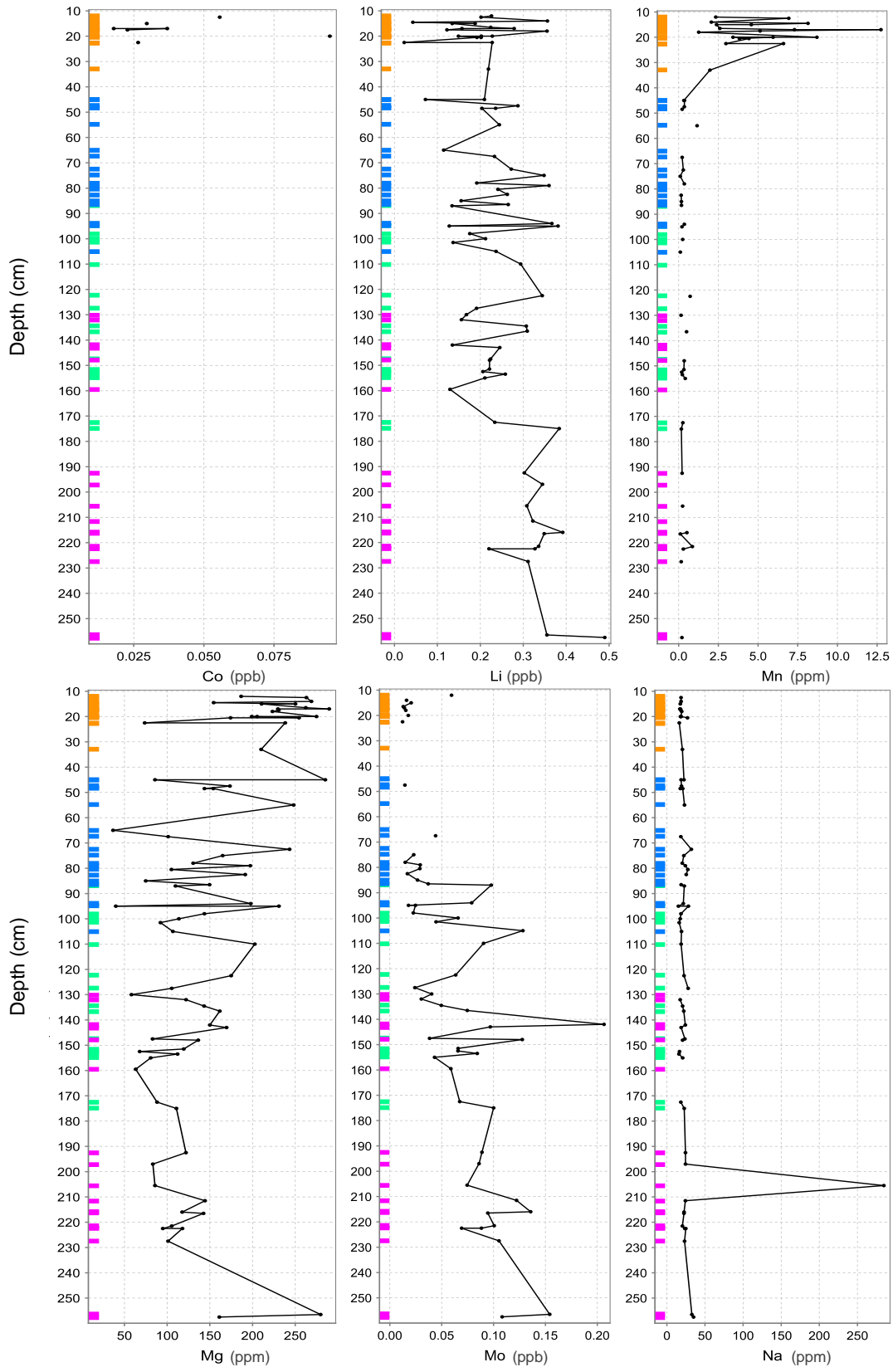


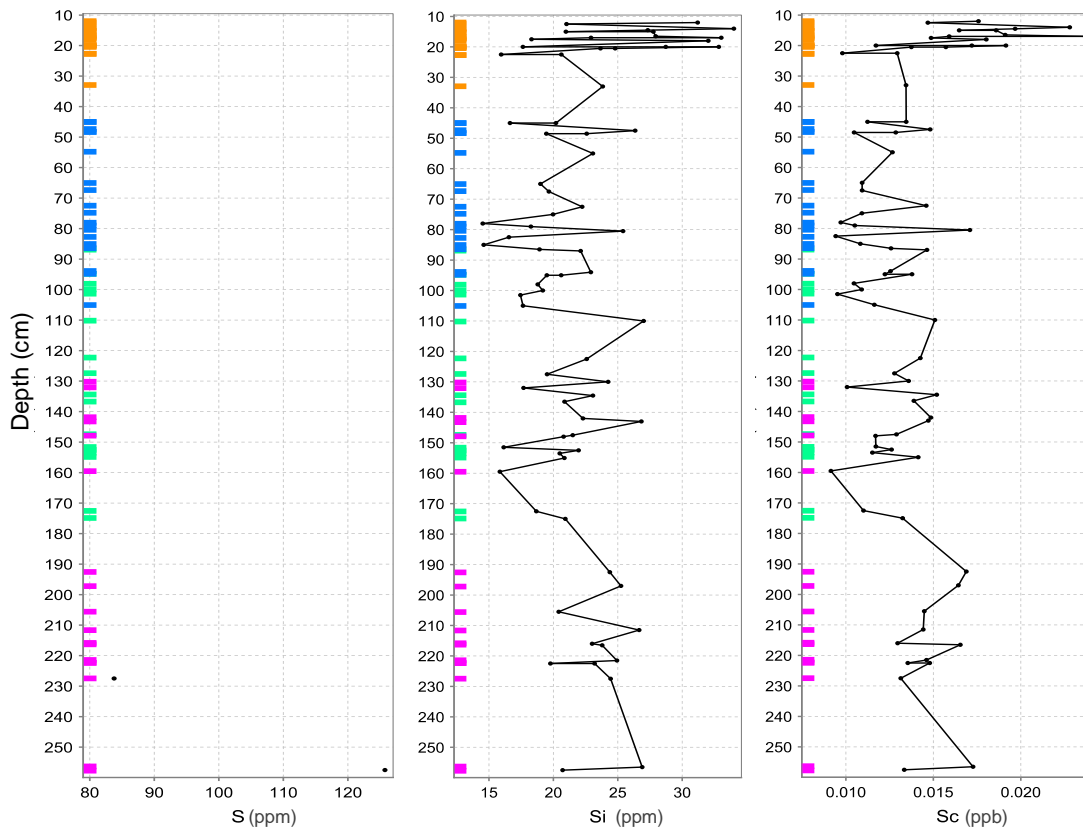
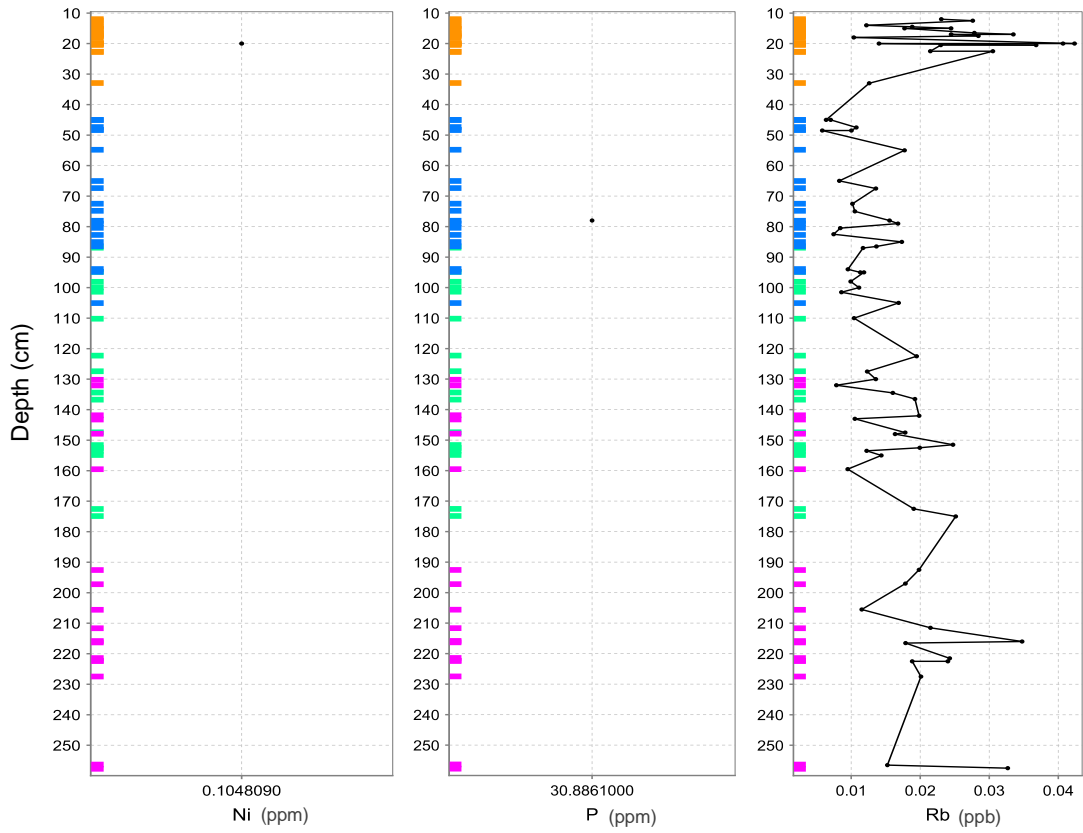


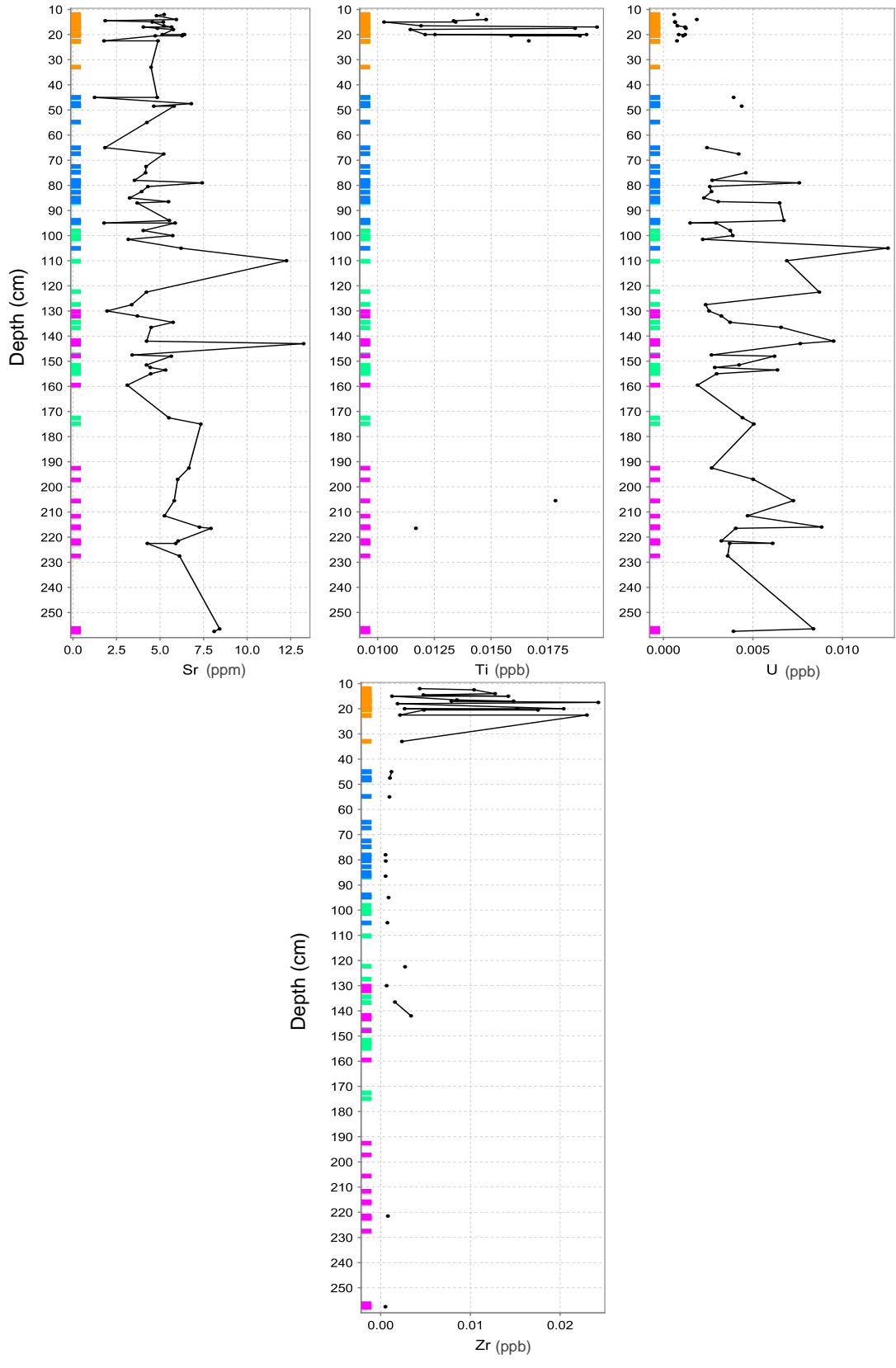
Appendix B: PEN Element Soil Profile Graphs

The following figures are depth versus plant extractable element concentration graphs. Soil sample depth of each soil sample plotted against plant extractable elemental concentrations of each soil sample. Data is compiled from all 19 soil profiles. Sampling depths are distinguished by colour on the left side of the graph: Section 1 = orange, section 2 = blue, section 3 = green, and section 4 = purple. Spline curves on these graphs are meant to illustrate element concentration trends and do not imply vertical connectivity among soils samples, because markers on the graphs represent individual soils samples selected from different locations on the island.

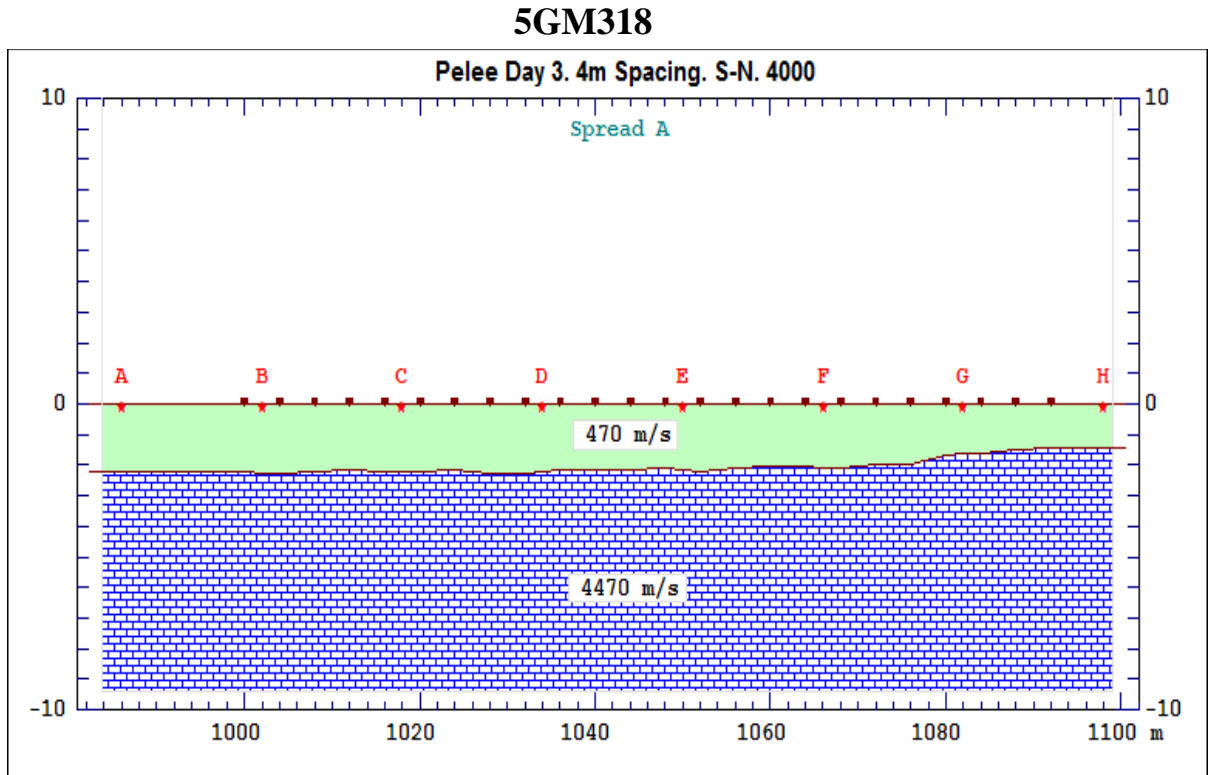






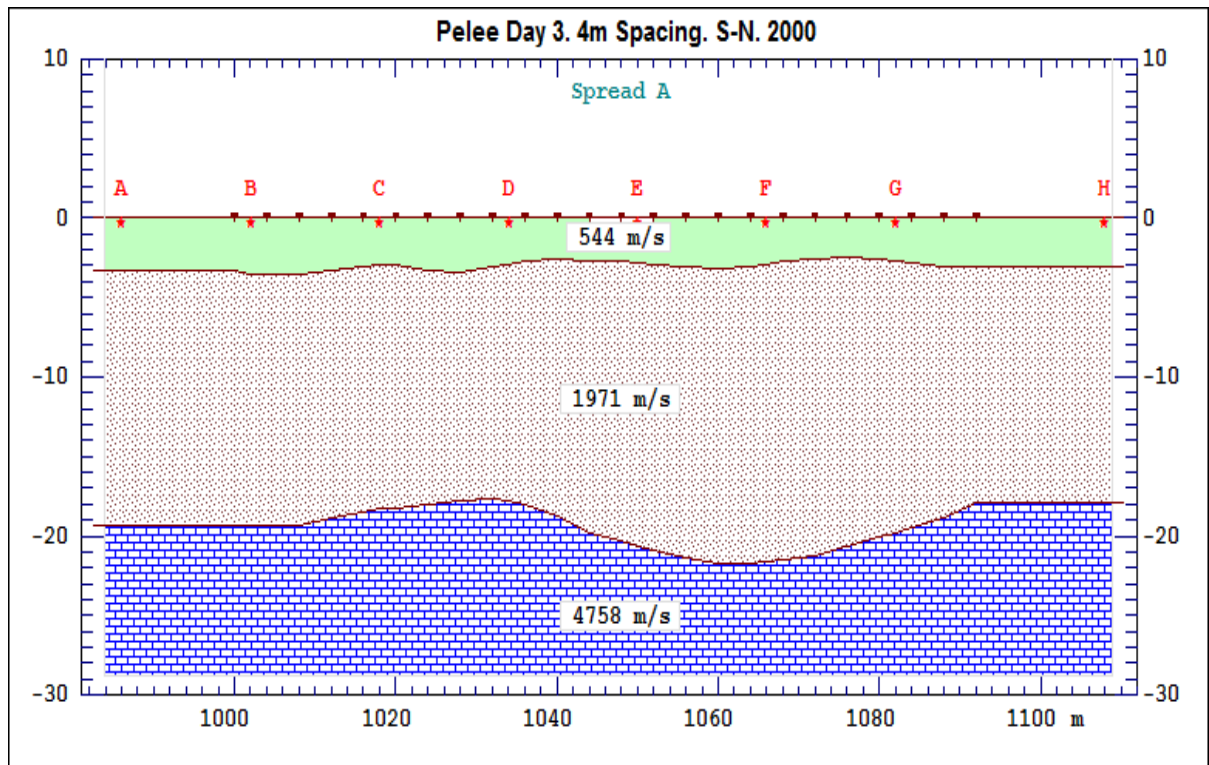


Appendix C: Seismic Refraction Figures



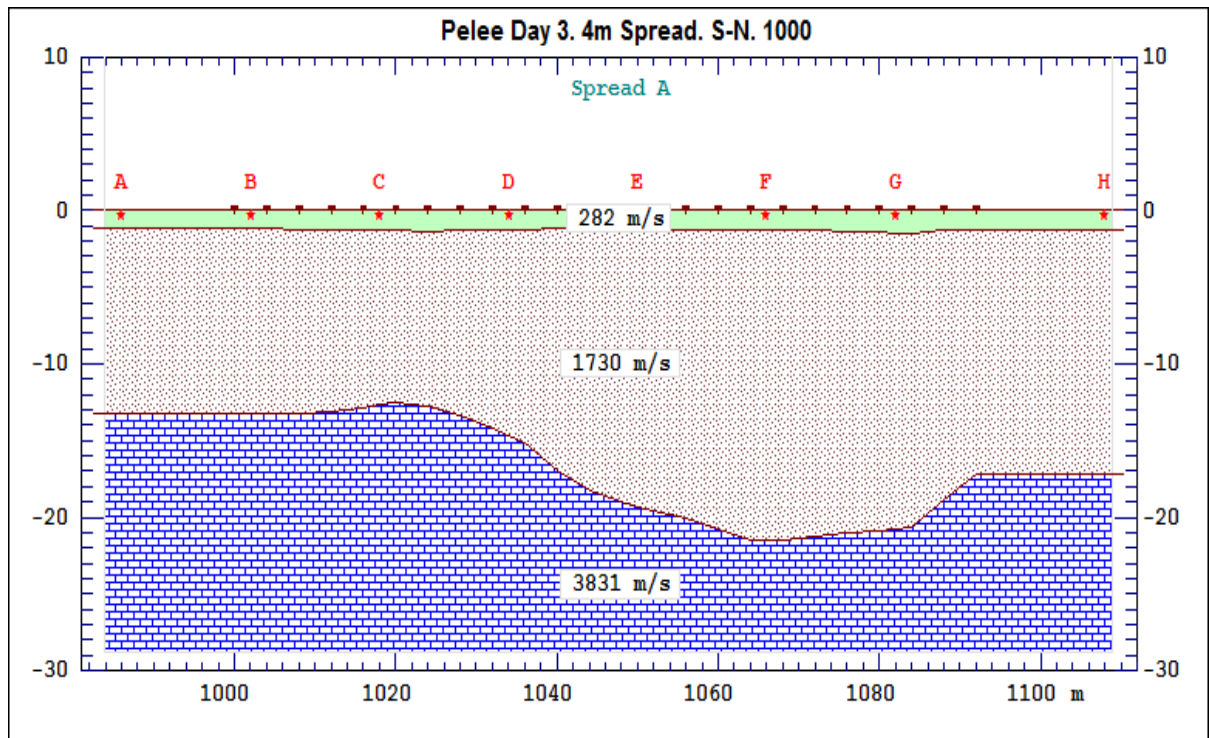
Seismic refraction depth profile from 24 channel linear array with 4 m spacing of field 5GM318, indicating depth of soil layers. The green layer represents soil thickness and the blue layer represents limestone bedrock thickness. The y-axis is depth in meters and the x-axis is horizontal distance in meters from south to north. The red letters indicate the location of the seismic source (steel plate and hammer) and brown dots indicate the locations of the geophone receivers. The numbers within the soil layers indicate the velocity of seismic waves passing through each layer.

10CF



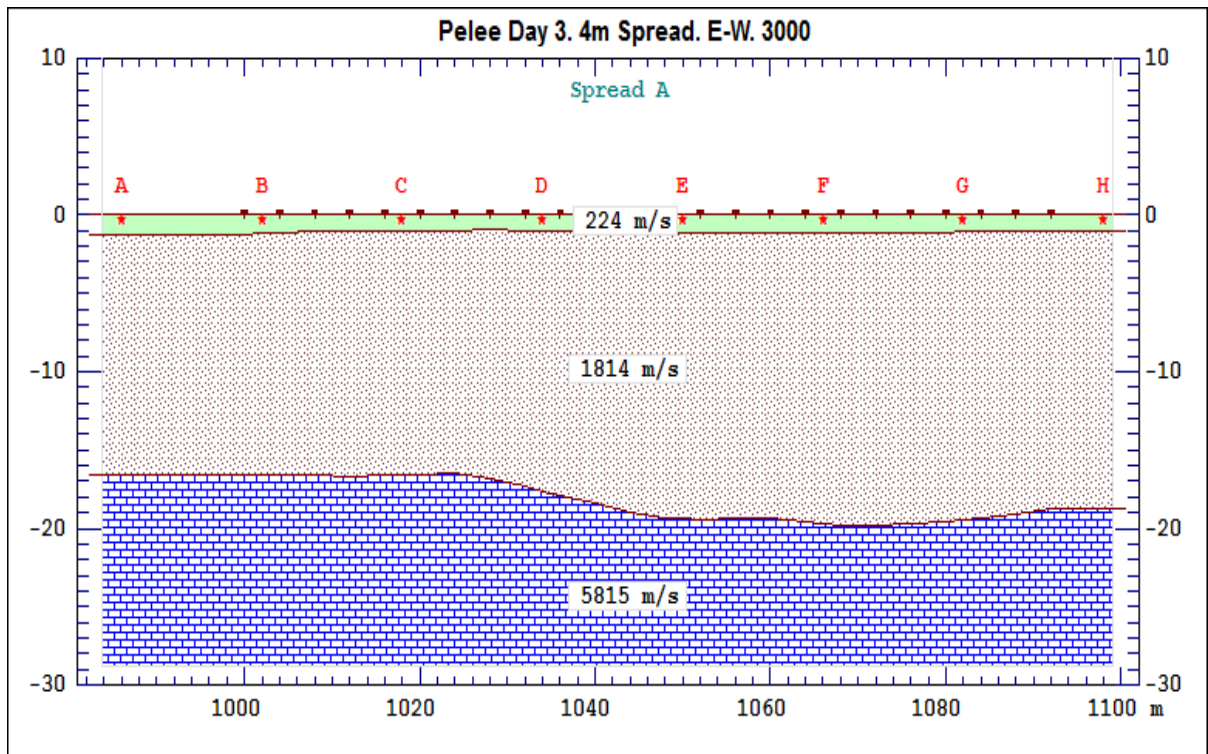
Seismic refraction depth profile from 24 channel linear array with 4 m spacing of field 10CF, indicating depth of soil layers. The green layer represents soil thickness, the grey layer represents till thickness, and the blue layer represents limestone bedrock thickness. The y-axis is depth in meters and the x-axis is horizontal distance in meters from south to north. The red letters indicate the location of the seismic source (steel plate and hammer) and brown dots indicate the locations of the geophone receivers. The numbers within the soil layers indicate the velocity of seismic waves passing through each layer.

13CF



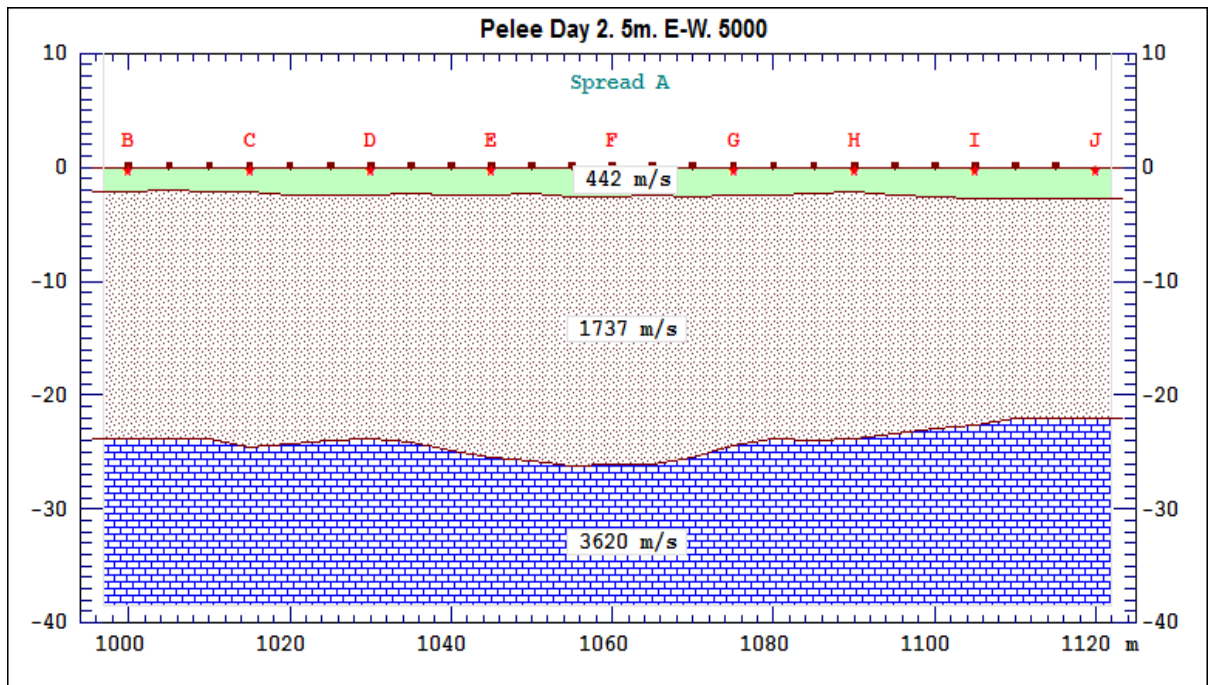
Seismic refraction depth profile from 24 channel linear array with 4 m spacing of field 13CF, indicating depth of soil layers. The green layer represents soil thickness, the grey layer represents till thickness, and the blue layer represents limestone bedrock thickness. The y-axis is depth in meters and the x-axis is horizontal distance in meters from south to north. The red letters indicate the location of the seismic source (steel plate and hammer) and brown dots indicate the locations of the geophone receivers. The numbers within the soil layers indicate the velocity of seismic waves passing through each layer.

15A



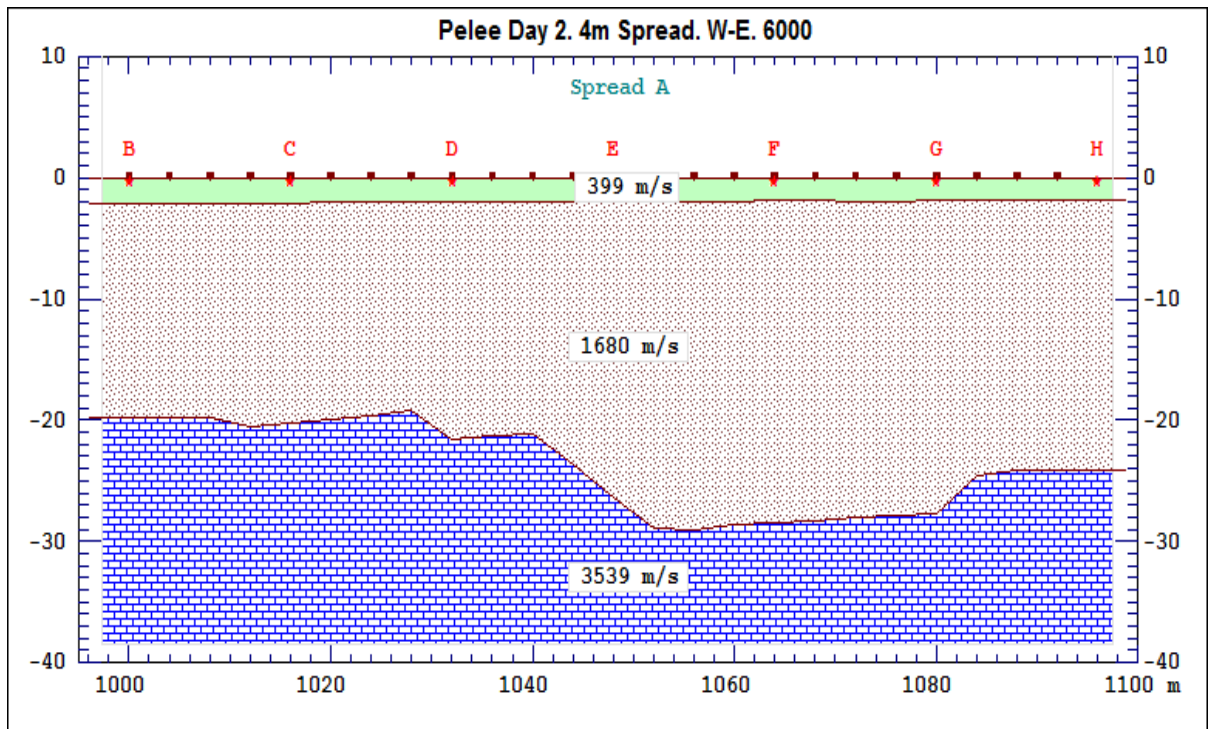
Seismic refraction depth profile from 24 channel linear array with 4 m spacing of field 15A, indicating depth of soil layers. The green layer represents soil thickness, the grey layer represents till thickness, and the blue layer represents limestone bedrock thickness. The y-axis is depth in meters and the x-axis is horizontal distance in meters from east to west. The red letters indicate the location of the seismic source (steel plate and hammer) and brown dots indicate the locations of the geophone receivers. The numbers within the soil layers indicate the velocity of seismic waves passing through each layer.

22CH



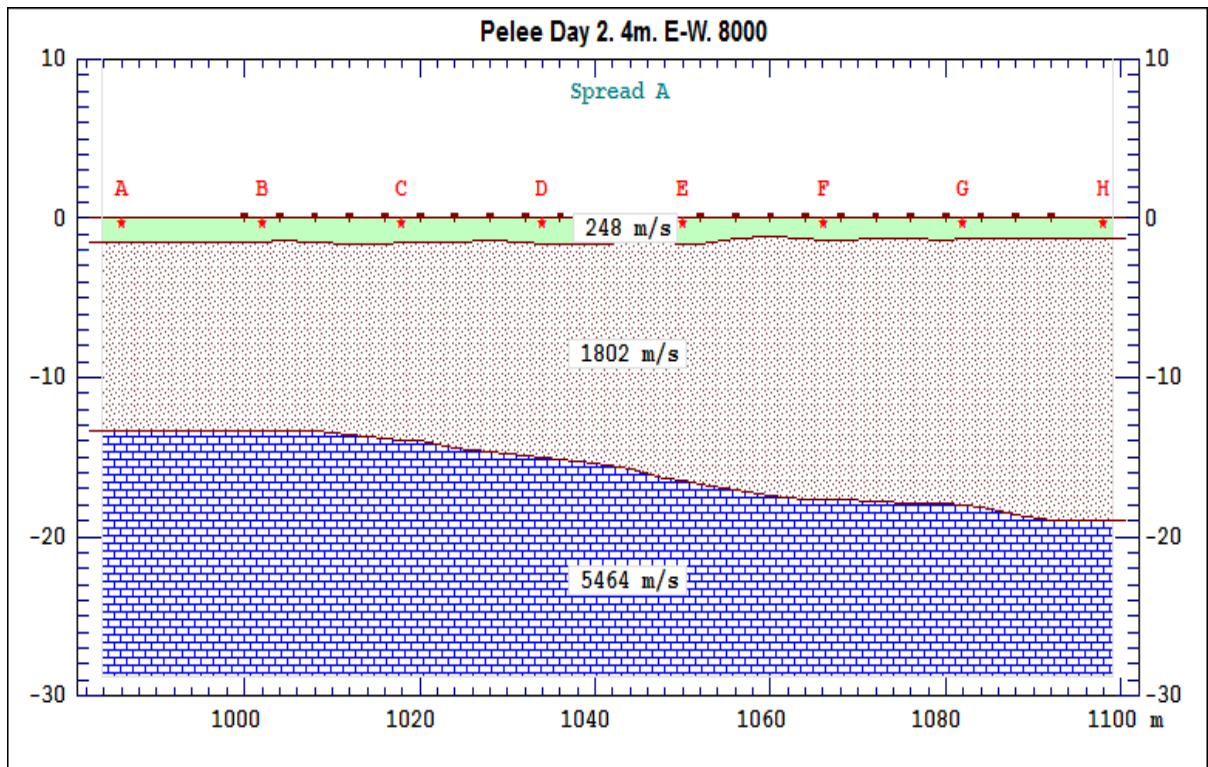
Seismic refraction depth profile from 24 channel linear array with 5 m spacing of field 22CH, indicating depth of soil layers. The green layer represents soil thickness, the grey layer represents till thickness, and the blue layer represents limestone bedrock thickness. The y-axis is depth in meters and the x-axis is horizontal distance in meters from east to west. The red letters indicate the location of the seismic source (steel plate and hammer) and brown dots indicate the locations of the geophone receivers. The numbers within the soil layers indicate the velocity of seismic waves passing through each layer.

23CH



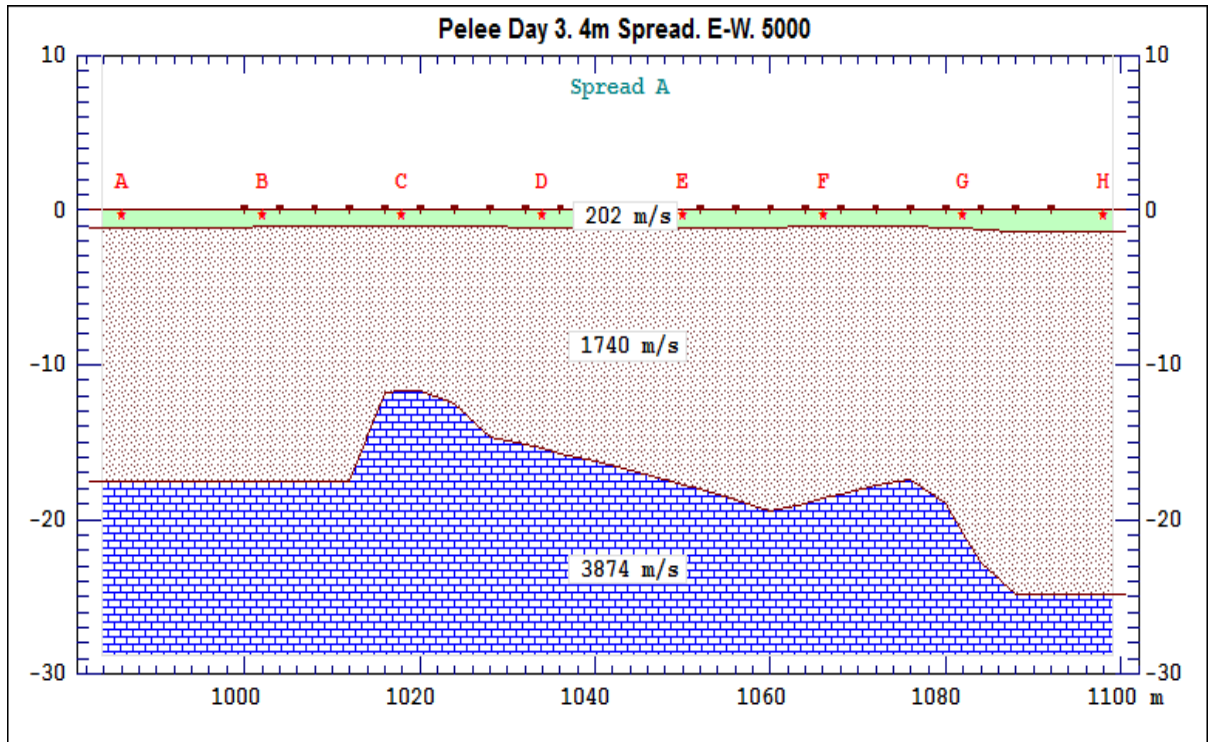
Seismic refraction depth profile from 24 channel linear array with 4 m spacing of field 23CH, indicating depth of soil layers. The green layer represents soil thickness, the grey layer represents till thickness, and the blue layer represents limestone bedrock thickness. The y-axis is depth in meters and the x-axis is horizontal distance in meters from west to east. The red letters indicate the location of the seismic source (steel plate and hammer) and brown dots indicate the locations of the geophone receivers. The numbers within the soil layers indicate the velocity of seismic waves passing through each layer.

24CF

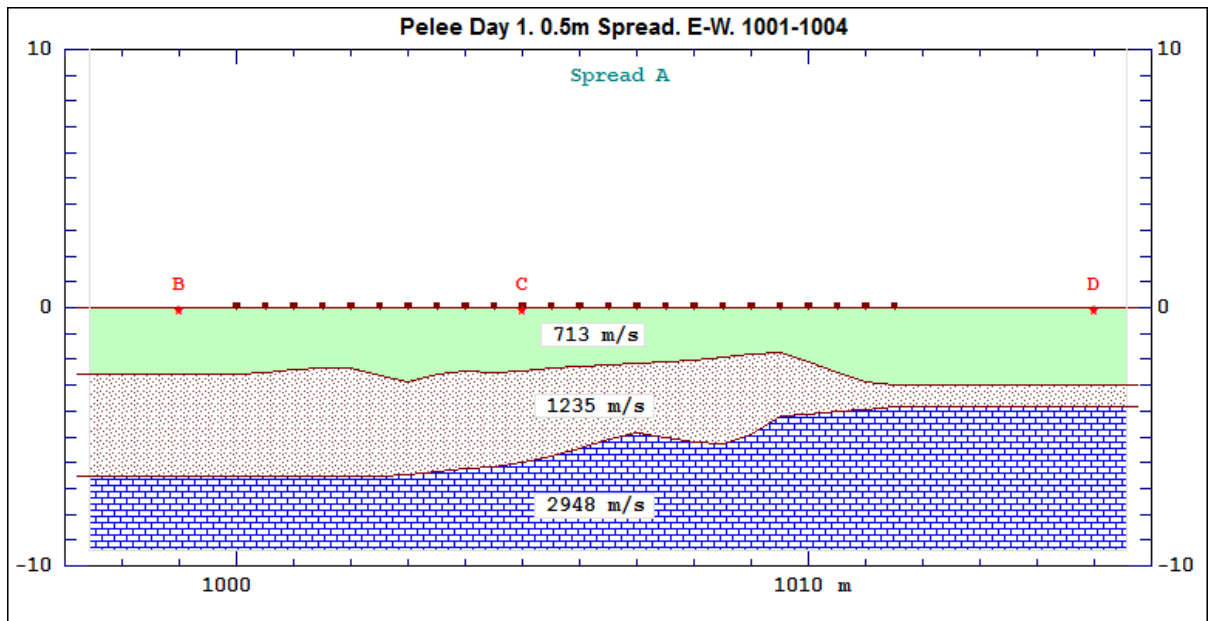


Seismic refraction depth profile from 24 channel linear array with 4 m spacing of field 24CF, indicating depth of soil layers. The green layer represents soil thickness, the grey layer represents till thickness, and the blue layer represents limestone bedrock thickness. The y-axis is depth in meters and the x-axis is horizontal distance in meters from east to west. The red letters indicate the location of the seismic source (steel plate and hammer) and brown dots indicate the locations of the geophone receivers. The numbers within the soil layers indicate the velocity of seismic waves passing through each layer.

26CF

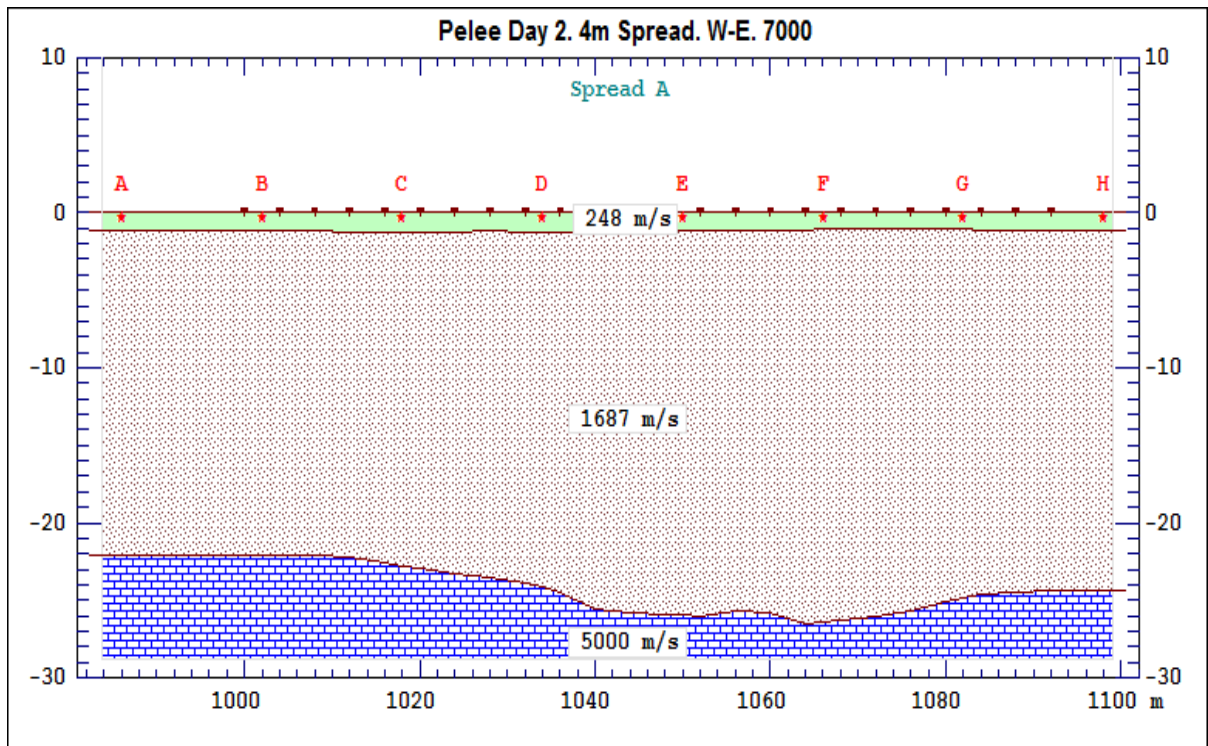


Seismic refraction depth profile from 24 channel linear array with 4 m spacing of field 26CF, indicating depth of soil layers. The green layer represents soil thickness, the grey layer represents till thickness, and the blue layer represents limestone bedrock thickness. The y-axis is depth in meters and the x-axis is horizontal distance in meters from east to west. The red letters indicate the location of the seismic source (steel plate and hammer) and brown dots indicate the locations of the geophone receivers. The numbers within the soil layers indicate the velocity of seismic waves passing through each layer.

27CS

Seismic refraction depth profile from 24 channel linear array with 0.5 m spacing of field 27CS, indicating depth of soil layers. The green layer represents soil thickness, the grey layer represents till thickness, and the blue layer represents limestone bedrock thickness. The y-axis is depth in meters and the x-axis is horizontal distance in meters from east to west. The red letters indicate the location of the seismic source (steel plate and hammer) and brown dots indicate the locations of the geophone receivers. The numbers within the soil layers indicate the velocity of seismic waves passing through each layer.

28CH



Seismic refraction depth profile from 24 channel linear array with 4 m spacing of field 28CH, indicating depth of soil layers. The green layer represents soil thickness, the grey layer represents till thickness, and the blue layer represents limestone bedrock thickness. The y-axis is depth in meters and the x-axis is horizontal distance in meters from west to east. The red letters indicate the location of the seismic source (steel plate and hammer) and brown dots indicate the locations of the geophone receivers. The numbers within the soil layers indicate the velocity of seismic waves passing through each layer.

Curriculum Vitae

Name: Lindsay Blythe

Post-secondary Education and Degrees:

The University of Western Ontario
London, Ontario, Canada
2010-2014 B.A. Kinesiology

The University of Western Ontario
London, Ontario, Canada
2015-2017 B.Sc. Geology

The University of Western Ontario
London, Ontario, Canada
2017-present M.Sc. Geology

Honours and Awards:

J. Malcolm Slack Earth Science Award
2018, 2019, 2020

Robert W. Hodder International Geoscience Field Experience Award
2019

Earth Sciences International Field School Global Opportunities Award
2019

Related Work Experience

Teaching Assistant Origin and Geology of the Solar System (EARTHSCI 1086)
The University of Western Ontario
2019

Teaching Assistant Earth, Art, and Culture (EARTHSCI 1089)
The University of Western Ontario
Winter 2018, Fall 2018

Teaching Assistant Earth Rocks (EARTHSCI 1022)
The University of Western Ontario
2017